THE EFFECT OF WHOLE OVARY CRYOPRESERVATION IN SHEEP

BY

ADWOA YAABA DADSON, MSC

SUPERVISORS: JUAN HERNANDEZ-MEDRANO, DR

ADAM WATKINS, DR

Thesis submitted to The University of Nottingham for the degree Of Doctor of Philosophy

University of Nottingham
Academic Unit of Lifespan and Population Sciences
School of Medicine
Queen's Medical Centre
Nottingham

AUGUST 2025

DECLARATION

I hereby declare that this thesis is my own work and that it has not been submitted anywhere for any other degree or award. The work presented herein is my own work and where other sources of information have been used, they have been duly acknowledged.

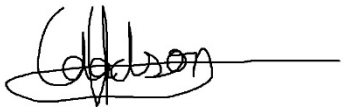

Adwoa Yaaba Dadson

TABLE OF CONTENTS

ACKNOWLEDGEMENTS

My foremost and deepest gratitude goes to the Almighty God for His grace, mercy, and guidance throughout my PhD journey.

I am profoundly grateful to Dr. Walid Maalouf for accepting my research proposal and application, allowing me to begin this academic pursuit. I extend my sincere appreciation to my supervisor, Dr. Juan Hernandez Medrano, for his invaluable advice, expert guidance, and unwavering support. A special thank you to Dr. Adam Watkins for serving as my internal assessor and supervisor, and for his insightful feedback during the compilation of this thesis.

My warmest appreciation also goes to Nader Eid, Afsaneh Khoshkerdar, and Klaountia Dimitra Makri for their stimulating discussions and encouragement, which provided great comfort during these past years. I also thank Nichola Baker and Dr. Hannah Morgan for their assistance with laboratory training and the techniques essential for my research.

I gratefully acknowledge the University of Nottingham and the Vice Chancellor Scholarship for Research for providing the funding that made this study possible.

Finally, I want to express my deepest thanks to my family and friends, whose support extended far beyond the academic. My parents, Mr. Joseph Dadson and Mrs. Judith Dadson, have been an immense source of financial support, and I am eternally grateful for their continued presence. I am also grateful to the BBGG/PAPS members, especially Pierro and Seyram Ahorsey, for consistently providing an environment that fostered my spiritual and emotional well-being. My sincere love and gratitude also go to Lucy Fiadonu, Sarah Andrews Okyne, Gregory Lamusah, Mr. and Mrs. Edusei, Madam Sarah, Mr. and Mrs. Danso, Golnar Mahani, Mostafa Azizkhani, Fatma

Poyraz Ciddi, Kwesi Asante, Mr Osei and Mrs Felicia Danquah who have all provided support in various ways.

ABSTRACT

The potential of whole ovary cryopreservation (WOCP) to restore ovarian function and fertility has been demonstrated in sheep, resulting in multiple live births from primordial and preantral follicles. However, the impact of WOCP on oocytes from antral follicles, their viability, and the long-term effects on ovarian tissue, oocytes, and subsequent embryos remain unclear. This study aimed to investigate the viability and maturation capacity of antral follicle oocytes following WOCP, along with variations in the transcriptomic profile and DNA methylation patterns in sheep ovarian tissue.

The study commenced with *in vitro* maturation (IVM) of antral follicle oocytes, assessing nuclear maturation using DAPI after 24 hours. WOCP's immediate effects on oocyte viability and apoptosis were examined using propidium iodide (PI) and TUNEL, respectively. Chromatin configuration of germinal vesicle (GV) oocytes and qualitative analysis of connexin 37 and 43 were performed to assess cell-to-cell communication. A comprehensive transcriptomic analysis using microarray and global DNA methylation assessment was performed on ovarian tissue post WOCP. Lastly, a scoping review to examine evidence related to epigenetic changes associated to oocyte and ovarian tissue cryopreservation (OTC).

The evaluation of nuclear maturation revealed a significantly lower maturation rate in the WOCP group (8%, n = 1/64) compared to the control (fresh) group (67%, n = 60/90). Proportions of PI-stained cells were relatively close between the WOCP and control groups (fresh group 17.1%; WOCP group 38.6%, $p > 0.05$). However, a significant difference in apoptotic index was observed between the control (fresh) group (26.6%) and WOCP (75.4%). Cryoprotectant exposure predominantly induced a condensed pattern of chromatin fibres (SNE- 54%) in GV-stage oocytes,

with noticeable decondensed patterns (NSN- 36%) and abnormal condensation, highlighting cryopreservation-induced alterations. Microarray analysis identified 2557 genes out of an initial 24,596 genes as statistically significant ($p<0.05$), but none remained significant after FDR correction. Despite this, 114 genes were selected for further analysis as potential candidates for differential expression. Gene Ontology (GO) enrichment analysis revealed changes in fundamental cellular activities, including metabolic processes, biological regulation, and cell proliferation, with significant positive enrichment in signalling and transport pathways, and negative enrichment in methylation-related annotations. KEGG pathway analysis showed upregulation of ribosomal genes (e.g., RPL11, RPL29) suggesting increased protein synthesis, and neurodegenerative disease-associated genes (e.g., NDUFA1, NDUFS5) integral to mitochondrial oxidative phosphorylation and thermogenesis, indicating increased ATP demands and cold-induced metabolic adaptations. Conversely, downregulation of autophagy (ATG16L1, ATG9A) and lysine degradation pathways (ALDH9A1, SETMAR) was observed, suggesting compromised cellular quality control. Furthermore, pro-apoptotic genes (BAX, STC2) were upregulated, while anti-apoptotic BCL2 was downregulated, indicating increased cellular susceptibility to apoptosis. Downregulation of transcriptional regulators (zinc finger proteins) and key signalling pathways like WNT4, GRM7, and GRM8 was also identified, suggesting disruptions to ovarian development and follicle activation.. Global DNA methylation exhibited no significant difference between the control group and WOCP. The review highlighted that cryopreservation, particularly vitrification, induced significant epigenetic alterations, including DNA methylation, histone modification, and microRNA expression changes, in oocytes and ovarian tissue across species.

In conclusion, this study unveils the intricate molecular and cellular responses of antral follicle oocytes to WOCP. The observed detrimental effects emphasise the challenges in

preserving delicate ovarian tissue structures, underscoring the necessity for optimized cryopreservation protocols. The study highlights the crucial role of cumulus cells in oocyte maturation and stresses the importance of their integrity during cryopreservation. Furthermore, insights into chromatin configuration and DNA methylation patterns provide valuable information on adaptive responses and epigenetic changes induced by WOCP. Dysregulation of gene expression in WOCP ovaries, particularly in pathways associated with metabolic processes and follicular development, underscores the complexity of reproductive outcomes post cryopreservation. Overall, the findings underscore the ongoing need for refinement in cryopreservation techniques to ensure the preservation of ovarian tissue integrity and optimize reproductive outcomes.

LIST OF FIGURES

LIST OF TABLES

LIST OF PRESENTATIONS

NATIONAL AND INTERNATIONAL CONFERENCES

ADWOA Y. DADSON, JUAN HERNANDEZ-MEDRANO, MARCOS CASTELLANOS-URIBE, IQBAL KHAN, ADAM WATKINS 2023. Transcriptomic profile of sheep ovarian cortex & the effect of whole ovary cryopreservation on DNA methylation. This presentation contains results obtained from Chapter 6 and presented as rapid fire poster presentations programme at the Fertility 2023 Annual Meeting, Belfast, 10-13 January 2023.

ADWOA Y. DADSON, JUAN HERNANDEZ-MEDRANO, WALID MAALOUF 2021. Epigenetic modifications after female fertility preservation by cryopreservation: a scoping review. This work was presented by poster at the Fertility 2020 Annual Meeting, 6-8 January 2021.

ADWOA Y. DADSON, DIAN WANG, JUAN HERNANDEZ-MEDRANO, WALID MAALOUF 2020. The effect of ovine whole ovary cryopreservation on the antral follicle oocyte and its developmental potential. This work was also presented during the 36th virtual Annual Meeting of the European Society of Human Reproduction and Embryology from 5 - 8 July 2020.

ADWOA Y. DADSON, DIAN WANG, JUAN HERNANDEZ-MEDRANO, WALID MAALOUF 2020. The effect of ovine whole ovary cryopreservation on the oocyte and its developmental potential. This work was presented by poster at the Fertility 2020 Conference, Edinburgh, 9-11 January 2020.

LIST OF ABBREVIATIONS

5-mC	5 Methyl Cytosine
AMH	Anti-Müllerian hormone
ANOVA	Analysis of variance
ART	Assisted reproductive technology
ASRM	American Society for Reproductive Medicine
BCB	Brilliant cresyl blue
bFGF	Fibroblastic growth factor
BMP	Bone morphogenetic proteins
BSA	Bovine serum albumin
C	Clumped
CC	Cumulus cell
cDNA	Complementary deoxy ribonucleic acid
COC	Cumulus oocyte complexes
COS	Controlled ovarian stimulation
CPA	Cryoprotectant
CX	Connexin
DAB	Diaminobenzidine
DAPI	4' ,6-diamidino-2-phenyl indole
DAZL	Deleted in Azoospermia-Like
DMSO	Dimethyl sulfoxide
DNA	Deoxy ribonucleic acid
DPBS	Dulbecco's phosphate-buffered saline
EG	Ethylene glycol
ELISA	Enzyme-linked immunoassay
ESHRE	European Society of Human Reproduction and Embryology
FBS	Foetal bovine serum

FCS	Foetal calf serum
FDR	False discovery rate
FMR1	Fragile X Messenger Ribonucleoprotein 1
FOXO3a	Forkhead box O3a
FSH	Follicle stimulating hormone
G6PD	Glucose-6-phosphate dehydrogenase
GDF9	Growth differentiation factor 9
GESA	Gene Set Enrichment Analysis
GO	Gene ontology
GV	Germinal vesicle
GVBD	Germinal vesicle breakdown
H&E	Haematoxylin-eosin
hCG	Human chorionic gonadotropin
HSE	In-house media
ICSI	Intracytoplasmic sperm injection
IHC	Immunohistochemistry
IVF	*In vitro* fertilisation
IVM	*In vitro* maturation
KEGG	Kyoto Encyclopaedia of Genes and Genomes
KITL	KIT Ligand
KITL-KIT	KIT Ligand - KIT Proto-Oncogene, Receptor Tyrosine Kinase interaction
LH	Luteinising hormone
LIF	Leukaemia inhibitory factor
MI	Metaphase of the first meiotic division
MII	Metaphase of the second meiotic division
mRNA	Messenger ribonucleic acid
mTOR	Mammalian (mechanistic) target of rapamycin
N	Netlike

NADPH	Nicotinamide Adenine Dinucleotide
NES	Normalised enrichment score
NHS	Normal Horse Serum
NSN	Nonsurrounded nucleolus
OC	Ovarian cryopreservation
OCT4	Octamer-binding transcription factor 4
OD	Optical density (absorbance)
OHSS	Ovarian Hyperstimulation Syndrome
OMI	Oocyte maturation inhibitor
OTC	Ovarian tissue cryopreservation
OXPHOS	Oxidative phosphorylation
PBS	Phosphate buffer saline
PC	Positive control
PCA	Principal components analysis
PCOS	Polycystic Ovary Syndrome
PCR	Polymerase chain reaction
PFA	Paraformaldehyde
PI	Propidium iodide
PI3K	Phosphatidylinositide 3-kinase
POI	Premature ovarian insufficiency
POF	Premature ovarian failure
PPP	Pentose phosphate pathway
PROH	Propylene glycol
PTEN	Phosphatase and Tensin homolog
R5P	Ribose 5-phosphate
RIN	RNA integrity number
RNA	Ribonucleic Acid
ROS	Reactive oxygen species

RRBS	Reduced representation bisulfite sequencing
SCF	Stem cell factor
scRNA-Seq	Single-cell RNA Sequencing
SEM	Standard error of the mean
SN	Surrounded nucleolus
SNE	Nuclear envelope
STRA8	Stimulated by Retinoic Acid 8
TGF-β	Transforming Growth Factor beta
TI	Telophase I
TP	Transplantation
TSC	Tuberous sclerosis complex
TZP	Transzonal projections
TUNEL	Terminal Transferase dUTP Nick End Labelling
WNT	Wingless-related integration site
WOCP	Whole ovary cryopreservation
ZP	Zona pellucida

CHAPTER ONE: LITERATURE REVIEW

1.1 INTRODUCTION

Premature ovarian failure (POF) now known as premature ovarian insufficiency (POI) is a condition where the normal functioning of the ovaries is halted in women below the age of 40. The condition is characterised by amenorrhoea or oligomenorrhea, elevated gonadotrophins and sex steroid deficiency (low oestradiol) (Maclaran et al., 2010; Webber et al., 2016). Although POI may be caused by autoimmune and genetic diseases such as Turner syndrome, the condition is increasingly iatrogenic. The prevalence of iatrogenic POI has risen as access to surgical management options, chemotherapy, and radiotherapy has increased. The overall prevalence of POI is approaching 4% of women before the age of 40 (Li et al., 2023), up from earlier estimates of approximately 1% for non-iatrogenic cases (Fenton, 2015). Ovaries are very sensitive due to their nature, presence of hormone receptors, producing oocytes and hormones for reproduction, making them easily prone to the cytotoxic effect of chemo- and radio-therapy) leading to POI (Meirow and Nugent, 2001). Hence, fertility preservation has become a rapidly growing specialty.

The incidence of cancer is rapidly increasing on a global scale. In 2012, an estimated 14.1 million new cancer cases were reported worldwide (Torre et al., 2016b). This number was projected to rise to 18.1 million new cases with 9.6 million deaths in 2018 (Bray et al., 2018). By 2020, the estimates had increased further, with 19.3 million new cancer cases and nearly 10 million cancer-related deaths (Sung et al., 2021). Despite the high number of deaths, these estimates suggest that the survival rate is also improving, thanks to advancements in therapeutic treatments (Siegel et al., 2012). In England and Wales, cancer survival has seen improvement with 50% of

people diagnosed with cancer surviving for ten years or more, doubling in the last 40 years in the United Kingdom (Quaresma et al., 2015).

It has also been observed that cancer survival is higher in women than men (Quaresma et al., 2015). This observation can be attributed to a variety of factors, including the types of cancers that are more prevalent in each gender and biological differences. Women often have better cancer-specific survival rates for several types of cancer, such as lung, liver, colorectal, pancreatic, stomach, and oesophageal cancers, while men tend to have better outcomes in bladder cancer (He et al., 2022). One contributing factor is that women are more frequently diagnosed with cancers that affect the reproductive system, such as breast and uterine cancers, which often have better prognoses, especially when detected early. Additionally, women are more likely to be diagnosed with adenocarcinoma, a type of cancer that generally responds better to treatment. Biological differences, such as tumour characteristics and responses to treatment, also play a role. For example, even after adjusting for major prognostic factors like histologic subtype, stage at diagnosis, and treatment received, women with lung cancer were found to survive significantly longer than men. These factors, combined with lifestyle differences, contribute to the observed gender disparities in cancer survival rates (He et al., 2022).

Finally, the number of children and young adults with cancer seems to be increasing yearly (Siegel et al., 2012). In the UK, cancer incidence rates in children have increased by 12% with rates in girls having increased by around 15% since the 1990s (Cancer Research, UK). These translate into a growing population of cancer survivors highlighting the importance of fertility preservation prior to the commencement of toxic treatments.

Fertility preservation options may not yield positive results for women diagnosed with POI due to depleted ovarian reserve. However, for women who are about to undergo cancer treatment,

fertility preservation options offer a valuable opportunity. Such patients at risk of POI including patients with POI in its early stages are presented with three alternatives for fertility preservation, which includes embryo cryopreservation, oocyte cryopreservation and ovarian tissue cryopreservation (OTC) (Webber et al., 2016). Oocyte cryopreservation and embryo cryopreservation techniques require the use of mature oocytes and therefore the patient will have to undergo ovarian stimulation, to induce the development of multiple preovulatory follicles yielding multiple mature oocytes. In the case of pre-pubertal patients who have not begun ovulation and menstruation, and adults who are ineligible for ovarian stimulation due to the urgency to begin cancer treatment, their best and only option is OTC (Practice Committee of American Society for Reproductive, 2019). Thus, either ovarian-cortex fragments or the whole ovary with its vascular pedicle can be cryopreserved. Since the first successful live births post transplantation of cryopreserved ovarian tissue, OTCP-TP has progressed from a revolutionary experimental procedure to an accepted clinical treatment in many centres (Donnez et al., 2004; Donnez et al., 2013; Gellert et al., 2018). To date, hundreds of graft TPs have been performed with over 130 live births and a pregnancy rate of between 30 and 50% (Gellert et al., 2018). The technique has also been seen to return ovarian function to 95% of ovarian tissue transplantations, however, the life span of the graft is shortened due to ischemia leading to the loss of follicles and the limited oocyte reserve transplanted (Maltaris et al., 2007; Nisolle et al., 2000). In some cases, a single graft has maintained function for years, producing as many as four consecutive pregnancies, while other grafts cease functioning within a few months (Andersen et al., 2012; Donnez and Dolmans, 2015a). In contrast, whole ovary cryopreservation (WOCP) for later autotransplantation theoretically presents an attractive alternative to OTC. This method could

improve follicle survival and maintain endocrine and reproductive functions for a much longer period, as it includes vascular transplantation.

This chapter will present an insight to the physiology and anatomy of the human ovary. It also discusses the process of follicle (folliculogenesis), oocyte development (oogenesis) particularly in humans with a few references to other mammals. We look at female fertility preservation, current options and practice as well as the main technique applied, cryopreservation, the science and techniques, methods under development. Finally, I discuss the OTC and delve into the aims and objectives of this study.

1.2 OVARIAN PHYSIOLOGY

The female reproductive tract consists of five main portions each having a critical function in reproduction (**Figure 1.1**). The ovary develops and houses the oocytes until they are ovulated into the fallopian tubes/oviducts where fertilisation occurs. The fertilised egg begins cell division in the fallopian tube and moves into the uterus at the blastocyst stage and implants into the uterine wall where it develops into a full foetus, passes through the cervix and then the vagina at birth (**Table 1.1**).

Table 1.1 Major mammalian female reproductive organs, locations, and function.

Organ	Function
Ovaries	Produces, stores, and develops oocytes
Fallopian tubes/oviduct	Transports oocytes from the ovary, is the site of fertilisation and transports blastocyst to the uterus
Uterus	Supports a developing embryo and foetus
Cervix	Permits passage between the uterus and the vagina
Vagina	Receives penis during intercourse, acts as the birth canal, passes menstrual flow

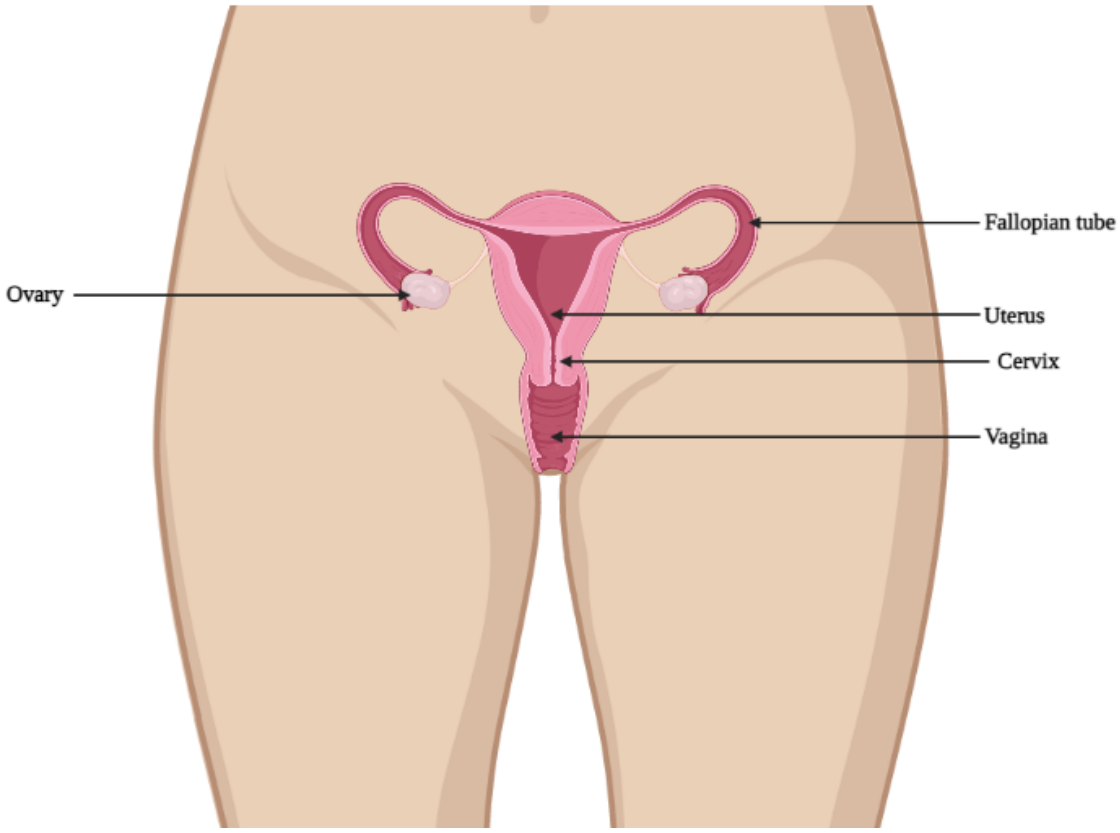

Figure 1.1.The female reproductive tract showing the main components; ovary, fallopian tube, uterus, cervix and vagina**.** Image was created using Biorender

Women are naturally born with a right and left ovary with all the oocytes they would have in their lifetime in non-growing follicles known as primordial follicles. The ovary is about the size and shape of an almond at birth and with a volume that changes with age, i.e., 0.7ml at 2 years of age to a peak of 7.7ml at age 20, declining to about 2.8ml at menopause in women (Kelsey et al., 2013). The ovaries are situated in the lateral wall of the lower pelvis on either side of the uterus below and behind the fallopian tubes. Each ovary is attached to the upper part of the uterus by the round ligament of the ovary (**Figure 1.1**).

The ovary consists of a thick cortex surrounding the vascular medulla (**Figure 1.2**). The cortex surrounding the medulla consists of a framework of connective tissue covered by the germinal epithelium, i.e., ovarian follicles. At birth, the ovary contains a finite pool of primordial follicles, each with an oocyte arrested in the diplotene stage of prophase I. From this time onwards, and throughout childhood, a proportion of these primordial follicles are continuously recruited to grow into primary and secondary (preantral) follicles; however, follicular growth up to these stages occurs independently of gonadotropins. With the onset of puberty, the activity of the hypothalamic–pituitary–gonadal axis supports further development of follicles to the antral and pre-ovulatory stages. Oocytes within these developing follicles remain arrested at prophase I until the LH surge at ovulation, when meiosis I is completed, and the ruptured follicle differentiates into a corpus luteum (**Figure 1.2**).

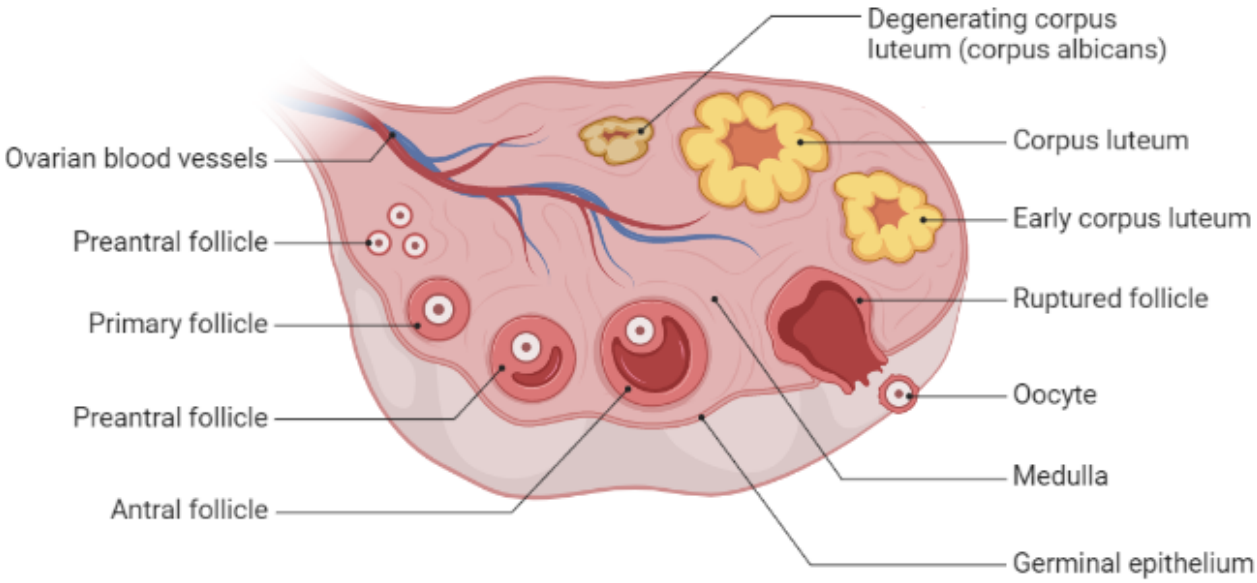

Figure 1.2. An illustration of a post puberty ovary showing the various follicle stages, blood vessels, cortex and medulla of the ovarian tissue. Image was created using Biorender.

1.3 OOCYTE DEVELOPMENT

1.3.1 Oogenesis

Oogenesis is the differentiation of the female diploid oogonium to form a mature haploid ovum suitable for fertilisation (Gilbert, 2000). During this process, the oocyte undergoes two major phases of unequal divisions, the first meiotic division (also known as reductional division or meiosis I) to form the haploid secondary oocyte and the first polar body and the second meiotic division (meiosis II) to form the ovum and second polar body which only occurs after fertilisation (Wang and Pepling, 2021). The process of oogenesis begins during foetal life and continues until the end of the female's reproductive lifespan.

In the human embryo, the precursor cells of the ovum begin their journey outside the body of the embryo where they form in the wall of the yolk sac at around 24 days of gestation. These

cells known as primordial germ cells migrate from the wall of the yolk sac to the developing gonads (primitive undifferentiated gonads/ gonadal ridges) around 5th week of gestation (Hardy et al., 2000). At 6-7 weeks of gestation, these cells would have arrived in the gonadal ridge (genital ridge), lose their migration properties but continue to divide by mitosis and become oogonia (Motta et al., 1997). The number of oogonia at this stage range in the 1000s however, they divide rapidly due to their remarkable mitotic activity, between 8 weeks to approximately 24 weeks of gestation resulting in roughly 6-7 million oogonia (Motta et al., 1997).

During this period, a critical transition occurs as the germ cells switch from mitotic division to meiotic division. This switch from mitosis to meiosis is a complex process that begins around 11-12 weeks of gestation and progresses in an anterior-to-posterior wave across the ovary. The transition is regulated by intricate molecular mechanisms, with retinoic acid playing a central role. Retinoic acid is synthesized in the mesonephros and diffuses into the developing ovary, where it initiates the meiotic program (Bowles et al., 2006). The action of retinoic acid induces the expression of genes necessary for meiotic entry, most notably STRA8 (Stimulated by Retinoic Acid 8) (Childs et al., 2011). STRA8 is a key regulator of meiotic initiation, activating other meiosis-specific genes and promoting the formation of meiotic chromosomal structures (Anderson et al., 2008). Simultaneously, the expression of pluripotency genes like octamer-binding transcription factor 4 (OCT4) is downregulated, marking the commitment of germ cells to the meiotic fate (Childs et al., 2011). Another crucial factor in this transition is the DAZL (Deleted in Azoospermia-Like) protein. DAZL acts as a licensing factor, making germ cells competent to respond to retinoic acid and initiate meiosis. It does this by regulating the translation of key meiotic proteins and by promoting the expression of meiosis-specific genes (Lin et al., 2008).

As oogonia enter meiosis, they become primary oocytes and begin to form primordial follicles. The timing of this transition is crucial, as it determines the final number of oocytes available for a female's reproductive lifespan. The meiotic process in oocytes is unique in that it arrests at the diplotene stage of prophase I, a state known as the dictyate stage. This arrest can last for decades until just before ovulation (Wear et al., 2016).

After 24 weeks of gestation, the number of oogonia drops rapidly. Most oogonia degenerate, which may be a result of genetic errors occurring during crossing-over, as well as metabolic and/or vascular disturbances during this period. The remaining oogonia enlarge and enter into the first meiotic division (Motta et al., 1997; Pinkerton et al., 1961; Sun et al., 2017), at which point they are called primary oocytes.

These oocytes progress through the first meiotic prophase proceeding through the leptotene, zygotene, and pachytene stages until the diplotene stage, at which point they are arrested due to the presence of an oocyte maturation inhibitor (OMI) factor secreted by the somatic cells surrounding the oocyte until puberty (Mira, 1998). The oocytes differ greatly in the rate at which they proceed through meiosis, and about a quarter remain as oogonia failing to enter meiosis at all, undergoing atresia. It is during this stage that somatic (pre-granulosa) cells enclosure the oocyte, forming primordial follicles, the earliest stage of follicular development.

With the onset of puberty, groups of primordial follicles are activated for development periodically with one primordial follicle becoming dominant and its oocyte resuming meiosis. Thus, in humans, after the first part of meiosis begins in the foetus, the signal to resume meiosis is not given until roughly 12 years later (Gilbert, 2000). In fact, some oocytes are maintained in meiotic prophase I for nearly 50 years. Additionally, out of about a million primary oocytes present at birth, only about 400 mature during a woman's lifetime (Findlay et al., 2015; Hansen et al., 2008;

Oktem and Oktay, 2008). At puberty and each subsequent ovarian cycle, the oocyte of the dominant follicle resumes meiosis, reaching telophase I just before the ovulation, forming two unequally sized daughter cells each with haploid number of chromosomes. One daughter cell retains nearly the entire cellular volume and components (cytoplasm) forming the secondary oocyte whereas the other contains mainly half of the chromosomes with hardly any cytoplasm forming the first polar body (Oktem and Oktay, 2008).

The secondary oocyte which enters the second meiotic division at the time of ovulation also arrests at metaphase II only to resume and complete meiosis after fertilisation. During the second meiotic division, a similar unequal cytokinesis takes place where most of the cytoplasm is retained by the mature egg (ovum), and a second polar body is extruded with minimal cytoplasmic content.

Mammalian meiosis is initiated by an extrinsic signal—retinoic acid—and consists of meiosis I and II, each of which is divided into prophase, metaphase, anaphase, and telophase (Bowles and Koopman, 2007; Koubova et al., 2006). Prophase of meiosis I (abbreviated as prophase I) is the first and most complex stage of meiosis, where homologous chromosomes, one inherited from each parent, come together in a process called synapsis. This pairing allows for the exchange of genetic material between homologous chromosomes, a phenomenon known as crossing-over or recombination. This exchange of genetic information during crossing-over contributes to genetic diversity among offspring. Based on chromosomal packaging, prophase itself is subdivided into five stages: leptotene, zygotene, pachytene, diplotene, and diakinesis (**Table 1.2**).

Meiosis II is characterized by its simplicity and brevity compared to the preceding meiosis I stages. It can be likened to mitosis for the haploid cells generated in the initial round of cellular

division during meiosis I. These haploid cells commence the second round of division already possessing a single copy of each chromosome (haploid set/1n), a result of the events in meiosis I. Within these haploid cells, each chromosome comprises a single chromatid. The subsequent phases of meiosis II involve the separation of sister chromatids, ultimately yielding four haploid cells, each with a distinct combination of non-duplicate chromosomes. A diagram of this meiotic process is presented in **Figure 1.3** below.

Table 1.2. A brief description of the processes that take place in meiosis I and meiosis II of oogenesis. Image Credit: (Gantchev et al., 2020)

Phase	Stage	Description
Meiosis I	**Prophase I**	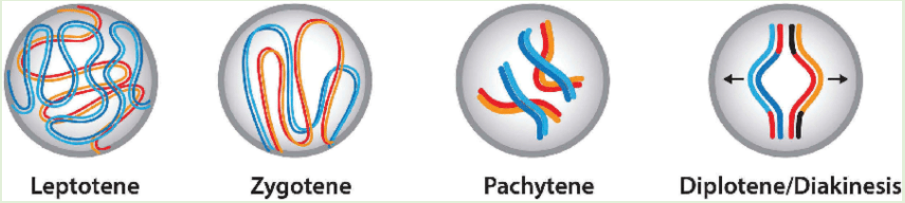 **Leptotene** • Chromosomes (consisting of two chromatids) appear as slender threads **Zygotene** • Pairing of homologous chromosomes (bivalent) **Pachytene** • Four chromatids become visible (tetrahed) • (Meiosis arrest occurs here) **Diplotene/Diakinesis** • Crossing over (synapsis of two central chromatids) • Formation of chiasmata • Chromosomes after genetic exchange migrate towards the nuclear membrane
	Metaphase I	• The spindle begins to form • The spindle apparatus attaches to the chromosomes • Homologous chromosomes are manoeuvred onto the equatorial plane/metaphase plate at the centre of the cell.
	Anaphase I	• Separation begins by the pulling of one entire chromosome of the two of each present to the opposite pole by the spindle fibres (there is no splitting of chromosome) *(The sister chromatids stay together during anaphase I; they remained paired together into the next phase, telophase)*
	Telophase I	• Chromosomes which were pulled apart during the previous phase complete their journey to the opposite poles of the cell. • Cytokinesis (division of one cell into two daughter cells) starts and completes resulting in two haploid cells..

Meiosis II	**Prophase II**	• Chromosomes condense, much as they did in meiosis one. • The nuclear envelope unravels • The mitotic spindle is formed, and the centrosomes migrate to the far poles of the cell. *(The mitotic spindle is formed by microtubules linking the centrosomes with the chromosomes.)*
	Metaphase II	• Mitotic spindle and microtubules move the chromatids onto the metaphase plate.
	Anaphase II	Oocyte prepares for division as • the sister chromatids are split apart from one another • pulled towards opposite ends of the cell
	Telophase II	• Cytokinesis occurs • Nuclear membranes reform • Two daughter cells are formed, the zygote and second polar body. Each of the cells having a single chromatid.

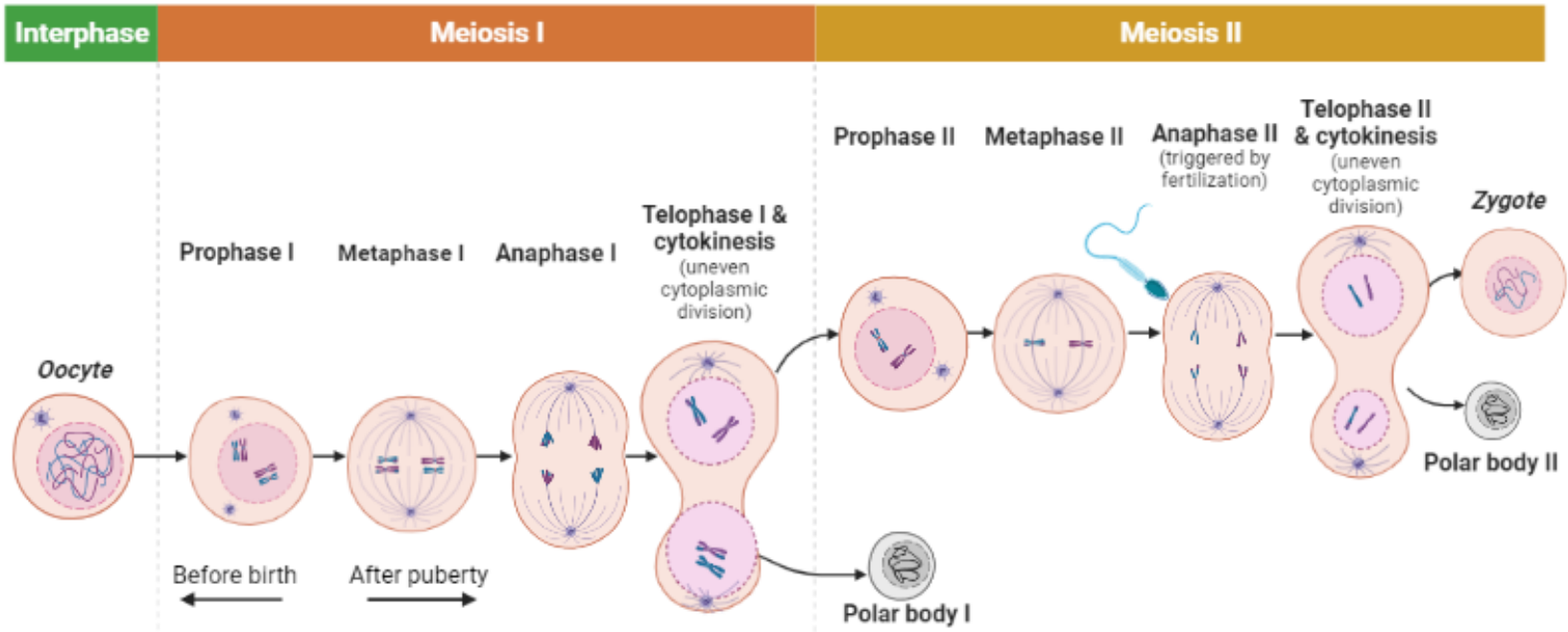

Figure 1.3. Oogenesis begins when the 2n oogonium undergoes mitosis, producing a primary oocyte. The primary oocytes are arrested in prophase I before birth. After puberty, meiosis of one oocyte per menstrual cycle continues, resulting in a secondary oocyte that arrests in metaphase II and expulsion of the first polar body (Polar body I). Upon ovulation and fertilization, meiosis is completed, resulting in the expulsion of the second polar body (Polar body II) and the formation of the zygote. Image was created using Biorender

1.4 FOLLICULOGENESIS & THE MENSTRUAL CYCLE

Oogenesis, previously discussed is accompanied by folliculogenesis, a process that involves the development and growth of the primordial follicle into a Graafian follicle (Hirshfield, 1991). In normal cycling women, a single (dominant) follicle is selected for ovulation approximately ten weeks before the actual release of the oocyte (Conti and Chang, 2016). This phase, known as the menstrual cycle, involves the sequential maturation and release of the oocyte. The term "menstrual cycle" is derived from the cyclical shedding of blood and endothelial tissue, constituting the uterine lining, which occurs monthly in response to hormonal interactions. In non-primate mammals however, the endometrium is reabsorbed by the walls of the uterus in a process described as the oestrous cycle (Catalini and Fedder, 2020). This section will however cover the menstrual cycle and where possible the pattern will be compared to other species.

1.4.1 Folliculogenesis

As previously stated in oogenesis, all the oocytes used over a female mammal's lifetime are present at birth in a finite pool of structures known as follicles. There are two types of follicles in the adult ovarian follicle pool: dormant primordial follicles and growing follicles. The dormant primordial follicles, which constitute the ovarian reserve, make up a larger proportion of the follicle pool in the human ovary compared to the growing follicles (90% vs. 10%, respectively) (Oktem and Urman, 2010) , this proportion is not fixed. With advancing age, the number of primordial follicles diminishes progressively, while the relative proportion of growing follicles increases until the reserve is nearly exhausted (Wallace and Kelsey, 2010). Primordial follicles possess a single layer of flattened granulosa cells enclosing the oocyte arrested in the diplotene stage of prophase I , as described in the previous section (Mira, 1998; Wang and Pepling, 2021). These pre-granulosa cells lack the features typical of granulosa cells in growing follicles, such as

the ability to undergo mitotic division, expression of gonadotropin receptors, and steroidogenic activity to produce oestrogen and progesterone (Oktay et al., 1997). Folliculogenesis begins with the activation of these dormant primordial follicles developing through various stages and ending with an luteinising hormone (LH) surge signalling the release of the oocyte (**Figure 1.4**). Primordial follicle activation commences shortly before birth with most follicles developing to the preantral follicle stage (Ford et al., 2020)

The activation of primordial follicles is a finely orchestrated process that depends on the intricate interplay between pre-granulosa cells and oocytes within the follicular microenvironment. Several key signalling pathways, including the Mammalian (mechanistic) Target of Rapamycin (mTOR) and Wingless-related Integration site (WNT) pathways in granulosa cells, the mTOR and Phosphatidylinositide 3-kinase (PI3K) pathway in oocytes, as well as the communication channel involving KIT Ligand - KIT Proto-Oncogene, Receptor Tyrosine Kinase interaction (KITL-KIT) between granulosa cells and oocytes, are essential for this activation (McLaughlin et al., 2011; Zhang et al., 2023).

In this process, the mTOR signalling pathway within granulosa cells plays a pivotal role. It serves as a sensor, detecting changes in the surrounding nutrient levels and other factors. When these conditions are favourable, granulosa cells respond by increasing the secretion of KIT Ligand (KITL). Once KITL binds to its receptor on the oocyte membrane, it triggers the activation of the PI3K signalling pathway within the oocyte itself. This activation cascade ultimately leads to the initiation of primordial follicle activation promoting cell survival and proliferation (Dunlop and Anderson, 2014; Zhang et al., 2023).

Control mechanisms include inhibitory factors like Phosphatase and Tensin homolog (PTEN) and Forkhead box O3a (FOXO3a), with their deficiency leading to premature ovarian

activation (Reddy et al., 2008). The Hippo signalling pathway, influenced by cell density, and factors such as bone morphogenetic proteins (BMP4, BMP7), leukaemia inhibitory factor (LIF), and fibroblastic growth factor (bFGF) contribute to primordial to primary follicle transition (Kawamura et al., 2013). Conversely, anti-Müllerian hormone (AMH) acts as a key inhibitory factor, suppressing primordial follicle recruitment and indirectly reducing the expression of activating factors like stem cell factor (SCF) and bFGF (Dunlop and Anderson, 2014; Skinner, 2005).

Following the activation of primordial follicles into primary follicles, the subsequent stage involves their development into secondary or pre-antral follicles. This process necessitates further growth of the oocyte and proliferation of granulosa cells. The involvement of members of the Transforming Growth Factor beta (TGFβ) superfamily, such as activin, enhances granulosa cell proliferation, and the growth becomes gonadotrophin-sensitive (Dong et al., 1996). The oocyte-expressed proteins growth differentiation factor 9 (GDF9) and BMP15 play crucial roles in the development of follicles beyond the primary stage, regulating cell proliferation within the follicle and SCF expression. Additionally, anti-Mullerian hormone (AMH) inhibits FSH sensitivity during this stage and its decline aligns with an increase in aromatase expression, impacting the follicle's ability to produce oestradiol. AMH not only controls the rate of follicles leaving the primordial pool but also potentially influences the selection of the dominant follicle (Broer et al., 2014).

The communication between the oocyte and surrounding somatic cells occurs bidirectionally through gap junctions and transzonal projections, this communication allows essential molecules to pass between the oocyte and granulosa cells, contributing to the coordinated development of the follicle (Fair et al., 1997).

Primary follicles evolve from primordial follicles as the oocytes initiate growth, and pre-granulosa cells transform into cuboidal, actively dividing cells (Da Silva-Buttkus et al., 2008). This transformation is mediated by paracrine factors like GDF9 (Dong et al., 1996). These primary follicles increase from 29 µm in size to about 150–200 µm in diameter with their granulosa cells also multiplying forming a concentric second layer around the oocyte to become the secondary follicle (Guzel and Oktem, 2017). During this progression, other significant changes also takes place simultaneously. This includes the establishment of gap junctions between the oocyte's surface membrane and neighbouring granulosa cells, the deposition of zona pellucida (ZP) material around the oocyte, the synthesis of cortical granules within the oocyte's cytoplasm and reorganization of the nucleolus (Fair et al., 1997).

The secondary follicle further develops into the preantral follicle, marked by granulosa cell differentiation and multiplication. Stromal cells surrounding the ovary align themselves around the edge of the follicle, and differentiate into theca cells, synthesizing androgens (Simon et al., 2020). The preantral follicle transitions into an antral follicle with the formation of an antrum containing follicular fluid produced by the granulosa cells, marking a shift to entirely gonadotrophin (Follicle Stimulating Hormone (FSH))-dependent status (Candelaria et al., 2020; Craig et al., 2007). The antrum development leads to the differentiation granulosa cells into cumulus cells surrounding the oocyte and promoting its maturation, and mural granulosa cells around the inner aspect of the follicle, producing sex steroids. Throughout this process, the oocyte undergoes significant growth but remains in the dictyate state. Gonadotrophin receptors expressed by granulosa and theca cells drive sex steroidogenesis with theca cells becoming luteinising hormone (LH) responsive (thus producing androgen) and granulosa cells responding to FSH (and converting theca cell-derived androgen to oestradiol by aromatization). The follicle destined for

ovulation is now around 10–12 mm in diameter (Baerwald et al., 2011). Ovulation is then triggered by an LH surge, and an antral follicle becomes preovulatory if both granulosa and theca cells express LH receptors. The innermost of cumulus cells will stay with the ovulated oocyte which surrounds the oocyte in the fallopian tube. During the gradual increase of the antrum, the oocyte undergoes a 500-fold increase in volume (corresponding to an increase in oocyte diameter from 10 μm in a primordial follicle to 80 μm in a fully developed follicle) (Dong et al., 1996).The intricate interplay of various factors guides the dynamic process of folliculogenesis.

The rise in gonadotropic production at puberty facilitates successive follicle growth and ovulation. Throughout the reproductive years, primordial follicles are continuously activated in a dynamic process that persists until menopause. This activation marks the committing step into folliculogenesis, where activated primordial follicles follow one of two paths: they either progress to ovulation or undergo atresia.

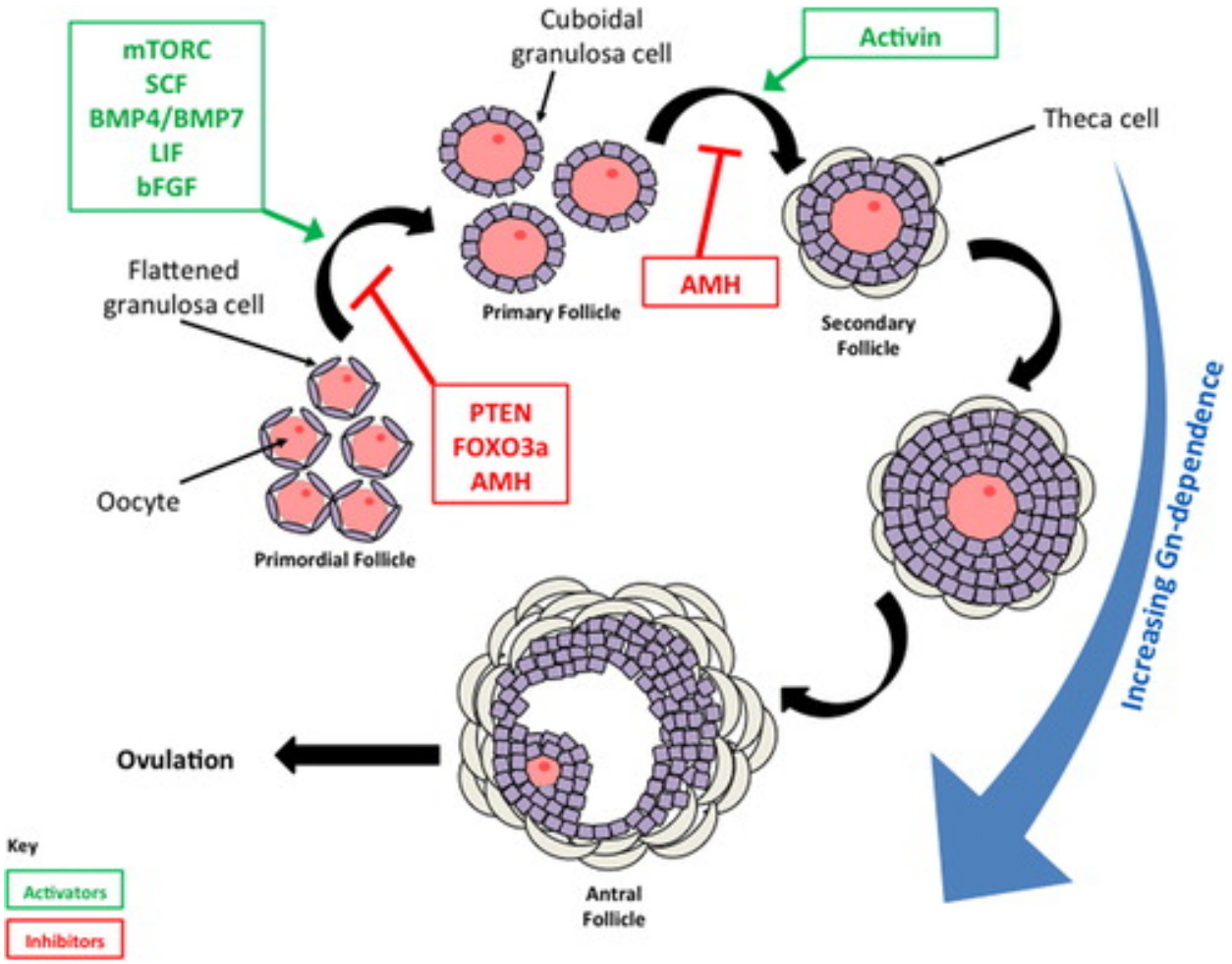

Figure 1.4. A summary of folliculogenesis. The primordial follicle pool develops into primary then secondary follicles independently of gonadotrophins, but the process is closely regulated by activating (green box) and inhibitory (red box) factors. Growth from a secondary follicle to an antral follicle is increasingly gonadotrophin-dependent, with ovulation being entirely gonadotrophin-dependent. Adapted from (Dunlop and Anderson, 2014)

1.4.2 Menstrual Cycle

The first day of vaginal blood flow is considered to be day 1 of the menstrual cycle ending on the first day of the next period. This periodic shedding which is the representation of the exuviating of endometrial tissue and blood vessels lining in the uterus would have aided the implantation of the blastocyst. The duration of the menstrual cycle in humans range from 24 to 32

days with ovulation occurring on day 14 for an average cycle of a 28-day period. Each ovulation is preceded by a period of oestradiol dominance and followed by a period of progesterone dominance. As the oestradiol are secreted by the follicles, the period of the menstrual cycle preceding ovulation is referred to as the follicular phase. Similarly, the period following ovulation is referred to as the luteal phase and progesterone is predominantly secreted by the corpus luteum during this phase. There are major differences between species in both the overall length of the cycle and in the relative duration of its follicular and luteal phases (**Table 1.3**). These differences mask a fundamentally similar organisation, resulting only from minor modifications to the basic pattern.

Some other mammals such as sheep, mouse, dogs, cats and pigs have an estrous cycle instead where the female is typically only receptive to mating during a specific period called estrus or heat, which is marked by hormonal changes and behavioural signs. Heape, in 1900 was the first to use the word estrus to describe the cycle and went further to define the four phases, namely proestrus, estrus, metestrus and diestrus. The proestrus phase corresponds to the follicular phase of the menstrual cycle, which is characterised by the elevation in circulating oestradiol concentration with a minimal surge in prolactin, leading to a gradual increment of FSH release and LH as follicles mature and the uterus enlarges. The peak in FSH concentration with an associated rapid decline in oestradiol levels correlates with ovulation in the estrus phase. The metestrus and diestrus phase are homologous to early and late luteal phases of the reproductive cycle, respectively, with the formation of the corpus luteum high levels of progesterone (Ajayi and Akhigbe, 2020; Heape, 1900).

Table 1.3 Menstrual/Estrous cyclicity in different species (Ajayi and Akhigbe, 2020; Bartlewski et al., 2011; Forde et al., 2011; Soede et al., 2011).

Species	Length of cycle (days)	Follicular phase (days)	Luteal phase (days)
Human	24–32	10–14	12–15
Cow	18–24	4–6	14–18
Sheep	16–17	1–2	14–15
Rat	4–5	2	2–3
Mouse	4-6	1-3	2-4
Pig	18-24	5-7	13-15

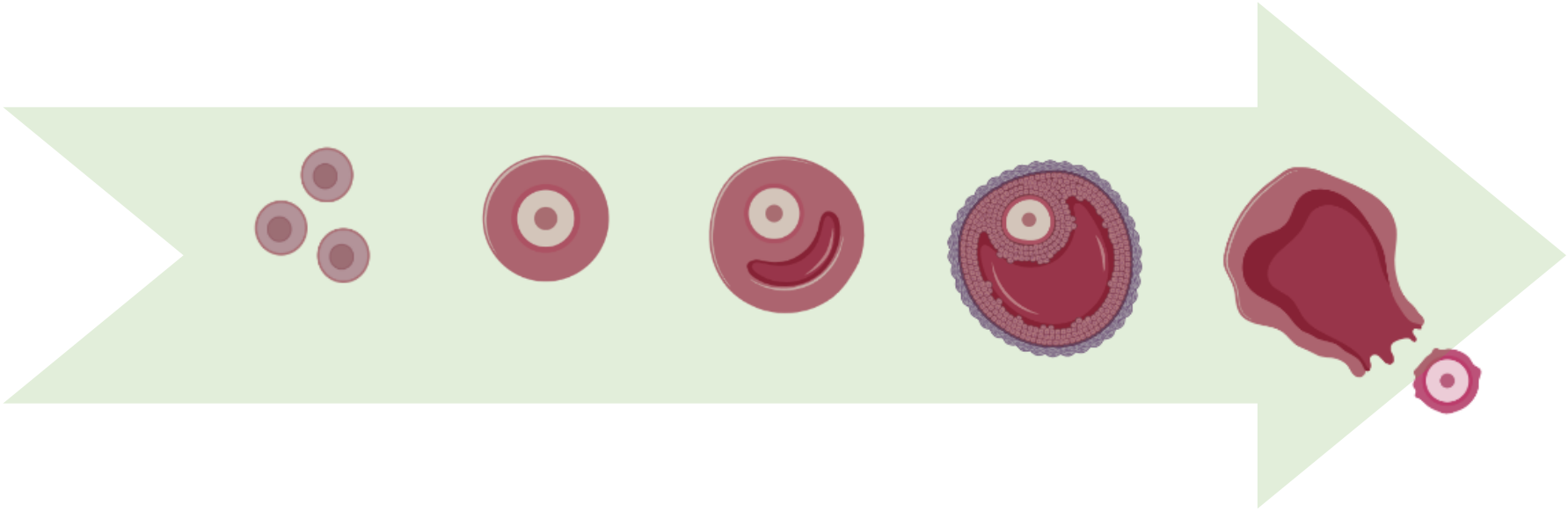

	Primordial follicle	Secondary follicle	Preantral follicle	Antral follicle	Ruptured follicle
	30 µm	F - >200 µm		F - >1-6 mm	
		O – 90 µm		O – 120 µm	
	30 µm	F - >200 µm		F – 200-400 µm	
		O – 40 – 80 µm		O – 80 -120 µm	
	20 µm	F - >200 µm		F – 300-400 µm	
		O – 70 – 75 µm		O – 75 µm	

Figure 1.5 An illustration of the follicle development stages showing the progression of follicles from the primordial stage to the ovulatory stage (Figures not drawn to scale). Also showing the approximate diameter of the follicle (F) and oocyte (O) at each stage for humans, sheep and mouse. Image was created using Biorender

1.4.2.1 Follicular phase

The menstrual cycle's follicular phase initiates from the onset of menstrual flow and extends until ovulation. In monovulatory species, such as humans, the follicular phase begins with the recruitment of a cohort of ovarian follicles under the influence of rising FSH levels. This rise in FSH occurs due to a decline in inhibin A and steroid production by the regressing corpus luteum from the previous cycle (Groome et al., 1996). As these follicles grow, they begin to produce increasing amounts of oestradiol and inhibin B, which in turn exert negative feedback on the pituitary gland, leading to a reduction in FSH levels (Groome et al., 1996). Among the recruited follicles, one becomes more sensitive to FSH due to having more FSH receptors and a better blood supply, allowing it to continue growing even as FSH levels decline. This follicle, known as the dominant follicle, suppresses the growth of other less developed follicles, which undergo atresia, or programmed cell death (Mihm and Evans, 2008). The dominant follicle continues to mature, producing higher levels of oestradiol, which eventually triggers a surge in LH. This LH surge marks the end of the follicular phase and leads to ovulation, where the mature oocyte is released.

In contrast, polyovulatory species, such as sheep and rodents, experience a different dynamic during the follicular phase. These species also recruit multiple follicles in response to rising FSH levels at the beginning of the reproductive cycle. However, unlike monovulatory species, where typically only one follicle achieves dominance, polyovulatory species can support the growth of several follicles simultaneously (Fortune, 1994). As these follicles develop, they produce increasing levels of oestradiol and inhibin, which, similar to monovulatory species, reduce FSH levels through negative feedback mechanisms. Despite the reduction in FSH, several follicles in polyovulatory species are able to maintain their growth due to their enhanced sensitivity to the hormone and the influence of local ovarian factors. These dominant follicles continue to mature

and prepare for ovulation, resulting in the release of multiple oocytes during the ovulatory event. This process increases the likelihood of multiple fertilizations and is an evolutionary strategy that maximizes reproductive success, especially in environments where competition for mates or resources is high (Fortune, 1994).

In both monovulatory and polyovulatory species, the follicular phase is characterized by a delicate balance of hormonal signals and local ovarian factors that regulate the growth and selection of follicles. In monovulatory species, this process ensures the maturation of a single, viable follicle, optimizing the chances of successful reproduction in each cycle. In polyovulatory species, the simultaneous maturation of multiple follicles allows for the release of multiple oocytes, enhancing the potential for multiple offspring. The mechanisms underlying follicular development and dominance are finely tuned to the reproductive strategies of each species, ensuring that the process is well-adapted to their specific reproductive needs and environments.

1.4.2.2 Ovulation

Ovulation typically occurs around 10-12 hours after the peak of LH. To reach the critical concentration of oestradiol necessary for positive feedback, the dominant follicle is usually >15mm in diameter as observed on ultrasound (Cahill et al., 1998). The onset of the LH surge occurs approximately 34 to 36 hours before ovulation, serving as a reliable predictor for timing ovulation. The LH surge induces luteinization of thecal and granulosa cells forming the corpus luteum responsible for progesterone synthesis required for the midcycle FSH surge, and stimulates the resumption of meiosis in the oocyte, leading to the release of the first polar body. Once the follicle is released, it is caught by the fimbriae of the fallopian tubes. The oocyte remains in metaphase II of meiosis II unless fertilization occurs.

1.4.2.3 Luteal phase

This phase typically spans 14 days in most women. Following ovulation, the remaining granulosa cells, not released with the oocyte, undergo enlargement, adopt a vacuolated appearance, and accumulate a yellow pigment called lutein. These luteinized granulosa cells, in conjunction with newly formed theca-lutein cells and surrounding ovarian stroma, constitute what is referred to as the corpus luteum. Functioning as a transient endocrine organ, the corpus luteum primarily secretes progesterone, preparing the oestrogen-primed endometrium for potential implantation of a fertilized ovum. Dissolution of the basal lamina and capillary invasion into the granulosa layer occur in response to angiogenic factors secreted by granulosa and thecal cells. Around eight or nine days post-ovulation, roughly coinciding with the anticipated implantation period, peak vascularization is achieved. This timeframe corresponds to peak serum levels of progesterone and oestradiol. The central cavity of the corpus luteum may accumulate blood, leading to the formation of a hemorrhagic corpus luteum. The corpus luteum's lifespan depends on sustained LH support, with its function diminishing towards the end of the luteal phase unless human chorionic gonadotropin (hCG) is produced by a pregnancy. In the absence of pregnancy, luteolysis of the corpus luteum occurs under the influence of oestradiol and prostaglandins, resulting in the formation of scar tissue known as the corpus albicans.

1.4.2.4 Menstruation

When pregnancy does not occur, the decline in corpus luteum function leads to a reduction in steroid hormone levels i.e., progesterone. This progesterone withdrawal causes increased coiling and constriction of spiral arterioles, ultimately resulting in tissue ischemia as blood flow to the superficial endometrial layers (the spongiosa and compacta) decreases. The endometrium releases prostaglandins, triggering contractions of uterine smooth muscle and the shedding of degraded endometrial tissue (Henzl et al., 1972).

Menstrual fluid consists of desquamated endometrial tissue, red blood cells, inflammatory exudates, and proteolytic enzymes. The typical duration of menstrual flow ranges from four to six days, although the normal span for women varies from as little as two days to as long as eight days. As mentioned earlier, the average menstrual blood loss is around 30 ml, with amounts exceeding 80 ml considered abnormal.

1.5 PREMATURE OVARIAN INSUFFICIENCY (POI)

As mentioned earlier POI is defined as amenorrhea due to a cessation of ovarian function before the age of 40 (Webber et al., 2016). It is a state of female hypergonadotropic hypogonadism and can manifest as primary amenorrhea with onset before menarche or secondary amenorrhea in a woman who previously had regular menstrual cycles. The condition is caused by chromosomal and genetic defects (Turner syndrome, Fragile X syndrome (Fragile X Messenger Ribonucleoprotein 1(FMR1) gene premutation)), autoimmune processes, chemotherapy, radiation, infections and surgery as well as some unidentified (idiopathic) causes (Rudnicka et al., 2018).

The first case report originates from 1942 by Fuller Albright, who termed the condition "primary ovarian insufficiency (Albright et al., 1942). It has also been known as "premature ovarian failure" and "premature menopause" which was too distressing for the patients, stigmatising irreversible failure and indicating a severe condition with complete follicular exhaustion (Komorowska, 2016), hence the new European Society of Human Reproduction and Embryology (ESHRE) guidelines proposed the term "premature ovarian insufficiency" for use in research and clinical practice (Webber et al., 2016).

Previously the prevalence of POI before the age of 40 years was 1%, in the longitudinal cohort study of Coulam and colleagues from long-term follow-up of a birth cohort of 1858 women in Rochester, Minnesota, which aimed at establishing the age-specific incidence of POI (Coulam et al., 1986). However, a recent study which collected data from 13 studies in 10 countries has shown an increased number of women worldwide experience POI, with the prevalence of 3.5% which was similar to 3.7% obtained in a 2019 study (Golezar et al., 2019). The study comprised 1,127,299 women, of whom 25,107 were POI patients over the past 20 years (Li et al., 2023). By subgroup analysis, the prevalence of POI among women with iatrogenic aetiology was 11.2%, followed by autoimmunity (10.5%). Also, the prevalence of POI by region was 11.3% at the highest in North America followed by South America (5.4%); and the prevalence of POI was 5.3% in a developing country, which was higher than 3.1% in a developed country(Li et al., 2023).

1.6 FEMALE FERTILITY PRESERVATION

As previously mentioned, POI resulting from medical treatment, has raised a growing interest in fertility preservation. In detail, these treatments including chemotherapy, radiation and surgery are indicated for conditions such as haematological diseases (leukaemia, Hodgkin's lymphoma, and non-Hodgkin's lymphoma), breast cancer, sarcoma and some pelvic cancers. Now, an important process during cancer treatment is a discussion with the patient about the risk of infertility and reviewing potential options for fertility preservation prior to initiation of the treatment or referring them for counselling (Walker et al., 2022).

Fertility preservation is also an option for women growing older and wanting to postpone childbirth for a variety of social reasons including career demands, because the ability of oocytes to be fertilised and develop to term dramatically decreases in parallel with age (Kuwayama et al.,

2005). In females, fertility rates are reported to increase upon entry into puberty, peaking in the early 20s and declining thereafter, with the decline increasing significantly after the age of 35 years (Kasapoğlu and Seli, 2020). This reproductive aging process is also characterized by a quantitative and qualitative deterioration in ovarian reserve, associated with increases in aneuploidy and higher rates of miscarriage (Esencan et al., 2021; Qiao et al., 2014). All these highlight the importance of female fertility preservation.

In 2020, the ESHRE published the Female Fertility Preservation Guidelines which is the first evidence-based guideline for healthcare professionals guiding the decisions of women prepping to undergo gonadotoxic treatments, transgender men or any woman considering fertility preservation in Europe (Anderson et al., 2020). The options included oocyte cryopreservation, embryo cryopreservation and ovarian tissue cryopreservation which will be described further in this chapter.

Table 1.4. A summary of the advantages and disadvantages of the three main fertility preservation options.

Fertility Preservation	Advantages	Disadvantages
Embryo cryopreservation	• It is a well-established and most reliable technique • There is no risk of reimplanting malignant cells • It presents a higher pregnancy rate	• It can only be offered to post-puberal women with a male partner/donor • It requires time for controlled ovarian stimulation • It does not restore fertility but provides a chance for pregnancy/birth • The procedure takes 2-5 weeks and may cause a delay in cancer treatment • It raises some ethical issues and concerns surrounding embryo freezing • It cannot be offered to women who have hormone-sensitive cancers • The procedure is expensive
Oocyte cryopreservation	• It can be offered to single women and women who don't want to use a sperm donor • There is no risk of reimplanting malignant cells • There are no ethical issues	• It requires time for controlled ovarian stimulation • It does not restore fertility but provides a chance for pregnancy/birth • It can only be offered to post-puberal women • At least 20 vitrified oocytes are required to achieve a live birth • It cannot be offered to women who have hormone-sensitive cancers • Not suitable for Polycystic Ovary Syndrome (PCOS) patients due to high risk of Ovarian Hyperstimulation Syndrome (OHSS)
Ovarian tissue cryopreservation	• It is an option for pre-puberal girls • It does not delay oncologic treatments • It restores ovarian function and allows natural pregnancy after auto-transplantation • There is no need for a partner or sperm donation • It does not require controlled ovarian stimulation	• It is an invasive surgical procedure under general • anaesthesia • The success rates are relatively low • There is a potential risk of cancer recurrence

Beyond cryopreservation, several innovative fertility preservation methods are being explored. These include ovarian suppression (Lambertini et al., 2019a), stem cell technology, *in vitro* follicle growth, and artificial ovaries, each offering unique approaches to safeguarding reproductive potential.

Ovarian suppression using Gonadotropin-Releasing Hormone agonists (GnRHa) is a clinical practice aimed at temporarily halting ovarian function during chemotherapy to protect the ovaries from damage (Lambertini et al., 2019a). This approach is intended to preserve ovarian function and lower the risk of POI. While it shows promise in maintaining ovarian function, its effectiveness as a fertility preservation strategy is still under investigation and does not replace established methods such as embryo or oocyte cryopreservation. For example, a meta-analysis found that 93% of women treated with GnRHa maintained ovarian function, compared to 48% of those who did not receive this treatment (Clowse et al., 2009; Lambertini et al., 2019b). Despite these encouraging results, the evidence regarding its role in fertility preservation is still evolving, with ongoing trials working to better understand its mechanisms and efficacy. While GnRHa is recommended to protect ovarian function during chemotherapy, its effectiveness as a fertility preservation method is still considered insufficient compared to cryopreservation techniques (Oktay et al., 2018).

Stem cell technology presents a groundbreaking approach by potentially generating gametes from pluripotent stem cells. This method could be transformative for individuals who have lost their natural gametes due to medical treatments or diseases. Although recent advancements have shown the possibility of creating primordial germ cells from stem cells, significant research is needed to ensure safety and efficacy before this technology can be applied clinically (Vermeulen et al., 2019).

In vitro follicle growth is an experimental technique that involves maturing ovarian follicles outside the body (Vitale and Dolmans, 2024). This method holds potential for women who cannot undergo traditional fertility preservation procedures. The success of this technique relies on creating a sophisticated culture environment that supports follicle growth and maturation to a stage where fertilization is possible. Current research is focused on optimizing these culture conditions to improve the viability of this approach for clinical use (Vitale and Dolmans, 2024).

Artificial ovaries involve creating bioengineered structures capable of supporting follicle growth and development (Cho et al., 2019). These structures can be transplanted back into the body to restore endocrine function and fertility. While animal studies have shown successful follicular development and pregnancies, challenges remain in improving follicular recovery rates, optimizing scaffold designs, and ensuring genetic safety before this method can be widely applied in humans (Cho et al., 2019).

Together, these innovative approaches represent the future of fertility preservation, offering hope for individuals facing infertility due to medical treatments or other factors. Each method is at a different stage of development, with ongoing research aimed at overcoming current limitations and ensuring their safe and effective application in clinical settings.

1.7 CRYOPRESERVATION

Cryopreservation is a procedure that involves cooling cells, tissues, organs and other biological structures to low temperatures, pausing the general activity including biochemical and enzymatic reactions to preserve its biological integrity (Mandawala et al., 2016). These biological structures are then stored in liquid nitrogen at -196˚C long term where its physiological processes

remain halted and can be stored for different time ranges depending on the cell, tissue or organ (Pegg, 2007).

In assisted reproductive technology (ART), cryopreservation has improved the efficiency of treatment by enabling the storage of sperm, oocytes , embryos, and ovarian tissue for periods up to several years (Aflatoonian et al., 2013; Dinh et al., 2022; Szell et al., 2013). The technique has contributed to the reduction or abolishment of the risk of multiple pregnancies due to the transfer of multiple embryos to achieve a pregnancy (Griesinger et al., 2011; Health, 2006). It also reduces the number of ovarian stimulation cycles (Lainas et al., 2009), allows delaying the embryo transfer during an *in vitro* fertilisation (IVF) cycle to prevent ovarian hyperstimulation syndrome and optimizing endometrial preparation (Levi Setti et al., 2013). Finally, embryo, oocyte and ovarian cryopreservation preserves the reproductive capacity in women who are at risk of infertility because of gonadotoxic medical treatments or who wish to postpone their reproductive plans (Argyle et al., 2016).

Spermatozoa became the first cell recorded in history to be successfully cryopreserved (Polge et al., 1949), posing some advantages for the technique in research and clinical applications. Today, aside the spermatozoa, and the cryopreservation of oocytes, embryos and ovarian tissue, cryopreservation is applied in regenerative medicine, transplantation medicine and conservation of animal and plant species.

The major steps in cryopreservation are (1): the incubation of cryoprotectants (CPAs) with cells or tissues before cooling; (2) cooling of the cells or tissues to a low temperature and its storage; (3) warming of the cells or tissues; and (4) removal of CPAs from the cells or tissues after thawing (Gao et al., 2016).

1.7.1 Cryoprotectants

Freezing and thawing of cells and tissue causes osmotic shock and physical damage by the formation of both intra- and extracellular ice crystals leading to cell death, hence the use of cryoprotective agents or CPA (Vincent and Johnson, 1992; Whaley et al., 2021). The successful cryopreservation of cells and tissues has been gradually increasing in recent years with the use of CPAs. These CPAs alter the freezing process by manipulating the rate of ice crystal formation and the transport of water in and out of the cell (osmosis). These CPAs therefore control the risk of shock effects and osmotic damage in the cell as far as possible by either penetrating the cell membrane or not (Arav, 2014).

The CPAs can therefore be divided into two categories which is the penetrating/permeating and non-penetrating/ non-permeating. Permeating cryoprotectants are miscible in water and work by penetrating the cell membrane forming hydrogen bonds with intracellular water molecules and lowering the ice nucleation temperature of the resulting mixture thereby preventing ice crystallization (Pereira and Marques, 2008). They also help to stabilize the cell membranes and protect the cytoskeleton. Such CPAs include dimethyl sulfoxide (DMSO), glycerol, ethylene glycol and propylene glycol (1,2-propanediol; PROH). Conversely, non-permeating cryoprotectants are unable to pass through the cell membrane, remain extracellular and act by increasing the osmolarity of the medium outside the cell and causing the cell to dehydrate by the drawing of water from the intracellular space (inside the cell) into the surrounding medium (**Table 1.5)** (Karlsson, 2002). These CPAs are used together with a permeating cryoprotectant to increase the net concentration of the permeating cryoprotectant inside the cell and to prevent ice-crystal formation (Ali and Shelton, 1993; Yong et al., 2020). Some thawing protocols commonly use a high concentration of non-permeating cryoprotectants such as sucrose (Jain and Paulson, 2006).

Other commonly used non-permeating CPAs include disaccharides, such as galactose and trehalose, and compounds with higher molecular weight such as polyvinyl pyrrolidone, hydroxyethyl starch, 2-methyl 2,4-pentanediol, polyethylene glycol and ficoll (Amorim et al., 2011; Yong et al., 2020). **Table 1.6** below shows a few of these cryoprotectants and the area of cryopreservation they are applied. The characteristics of a good cryoprotectant is low toxicity at high concentrations, high solubility, low molecular weight, lower freezing point and ability to protect cell from injury.

Table 1.5 Comparison of penetrating and non-penetrating cryoprotectants

Permeating Cryoprotectant	Non-permeating Cryoprotectant
• Penetrate the cell membrane • Small molecules • Form hydrogen bond with water molecules to prevent ice crystal formation • Used at low concentration in water and they lower the freezing temperature	• Do not penetrate the cell membrane • Macromolecules • Dehydrate the intracellular space of the cell by drawing out water • Mostly used in combination with a permeating cryoprotectant

Table 1.6 Commonly used cryoprotective agents and what they have been used to cryopreserve successfully.

Membrane permeability	CPA	Applied in cryopreservation
Permeable	Dimethyl sulfoxide (DMSO	Bone marrow Dental pulp Embryo (combined with EG or propylene glycol) Embryonic stem cells (alone or combined with EG) Microorganisms Oocyte (combined with EG) Testicular cell/tissue
	Glycerol	Microorganisms Red blood cell Spermatozoa
	Ethylene glycol (EG)	Amniotic fluid Dental pulp
	Propylene glycol (1,2-propanediol)	Embryo Hepatocytes Oocytes
Non-permeable	Trehalose	Embryo Ovarian tissue (combined with vitrification) Red blood cell Spermatozoa Stem cells (combined with propylene glycol)

1.7.2 Techniques in cryopreservation

Currently, cryopreservation for animal germplasm can be achieved by two main cryopreservation methods, i.e., slow freezing and vitrification (**Table 1.7**) (Mandawala et al., 2016). Slow freezing involves a steady cooling of samples at a rate of 0.5-2˚C/min followed by

rapid thawing, whereas vitrification avoids the formation of ice crystals by rapid cooling and thawing (Mandawala et al., 2016).

In slow freezing, the temperature of the freezer is slowly lowered by an automatic controlled freezing programme either computer controlled or manually using controlled-rate freezing devices, reducing the formation of ice crystals. The concentration of cryoprotectant in the medium is relatively low and increases as the temperature is lowered and water freezes, leading to further dehydration of the cell by osmosis. The type of cell determines the optimum cooling rate due to variances in their capacities to transport water across the plasma membrane. (Shen et al., 2003). This ensures that enough water is lost and replaced by CPA and the cells are not exposed to adverse conditions for too long caused by too fast or too slow freezing rates, respectively.

Vitrification on the other hand seeks to avoid the formation of ice crystals using higher concentrations of cryoprotectants and rapid cooling. Here, water becomes extremely viscous with properties of a solid instead of becoming crystalline during the cooling process (Pegg, 2002). The rapidity of the cooling process and the high concentration of cryoprotectants mean that the water molecules are unable to form themselves into the lattice structure of ice crystals, thus avoiding damage to the cells (Whaley et al., 2021). The cell is placed in a hyper-osmotic medium, which results in very fast dehydration, and is then cooled rapidly by placing it onto a metal block in liquid nitrogen. In order to obtain the ultra-rapid cooling rates required, very small volumes are used, typically around 1µl. The whole procedure takes only a few minutes, and no mechanized equipment is involved, making it an attractive option for the laboratory.

Although both methods are effective, they each have ultimate advantages and shortcomings. For slow freezing, the major disadvantage would be the requirement of specialised equipment and the possible damage to cells by the formation of intracellular ice crystals. Whereas

osmotic damage due to elevated concentration of cryoprotectants and small sample volume are the major disadvantages of vitrification (Hunt, 2011).

Table 1.7 Comparison between the slow-freezing and vitrification methods.

Feature	Slow freezing	Vitrification
Duration	The procedure lasts 3+ hours	Takes less than 10 min (fast)
Equipment	Requires both a computer and a freezing machine	Does not require any specialised machine
Cost	Expensive	Inexpensive
CPA concentration	Low concentration	High concentration
Formation of ice crystal	High risk of occurrence	Low or no risk of occurrence
CPA toxicity	Lower risk	Higher risk
Status of system	Closed system only	Opened or closed system

There is another technique in cryopreservation which is also characterized by exceptionally fast cooling rates to prevent ice crystal formation and has found valuable applications in fertility preservation. The technique known as ultrarapid freezing differs from vitrification in the approach and the state in which the material is preserved as vitrification involves the creation of a glass-like, amorphous solid without the formation of ice crystals. The technique does not employ the use of programmable machines and requires a lower concentration of CPA than vitrification (AbdelHafez et al., 2010). One notable example is its use in the cryopreservation of sperm, where the rapid

cooling prevents the formation of ice crystals that could damage the delicate structure of sperm cells (Schuster et al., 2003). Additionally, ultrarapid freezing has been applied to preserve embryos (AbdelHafez et al., 2010). By swiftly reducing the temperature of embryos, ultrarapid freezing minimizes the risk of ice crystal formation, preserving the viability of these early-stage embryos. The technique has also proven effective in the cryopreservation of oocytes, a vital aspect of fertility preservation for women undergoing medical treatments that may compromise their reproductive capacity.

1.7.3 Application of cryopreservation in female fertility preservation

1.7.3.1 Embryo cryopreservation

In 1996, the first case of embryo cryopreservation for fertility preservation was reported where a woman diagnosed with breast cancer went through conventional IVF prior to treatment by chemotherapy (Jang et al., 2017). Presently, the indications of embryo cryopreservation have advanced alongside the technique and its success rate. Most routinely, surplus embryos from IVF cycles are cryopreserved to maximize the pregnancy potential of each oocyte stimulation.

Despite the higher rates of success, the technique is feasible only for post pubertal women with a partner (or using donor sperm) (Donnez and Dolmans, 2015a). Another limitation is the ethical and legal issues that need to be considered, for example in some countries embryo cryopreservation is forbidden by law both in ART and fertility preservation, and embryo cryopreservation is performed notwithstanding the current regulations in very specific cases (Brezina and Zhao, 2012). Moreover, cryopreserved embryos belong to both parents, and this aspect becomes problematic to manage after many years of cryopreservation, as relationships can be dissolved. Another limitation of the procedure is the inability to restore fertility in women, having no effects on cycle restoration or resuming ovulation, despite providing the possibility of

pregnancy. Finally, the procedure is not feasible in patients requiring immediate chemotherapy, due to the 10-15 days of controlled ovarian stimulation (COS) program to induce multiple follicular growth and oocytes retrieval (Donnez et al., 2010).

Cryopreservation of embryos can be done at different stages of development, either the zygote stage, cleavage stage or blastocyst stage usually determined by the clinic and/or hospital policy or the indications (reason) for cryopreservation. Cryopreserving embryos at the zygote stage allows a maximum number of embryos to be stored; however, this does not reflect the quality or ability of the embryos for further development. Cryopreservation at the blastocyst stage on the other hand has been demonstrated to have the best survival and implantation rates with comparable success rates to the transfer of fresh blastocysts (Korkidakis et al., 2021; Pavone et al., 2011; Sunkara et al., 2010).

Embryo cryopreservation has been achieved with both cryopreservation methods, however, vitrification has shown higher cryosurvival rates and proved to be an effective method for cryopreserving embryos at all developmental stages (Li et al., 2014; Rienzi et al., 2016).

1.7.3.2 Oocyte cryopreservation

As mentioned earlier, oocyte cryopreservation is a fertility preservation option for women at risk of POI, particularly patients who are going to be exposed to gonadotoxic therapies or radiation. However, the technique is also employed when couples do not consent to creating excess embryos for ethical or religious reasons and the male partner is unable to provide semen on the day of oocyte collection in oocyte donation programmes during IVF cycles (Cobo et al., 2011; Practice Committee of the American Society for Reproductive Medicine. Electronic address, 2021)) or 'social egg freezing' in anticipation of age-related fertility decline which has become more widely accepted (Argyle et al., 2016; Stoop et al., 2014).

The first reported pregnancy from cryopreserved oocytes was 1986 in Australia using DMSO as the CPA (Chen, 1986). Slow freezing was the method of choice during that time up until recently when vitrification became the more favoured approach to oocyte cryopreservation as slow freezing is not very effective resulting in low pregnancy rates and higher oocyte damage (Argyle et al., 2016; Iussig et al., 2019). The first live birth following oocyte vitrification was reported in 1999 where a healthy baby girl was born to a 47-year-old woman following vitrification of mature oocytes (Kuleshova et al., 1999). Here, the oocytes were vitrified in a combination of ethylene glycol and sucrose in open pulled straws. Indeed, slow freezing oocytes has generated multiple births, but vitrification has reported improved post-thaw survival rates preserving oocyte developmental ability and internal structures more efficiently (Antinori et al., 2007; Cobo et al., 2008; Smith et al., 2010).

In 2006, a meta-analysis examining oocyte cryopreservation suggested that the use of vitrification could enhance pregnancy rates, although the number of recorded pregnancies at that time was limited (Oktay et al., 2006). Subsequent comparisons of IVF outcomes between slow-frozen and vitrified oocytes demonstrated superior survival, fertilisation, and pregnancy rates with vitrification (Cao et al., 2009; Fadini et al., 2009; Smith et al., 2010). Notably, Fadini et al. (2009) reported significantly higher pregnancy rates (18.2% versus 7.6%). Growing evidence supports the efficacy of IVF with vitrified oocytes, suggesting comparable outcomes to IVF using fresh oocytes, with oocyte survival rates exceeding 84% (Nagy et al., 2009) (Almodin et al., 2010; Rienzi et al., 2012; Ubaldi et al., 2010). Compared to 1999, when nearly 100 cryopreserved oocytes were needed to achieve a single pregnancy (Porcu, 1999), advancements have reduced this number to just 20 vitrified oocytes. However, this number is significantly influenced by the age of the oocyte (Cobo et al., 2016; Cobo et al., 2015). Randomized controlled trials have reported clinical

pregnancy rates per transfer ranging from 35.5% to 65.2% (Cobo et al., 2008; Parmegiani et al., 2011; Rienzi et al., 2010). A recent meta-analysis of five studies found no significant differences in fertilization rates, embryo cleavage, high-quality embryos, and ongoing pregnancy between vitrification and fresh oocyte groups (Cobo and Diaz, 2011).

The procedure of oocyte cryopreservation is typically carried out with mature oocytes (MII stage oocytes). The procedure begins with a 10 – 14 days hormone treatment for ovarian stimulation, hence patients requiring an immediate start to cancer treatments may not have enough time for the cycle (Cakmak and Rosen, 2013). Additionally, the drugs given to stimulate the ovaries increase the levels of oestrogen which may encourage some cancers to grow, such as breast cancer (Momenimovahed et al., 2019; Pfeifer et al., 2016).

Oocytes at MII stage are not only difficult to equilibrate with CPA, but they are also quite sensitive to physical/chemical injury due to their vulnerable spindle apparatus (Iussig et al., 2019; Stachecki and Cohen, 2004). Hence, the major concerns for oocyte cryopreservation is the stability of microtubules and microfilaments as well as the hardening of the zona pellucida and release of cortical granules which provides a physiological block to polyspermic fertilization hence low fertilisation rates (Gook et al., 1995; Zenzes et al., 2001). However, studies showed the ability of human, bovine and mouse oocytes to retain their chromosomal integrity after cryopreservation (Stachecki et al., 2004) and the introduction of intracytoplasmic sperm injection (ICSI) rectified the fertilisation issues reported in the first successful childbirth after vitrification (Kuleshova et al., 1999; Porcu et al., 1997).

As previously mentioned, vitrification has gradually become the method of choice after researchers extensively revisited and modified the procedures to improve laboratory and clinical results mainly with the help of animal research. The current and most used protocol for oocyte

vitrification consists of a two-step procedure involving the stepwise addition of CPAs in cryomedia, a first equilibration phase (5-15 min) in a solution containing 7.5% v/v ethylene glycol and 7.5% v/v DMSO and incubation in vitrification solution with 15% v/v ethylene glycol and 15% v/v DMSO, plus 0.5 mol/L sucrose (up to 1 min). The oocyte is then transferred onto thin plastic filmstrip attached to a holder and protected by a tubular cap and finally plunged in liquid nitrogen at −196°C, where it is stored until use (Kuwayama, 2007).

Compared to slow freezing, oocyte vitrification is reported to yield a higher survival rate (Rienzi et al., 2017) despite the changes made to improve the procedure. Briefly, DMSO which was used in the first instances was subsequently replaced with PROH (1.5 mol/L) and sucrose (0.1 mol/L) as CPAs, using a protocol similar to that applied routinely in embryo cryopreservation (Gook et al., 1993; Kuwayama, 2007). As the procedure presented limited success with only 2.3 implantations per 100 thawed oocytes (Gook and Edgar, 2007), new suggestions found that doubling the sucrose concentration in the freezing solution (from 0.1 to 0.2 mol/L) resulted in a statistically significant increase in oocyte survival (34% and 60%, respectively). Moreover, a longer exposure (10.5-15 min vs 0.5-10 min) to freezing solutions before lowering the temperature further improved the survival rate, fertilization rate and cleavage rates (Fabbri et al., 2001; Gook and Edgar, 2007)).

Also, the randomized controlled trials supporting similar success rates between IVF with vitrified/warmed oocytes and fresh oocytes primarily used open vitrification systems (Cobo et al., 2008; Parmegiani et al., 2011; Rienzi et al., 2010). Concerns about the sterility of open systems led to investigations into liquid nitrogen sterilization and storage in vapor phase liquid nitrogen to reduce contamination (Parmegiani et al., 2010). Closed vitrification systems were introduced to address contamination concerns, demonstrating bacterial-free results. However, debates arise over

the efficiency of closed systems due to decreased cooling rates, with studies suggesting potential drawbacks such as less effective preservation of oocyte ultrastructure and lower fertilization, cleavage, and clinical pregnancy rates (Vajta et al., 2015). Despite these concerns, other studies advocate for closed vitrification, emphasizing excellent clinical outcomes and an aseptic environment (Smith et al., 2010; Stoop et al., 2012). The warming rate is highlighted as crucial for oocyte survival in vitrification protocols, and optimal outcomes are more likely when vitrification and warming are conducted using matched protocols within the same clinic (Brison et al., 2012).

1.7.3.3 Ovarian cryopreservation

Cryopreservation of oocytes and embryos have now become well-established techniques for fertility preservation in many centres if not all (Practice Committee of American Society for Reproductive, 2019). On the other hand, ovarian tissue cryopreservation (OTC) is not necessarily a new technique but newly introduced clinically. Its use has been increasingly employed to treat POI and restore fertility in young cancer patients (Kolibianaki et al., 2020) with ovarian activity restored in over 95% of reimplanted thawed tissue (Donnez and Dolmans, 2017; Gellert et al., 2018). OTC and transplantation (TP) has also resulted in over 130 successful live births globally as of June 2017 and is now accepted as a successful fertility preservation option for women (Dolmans et al., 2020; Donnez and Dolmans, 2017; Kristensen and Andersen, 2018).

OTC, which permits the sectioning of the ovarian cortex for cryopreservation, was first employed clinically in Europe and the United States in the late 1990s, but the first live birth after OTC & TP was reported in 2004 (Donnez et al., 2004). It has shown a successful pregnancy rate of 27.5% to 31% in humans by 2016 (Jensen et al., 2015; Van der Ven et al., 2016b) with other centres reporting a 50% and a live birth rate of 41% in a series of 60 patients in 2020 (Shapira et al., 2020). This strategy of fertility preservation benefits girls and young women requiring

gonadotoxic treatments, patients unable to undergo ovarian stimulation for oocyte cryopreservation and is the only option for prepubertal girls. OTC & TP does not only preserve the follicular reserve but with subsequent TP, it restores ovarian endocrine function (Donnez and Dolmans, 2015b). Additionally, the technique is rapid and does not require consideration of the menstrual cycle while preserving a large number of follicles. In 2013, the American Society for Reproductive Medicine (ASRM) removed the "experimental" label associated with ovarian cryopreservation (Practice Committees of the American Society for Reproductive and the Society for Assisted Reproductive, 2013).

OTC has demonstrated a consistent rise in endocrine function recovery and live birth rates after re-implantation. However, it is observed that the proportion of healthy primary follicles in frozen tissue tends to decrease compared to fresh tissue generally (Bahroudi et al., 2022). Deansely et al. was the first to perform OTC successfully in the 1950s using rat as the model (Deanesly, 1954) and has since been studied in animals for over 65 years. Pieces of the rat ovaries were soaked in glycerol-saline, frozen to –79°C, thawed and implanted subcutaneously in different ovariectomized adult females. Even though part of the implanted tissue decayed, some of the follicles and oocytes, recovered rapidly and formed functional grafts. As sheep ovaries are similar in characteristics to that of humans, Newton and his colleagues in 1996 performed successful TPs in sheep (Newton et al., 1996) and the first human ovarian TP with cryopreserved ovarian tissue was later performed by Dr. Oktay in 1999 (Oktay and Karlikaya, 2000). Since then, researchers have explored freezing ovarian tissue with a variety of solutions and three common techniques in cryopreservation; vitrification, slow-freezing, and ultrarapid freezing (Abedelahi et al., 2013). The three mentioned techniques have produced different results in research conducted in recent years; therefore, researchers are seeking to improve these techniques to obtain better results. For example,

in one investigation involving foetal ovaries, ultrarapid freezing displayed a notable central necrosis rate of 14%, while 85% of somatic cells and 75% of oocytes survived the process (Zhang et al., 1995). Meanwhile, a study by Locatelli and Calais using slow-freezing in immature ewes showcased similar reductions in the proportion of primary follicles and an increase in growing follicles during both fresh and frozen ovarian tissue cultures (Locatelli et al., 2019). Another facet of the comparison involves the cryopreservation methods—vitrification closed, vitrification open, and slow freezing. Post-thawing/warming, histomorphological analysis showed no disparity between slow freezing and vitrification open ovaries, although vitrification open exhibited higher apoptosis levels after ovarian culture. Furthermore, the expression of follicular AMH and BMP15 genes associated with folliculogenesis was diminished in ovaries subjected to vitrification open (Terren et al., 2019). Again, research has shown that some modifications, such as adding antioxidants and synthetic polymers to the vitrification solutions to reduce oxidative stress, can inhibit apoptosis and improve follicles morphology (Bahroudi et al., 2022).

Even though OTC is a clinically adapted treatment leading to successful pregnancy and birth (Donnez et al., 2004; Donnez et al., 2013), it provides only a limited oocyte reserve and therefore provide a relatively brief fertile window before complete depletion of oocytes contained within the graft (Jensen et al., 2015; Maltaris et al., 2007). This shortened lifespan leads to a 60% loss of primordial follicles due to ischemia prior to revascularisation rather than cryodamage (Maltaris et al., 2007; Nisolle et al., 2000; Zhou et al., 2016).

In contrast, whole ovary cryopreservation (WOCP) for later autotransplantation, presents a promising approach suggested to address the limitations presented by cryopreservation and autografting of ovarian-cortex cryopreservation (Donnez et al., 2010). Thus, it allows the preservation of the entire ovary's follicle reserve, complete and immediate revascularization and

the potential for full restoration of ovarian function with the avoidance of significant loss of follicles (Donnez et al., 2010). Until recently WOCP has been indicated to have detrimental effects on ovarian follicle population, which is attributed to an acute loss of vascular patency in sheep (Campbell et al., 2014). However, utilizing optimized cryopreservation and post-operative anti-coagulant regimes has led to the success of natural fertility and even live birth in sheep (Campbell et al., 2014; Torre et al., 2016a). These results are indeed positive and its implications are more relevant as the physiology of sheep ovaries has been found to be similar to that of human (Gosden et al., 1994).

The key challenges associated with cryopreserving and transplanting a whole ovary are (A) the surgical expertise needed for the retrieval of the entire ovary along with its vascular pedicle, (B) the cryopreservation method applied for freezing the complete organ, and (C) the successful implementation of functional vascular reconnection upon thawing. These challenges have gradually been explored in rodents and sheep leading to the improvement of the technique and full restoration of ovarian function, fertility and successful birth in sheep (Campbell et al., 2014). In this study, post-thaw interventions for slow-frozen whole ovaries were explored. The authors observed that the addition of survival factors did not confer benefits. However, administering aspirin before surgery led to increased rates of ovarian function resumption. Despite this improvement, the follicle survival rate within grafts with restored function was only 20%. The subsequent part of the study explored combining preoperative aspirin with postoperative anticoagulation regimens, achieving a remarkable 100% restoration of ovarian function in 14 cases. These cases exhibited high rates of natural fertility, with a 64% pregnancy rate and a 29% live birth rate. Upon degrafting 11 to 23 months later, histological examination revealed an impressive 60–70% follicle survival rate. The significant improvement in success rates was

attributed to an optimal slow-freezing protocol for ovine ovaries (DMSO 1.5 M perfused for 60 min) and the use of anti-thrombotic agents to prevent postoperative clotting. Torre et al. (2014) further supported this success by transplanting both vitrified and slow-frozen whole ovaries to sheep without anti-thrombotic therapy, although resulting follicle survival rates remained poor in both groups at degrafting three years later (<99%).

Prior to this, Imhof et al. achieved the first live birth after transplanting a cryopreserved whole ovary in sheep (large animal model), but observed low follicle survival rates over time, indicating the need for improvement (Imhof et al., 2006). Different surgical techniques, including alternative vascular pedicle approaches, were explored, but significant follicle loss was observed, even with fresh ovaries subjected to perfusion (Onions et al., 2013). Follow-up studies have investigated the impact of cryopreservation and perfusion on vascular patency, follicle survival, and ovarian function (Onions et al., 2013).

While some success has been achieved with optimal slow-freezing protocols and anti-thrombotic agents, challenges remain, including the need for specific anti-thrombotic strategies. Combining aspirin with postoperative anticoagulation regimens has shown promise in improving ovarian function, leading to increased rates of natural fertility. However, before clinical implementation, further research is required to determine ideal cryoprotectant perfusion times, optimize anticoagulant treatments, and ensure the health of offspring resulting from the procedure. Overall, progress has been made, but refinements are needed for WOCP and transplantation to become viable clinical practice. However, the technique being successful on its own provides an option for a higher follicle reserve and therefore could be combined with oocyte isolation, *in vitro* maturation (IVM), IVF and ICSI as an alternative to transplantation.

Until now, only a few research teams have tackled the intricate task of vascular transplantation involving fresh whole ovaries in humans, with no attempts to transplant a cryopreserved whole ovary (Hossay et al., 2020; Mhatre et al., 2005; Silber et al., 2008). The latest study on fresh whole ovary transplantation dates back to 2008, demonstrating the technical feasibility of orthotopic vascular transplantation and resulting in a healthy live birth (Silber et al., 2008). Cryopreserving whole human ovaries has been undertaken by limited teams. Martinez-Madrid et al. (2007) developed a successful slow-freezing protocol, noting a decrease in viable follicles after thawing but without apoptosis or structural alterations (Martinez-Madrid et al., 2007). Another team proposed a different slow-freezing protocol based on cow ovaries, achieving over 90% morphologically normal follicles after thawing (Westphal et al., 2017). Patrizio et al. (2008) successfully cryopreserved 11 premenopausal human ovaries using directional freezing, showing no histological differences compared to fresh control ovaries (Patrizio et al., 2008). Due to the challenge of obtaining premenopausal human ovaries, Milenkovic et al. suggested using postmenopausal ovaries for developing cryopreservation protocols, offering an opportunity to establish optimal procedures applicable to premenopausal ovaries (Milenkovic et al., 2011). Developing an effective freezing/thawing protocol for the human ovary is crucial for future transplantation experiments by microsurgery experts.

1.8 RATIONALE AND HYPOTHESIS

1.8.1 Rationale

Developing a successful cryopreservation protocol for large organs, such as whole ovaries, presents substantial challenges due to the increasing biological complexity involved (Woods et al.,

2004). Key issues include addressing heat and mass transfer, ensuring uniform distribution of cryoprotectants, and preventing ice formation, all of which are essential for maintaining tissue integrity (Pegg, 2007). Studies on porcine and sheep ovaries highlight the protective role of cryoprotectants in maintaining ultrastructural integrity and preventing disruption of ovarian architecture (Imhof et al., 2004; Wallin et al., 2009). Achieving optimal cryoprotectant distribution, especially within blood vessels, is crucial to prevent irreversible endothelial cell disruption and thrombotic events after transplantation. However, attaining ideal distribution without inducing toxicity remains challenging due to the size and complexity of the organ. While *in vivo* perfusion attempts have been explored, *in vitro* perfusion is considered more effective for ensuring cryoprotectant penetration (Isachenko et al., 2014). Nevertheless, both perfusion and cryopreservation techniques can adversely affect ovarian vasculature, particularly the microvasculature in the ovarian medulla, contributing to poor follicle outcomes in animal studies despite maintaining vascular patency at the anastomotic site (Onions et al., 2013). These challenges highlight the intricate nature of cryopreserving and transplanting whole ovaries, requiring careful consideration of various factors to optimize success.

Slow freezing has emerged as a successful technique for cryopreserving whole ovaries, with documented live births resulting from slow-frozen ovaries. Studies indicate that slow freezing can achieve favourable post-thaw viability and functional outcomes, especially in large animal models like sheep and cows. Significantly, all reported live births following whole ovary cryopreservation and transplantation have been associated with the slow-freezing procedure (Campbell et al., 2014; Torre et al., 2016a).

Autotransplantation of cryopreserved ovarian tissue cortex has demonstrated a birth rate of approximately 35%, as evidenced by Van der Ven et al. (Van der Ven et al., 2016a). The number

of pregnancies and live births has notably surpassed 200 in 2020, according to Dolmans et al. (Dolmans et al., 2020) and Khattak et al. (Khattak et al., 2022). In the context of human OTC and TP, slow freezing remains the preferred technique based on favourable live birth outcomes. Studies have scrutinized the drawbacks of slow freezing, including ice crystal formation leading to higher DNA fragmentation levels (Xiao et al., 2013), gene under-expression (Labrune et al., 2020), and metabolic and secretory issues (Einenkel et al., 2022). It is also suggested that slow-freezing OTC in humans is associated with significant telomere shortening, altered senescence markers, and mitochondrial structural changes (Kim et al., 2021).

Finally, the study by Campbell et al. (2014) demonstrated successful restoration of ovarian function and fertility in sheep following WOCP and autotransplantation. However, several key observations warrant further investigation. Notably, ovulation resumed approximately 21 days post-transplantation, suggesting that antral follicles present at the time of the procedure were unable to ovulate immediately. This delay indicates potential compromise of these follicles during the cryopreservation and transplantation process. Furthermore, while high ovulation and fertilization rates were achieved, the relatively low live birth rate points to possible issues with oocyte quality or developmental competence. These findings highlight critical knowledge gaps in our understanding of how WOCP affects follicular and oocyte health, particularly in antral follicles.

1.8.2 Hypothesis

Given these potential complications, I hypothesise that the slow freezing technique used by Campbell et al. (2014), while capable of restoring ovarian function and fertility in sheep, introduces subtle yet significant cellular and molecular changes in ovarian tissue. These alterations may particularly affect antral follicles, compromising their immediate viability post-transplantation and potentially impacting oocyte developmental competence. Specifically, I

propose that oocytes from antral follicles subjected to WOCP may exhibit increased DNA fragmentation, elevated apoptosis rates, and impaired maturation capacity.

It is important to determine whether growing, antral follicles are affected by cryopreservation because these follicles contain oocytes that are already advanced towards developmental competence and represent the most immediate potential source of viable gametes following tissue retrieval. If preserved successfully, they can be matured and fertilised *in vitro*, offering patients a direct pathway to achieving pregnancy without the need for lengthy follicle growth periods. By contrast, primordial and early pre-antral follicles may tolerate cryopreservation better, but would require prolonged development to reach maturity, making them less immediately useful clinically. Thus, understanding the vulnerability of antral follicles to cryoinjury is essential for assessing the true reproductive potential of cryopreserved ovarian tissue.

This question is especially important in clinical contexts where ovarian tissue cannot be reimplanted after cryopreservation, such as in patients with haematological cancers or other conditions with a high risk of reintroducing malignant cells through transplantation. In these situations, the only safe route to using the preserved tissue is through IVM of oocytes from antral follicles. If these follicles are damaged by cryopreservation, the utility of WOCP in such patients would be severely limited. Therefore, assessing the survival, quality, and developmental competence of antral follicle oocytes after WOCP is critical both for optimising protocols and for determining the genuine clinical applicability of this fertility preservation approach.

Furthermore, the observed discrepancy between high ovulation and fertilisation rates and relatively low live birth rates suggests a potential compromise in the molecular makeup of the ovarian tissue and oocyte quality. This may involve subtle alterations in gene expression,

epigenetic modifications, or other molecular mechanisms that ultimately impact embryo development and pregnancy outcomes.

1.9 MAIN OBJECTIVE

The main objective of this study was to investigate the effects of the WOCP and thawing protocol, as described by Campbell et al. (2014), on ovine ovarian tissue, focusing particularly on oocyte viability, oocyte DNA fragmentation, histological integrity, ovarian tissue transcriptomic profiles, and DNA methylation. This study aims to characterize the cellular and molecular changes that occur within ovarian tissue and oocytes during the cryopreservation process. By elucidating these changes, we aim to understand the potential impact of cryopreservation on ovarian function and oocyte quality, ultimately leading to advancements in cryopreservation techniques.

Sheep were chosen as the model for this series of experiments for two main reasons: firstly, due to the success of previous experiments in the unit which had used sheep, and secondly, because of the ready availability of biological material from nearby abattoirs. The specific aim of each experimental feature is further discussed separately in the individual experimental chapters as described below.

First, I aimed to replicate the cryopreservation, thawing and rapid warming of ovine whole ovary as described by Campbell et al. (2014) and to access the viability of the oocytes from the visible antral follicles post warming using IVM, DNA fragmentation. **(Chapter two, effect of WOCP on antral follicle oocyte structure and development).**

Secondly, to evaluate the impact of cryopreservation on cell proliferation and cumulus-oocyte complex interactions within ovarian tissue using immunohistological techniques,

specifically Ki67 staining for cell proliferation and connexin staining for cell-cell interactions. **(Chapter three, effect of WOCP on oocyte – cumulus cell contact and interaction).**

Thirdly, to investigate the molecular and epigenetic changes induced by WOCP in sheep ovarian tissue by analysing the transcriptome using microarray technology and assessing global DNA methylation patterns. (**Chapter four, the effect of WOCP on transcriptome and global DNA methylation of the sheep ovary).**

Finally, a scoping review was conducted to examine the current literature on the epigenetic impact of oocyte and ovarian tissue cryopreservation. This review aimed to map and synthesise the evidence within this area, highlight knowledge gaps, and provide a broader context for interpreting the experimental findings of this thesis. (Chapter Five, **epigenetic changes after oocyte or ovarian tissue cryopreservation: a scoping review**)

By addressing these specific aims, this study provides both experimental data and a critical review of existing research, together offering a comprehensive evaluation of the impacts of WOCP on ovine ovarian tissue and the potential epigenetic implications of cryopreservation. Together, these findings contribute towards the development of safer and more effective cryopreservation protocols for large organs such as whole ovaries.

CHAPTER TWO : EFFECT OF WOCP ON ANTRAL FOLLICLE OOCYTE STRUCTURE AND DEVELOPMENT

2.1 INTRODUCTION

Developing a successful cryopreservation protocol for large organs like whole ovaries is extremely challenging (Fahy et al., 2006). Unlike a single cell, numerous issues are associated with freezing and thawing of a whole ovary while preserving its viability upon thawing, including heat and mass transfer, poor heat transfer between the core and periphery of the organ, and adequate distribution of the cryoprotectant throughout the organ to prevent ice formation due to its composition of many different cells that vary in size, shape and water content (Arav and Natan, 2009; Onofre et al., 2016; Pegg, 2007). Additionally, in the ovary, there is a presence of follicles at different stages of growth and maturation. Based on this, it is highly conceivable that cryopreservation will affect the different cell types within the ovary, both somatic and germ line, variably.

Freezing-induced damage to oocytes is frequently unavoidable. Prior literature has documented the occurrence of shrinkage and vacuolization in frozen-thawed human oocytes (Bianchi et al., 2014; Nottola et al., 2016; Palmerini et al., 2014). While these macroscopic changes are observable directly under the microscope, gaining a deeper understanding of oocyte freezing damage necessitates molecular and cellular-level detection methods.

Cryoinjury often triggers apoptosis in oocytes, impacting their subsequent developmental potential. Apoptosis is a cellular response to physiological and pathological signals and changes in external environmental conditions (Hu et al., 2012). Its primary characteristic is the fragmentation of DNA within cells. Additionally, the freezing process affects the integrity and

permeability of the oocyte membrane due to chemical and physical pressure Moussa et al. (2014). The normal function of the cell membrane is closely intertwined with the viability and developmental capacity of oocytes (Hoshino, 2018).

In a previous study with sheep ovarian tissue fragments comparing the two primary cryopreservation methods, i.e., slow freezing and vitrification, vitrification was found to better preserve follicular morphology when compared to slow freezing using haematoxylin-eosin (H&E) staining and caspase-3 immunohistochemistry (Labrune et al., 2020). While vitrification better preserved follicular morphology, both techniques showed equivalent apoptotic rates—a finding that contrasts with expectations given vitrification's reduced ice crystal formation. Conversely, another study, specifically focusing on apoptosis assessment in cortical and medullar tissues following WOCP and rapid thawing, did not associate the technology with any signs of apoptosis or ultrastructural alterations in any cortical or medullar regions. In their study, they employed terminal deoxynucleotidyl transferase-mediated biotinylated deoxyuridine triphosphates nick end-labelling (TUNEL) technology for detecting DNA fragmentation and immunohistochemistry (IHC) for active caspase-3 to identify cells programmed to undergo apoptosis (Martinez-Madrid et al., 2007).

These discrepancies highlight critical differences in experimental design and biological responses. Cortical fragments lack vascular networks, potentially exacerbating ischemic stress during processing and amplifying apoptosis signals. Furthermore, detection methods differ: TUNEL identifies late-stage DNA fragmentation, while caspase-3 immunohistochemistry detects early apoptotic signalling, potentially influencing sensitivity to apoptotic markers. Additionally, WOCP's vascular perfusion likely enables more uniform cryoprotectant distribution compared to fragment immersion, reducing localized cellular stress. These factors complicate direct

comparisons between studies and underscore the need for standardized methodologies when evaluating cryopreservation outcomes. Moreover, these findings highlight the necessity for thorough investigations into any new cryopreservation methodology to ensure comprehensive understanding of its effects on tissue integrity and cellular viability.

2.1.1 Chromatin configuration

Chromatin, the intricate combination of DNA and proteins constituting the genetic material in the cell nucleus, undergoes dynamic transformations during oocyte growth. At the germinal vesicle (GV) stage, chromatin transitions from a diffuse or decondensed configuration in growing oocytes to a progressively condensed state around the nucleolus as maturation concludes. This structural shift coincides with global transcriptional repression, reflecting the chromatin's role in coordinating gene expression across developmental stages. In bovine oocytes, five distinct GV chromatin configurations have been characterized: nonsurrounded nucleolus (NSN) with diffuse chromatin throughout the GV, netlike (N) with reticular chromatin patterns, clumped (C) with aggregated chromatin masses, surrounded nucleolus (SN) with heterochromatin encircling the nucleolus, and floccular (F) with chromatin clusters near the nucleolus and nuclear envelope (Liu et al., 2006). Sheep oocytes exhibit similar configurations—NSN, SN, and a unique surrounded nucleolus with peripheral chromatin (SNE), where chromatin condenses around the nucleolus and nuclear membrane (Russo et al., 2007). These configurations are evolutionarily conserved, with mouse and human studies identifying analogous NSN and SN states linked to transcriptional activity and developmental competence.(Debey et al., 1993; Demond et al., 2025; Zuccotti et al., 1995)

The relationship between chromatin configuration and transcriptional activity is pivotal for oocyte developmental potential. During the NSN phase, oocytes exhibit high transcriptional activity, synthesizing maternal mRNAs and proteins critical for early embryogenesis (De La Fuente et al., 2004; Zuccotti et al., 1995; Zuccotti et al., 2002). As chromatin condenses into the SN configuration, transcriptional activity declines, marking a transition to a transcriptionally quiescent state. This repression is not merely a passive consequence of chromatin compaction but an active process ensuring the preservation of maternally derived transcripts and epigenetic stability (Bouniol-Baly et al., 1999). For instance, SN-configurated oocytes in mice and humans show reduced expression of transposable elements and enhanced DNA methylation patterns, which safeguard genomic integrity during meiotic resumption and fertilisation (Miyara et al., 2003). The transcriptional silencing in SN oocytes coincides with the completion of molecular stockpiling, enabling these cells to prioritize translational rather than transcriptional activity during maturation—a prerequisite for successful embryonic development (Albertini and Olsen, 2013).

The developmental implications of this transcriptional regulation are profound. Oocytes retaining the NSN configuration often exhibit lower meiotic competence, as persistent transcription disrupts the coordinated storage of maternal factors required for fertilisation and zygotic genome activation. Conversely, SN-configurated oocytes, with their condensed chromatin and silenced transcription, demonstrate superior developmental outcomes, including higher rates of meiotic completion, fertilisation, and embryo formation. This dichotomy arises because transcriptional quiescence in SN oocytes allows for the selective stabilisation of essential transcripts while eliminating noise from unnecessary gene expression, thereby optimising the oocyte's metabolic and epigenetic readiness for subsequent developmental milestones. In sheep, the SNE configuration further refines this balance, with chromatin condensation near the nuclear

envelope potentially facilitating spatial organization of transcriptional machinery during the final stages of oocyte maturation. These findings underscore that chromatin configuration serves not merely as a morphological marker but as a functional determinant of oocyte quality, integrating structural, transcriptional, and epigenetic factors to gatekeep developmental competence.

To fully appreciate the significance of chromatin dynamics in oocyte development, it is essential to understand the various configurations observed within the germinal vesicle (GV). In bovine oocytes, for instance, five distinct patterns have been identified. The Nonsurrounded nucleolus (NSN) configuration is characterized by diffuse chromatin distributed throughout the entire GV, indicative of active transcriptional states. The Netlike (N) configuration presents a more organized chromatin pattern, resembling a network. The Clumped (C) configuration shows chromatin gathered into distinct clumps. The Surrounded nucleolus (SN) configuration is unique, featuring a nucleolus entirely enveloped by heterochromatin, a state associated with transcriptional repression. Finally, the Floccular (F) configuration exhibits chromatin concentrated near the nucleoli and nuclear envelope. In sheep oocytes, a simpler classification exists, with NSN and SN configurations similar to those in bovine, alongside the SNE pattern, where chromatin clusters near both the nucleolus and the nuclear envelope. These diverse configurations reflect varying stages of oocyte maturation and are crucial indicators of developmental potential (Liu et al., 2006; Russo et al., 2007)

2.1.2 Rationale and hypothesis

As indicated previously, all live births reported after WOCP and TP to date were obtained using the slow freezing procedure. In the first report by (Imhof et al., 2006), it was reported four sheep showed postoperative luteal function. One sheep conceived after spontaneous mating and delivered a healthy lamb 545 days after transplantation. In the study by Campbell et al which

employed antithrombotic therapy resulted in total acute restoration of ovarian function in 14/14 ewes within 3 weeks of WOCP & TP, with 9/14 ewes becoming pregnant and 4/14 giving birth to a total of seven normal lambs. Finally, Torre et al had one ewe delivering twins 527 days after transplantation. These reports indicate that the successful restoration of ovarian function did not occur in antral follicles. Antral follicles have a higher risk of cryoinjury compared to earlier stages of development due to the presence of intrafollicular fluid possibly forming ice crystals. Ideally the competence of an oocyte will collectively be its ability to mature, be fertilised and develop into an embryo, establish a pregnancy and produce a healthy offspring.

Therefore, the hypothesis of this study is that slow freezing of the whole ovary induces DNA fragmentation, apoptosis, growth impairment, cell membrane vulnerability and causes changes in chromatin configuration to germinal vesicle oocytes in antral follicles in sheep.

This study proposes that subjecting the entire ovary to a slow freezing process induces a cascade of detrimental effects on germinal vesicle oocytes located within antral follicles in sheep. The rationale behind this hypothesis is grounded in the well-established challenges associated with slow freezing, including the potential for DNA fragmentation, apoptotic responses, growth impairment, and alterations in chromatin configuration. Slow freezing, as a cryopreservation technique, has been known to introduce stressors such as ice crystal formation and osmotic imbalances, particularly impacting the delicate structures and developmental potential of oocytes. The vulnerability of germinal vesicle oocytes within antral follicles to these cryopreservation-induced stresses underscores the need for a comprehensive investigation into the specific repercussions on DNA integrity, cellular viability, growth dynamics, and chromatin organization. By delving into these intricate aspects, the study aims to provide nuanced insights essential for

optimizing slow freezing protocols and preserving the reproductive capacity of sheep, contributing to advancements in ovarian cryopreservation techniques.

2.1.3 Aims and objectives

Given the well-established similarities in ovarian morphology and function between sheep and humans, the sheep model proves to be a valuable resource for studying follicular dynamics with potential applications in human reproductive research. The primary objective of this study is to evaluate the impact of WOCP on the viability and maturation capacity of GV oocytes from antral follicles in sheep, focusing on whether WOCP impairs their ability to mature *in vitro* (IVM). Additionally, the study seeks to determine whether different IVM media, specifically commercially available BO-IVM compared to laboratory-prepared M199-based media, can improve the maturation outcomes of oocytes obtained from WOCP-treated ovaries. A further aim is to assess the effects of WOCP on DNA integrity, cell viability, and chromatin configuration in GV oocytes, using TUNEL assays and propidium iodide staining to quantify DNA fragmentation and viability while analysing chromatin orientation to identify potential disruptions in key configurations such as NSN, SN, or SNE. Collectively, these aims address critical gaps in understanding the effects of WOCP on antral follicle oocytes and provide insights into optimizing cryopreservation protocols for fertility preservation.

2.2 METHODS AND MATERIALS

2.2.1 Experimental design

As a preliminary step for the IVM study in the sheep oocytes, a comparative analysis of two IVM media: a commercially available medium, BO-IVM (IVF Bioscience, UK), and a in-

house prepared medium consisting of M199 supplemented with FSH, LH, and oestradiol. The efficiency, effectiveness, and consistency of each medium in supporting oocyte maturation was evaluated.

To evaluate the effect of whole ovary cryopreservation, thawing and rapid warming, oocytes were assessed after randomly allocating them into fresh and WOCP. WOCP and thawing was carried out as described by (Campbell et al., 2014). Cumulus oocyte complexes (COC) were then retrieved from the visible antral follicles and grouped into the various grades based on quality as described previously (Wood and Wildt, 1997). The oocytes were then assessed for viability and apoptosis using propidium iodide (PI) and terminal deoxynucleotidyl fluorescein-dUTP nick end labelling (TUNEL) respectively. Nuclear maturation was also assessed after IVM. Finally, a set of oocytes were stained with brilliant cresyl blue (BCB) and again put into IVM culture. A brief illustration of the experimental design is shown in **Figure 2.1** below.

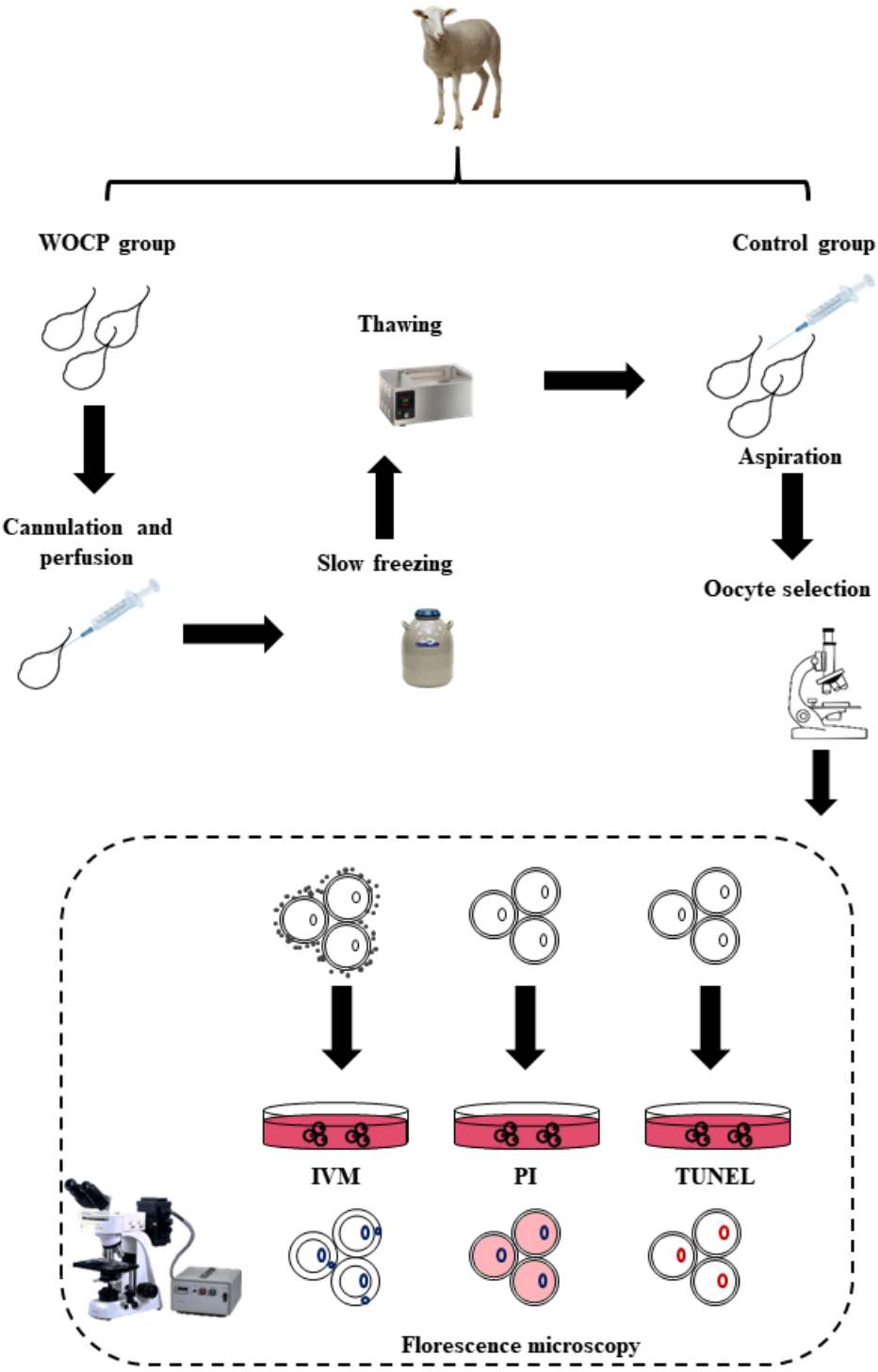

Figure 2.1 Flowchart of the experimental design. Sheep reproductive tracts retrieved from the abattoir. Out of the two ovaries from each sheep one was randomly selected as control and the other WOCP. Control oocytes were aspirated and matured or stained immediately with PI or TUNEL.WOCP were cannulated, perfused with CPA and transferred to the freezer for slow freezing after which they were thawed, and oocytes were aspirated and matured or stained. Images were taken with the fluorescence microscope and data analysed.

2.2.2 Ovarian tissue collection and whole ovary cryopreservation

No sheep was sacrificed for the sole purpose of this research Sheep reproductive tracts (n=8) (**Figure 2.2**) were transported in a sterile bag from the abattoir where.to the lab. The tracts were sterilised with 70% ethanol, cleaned and washed with Dulbecco's phosphate-buffered saline (DPBS) (Sigma-Aldrich, US). For each sheep, one ovary was randomly designated as the control (fresh), while the other underwent WOCP.

The ovary with its pedicle was dissected and cannulated using a 22G Leaderflex cannula with extension (0.7 mm × 20 cm, Vygon GmbH & Co., Aachen, Germany) and tied securely with a double mersilk suture (Ethicon, Inc, UK). The conditions of perfusion and cryopreservation were as described previously by Campbell et al., 2014. Each ovary (both WOCP and control) was placed into perfusion trays and first infused with heparinised (100 IU ml^{-1}) Ringer's solution at a rate of 1 ml/ min for 10 minutes using a syringe driven perfusion pump (Precidor Infors Ag Basel; ChemLab Scientific Products Ltd, Hornchurch, UK) fitted with a 50 ml syringe. This was done to remove blood and prevent blood clotting.

For the WOCP group of ovaries, they were immediately followed by a 60 minutes perfusion with the cryoprotective agent (CPA) (Leibovitz L-15 media supplemented with 1.5 mol l^{-1} dimethyl sulfoxide (DMSO) (Sigma-Aldrich, US), 0.1 mol l^{-1} sucrose (Sigma-Aldrich, US) and 10% (v/v) heat inactivated foetal calf serum (FCS) (Sigma-Aldrich, US) perfusion at a rate of 0.5 ml/ min. After this, the ovaries were placed in cryogenic vials and topped up with CPA. All solutions were filter sterilized using a 0.22um filter and 50ml syringe or 0.2µm Nalgene™ Rapid-Flow™ (Thermo Scientific™, UK), refrigerated and kept on ice prior to use.

Using a Planer controlled rate freezer (Kryo 550-16; Planer plc, Middlesex, UK) a slow-freezing cryopreservation protocol described by Campbell et al., 2014 was utilized. The conditions

of the program involved cooling to 0˚C before loading the samples. The chamber was then cooled to -9˚C at a rate of-1˚C min^{-1} and the temperature held for 5 min to allow manual seeding. After seeding, the temperature proceeded to reduce at a rate of-0.3˚C min^{-1} to -40˚C following which the temperature further reduced at a rate of -10˚C min^{-1} to a final temperature of -140˚C. Immediately after the freezing protocol, the cryogenic vials were plunged and stored in liquid nitrogen for at least 5 days prior to thawing and aspiration.

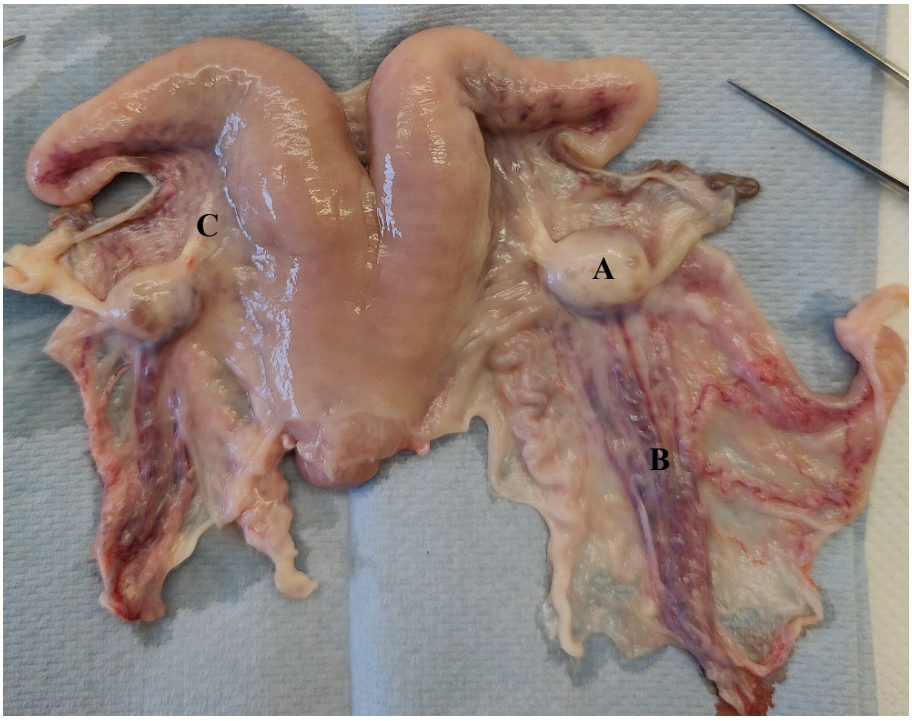

Figure 2.2 Pictures of the sheep reproductive tract showing A- ovary, B -uterine veins, C- fallopian tube.

2.2.3 Ovarian thawing

After 5 days, the frozen ovaries were removed from liquid nitrogen and allowed to sit at room temperature for two (2) minutes before being placed in a water bath at 37˚C for 30–40 minutes for thawing. Three sterile thawing media with reducing concentrations of DMSO (1M, 0.5M, 0M), Leibovitz L-15 media and 10% FCS were used for the thawing process. Each ovary

was then transferred to a perfusion tray and immersed in warm (37˚C) thawing media, beginning with the highest in DMSO concentration. The ovaries were perfused subsequently with each media (37˚C) for 10 minutes at a rate of 1ml min $^{-1}$ through the pre-existing cannula (**Figure 2.3**). After thawing, the ovaries were kept in the final thawing media (37˚C) (described above 0M DMSO) with no DMSO prior to oocyte aspiration.

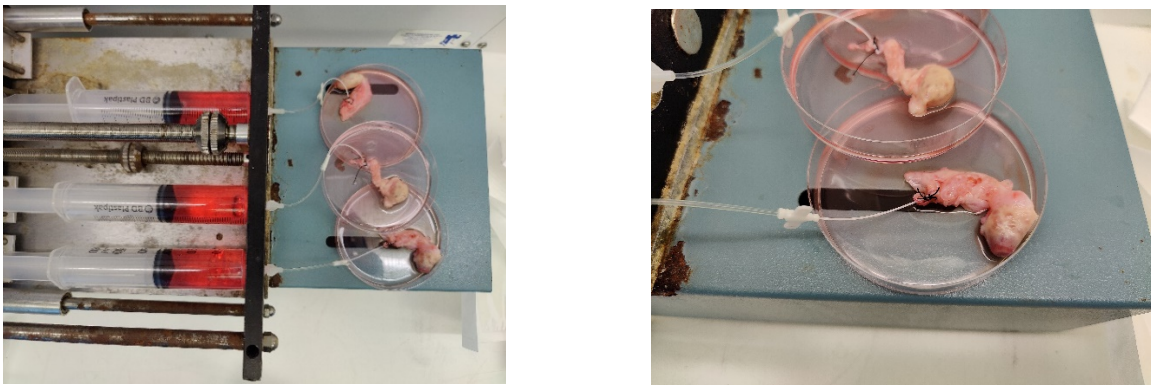

Figure 2.3 Pictures of thawed ovaries being perfused with warm thawing media at a rate of 1ml per min using a syringe-driven perfusion pump fitted with a 50 ml syringe through the pre-existing cannula in a perfusion tray while immersed in more warm (37˚C) thawing media.

2.2.4 COC collection

Using a 10 ml syringe and 21-gauge needle, all visible follicles on the ovary were aspirated and the contents emptied into a 5ml Falcon tube and kept warm at 37˚C. The contents (follicular fluid) were transferred into a dish containing warm oocyte wash media (37˚C) (IVF Bioscience, UK), and with the help of a dissection microscope, cumulus oocyte complexes (COCs) were identified, and transferred into clean warm wash media (37˚C). The oocytes were washed twice in warm wash media (37˚C) prior to subsequent experiments. The oocytes were graded based on their morphological appearance; grade A: oocytes surrounded by cumulus cells; grade B: oocytes partially surrounded by cumulus cells; grade C: oocytes not surrounded by cumulus cells; and

grade D: degenerated oocytes and cumulus cells. Grade A and B were considered normal COCs and grade C and D abnormal (**Figure 2.4**) (Talukder et al., 2011).

In this study, whole ovaries from different sheep were collected, cryopreserved, or used fresh as controls as described above. However, because the ovaries were retrieved from the abattoir setting and processed at different times, it was not possible to confidently pair ovaries from the same animal for experimental comparison. As a result, treatment and control groups were effectively created from independent ovaries rather than paired contralateral samples. This limitation meant that although the experimental design initially aimed to use paired ovaries from each sheep (thus controlling for inter-animal variability), the loss of paired identity required analyses to be conducted on unpaired groups. Consequently, potential animal-to-animal variation may have contributed additional biological variability to the dataset, reducing the statistical power and robustness of subsequent comparisons.

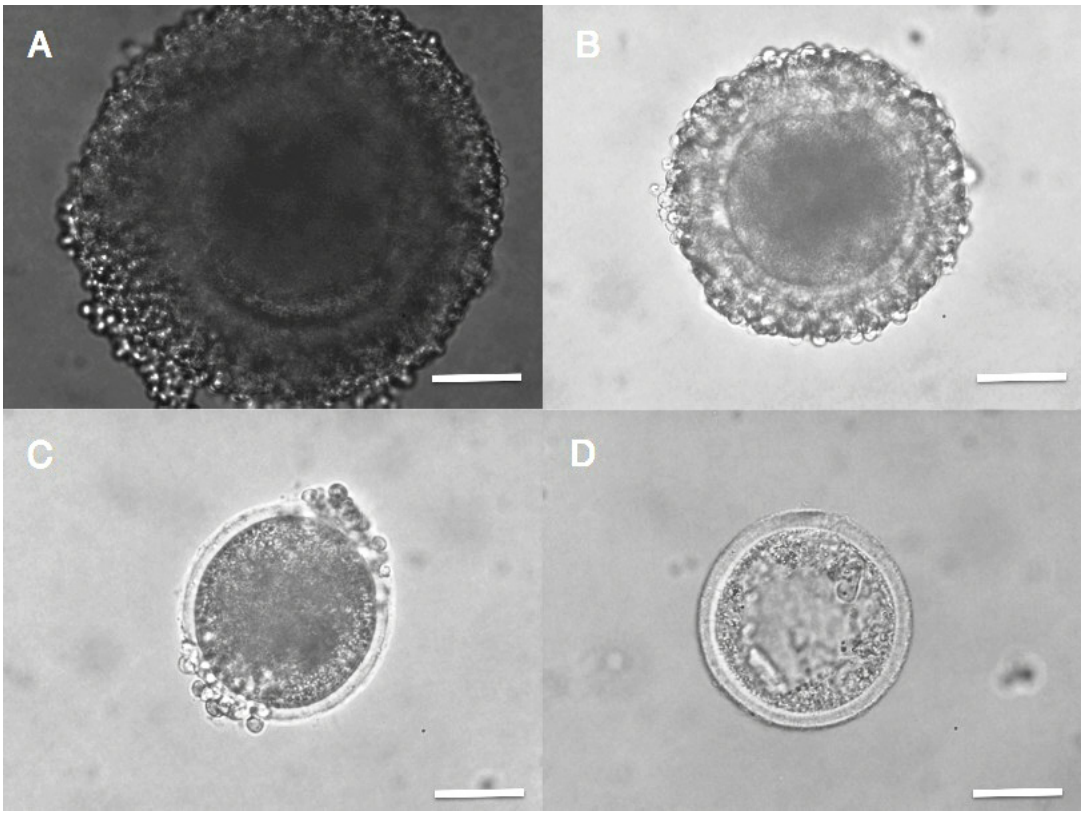

Figure 2.4 Representative photograph of COCs showing: A) Grade A; B) Grade B which are normal COCs; C) Grade C; D) Grade D (Abnormal COCs). Adapted from (Renata Gaya Avelar et al., 2012).

2.2.5 Oocyte viability assessment

Oocytes were assessed for viability based on membrane (oolemma) integrity using propidium iodide (PI) (Thermo Fisher Scientific™, UK) staining. PI only penetrates damaged cell membranes, binds to DNA and Ribonucleic Acid (RNA) by intercalating between base pairs emitting red fluorescence and indicating membrane damage thereby excluding viable cells. Oocytes were washed in 2 % bovine serum albumin (BSA) (Thermo Fisher Scientific™, UK) in PBS, treated with 80 IU/mL hyaluronidase to remove cumulus cells, fixed in 4% paraformaldehyde (Thermo Fisher Scientific™, UK) and stained with PI (50 µg/ml) for 10 minutes in the dark. The oocytes were then washed in 2 % BSA in PBS once again and mounted in 4′,6-diamidino-2-

phenylindole (DAPI) containing Vectashield Antifade Mounting Medium (Vector Laboratories, Inc) for observation under fluorescence microscopy. Non-viable cells emitted red fluorescence (PI-positive) as well as blue, indicating a disruption of the cellular membrane, while viable cells showed blue fluorescence without red (PI-negative), indicating an intact cell membrane.

2.2.6 Evaluation of apoptosis (TUNEL)

After thawing and warming described under **section 2.2.3**, COCs as isolated under **section 2.2.4** were fixed in paraformaldehyde (4%) (Thermo Fisher Scientific™, UK) for 1 hour at room temperature. Following three washes in 2 % BSA in PBS, COCs were treated with 80 IU/mL hyaluronidase to remove cumulus cells. Oocytes were permeabilised in PBS containing 0.2% Triton X-100 for 30 minutes at 38.5°C. Before staining, a few oocytes were allocated as positive and negative controls for the TUNEL reaction, and these were treated with 0.1 IU/µl DNAse I (Qiagen, UK) for 1 hour at 38.5°C. After three washes in BSA (2%), TUNEL staining was performed with In Situ Cell Death Detection Kit, TMR red (Sigma-Aldrich, US), according to the manufacturer's instructions. The kit is based on the detection of single- and double-stranded DNA breaks that occur at the early stages of apoptosis. The kit has two components, an enzyme solution and a label solution. For every reaction, the components were mixed immediately before use as one part enzyme solution to 9 parts label solution. A maximum of 45 oocytes were placed in a 30µl drop of TUNEL mixture for each group and incubated for an hour at 38.5˚C. Negative control samples had the terminal deoxynucleotidyl transferase enzyme omitted from this step. During the incubation period, TdT catalyses the addition of TMR-dUTP at free 3′-OH groups in single- and double-stranded DNA both of which are present in the TUNEL reaction mixture. Oocytes were mounted on glass slides with 10µl drop of Vectashield Antifade Mounting Medium with DAPI (Vector Laboratories, Inc) and observed using fluorescence microscope (Nikon DS – RiL camera

connected to Nikon eclipse 80i microscope with a Nikon digital imaging head and a Nikon super high-pressure mercury lamp power supply (Nikon Instruments, UK)). Oocytes with damaged sites of DNA emitted red fluorescence indicating apoptosis and were noted as apoptosis positive while oocytes emitting no red fluorescence were recorded as negative.

2.2.7 Chromatin configuration assessment

The chromatin configuration was assessed for all oocytes used for viability assessment and apoptosis evaluation in both fresh/control (n=260) and WOCP (n=155) groups. Due to DAPI staining which permitted the observation of these chromatin patterns in GV oocytes, their observed pattern was studied and compared to images depicted and defined by Russo et al in 2007 (**Figure 2.5**). The chromatin was classified into three major categories based on their condensation and distribution: diffuse chromatin in the whole nuclear area (NSN), condensed chromatin surrounding the nucleolus (SN), and condensed chromatin near the nucleolus and the nuclear envelope (SNE). Below is a brief description of these patterns (**Table 2.1**).

Table 2.1 A brief description of the chromatin classification based on the condensation and distribution as described by Russo et al. The three major classifications; nonsurrounded nucleolus (NSN), surrounded nucleolus (SN) and nuclear envelope (SNE).

Chromatin Classification	Description
Nonsurrounded nucleolus (NSN)	**i.** Numerous fibrillar strands of decondensed chromatin, which are intertwined together throughout the entire area of the nucleus **ii.** Strands of fibrillar decondensed chromatin similar to pattern in 'i' but were dispersed evenly throughout the entire nuclear area giving a diffused appearance
Surrounded nucleolus (SN)	Clumps of condensed chromatin fibres which were either distributed throughout the entire nuclear area or will mostly be confined in and around the nucleolus.
Nuclear envelope (SNE)	Clumps of completely condensed chromatin along the entire circumference of the nuclear envelope and surrounding the nucleolus as well.

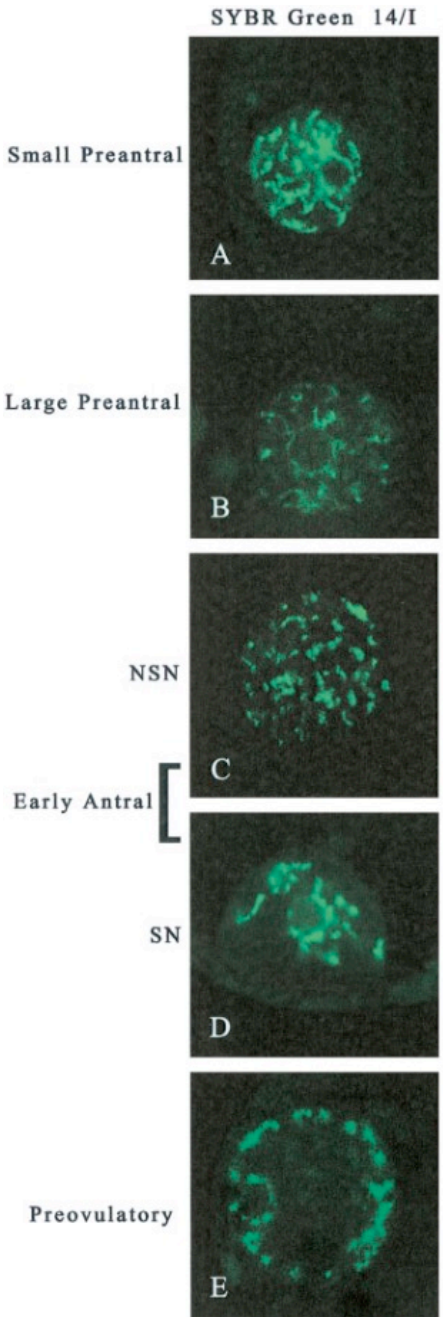

Figure 2.5 Representative digital images of sheep GVs showing different chromatin configuration**.** Chromatin counterstaining was performed with SYBR Green 14/I (green), which detects double-stranded DNA. A: GV example of a germ cell obtained from a small preantral follicle with diffuse chromatin (NSN) B: A GV example of an oocyte obtained from a large preantral follicle with the NSN chromatin. C and D: Two examples of oocytes obtained from early antral follicles with a NSN chromatin and a SN configuration, respectively. E: GV of a fully grown oocyte isolated from a preovulatory follicle where the chromatin assumes the SNE pattern. Adapted from (**Russo et al., 2007**).

2.2.8 Oocyte maturation

After systematically searching through follicular fluid collected as described in **section 2.2.4** and washed in warm (37˚C) wash media (IVF Bioscience, UK) or laboratory-prepared collection media holding medium (TCM-199 supplemented with 10% FCS), oocytes were distributed into 2 groups (normal and abnormal) based on morphology as mentioned earlier (**section 2.2.4**). COCs were washed in pre-optimized maturation media; commercial IVM media (BO-IVM, Bioscience, UK) or in-house media [(M199 (no HEPES), FCS (Sigma-Aldrich, US), follicle-stimulating hormone (FSH), luteinising hormone (LH), oestradiol, sodium pyruvate, cysteamine] composed of tissue culture medium 199 (TCM-199; Sigma-Aldrich, US) supplemented with 10% (v/v) foetal calf serum (FCS; Sigma-Aldrich, US), 25 mM sodium pyruvate, 50 IU/ml cysteamine (Sigma-Aldrich, US). Finally, COCs were cultured in a 4-well dish of 0.5ml maturation media with a maximum of 45 oocytes per well. The COCs were incubated at 38.5˚C and 5% CO_2 in humidified atmospheric air for 24 hours.

2.2.9 Fluorescent imaging

Fluorescence images were taken with a Nikon DS – RiL camera connected to Nikon eclipse 80i microscope with a Nikon digital imaging head and a Nikon super high-pressure mercury lamp power supply (Nikon Instruments, UK). Images were acquired with specialist imaging software, Volocity. The images taken after fluorescence imaging were split into individual channels and merged using ImageJ version 1.51a for windows (Wayne Rasband, National Institutes of Health, USA) to deduce the presence or absence of the specific stains (PI and TUNEL) applied to embryos.

2.2.10 Brilliant cresyl blue staining (BCB)

After aspiration, oocytes were washed in mPBS (PBS supplemented with 1 g/l glucose, 36 mg/l sodium pyruvate, 0.5 g/l BSA and 0.05 g/l gentamicin (Sigma-Aldrich, US). Following

the procedure of staining as previously described by (Catala et al., 2011), oocytes were incubated in 13 uM brilliant cresyl blue (BCB) (Sigma-Aldrich, US) diluted with mPBS for 1 hour at 38.5˚C in humidified air. After incubation, oocytes were washed in mPBS and classified into two groups depending on the colouration of the cytoplasm as observed under a light microscope: oocytes with blue cytoplasm or hypothetically grown oocytes (BCB+) and oocytes without blue cytoplasm colouration or hypothetically growing oocytes (BCB-).

2.2.11 Statistical analysis

Data in graphs are expressed as percentage mean unless otherwise stated. Data was tested for normality using the D'Agostino Pearson test for normality and homogeneity of variance using the one-way ANOVA. The groups were then compared using a Mann-Whitney U test, which is appropriate for unpaired data from two independent groups.

Although the original plan was to use paired data analyses by comparing contralateral ovaries from the same sheep, in practice this was not achievable because oocytes were pooled during collection, and the identity of paired ovaries from the same animal could not be maintained. This oversight effectively eliminated pairing information, which would have yielded more statistically powerful within-animal comparisons and greater control for inter-animal variability. Instead, unpaired analyses had to be performed. This distinction is a key methodological limitation: while unpaired testing remains valid for group-level comparisons, it does not fully exploit the potential strength of the design that would have been available had ovary pairing been preserved.

All data and statistics were analysed using GraphPad Prism version 8.0.2 for windows (GraphPad Software Inc., USA) and graphs were also generated with GraphPad Prism. P-values less than 0.05 were considered statistically significant. Data gathered for chromatin configuration analysis were organised into a contingency table, and a chi-square test was

performed to examine the association between chromatin configuration and experimental groups using GraphPad Prism.

2.3 RESULTS

2.3.1 Nuclear assessment of oocyte maturation post IVM

In the following set of data, oocytes were aspirated from fresh ovaries as well as frozen thawed ovaries. These oocytes were washed and carefully grouped into grade A, B, C and D as previously mentioned in **section 2.2.4**; Group A and B were considered as good quality oocytes while group C and D were considered as low quality oocytes. The oocytes were matured *in vitro* for 24 hours at 38.5˚C after which they were fixed and stained with DAPI for nuclear assessment. The oocytes were classified into various stages of development (GV, GVBD, MI, AI, TI & MII) as observed by nuclear assessment (**Figure 2.6**). GV & GVBD were considered immature, MI & AI were considered intermediate and TI & MII were considered mature oocytes.

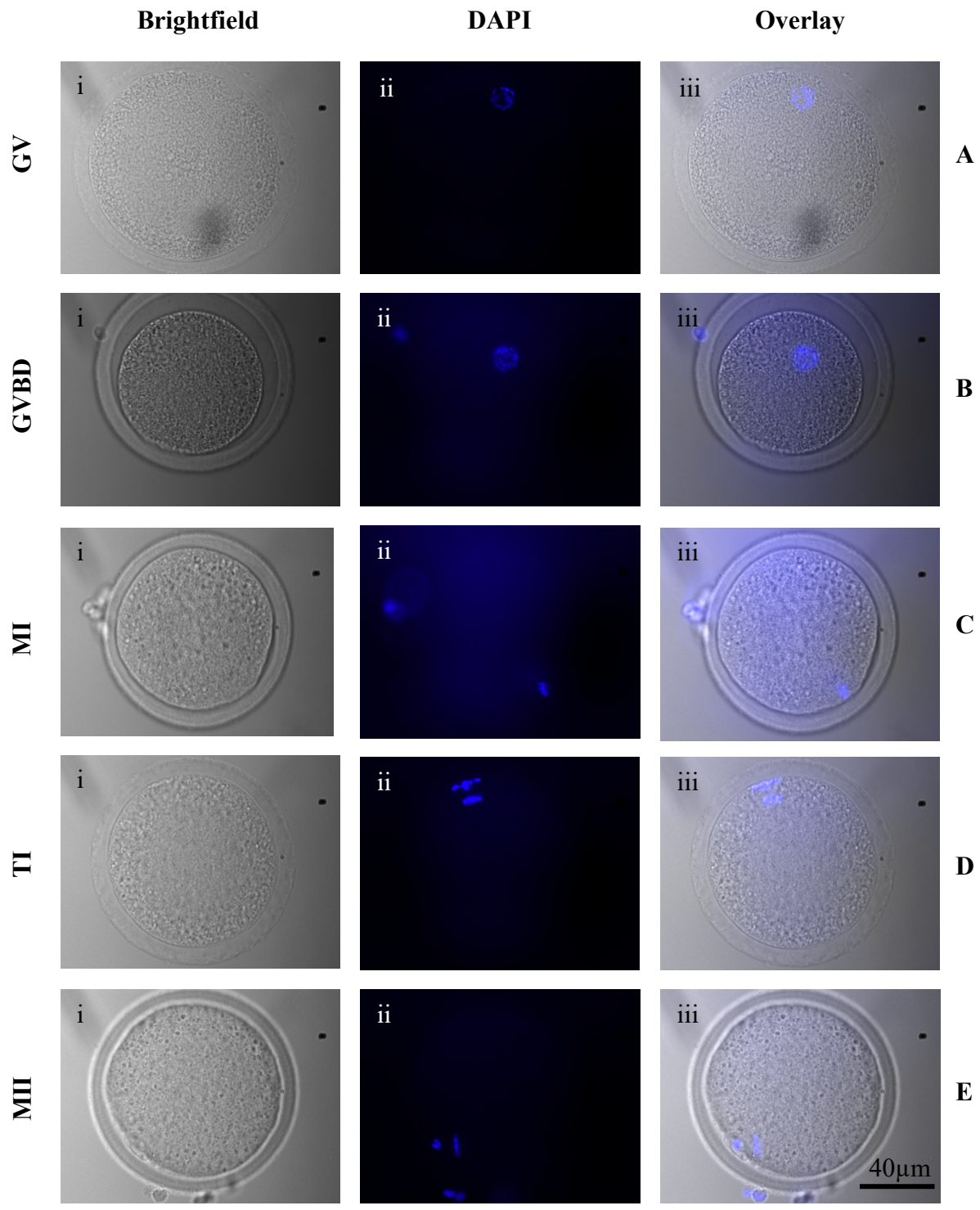

Figure 2.6 Representative images of oocytes displaying the different stages of maturation. Brightfield (i), DAPI fluorescent image (ii) and an overlay of both brightfield and DAPI images (iii) of sheep oocytes post 24 hours IVM culture. (A) GV, (B) GVBD (C) MI (D) TI and (E) MII. Scale bar = 40 µm.

2.3.1.1 The rate of in vitro maturation using commercial media vs. in-house prepared media

In-house media (HSE) reached a maturation rate of 40% while BO-IVM had a rate of 60% (**Figure 2.7)**, but these rates were not statistically different (p=0.335). Since BO-IVM demonstrated similar maturation rates to HSE media, and because of the consistency between lots, it was the preferred choice moving forward.

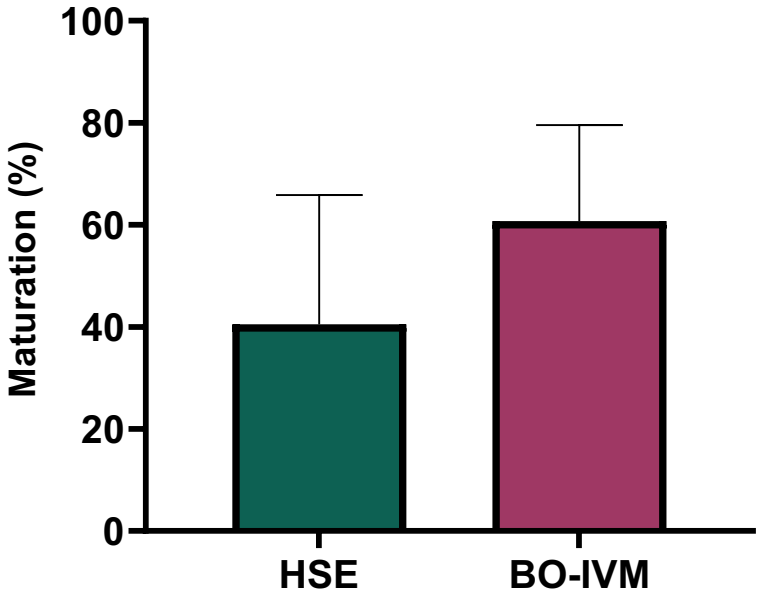

Figure 2.7 Bar graph illustrating the percentage of sheep oocytes reaching maturation after *in vitro* culture in HSE and BO-IVM media. The HSE group showed a 40% maturation rate, while the BO-IVM group achieved 60% maturation (p=0.335). Error bars represent the standard deviation (SD) of the mean maturation rate for each media condition.

2.3.1.2 The effect of WOCP on subsequent oocyte in vitro maturation (IVM)

After IVM, nuclear maturation assessment showed a higher percentage of oocytes from the control (fresh) group (67.14 %, n=60/90) reaching maturation, while WOCP group only had a single oocyte reaching the MII stage (8.3 %; n=1/64) (**Figure 2.8)**. Comparing oocyte maturation between control oocytes and WOCP according to Chi-square test, a significant association was found between the WOCP process and the percentage maturation outcome ($p < 0.0001$). The results also show most of the oocytes from the WOCP group remained at the

GV stage even after 24 hours of IVM while the contrary was observed in the control group (**Table 2.2**).

Table 2.2 Oocyte nuclear maturation assessment post IVM of both fresh and WOCP groups showing both the percentage and total number in each category.

	Immature	**Intermediate**	**Mature**
Control oocytes	0	32.86%	67.14%
(Fresh)	0	30	60
Oocytes from	55%	36.67%	8.3%
WOCP	43	20	1

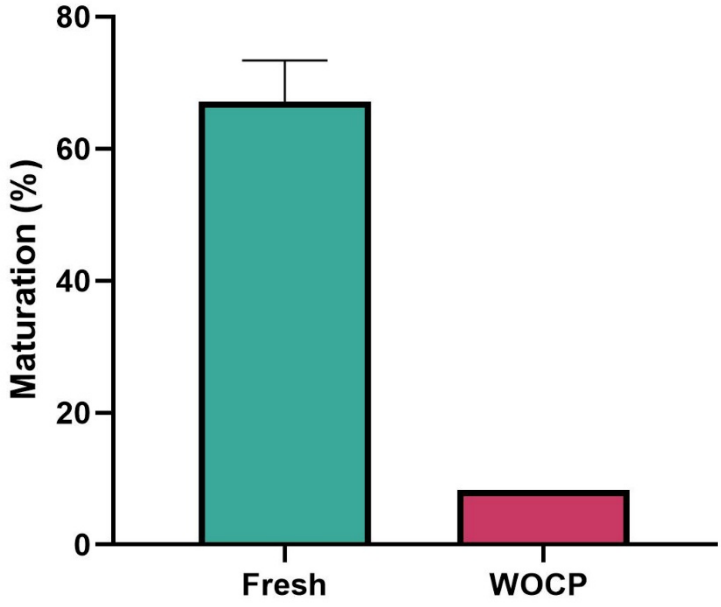

Figure 2.8 Comparison of oocyte maturation rates between control and WOCP groups. Bars represent the percentage of oocytes reaching the MII stage after IVM in control (n=60/90) and WOCP (n=1/64) groups. The difference between groups was statistically significant ($p < 0.0001$)

2.3 2 Effect of WOCP on COC morphological grading

Some oocytes from WOCP were observed to have cracked zona pellucida, spillage of cellular contents, change in shape, cytoplasmic atrophy and vacuolisation. As mentioned earlier, COCs were grouped into grade A, B, C and D as described by (Talukder et al., 2011). Group A and B were considered as good quality oocytes while group C & D were considered low quality. Due to the loss of cumulus cells and the above-mentioned characteristics observed in majority of the oocytes from frozen ovaries, oocytes from the WOCP group were graded mostly by the oocyte morphology rather than the COC. There was no significant difference in the proportion of COCs classified as A, B (termed AB) and C, D (termed CD) respectively between the two groups (WOCP, AB:54.3%, CD: 45.8%; control, AB: 54.5%, CD: 45.5%; $P \geq 0.05$). These COCs, after morphological assessment were split for the subsequent experiments using biological stains.

Table 2.3 Morphological grading of COCs retrieved from sheep antral follicles of control (fresh) and WOCP). The oocytes are grouped into normal (A&B) and abnormal (C&D).

Group	**Number of COCs for grading (n)**	**AB (%±SEM)**	**CD (%±SEM)**
Control	304	54.3%±8.0% (164)	45.8%±7.2% (140)
WOCP	236	54.5%± 12.7% (115)	45.5%±12.7% (121)

2.3.3 Effects of WOCP as assessed by biological stains

In the following set of data, oocytes were retrieved from WOCP ovaries stored in liquid nitrogen for at least one week. These oocytes were first graded based on morphological observation. They were then immediately stripped of their cumulus cells where present, fixed and stained with PI to assess the viability or assessed for DNA fragmentation with TUNEL assay.

2.3.3.1 Cell viability of oocytes after WOCP

After WOCP, oocytes were assessed for viability with PI (**Figure 2.9**). The WOCP group showed the highest percentage of cell membrane disruption (32.6 %) determined via PI staining, with the control group exhibiting a lower percentage of cell membrane disruption (19.8 %) (**Figure 2.10**). However, this did not show a significant difference between both groups ($p > 0.05$). A total of 202 oocytes from both control and WOCP ovaries were aspirated for PI staining, however, only 146 were successfully stained with DAPI confirming the presence of the nucleus. Out of this total, the control group had 76 and the WOCP group had 70 oocytes considered for the assessment of PI.

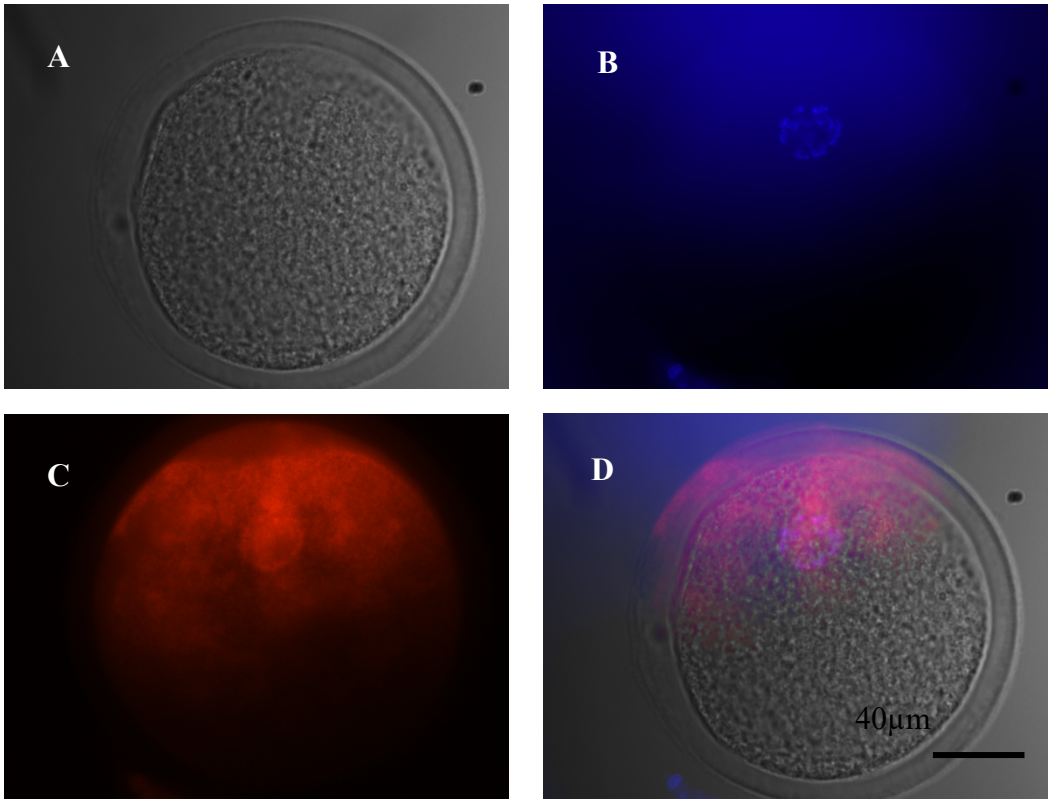

Figure 2.9 Representative fluorescent and brightfield images of sheep oocytes following PI staining.(A) Brightfield image, (B) 4‘, 6-diamidino-2-phenylindole (DAPI – blue), depicting cell nucleus, (C) propidium iodide (PI, red), depicting cytotoxicity, (D) composite overlay of all channels. Note that PI staining in oocytes may be affected by cytoplasmic RNA content which could impact nuclear-specific staining. Magnification at 40X. Scale bar = 40 µm.

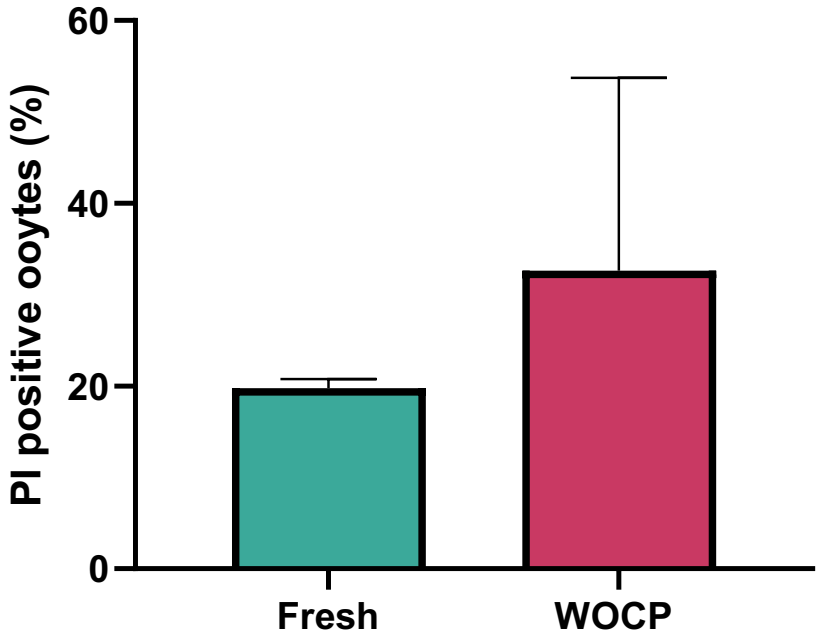

Figure 2.10 Bar graph illustrating the percentage of oocytes with cell membrane disruption as determined by PI staining in control and WOCP groups. The WOCP group showed 32.6% membrane disruption, while the control group exhibited 19.8%. Despite the apparent difference, statistical analysis revealed no significant difference between the groups ($p > 0.05$). Error bars in represent the standard deviation (SD).

2.3.3.2 Evaluation of apoptosis as assessed by the Terminal Deoxynucleotidyl Transferasemediated dUTP Nick End Labelling (TUNEL) assay in oocytes

Following WOCP, oocytes were assessed for DNA fragmentation using the TUNEL assay, and results were expressed as the 'apoptotic index' (in %). This index represented the number of TUNEL positive oocytes / the total number of DAPI stained oocytes. Positively stained oocytes were depicted by red fluorescence located in the region of the nucleus (**Figure 2.11**). A total of 200 oocytes were identified for TUNEL assay, however 145 were successfully stained with DAPI depicting the presence of the nucleus. The control group had a total of 76 and the WOCP had a total of 69. The control group had a lower apoptotic index (22.4%±24.8% SEM) compared to WOCP group (75.4%±26.6% SEM; $P<0.05$). (**Figure 2.12**).

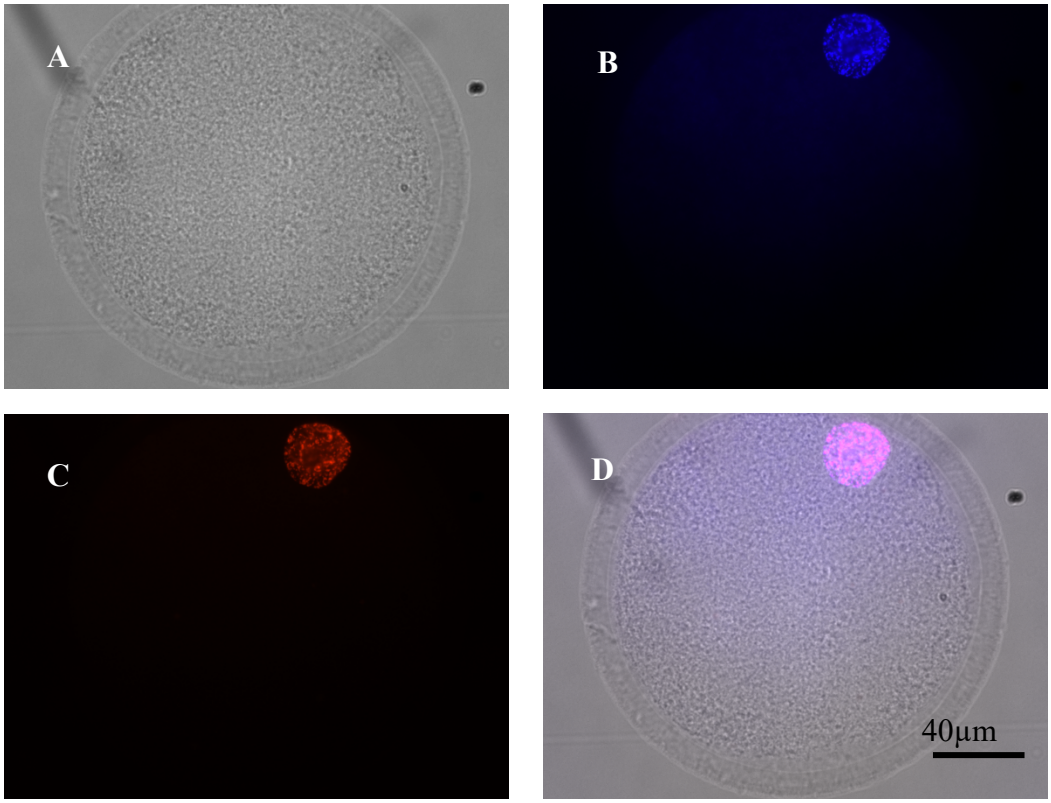

Figure 2.11 Representative fluorescent and brightfield images of sheep oocytes following TUNEL.(A) Brightfield image, (B) 4‘, 6-diamidino-2-phenylindole (DAPI – blue), depicting cell nucleus, (C) fluorescein-12-dUTP (TUNEL-red), depicting DNA fragmentation in the nucleus of the cell, (D) composite overlay of all channels. Magnification at 40X. Scale bar = 40 µm.

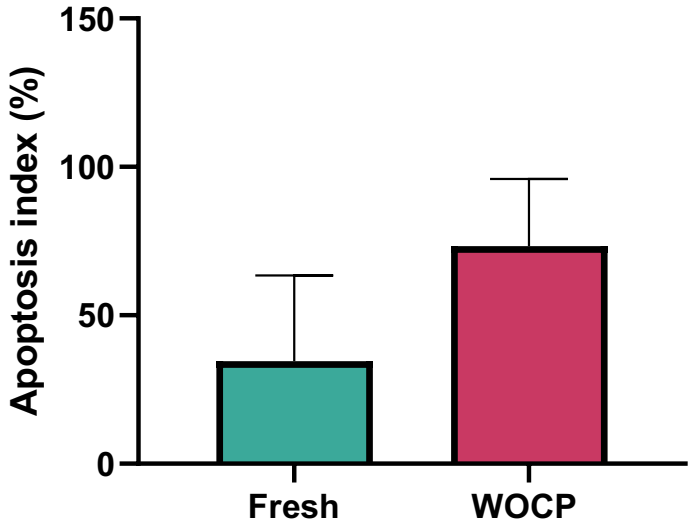

Figure 2.12 bar graph illustrates the apoptotic index (percentage of TUNEL-positive oocytes) in control and WOCP groups. The control group showed an apoptotic index of 22.4%, while the WOCP group exhibited 75.4%. Statistical analysis revealed a significant difference between the groups ($P<0.05$), indicating higher DNA fragmentation in WOCP oocytes. Error bars in represent the standard error of the mean (SEM).

2.3.4 Chromatin configuration assessment

All known chromatin configuration classifications were observed in both control (fresh) and WOCP groups. However, 218 oocytes (137 control, 81 WOCP) were excluded from classification due to image blurriness and unclear nuclear focus. Approximately, 54% (**Figure 2.14**) of the WOCP oocytes ($n = 40/74$, Chi-square, $p < 0.05$) displayed a condensed pattern of configuration (SNE) with chromatin fibres demonstrating fluorescence along the nuclear envelope as well as surrounding the nucleolus (**Figure 2.13B**). The major change in the pattern of configuration was observed with an increase in decondensed chromatin fibres (~36%) occupying the entire area of GV depicting an NSN configuration (**Figure 2.13A**) in WOCP oocytes ($n = 27/74$). Only ~13% of the control GV-oocytes ($n=17/123$, Chi-square, $p < 0.05$) exhibited this pattern of decondensed fibres. The total number of classified oocytes was 123 and 74 in the control and WOCP groups respectively (**Table 2.4**).

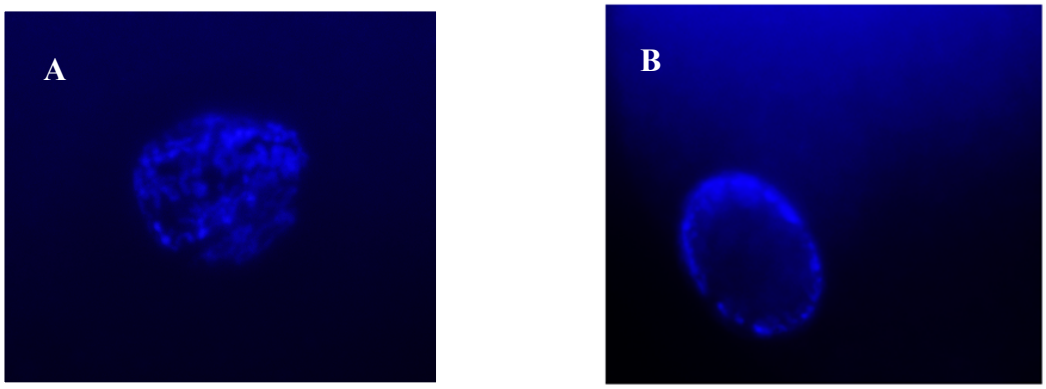

Figure 2.13 Representative images of cryopreserved sheep GVs showing different patterns of chromatin configurations followed by DAPI staining of the nucleus. A) An example of NSN pattern of chromatin configuration in a cryopreserved GV-oocyte B) An example of SNE pattern of chromatin configuration in a cryopreserved GV-oocyte.

Table 2.4 Total and individual number of oocytes classified according to the three major chromatin configuration groups in both fresh (control) and WOCP ovaries.

Chromatin Classification	**No. of GV oocytes**	
	Control	**WOCP**
NSN	17	27
SN	17	7
SNE	89	40
Total no. of oocytes classified	**123**	**74**
Total no. of oocytes not classified	*137*	*81*

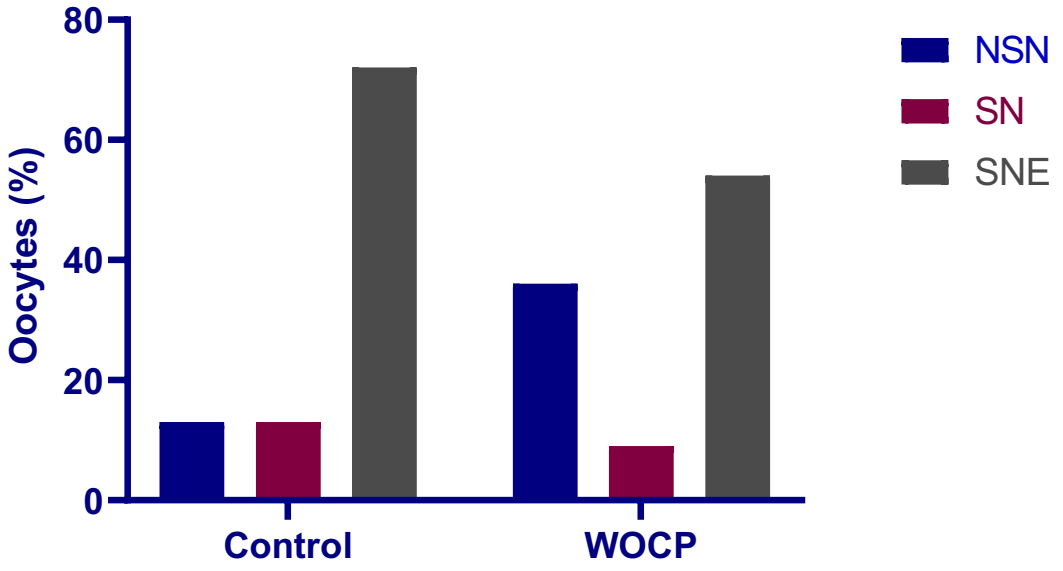

Figure 2.5 A bar graph representation of the percentage of oocytes classified in NSN, SN and SNE in both control and WOCP ovaries.

2.3.5 Effects of WOCP as assessed by biological stains

2.3.5.1 Oocyte screening by brilliant cresyl blue stain (BCB) post WOCP

In the following set of data, oocytes retrieved from both control and WOCP ovaries were stained in 13µM BCB prior to IVM for 24 hours to assess their quality and developmental competence. Oocytes were initially grouped into A&B and C&D groups prior to BCB staining to assess the number of oocytes that stained positive within the groups. BCB staining is a valuable technique that helps identify oocytes that have completed their growth phase (BCB+) versus those that are still growing (BCB-). BCB+ oocytes, which exhibit a blue cytoplasm, are generally considered more developmentally competent, while BCB- oocytes, which remain colourless, indicate high glucose-6-phosphate dehydrogenase activity and ongoing growth.

The results from the BCB staining reveal interesting patterns across the fresh and WOCP groups. In the fresh group, a total of 212 oocytes were assessed. Among the Grade A & B oocytes, 74 were BCB+ and 31 were BCB-. For the Grade C & D oocytes, 63 were BCB+

and 44 were BCB-. In the WOCP group, a total of 83 oocytes were evaluated. The Grade A & B category had 18 BCB+ and 14 BCB- oocytes, while the Grade C & D category showed 36 BCB+ and 15 BCB- oocytes. Unfortunately, all the oocytes in both the control and WOCP group remained in the GV stage after IVM.

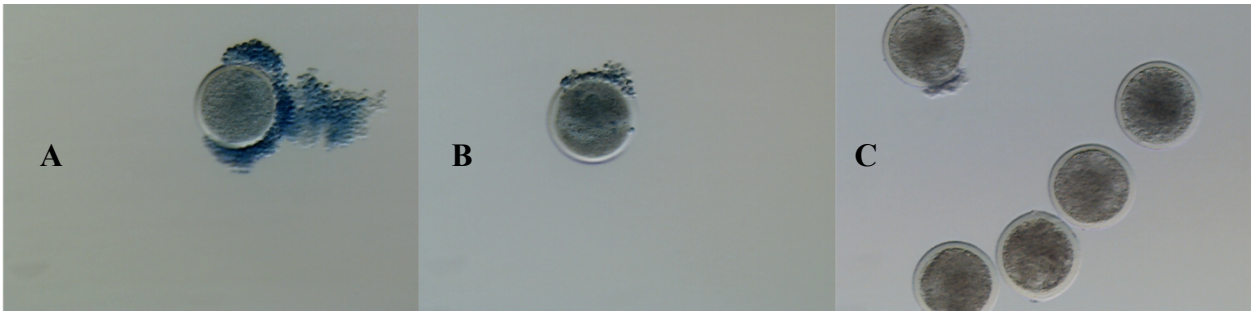

Figure 2.15 BCB staining in WOCP group. A: BCB positive stained COC (Grade B); B: BCB positive stained COC (Grade C); C: BCB negative stained COC (Grade D).

Table 2.5 Total number of oocytes showing BCB+ and BCB- staining between control and WOCP groups. BCB+ and BCB- represent BCB positive staining and BCB negative staining, respectively. The oocytes are also grouped into the normal (A&B) and abnormal (C&D) based on the morphological appearance of the oocytes.

	Grade A & B		**Grade C & D**	
	BCB+	***BCB-***	***BCB+***	***BCB-***
Fresh group	74	31	63	44
WOCP group	18	14	36	15

2.4 DISCUSSION

The objective of these experiments was to investigate whether WOCP affects the continued growth and development of antral follicle oocytes, with particular attention to potential underlying mechanisms such as membrane damage, DNA fragmentation, and possible changes in chromatin configuration. Consistent with the hypothesis, the results indicate a substantial reduction in the maturation potential of oocytes obtained from WOCP-antral follicles, aligning with significantly elevated rates of apoptosis. We also observed an elevated percentage of decondensed pattern of chromatin configuration.

2.4.1 Utilising commercially available media (BO-IVM) for *in vitro* maturation (IVM) of sheep oocytes compared to media prepared in the laboratory (HSE)

Initial trial comparing commercial media (BO-IVM) and in-house media revealed comparable maturation consistency (HSE media: 40%, BO-IVM: 60%, t test, $p = 0.335$), leading to subsequent IVM cycles utilizing BO-IVM due to its greater convenience and time efficiency. While in-house media (M199 supplemented with FSH, LH, and oestradiol) has been traditionally employed for IVM (Dhali et al., 2017), the present experiments explored the use of a commercially produced IVM media (BO-IVM) to enhance effectiveness, efficiency, and consistency. Preliminary studies were conducted to evaluate the maturity rates of oocytes cultured in BO-IVM and in-house media, with achieved maturation rates falling within the average IVM rates (~60–80%) observed in sheep oocytes (Zhu et al., 2018). Despite the commercial media exhibiting a higher maturation rate (60%) compared to the in-house media (40%), the difference was not statistically significant, affirming equal consistency in the maturation rates. Therefore BO-IVM was deemed suitable for sheep oocyte IVM based on these findings, providing evidence for its suitability in subsequent experiments.

2.4.2 WOCP induces structural alterations in the COC of antral follicles

After aspirating visible follicles from cryopreserved ovaries, it was observed that the COCs and oocytes could not escape some expected cryo-damages. These cryopreservation induced damages observed include, cracked zona pellucida, leaking of cellular contents, shrinking of cytoplasm, change in shape of oocyte and partial or full removal of cumulus cells, all of which are consistent in previous studies (Rana et al., 2013; Sathananthan et al., 1987). In the control group, 164 oocytes were graded normal, which is about 54 % of the total while the WOCP group had 115 normal oocytes equivalent to 49 %.

In a previous study, sheep oocytes retrieved from cryopreserved ovarian tissues had 70 % reaching metaphase II with no reports of excessive loss of cumulus cell layers (Al-aghbari and Menino, 2002). The study also recorded oocytes with up to five layers of cumulus cells which is contrary to the observation in this study. However, the study reported these finding on vitrified sheep ovarian tissues rather than slow freezing. Furthermore, in the study by Al-aghbari and Menino, 2002, the CPA was 35 % ethylene glycol (EG) whereas DMSO was used in the present study which could quite possibly explain the loss of cumulus cells due to the distinct physicochemical properties and cellular effects of these agents. EG is a smaller molecule with higher permeability and lower cytotoxicity compared to DMSO, which is more membrane-penetrating but also more toxic at higher concentrations or longer exposures. Studies have shown that EG generally preserves follicular morphology and viability better than DMSO in ovarian tissue cryopreservation, likely because EG causes less osmotic and oxidative stress to cells, including sensitive cumulus cells surrounding oocytes (Durli et al., 2014; El Cury-Silva et al., 2021). DMSO, while effective as a cryoprotectant, is also known to induce epigenetic changes and cellular stress responses that may contribute to cumulus cell damage or detachment during freezing and thawing (Nakamura et al., 2017). Additionally, residual DMSO levels after warming can be higher and more persistent than EG, potentially

exacerbating toxicity (Nakamura et al., 2017; Obata et al., 2018). This difference in toxicity profiles may underlie the increased cumulus cell loss observed in the present study using DMSO. Furthermore, the method of oocyte retrieval was different from the one employed in this study. The ovaries were slashed with a scalpel, allowed to sediment in DPBS in a tube for 10 minutes after which the oocytes were recovered. It is therefore unclear if the oocytes were recovered from antral follicles or preantral, although it is likely that they were from preantral due to the method of OTC.

2.4.3 Nuclear maturation rate in antral follicle oocytes is negatively affected by WOCP

In this study, nuclear maturation rate was significantly higher in control oocytes as compared to oocytes retrieved from WOCP ovaries (control group - 67 %; n=60/90, WOCP group 8 %; n=1/64, $p < 0.05$). This suggests that the slow freezing process and/or thawing process induced damage to the oocyte making it incapable of further maturity into metaphase II. As observed in fluorescence microscopy, a majority of these oocytes remained at the GV stage and failed to progress or even begin the process of maturation.

A possible explanation for the observed outcome in this study could be the absence of cumulus cells, which are vital for oocyte maturation, as germ cell development, meiotic progression, and the overall transcriptional pattern are regulated by cumulus cells (Matzuk et al., 2002). Throughout mammalian folliculogenesis, continuous bidirectional communication and nutrient exchange occur between cumulus cells (CCs) and oocytes (Coticchio et al., 2015; Russell et al., 2016; Wigglesworth et al., 2013). In antral follicles, gap junctions formed by connexin 37 (Cx37) establish connections between CCs and the oocyte (Kidder and Mhawi, 2002). These gap junctions enable the transfer of various small molecules, including ions, cyclic nucleotides (cAMP, cGMP), metabolites, amino acids, RNA transcripts, miRNAs, and more, from CCs to the oocyte. This intercellular communication is essential for oocyte maturation and the acquisition of competence (Dumesic et al., 2015; Kidder and Mhawi, 2002;

Wigglesworth et al., 2013). The oocyte attains full competence during the transition from prophase I to metaphase II, enabling it to undergo fertilization and generate a viable embryo. Importantly, paracrine signalling from CCs to the oocyte plays a crucial role in supporting meiotic resumption, facilitating nuclear and cytoplasmic maturation, and regulating transcriptional activity (Albertini et al., 2001). Therefore, the functions of cumulus cells generally reflect the oocyte's functional competence (Li et al., 2006; Li et al., 2008).

Previous work has reported that CPA causes a disorganisation of the actin filaments within transzonal projections through which cumulus cells establish physical contact with the oocytes (Younis et al., 1996). Although previous studies reported human and mouse cumulus-free immature oocytes showed remarkable maturation rate (Chian and Tan, 2002; Huang et al., 1999; Miki et al., 2006), these oocytes where retrieved from induced ovaries. In another study, it was reported that oocytes (GV/MI) retrieved from human ovaries following controlled ovarian stimulation require a short time for GVBD and maturation, although final rates of oocyte maturation is comparable to those from unstimulated ovaries (Cha and Chian, 1998). The stimulation protocol typically involves administration of gonadotropins to promote the growth and development of multiple follicles. These stimulated oocytes are also capable of maturing successfully without the support of cumulus cells (cumulus-free maturation), unlike oocytes from unstimulated ovaries, which generally rely on cumulus cell interactions for optimal maturation. The accelerated maturation observed in stimulated oocytes is likely due to enhanced signalling between the oocyte and cumulus cells induced by hormonal priming, which facilitates meiotic resumption and cytoplasmic maturation.

Similarly, the *in vitro* culture of denuded bovine oocytes revealed abnormalities in nuclear and cytoplasmic maturation, making them less likely to resume meiosis (Macaulay et al., 2016). Specifically, these abnormalities include arrest at earlier meiotic stages such as the GV stage, degenerated chromatin configurations, and failure to form a proper MII spindle or

extrude the first polar body, all indicative of impaired nuclear maturation. Cytoplasmic defects involve disrupted organelle distribution and altered metabolic activity, which are critical for oocyte developmental competence.

The authors attribute these defects primarily to the loss of bidirectional communication between the oocyte and its surrounding cumulus cells, which normally provide essential signals, nutrients, and regulatory molecules via gap junctions and transzonal projections. Without cumulus cells, oocytes lack this critical support, leading to impaired regulation of meiotic progression, cytoplasmic maturation, and gene expression. Transcriptomic analyses of partially denuded oocytes showed altered expression of genes involved in lipid homeostasis, mitochondrial function, chromatin remodeling, and epigenetic regulation, further explaining the compromised maturation capacity. Importantly, treatments that restore or mimic cumulus cell signaling, such as pro-cumulin supplementation, have been shown to partially rescue these defects, highlighting the crucial role of cumulus-oocyte interactions in oocyte quality and maturation (Macaulay et al., 2016).

Intriguingly, such abnormalities were not observed when mouse oocytes were co-cultured with cumulus cells (CCs) (Bahrami et al., 2022; Ge et al., 2008). Moreover, pig oocytes surrounded by CCs and co-cultured with supplemented CCs exhibited increased meiotic and developmental competencies (Matsunaga and Funahashi, 2017). These studies underscore the importance of the presence of cumulus cells, whether they are directly connected to the oocyte. Another study demonstrated that the maturation rate of human oocytes could increase from 57% to 82% after 48 hours, without affecting fertilisation or cleavage rates. Therefore, it might have been beneficial to consider co-culturing the oocytes with CCs for 48 hours rather than 24 hours (Barnes et al., 1996).

The subsequent question arises: is the loss of cumulus cells attributed to the freezing protocol, the CPA itself, or the duration of exposure to the CPA? In a proof-of-principle experiment in the laboratory, ovaries were directly immersed in liquid nitrogen without any CPA. Consequently, every oocyte retrieved from this ovary had completely lost its cumulus cells. This observation leads to speculation that prolonging the exposure time to the CPA could potentially enhance the effective cryopreservation of antral follicles. Unfortunately, we did not conduct a separate study exposing the tissue solely to the CPA. Such a study could have provided insights into the potential toxicity of the CPA to the cumulus-oocyte complexes (COCs).

2.4.4 WOCP causes significant level of apoptosis in oocytes of antral follicles but no significance in viability

Following this, the viability of oocytes between both groups showed no significant difference (control group 17.1%±14.9 %; WOCP group 38.6%± 21.8%, $p > 0.05$). However, with TUNEL, a significantly higher level of apoptosis was demonstrated in the WOCP group as compared to the control group (control group: 22.4%±24.8%; WOCP: 75.4%±26.6%, $p < 0.05$).

While the viability results did not reveal a significant difference between the two groups, the TUNEL assay demonstrated a substantially higher level of apoptosis in the WOCP group. This discrepancy suggests that despite seemingly intact viability, cryopreserved oocytes in the WOCP group experienced increased DNA damage, leading to elevated rates of programmed cell death. The findings align with existing literature on the challenges associated with cryopreservation, particularly the potential for stress-induced damage to cellular structures. Cryopreservation exposes cells to sub-zero temperatures, leading to ice crystal formation, osmotic imbalances, and oxidative stress. Such stressors can adversely affect cellular components, including DNA, and may result in apoptosis (Bojic et al., 2021; Estudillo

et al., 2021; Pegg, 2007). The higher level of apoptosis observed in the WOCP group is consistent with studies indicating that the freezing and thawing processes can induce DNA damage, compromising the overall health of the oocytes.

Interestingly, in sequential studies carried out in 2014 to compare the DNA integrity of oocytes after slow freezing and vitrification, it was demonstrated that slow freezing caused a higher level of DNA fragmentation in oocytes as compared to vitrification (Mathias et al., 2014). These results were however achieved with a Comet assay rather than a TUNEL. The Comet assay and TUNEL assay both detect DNA fragmentation associated with apoptosis but differ in sensitivity and specificity, leading to differences in estimating apoptosis rates. The study also investigated the level of DNA fragmentation in granulosa cells and found the same trend with significantly higher DNA fragmentation in granulosa cells from the slow freezing group. Again, the study demonstrated a significantly higher level of reactive oxygen species in ovarian tissue slow freeze-thawing group and therefore concluded that oocytes and granulosa cells are more susceptible to DNA damage during slow freeze- thawing as compared to vitrification. This study used immature oocytes from mouse ovarian tissue but in bovine, mature oocytes, a significant rate of DNA fragmentation was found after vitrification (Stachowiak et al., 2009).

These studies comparing different cryopreservation models have highlighted variations in cellular responses, supporting the notion that the technique employed plays a crucial role in determining outcomes. WOCP involves preserving the entire ovary, introducing a complex set of variables compared to individual oocyte cryopreservation. This complexity may lead to uneven distribution of stressors, affecting oocytes differently within the same ovary. The failure of the WOCP group to initiate nuclear maturation further underscores the impact of compromised DNA integrity on critical cellular processes. Literature suggests that DNA damage can disrupt the proper progression of cell cycle events, including nuclear maturation,

which is essential for successful oocyte development (Carroll and Marangos, 2013; Senturk and Manfredi, 2013). The observed link between increased apoptosis and reduced nuclear maturation in the WOCP group points to a potential causal relationship between cryopreservation-induced DNA damage and impaired oocyte maturation.

Prior research highlights the detrimental effects of temperature modifications during both cryopreservation and warming on cellular functions, leading to oocyte degeneration due to observed alterations in DNA integrity (Magnusson et al., 2008; Martinez-Burgos et al., 2011). The extent of cryoinjury is intricately linked to the method of cryopreservation and the type of CPA, with the degree of injury being dependent on these specific parameters (Men et al., 2003; Milenkovic et al., 2012). An illustrative example of the impact of cryopreservation methods on oocyte injury can be found in the study by Mathias et al. (2014). Furthermore, the choice of CPA can significantly influence the physiological integrity of oocytes, exemplified by the use of 1,2-propanediol in slow-freezing procedures, as evidenced by changes in the protein expression profile of oocytes compared to control and vitrified mouse oocytes (Larman et al., 2007). The detrimental effects of this specific cryoprotectant extend to increased intracellular calcium, reactive oxygen species (ROS) production, zona pellucida hardening, and decreased oocyte survival when rodent oocytes are exposed to this reagent (Gualtieri et al., 2021). These findings collectively emphasize the nuanced impact of cryopreservation parameters, including temperature modifications, cryoprotectant choice, and method, on oocyte health and viability.

2.4.5 Identifying and selecting high-quality oocytes based on their metabolic activity using BCB

The pentose phosphate pathway (PPP) serves as a pivotal glucose metabolic route, generating Nicotinamide Adenine Dinucleotide (NADPH) and ribose 5-phosphate (R5P) as an alternative to glycolysis (Gutnisky et al., 2014). An essential consideration is the cellular site

where the PPP influences oocyte maturation, with consensus suggesting that heightened PPP activity within cumulus cells triggers a meiosis-inducing signal impacting the oocyte, leading to GVBD (Downs et al., 1998).

Assessing PPP activity can be achieved through the BCB test (Wongsrikeao et al., 2006). The vital dye BCB allows for the selection of oocytes that have completed their growth phase based on Glucose-6-phosphate dehydrogenase (G6PD) activity, the initial enzyme in the PPP, which diminishes as the follicle develops (Lamas-Toranzo et al., 2018). Growing oocytes degrade the dye (lacking blue cytoplasmic coloration), indicating high PPP activity (BCB-), while BCB+ oocytes (displaying blue cytoplasmic coloration) indicate low PPP activity upon reaching their final size (Catala et al., 2011; Lamas-Toranzo et al., 2018; Manjunatha et al., 2007; Rodrıguez-González et al., 2002). Furthermore, oocytes stained BCB+ have demonstrated optimal development to the MII stage compared to BCB- (Alm et al., 2005; Catala et al., 2011). This study utilized BCB staining to evaluate the cytoplasmic activity of oocytes post WOCP and IVM. After 24 hours of maturation, all oocytes in both fresh and WOCP groups were observed to be colourless, despite zero maturation recorded. This suggests continuous energy utilization in the oocyte cytoplasm, as indicated by the initial dye uptake. Furthermore, rapid dye loss in BCB+ oocytes following one hour of incubation and washing also suggests the ongoing activity of G6PDH. This aligns with existing literature that indicates BCB staining as a reliable indicator of oocyte cytoplasmic maturation and metabolic activity.

2.4.6 Chromatin configuration

The chromatin configuration observed in antral follicles is a crucial aspect of oocyte development and maturation. Across different species, oocytes within antral follicles exhibit specific patterns of chromatin organisation, and these patterns can undergo changes as the oocytes progress through different stages of development. In sheep, for instance, oocytes from pre-antral follicles show an NSN configuration, which transitions to an SN pattern in early

antral follicles, and finally, oocytes from medium and pre-ovulatory follicles display the SNE pattern (Russo et al., 2007). This transition in chromatin configuration suggests a dynamic process linked to follicular growth and maturation. Similarly, bovine oocytes, the chromatin configuration undergoes changes during antral follicle development. Oocytes are initially at the NSN stage in follicles smaller than 0.7 mm, but as the follicles grow to 1.5 mm, the NSN pattern disappears, and N, C, and SN patterns begin to emerge (Liu et al., 2006).

The observed variations in chromatin configuration are species-specific and indicative of different stages of oocyte development, with potential implications for gene expression, transcriptional activity, and meiotic competence. In mice, SN-type oocytes exhibit transcriptional silence, while NSN-type oocytes are actively transcribing (Bouniol-Baly et al., 1999; De La Fuente and Eppig, 2001). This relationship emphasizes the significance of understanding chromatin patterns in the context of reproductive biology.

Due to the failure of oocytes derived from WOCP antral follicles to mature, the present study took a targeted approach to unravelling the impact of WOCP on these delicate chromatin configurations. The findings present a compelling narrative of significant alterations, with approximately 54% of oocytes subjected to WOCP displaying a condensed pattern characterized as surrounded nucleolus with additional chromatin condensation near the SNE. Simultaneously, an increase in decondensed chromatin fibres, constituting the NSN configuration, was observed. These alterations not only highlight the sensitivity of chromatin structures to cryopreservation processes but also prompt speculation about adaptive responses or stress-induced changes in oocytes during cryopreservation.

A noteworthy perspective arises from the decrease in the condensed SNE pattern in WOCP oocytes, reminiscent of the pattern observed during the final stages of normal GV-oocyte maturation. This prompts intriguing considerations about the potential defensive

mechanism deployed during cryopreservation. The early condensation observed in response to cryopreservation may serve as a protective strategy, compactly packaging chromatin fibres to shield against the cryodamage incurred during freezing (Kratochvílová et al., 2019). This defensive mechanism could be instrumental in preserving the genetic material integrity of oocytes throughout the cryopreservation process.

Beyond the morphological changes, the study delves into the implications for gene expression and transcriptional activity in WOCP oocytes. The increase in decondensed chromatin fibres, specifically the NSN pattern, suggests a shift towards a more transcriptionally active state. This holds significance in the context of oocyte maturation and subsequent embryonic development, as active transcription in NSN-type configurations is often associated with the expression of genes critical for these processes (Russo et al., 2007).

Moreover, the intimate relationship between chromatin configuration and meiotic competence is a focal point of consideration. Oocytes exhibiting a decondensed chromatin configuration, such as the NSN pattern observed in WOCP oocytes, are typically associated with heightened transcriptional activity but reduced meiotic competence whereas condensed chromatin (SN) correlates with transcriptional quiescence and enhanced developmental potential (Al-aghbari and Menino, 2002; Ferrer-Roda et al., 2024; Ma et al., 2013). This hints at a potential positive influence on the meiotic competence of WOCP-exposed oocytes, potentially impacting their ability to progress through meiosis.

While the study refrains from direct assessments of meiotic progression with these oocytes in particular, the increase in the NSN configuration in WOCP oocytes implies a potential for meiotic progression beyond the GV stage. This observation holds significance, as the NSN configuration is often correlated with oocytes more likely to progress through meiosis.

However, the previous study where oocytes were *in vitro* matured, showed the opposite where oocytes were unable to mature.

The intricate relationship between cryopreservation, cryoprotectant exposure, and the integrity of the granulosa-oocyte interface underscores the critical need for further refinement in cryopreservation protocols. Both cryopreservation and the exposure to cryoprotectants have been implicated in compromising the communication routes between granulosa cells and oocytes. This disruption has broader implications for the integration of oogenesis and folliculogenesis, and its untimely or defective occurrence can lead to specific defects in chromatin remodelling and meiotic competence (Albertini et al., 2003).

The disruption of communication pathways between granulosa cells and oocytes is not merely a mechanical consequence but has profound molecular and developmental repercussions. Inappropriately timed or defective chromatin remodelling resulting from disrupted communication pathways can impair meiotic competence. This emphasizes the intricate coordination required for the normal progression of oocyte development. One of the consequences of this loss in coordination is believed to stem from the failure to appropriately regulate gene expression in developing oocytes and the acquisition of meiotic competence.

In the context of ovarian tissue cryopreservation and transplantation, maintaining the integrity of the granulosa-oocyte interface becomes paramount. Disruptions in this interface can lead to aberrant gene expression and compromised meiotic competence, potentially impacting the success of ART procedures. Therefore, ongoing efforts to optimize cryopreservation techniques should not only focus on the physical preservation of oocytes but also on preserving the intricate cellular and molecular dialogues that are essential for normal folliculogenesis and oocyte development.

The failure of oocytes from WOCP tissue to mature *in vitro* can be attributed, in part, to the observed alterations in chromatin configuration. Typically, the transition from NSN to SN configuration is associated with transcriptional silencing and the acquisition of meiotic competence (Bouniol-Baly et al., 1999; De La Fuente and Eppig, 2001). The coexistence of both patterns in WOCP oocytes indicates an asynchrony in this developmental process, potentially compromising the oocytes' ability to properly regulate gene expression and progress through meiosis. The increased presence of NSN configuration in WOCP oocytes is particularly relevant, as NSN oocytes are generally associated with higher transcriptional activity but often exhibit lower developmental competence compared to SN oocytes (Kratochvílová et al., 2019). This aligns with the observed maturation failure, as NSN oocytes typically show reduced ability to resume and complete meiosis.

The altered chromatin configurations may also impact epigenetic regulation. Changes in histone modifications and DNA methylation patterns, which are closely tied to chromatin structure, could affect the oocytes' ability to properly activate genes necessary for maturation and early embryonic development (Kageyama et al., 2007).

In conclusion, the chromatin configuration changes observed in this study provide a mechanistic explanation for the maturation failure seen in the previous *in vitro* experiment. These alterations reflect a complex interplay of disrupted developmental processes, potentially compromised epigenetic regulation, and altered transcriptional activity, all of which are critical for successful oocyte maturation.

2.5 LIMITATIONS AND RECOMMENDATIONS

Several limitations in the present study warrant consideration, potentially influencing the robustness and generalizability of the results. Firstly, the ovarian tissue utilised in this

investigation was sourced from the reproductive tract of sheep at a local slaughterhouse, introducing variability in the age of the animals. This lack of strict age control may have implications for the study outcomes, emphasising the importance of accounting for age-related variations in future experiments.

Additionally, the estimation of the development potential of immature oocytes using BCB dye, while innovative, yielded unsatisfactory maturation rates for oocytes with both positive and negative BCB staining and in both the control and WOCP experimental groups. This discrepancy might be attributed to challenges in the operational techniques for immature oocyte handling and suboptimal culture conditions. To address this, future experiments would focus on refining the BCB staining procedure. This includes adjustments to the BCB dye concentration and the incorporation of a BCB staining control group to thoroughly investigate any potential negative effects on IVM of oocytes.

Furthermore, the analysis of chromatin configuration faced limitations, including a restricted and highly variable number of sections in both the fresh and frozen groups. The variability in section quality posed challenges for statistical analysis, impeding data interpretation. A significant number of GV-stage oocyte sections were excluded due to damage, and the reduced clarity hindered the differentiation between abnormal chromatin condensation patterns and typical configurations. Future studies could benefit from employing advanced optical imaging techniques, such as confocal microscopy, to gain deeper insights into DNA breaks and alterations in higher-order chromatin structures across various developmental stages (GV, MII, and early embryonic stages). This approach may offer a more dynamic understanding of chromatin behaviour aligned with different transcriptional levels.

An imperative avenue for future research involves directly evaluating meiotic progression and embryonic development. This will ensure a comprehensive understanding of

the reproductive implications associated with exposure to WOCP, aligning with the ongoing quest for a more nuanced comprehension of the experimental outcomes (Russo et al., 2007).

2.6 CONCLUSION

The outcomes regarding DNA fragmentation, morphological assessment, and cumulus cell loss unequivocally underscore the incapacity of antral follicle oocytes from WOCP tissue to attain maturation to the MII stage of meiosis. Despite the uncertainty surrounding cytoplasmic maturation, indicated by colourless oocytes after 24 hours of maturation, it suggests sustained cytoplasmic activity.

The application of BCB staining in this study yields valuable insights into post-WOCP and IVM oocyte cytoplasmic activity. The prolonged colourless state and swift dye loss in BCB-positive oocytes corroborate ongoing energy utilization and G6PDH activity. This aligns with established literature emphasizing the predictive value of the BCB test for oocyte quality and developmental competence.

In summary, the findings suggest a notable influence of WOCP on the chromatin configuration of antral follicle oocytes, potentially impacting gene expression, transcriptional activity, and meiotic competence. The increased prevalence of decondensed chromatin in WOCP oocytes hints at a more transcriptionally active state, potentially favourable for progressing through meiosis. However, a more comprehensive understanding of the reproductive implications of WOCP exposure necessitates direct assessments of meiotic progression and embryonic development in future studies.

CHAPTER THREE : EFFECT OF WOCP ON OOCYTE – CUMULUS CELL CONTACT AND INTERACTION

3.1 INTRODUCTION

In the early stages of growth, the oocyte releases glycoproteins that aggregate to form a translucent, acellular layer known as the zona pellucida (ZP) (Gupta et al., 2007). This layer serves as a boundary between the oocyte and granulosa cells (Gupta et al., 2007). As mentioned earlier (**Chapter 1.4**), during folliculogenesis, the primordial follicles transform in shape and quantity of cells, leading to the formation of an eccentrically positioned fluid filled cavity known as the follicular antrum within the granulosa cell layer (Rodgers and Irving-Rodgers, 2010). This fluid increases in volume, expanding the follicular cavity, causing the oocyte to shift towards its periphery (Gilchrist et al., 2004; Jaffe and Egbert, 2017).

The successful initiation of folliculogenesis and cytoplasmic maturation, plays a pivotal role in ensuring the proper functioning of the female reproductive system. This intricate process relies on the mandatory, precise control through interactions among the oocyte and granulosa cells, facilitated by transzonal projections (TZPs) which penetrate the zona pellucida, reaching the surface of the oolemma (Griffin et al., 2006; Kidder and Mhawi, 2002). Gap junctions which are important for cell physiology, allowing paracrine and juxtacrine signalling, signal transduction and secretory function are present in various mammalian organs and tissue including the ovary where they facilitate the exchange of ion and small metabolites less than 1 kDa (including second messengers such as Ca2+, inositol phosphates or cyclic nucleotides) between neighbouring cells (Goldberg et al., 2004; Kidder and Mhawi, 2002).

These gap junctions establish numerous connections between neighbouring granulosa cells, forming an extensive network of intercellular communication within the somatic cells (granulosa cells, cumulus cells) of the ovarian follicle. This network is particularly crucial

because the granulosa cell layer lacks a vascular supply (Strączyńska et al., 2022). This network has a hexameric structure known as a connexon and comprises proteins from the connexin family (Grazul-Bilska et al., 1997; Söhl and Willecke, 2004) including Cx26, Cx32, Cx37 and Cx43 which have been detected in ovarian follicles of different animals including rat, mouse, pig, sheep and cow (Grazul-Bilska et al., 1997). Most notably Cx43, is localised on the membranes of cumulus oophorous/granulosa cells and the oocyte itself in pig, sheep, rat and cow. The expression of this protein has been seen to increase as the follicle grows in response to FSH resulting in a larger expression in antral follicles (Granot et al., 2002; Johnson et al., 2002; Melton et al., 2001; Simon et al., 2006). Cx37 plays a key role in communication between the oocyte and granulosa cells (Nuttinck et al., 2000; Teilmann, 2005; Veitch et al., 2004). Studies have demonstrated that well-functioning gap junctions are essential for the oocyte to achieve both cytoplasmic and nuclear maturation (Carabatsos et al., 2000) as the interplay between the oocyte and the surrounding cumulus cells through gap junctions is key in controlling meiosis resumption (Luciano et al., 2004; Wigglesworth et al., 2013).

In sheep ovaries, Cx37 and Cx43 are present in both the granulosa and the theca cells of antral follicles whereas the expression of Cx26 is present in the theca layer of antral follicles as well as in the corpus luteum (Borowczyk et al., 2006a; Borowczyk et al., 2006b; Grazul-Bilska et al., 1998). Cx43 is mainly localized between cumulus cells and between the oocyte and cumulus cells, and, in addition the oocyte side of the zona pellucida (Pant et al., 2005). The presence of Cx32 and Cx43 was also detected in ovine corpus luteum. The Cx37 protein is predominantly situated in the larger blood vessels of the ovary, in certain granulosa and theca cells within ovarian follicles, and at the boundaries between cumulus cells and the oocyte (Borowczyk et al., 2006a). It has been further shown that both localization and expression of the ovarian connexins in the sheep is estrous cycle stage-dependent where an increased Cx43

expression has been reported in large antral follicles as compared with small antral follicles (Grazul-Bilska et al., 1998).

3.1.2 Rationale and Hypothesis

The oocyte achieves full competence during the transition from prophase I to metaphase II, allowing it to undergo fertilization and generate a viable embryo. Cumulus cells (CCs) play a crucial role in this process by providing paracrine signals to support meiotic resumption, facilitate nuclear and cytoplasmic maturation, and regulate transcriptional activity (Martinez et al., 2023).

In **Chapter 2**, it was observed that oocytes retrieved from antral follicles, appeared disconnected from their cumulus cells, and were unable to mature *in vitro*. Disruptions in communication pathways critical for integrating oogenesis and folliculogenesis have been associated with improperly timed or defective chromatin remodelling, leading to specific meiotic competence defects (Albertini et al., 2003) which we have seen in **chapter 2**.

Studies in mouse ovaries lacking Cx37 have reported meiotically incompetent oocytes (Carabatsos et al., 2000). Similarly, antisense knockdown of Cx43 in bovine COCs demonstrated the role of Cx43 in the meiotic maturation of bovine oocytes (Vozzi et al., 2001). Studies of defects in the development of the oocyte and granulosa cells in mice diagnosed with mutations in the genes encoding these proteins showed that the lack of the Cx43 stops the growth of the ovarian follicle during the early stages of development and blocks meiosis (Ackert et al., 2001; Norris et al., 2008). Conversely, disruption of gap junctions by silencing the Cx37 gene in mice resulted in the presence of decondensed chromatin in oocytes, typical for the GV stage and the interphase microtubule system, consequently leading to the inability to resume meiosis (Carabatsos et al., 2000).

Both cryopreservation and exposure to cryoprotectants have been found to compromise the integrity of the granulosa-oocyte interface, emphasizing the need for further optimization of cryopreservation protocols to mitigate the disruption of cellular communication routes in the ovary. Additionally, experimental evidence highlights that damage caused by extracellular ice poses a significant obstacle to the extension of cryopreservation techniques to multicellular systems (Pegg, 1987). For instance, vitrification of follicles can lead to cryoinjuries, resulting in the loss of membrane proteins, including Cx37 and Cx43 (Sampaio da Silva et al., 2016). Therefore, our hypothesis suggests that either the cryopreservation technique or the cryoprotectant used may have led to disruptions in the cellular communication routes of the oocyte and cumulus cells, rather than the aspiration method.

3.1.3 Objectives

Recognising the potential of gap junctions as reliable biomarkers for follicle health due to their crucial role in facilitating bidirectional communication between oocytes and granulosa cells, the primary objective of this study was to conduct a morphological visualization of the key proteins. This was achieved through immunohistochemical methods applied to the ovarian cortex following the process of WOCP and subsequent warming. The focus of the qualitative assessment was to gain insights into the spatial localization, intensity, and distribution patterns of Cx43 and Cx37, both before and after WOCP. This qualitative analysis serves as a crucial prerequisite for understanding the potential impact of the cryopreservation process on future follicle developmental capacity.

Additionally, the study aimed to assess cellular proliferation in ovarian tissue by analysing Ki67 expression, thereby providing insights into the viability, proliferative activity, and health of the follicle populations and stromal cells following the WOCP process. This approach also allowed evaluation of the potential impact of cryopreservation on follicle survival and the tissue's capacity to resume normal cellular activities.

3.2 METHODS AND MATERIALS

3.2.1 Experimental design

Ovaries, along with a 10–15 cm length of their associated pedicle, were excised from the reproductive tract upon retrieval from the abattoir. The ovaries were subjected to two different procedures: (i) immediate fixation in formalin (n = 3; Fresh group), and (ii) perfusion with Ringer's solution, CPA, and cryopreservation after ovarian arterial cannulation, following the method previously described (**Chapter 2.2.2**) and previously described by Campbell et al., 2014. After three weeks of cryopreservation, the ovaries were thawed using the method detailed in **Chapter 2.2.3** and Campbell et al., 2014 (n = 3; Cryopreserved group). With each sheep reproductive tract, one ovary was randomly treated as fresh and the other WOCP.

3.2.2 Tissue Fixation and Embedding

The ovary underwent fixation in 10% neutral buffered formalin for a minimum of 24 hours. Subsequently, the fixed tissue samples underwent processing and dehydration through an escalating ethanol series: 70%, 80%, 90%, and 100%. The tissue was then cleared using either xylene (Bouins fixed tissue) or Histo-Clear II (National Diagnostics, GA, USA; for FMS fixed tissue). The embedding medium, paraffin, was gradually and uniformly infiltrated into the tissue within embedding moulds. The infiltrated tissue was allowed to harden in a refrigerator, facilitating subsequent histological evaluation. Thin serial sections of 5 µm thickness, spaced 100 µm apart, were then cut from the tissue using a microtome.

3.2.3 Immunohistochemistry

3.2.3.1 Ki67

The slides were subjected to dewaxing by first immersing them in xylene (Sigma-Aldrich, US) for two cycles of 3 minutes each, followed by a single immersion in a 1:1 mixture of xylene and 100% ethanol (Sigma-Aldrich, US) for 3 minutes. Subsequently, the slides were

immersed in 100% ethanol for two cycles of 3 minutes each, then in 95% ethanol for 3 minutes, followed by sequential immersions in 70% ethanol and 50% ethanol for 3 minutes each. Finally, the slides were rinsed thoroughly with distilled water for 5 minutes each at room temperature to complete the rehydration process. Following this, they underwent three consecutive 5-minute washes with PBS (Sigma-Aldrich, US). Subsequently, the slides were immersed in a microwave-safe container with citrate buffer (Thermo Scientific™, UK), boiled on low heat for 5-7 minutes, and left to stand in the hot buffer for 20 minutes. After another three 5-minute PBS washes, the slides were treated with 3% hydrogen peroxide (Thermo Scientific™, UK) in water for 5 minutes, followed by an additional three 5-minute PBS washes.

For the establishment of a humid incubation chamber, Normal Horse Serum (NHS) blocking serum (Thermo Scientific™, UK) was applied to the slides and incubated for 20 minutes. Excess NHS was blotted away, and the Ki67 primary antibody (Vector Laboratories, Peterborough, UK) was introduced. Incubation occurred overnight at 4˚C, followed by another three 5-minute PBS washes. Biotinylated antibody was then administered to the slides and left to incubate for 30 minutes. The AB Elite complex was prepared and added to the slides, which were incubated for an additional 30 minutes at room temperature.

After three 5-minute PBS washes, the ABC reagent was applied to the slides and incubated for 30 minutes at room temperature. Subsequent to another three 5-minute PBS washes, the DAB substrate was added and left to incubate for 5 minutes. The slides underwent two 5-minute washes with distilled water. Finally, they were counterstained with Mayer's Haematoxylin for approximately 10 seconds, washed before undergoing dehydration and mounting.

Controls for antibody specificity included omission of the primary antibody (negative control) to confirm the absence of non-specific secondary antibody binding and chromogen

reaction; use of positive control tissue known to express Ki67 (rat spleen sections provided by the laboratory); and comparison against established nuclear staining patterns of Ki67 within germinal centres of lymphoid tissue to further validate antibody specificity.

3.2.3.2 Connexin 37 and 43

Serial sections of ovarian cortical tissue, each 5 µm thick and spaced 100 µm apart (n = 2), underwent staining for connexin 37 or connexin 43 using the Bond Max™ equipment from Leica Microsystems Ltd, UK, to visualize gap junctions. The tissue sections were initially dewaxed and rehydrated as part of the preparation process as described in section 3.2.3.1. The primary antibody, specific to Cx37 or Cx43, was then applied to the tissue sections and incubated for a duration ranging from 30 minutes to 1 hour. Subsequently, the sections were thoroughly washed 3 times with PBS.

Following the primary antibody incubation, a secondary antibody was applied and incubated for an additional 30 minutes to 1 hour. A subsequent round of PBS washing was performed to remove any unbound secondary antibody. To visualize the presence of connexin proteins, DAB was applied as a chromogen and incubated for a period ranging from 15 to 30 minutes.

Finally, the stained tissue sections were observed under a light microscope (Nikon eclipse 80i microscope) to visualize the gap junctions. In the microscopy analysis, connexin 37 and 43 proteins were identified by their distinct brown staining patterns.

Controls for connexin staining included omission of the primary antibody (negative control) to evaluate non-specific binding from the secondary antibody and chromogen, as well as the use of positive control tissues known to express connexins—rat heart tissue for Cx43 and previously validated ovary tissue for Cx37. Expected localisation patterns, characterized

by punctate staining at cell junctions, were corroborated by comparison with established descriptions in the literature to further confirm the validity and specificity of the staining.

3.2.4 Image analysis

3.2.4.1. Ki67

After the staining process, 'Volocity' image analysis software (Improvisionw, PerkinElmer; Cambridge, UK) was utilized to capture random images of the ovarian stroma for each tissue section (n = 3 per tissue section). Subsequently, all positively stained and counterstained cells in each image were quantified using the same 'Volocity' software, and the percentage of cells expressing Ki67 was calculated. Due to non-normal distribution of the data, a comparison between time 0 and post-treatment tissue was conducted using the Wilcoxon-signed rank test. The observer was not blinded to the treatment assignment. This lack of blinding carries the risk of observer bias: prior knowledge of treatment group could have subconsciously influenced the consistency of cell identification, the thresholds applied to define positivity, or the interpretation of borderline staining, potentially inflating or minimizing apparent differences between groups. Although the same analytical settings were applied across all images to limit this effect, the risk of bias cannot be entirely excluded.

3.2.4.2 Connexin 37 & 43

Upon completion of immunohistochemical staining for Cx43 and Cx37, the processed tissue sections were subjected to examination using a Nikon DS – RiL camera connected to Nikon eclipse 80i microscope with a Nikon digital imaging head. Photomicrographs were systematically captured at 20x or 40x magnification to ensure optimal visualization of cellular details and staining characteristics.

A thorough qualitative assessment of the staining patterns and distribution of both Cx43 and Cx37 was carried out within the ovarian tissue. The staining was visualized as a distinct brown colour resulting from specific chromogenic reactions (DAB), for positive staining. The

expected staining patterns for Cx43 and Cx37 included positive punctate staining, potentially appearing as distinct brown spots or dots, localized between adjoining cells, particularly in areas involving cumulus-oocyte connections. The intensity of the brown staining and its distribution were crucial aspects of the qualitative analysis. The observer was not blinded to treatment assignment, introducing the possibility of subjective bias. Awareness of group allocation may have influenced the perception of staining intensity or subtle differences in distribution and could also have shaped the choice of representative images. This presents the risk of unintentionally reinforcing expected outcomes and overestimating treatment-associated effects. While standardized imaging protocols and systematic selection criteria were used to reduce subjectivity, these potential sources of bias remain a limitation of the study.

Representative images were selected from the pool of systematically captured photomicrographs to provide a comprehensive record of staining patterns. For each tissue section, multiple fields were first acquired at 20x and 40x magnification to include both stromal and follicular regions. Selection of representative images was then guided by pre-defined criteria: (i) adequate preservation of tissue morphology without significant artefacts such as folds, tearing, or uneven staining; (ii) clear visualisation of positive stain; and (iii) presence of follicles at varying maturational stages allowing documentation of the variation in connexin (Cx37 and Cx43) localisation and intensity that occurs during folliculogenesis. In addition, images were selected from both fresh ovarian tissue and WOCP tissue to enable comparison of staining characteristics between groups. The aim was to capture a spectrum of staining responses—ranging from weak to more intense signals—rather than highlight only isolated areas of strong positivity.

3.3 RESULTS

3.3.1 Ki67 expression

Ki67 immunostaining was employed to evaluate the proliferative activity of cumulus cells in the ovarian tissue samples (**Figure 3.1**). The Ki67-positive cell percentages within the cumulus cell population were assessed in both the control and WOCP groups. While a noticeable trend of increased Ki67-positive cumulus cell percentages was observed in the WOCP group (72.9%) compared to the control group (71.46%), the difference did not reach statistical significance (p-value<0.5).

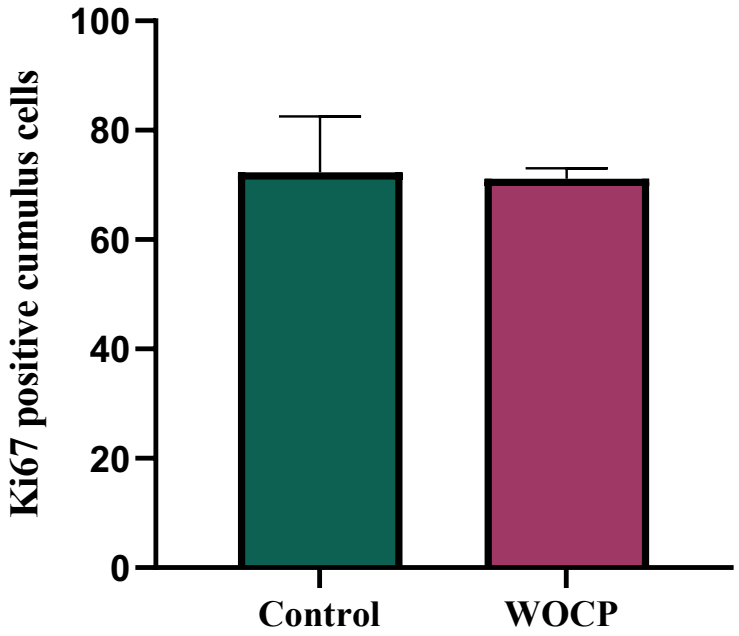

Figure 3.1 Graph showing the mean percentage of cumulus cells staining positive for the Ki67 antigen protein in ovarian tissue collected before (control) and following WOCP (WOCP).*Significant difference ($P < 0.05$) between control and post-WOCP readings. Error bars in represent the SEM.

3.3.2 Localisation of Connexin 37 and 43 expression post WOCP

Upon microscopic examination of immunohistochemically stained ovarian tissue sections, distinct patterns of Cx37 expression within the gap junctional network were observed.

In the control group, Cx37 protein predominantly localized in larger blood vessels within the stromal tissue of the ovarian cortex and medulla. Furthermore, Cx37 expression was detected at the borders between oocytes and cumulus cells, along with some granulosa cells, showing notable presence along cellular borders and within the cytoplasm. Weak staining in theca cells was observed, primarily in a limited number of follicles, and exhibited a punctate pattern, highlighting the existence of gap junctions in these regions.

Following WOCP and subsequent warming, the qualitative analysis indicated a consistent presence of Cx37 in similar locations. The staining patterns within the blood vessels, at the oocyte-cumulus cell borders, and in granulosa cells remained observable. However, a notable difference was observed in Cx37 staining post-WOCP, particularly in the reduced distinctness between the oocyte and the cumulus cells of the antral follicles compared to the control group. This suggests potential alterations in Cx37 distribution and intensity, emphasizing the impact of cryopreservation on the gap junctional network in ovarian tissue.

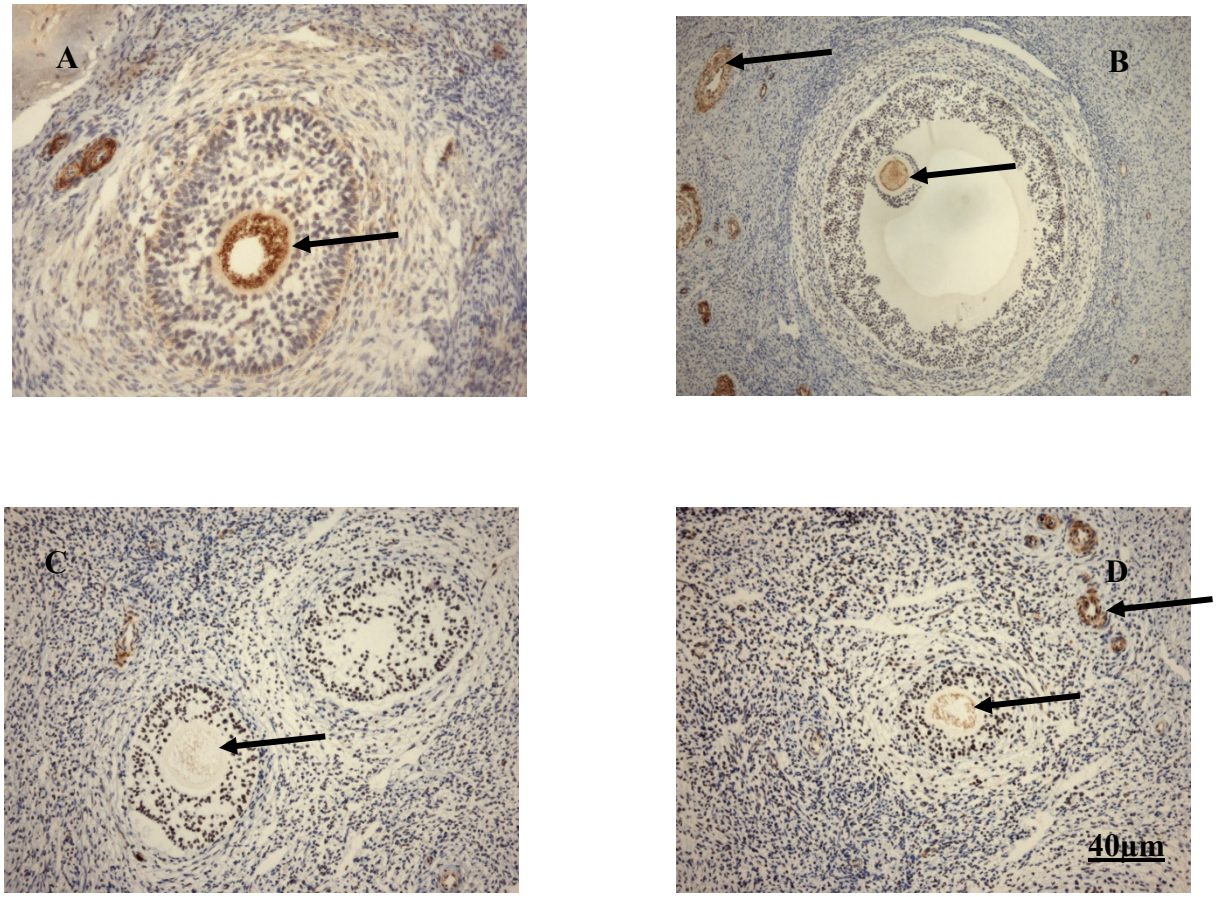

Figure 3.2 Representative Cx37 protein expression (arrows) in the secondary follicle of the control group (A), in antral follicle and blood vessel of the control group (B), in secondary follicle and early antral follicle of the WOCP group (C), secondary follicle and blood vessels of the WOCP group (D). Bar = 40 x.

Concomitantly, Cx43 staining in the control group exhibited prominent localization between adjoining cumulus cells and between the oocyte and cumulus cells in all COCs, irrespective of follicular size. Additionally, positive staining was observed on the oocyte side of the zona pellucida, while theca cells showed few and scanty spots of staining in between some cells.

Post-WOCP, qualitative analysis revealed a consistent presence of Cx43 in the previously mentioned locations. However, the staining patterns between adjoining cumulus cells and between the oocyte and cumulus cells appeared notably faint. Importantly, the intensity of Cx43 staining tended to decrease post-WOCP compared to the control group,

suggesting potential alterations in Cx43 distribution and intensity following cryopreservation of the whole ovary. Despite the decreased intensity, positive staining on the oocyte side of the zona pellucida remained distinct in WOCP tissue.

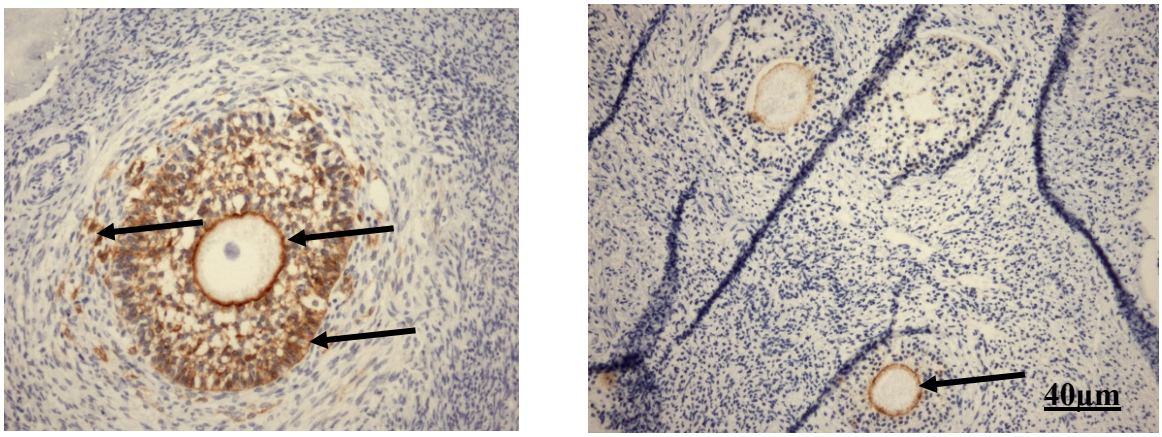

Figure 3.3 Representative Cx43 protein expression (arrows) in the secondary follicle (theca cells, cumulus cells, around the oocyte) of the control group (A), the secondary follicle (around the oocyte) of the WOCP group (B). Bar = 40 x.

3.4 DISCUSSION

The underlying hypothesis of the study was that the defects observed in Chapter 2 may stem from disruptions in the communication pathways between oocytes and cumulus cells, potentially induced by the cryopreservation technique or the cryoprotectants employed. This hypothesis is in line with the observation that damage from extracellular ice can result in the disruption of membrane proteins, including Cx37 and Cx43 (Tanpradit et al., 2015). The qualitative analysis conducted in this study revealed a reduction in these membrane proteins' presence between the oocyte and cumulus, as well as adjoining cumulus cells. This suggests a plausible connection between cryopreservation-induced changes and the integrity of cellular communication in the ovary, supporting the study's central hypothesis.

The Ki67 immunostaining results revealed the proliferative activity of cumulus cells in ovarian tissue samples, providing insights into the impact of WOCP. In the control group, the mean percentage of Ki67-positive cumulus cells was 72.97%, while in the WOCP group, it was slightly lower at 71.46%.

Despite the numerical decrease in the mean percentage of Ki67-positive cumulus cells in the WOCP group, the difference did not reach statistical significance (p-value: 0.42). This suggests that, based on the Ki67 marker, there was no significant difference in the proliferative activity of cumulus cells between the control and WOCP groups.

Studies employing Cx37 and Cx43 knockout models have elucidated the essential roles of both connexins in the growth and development of ovarian follicles, each contributing differently to specific cell types within the follicle. Cx37 protein in cows was identified in both oocyte and granulosa cell compartments, with a primary localization observed during the preantral stages of follicular development (Nuttinck et al., 2000). In mice, Cx37 protein was primarily confined to cumulus cells and the oocyte, though some immunoreactivity extended to granulosa cells more distant from the oocyte (Simon et al., 2006). Conversely, in sheep, Cx37 protein was found at the oocyte-cumulus borders and in certain granulosa and theca cells (Borowczyk et al., 2006a) which is consistent with the observation of the in the control group of this study. This suggests that the staining protocol was successful and Cx37 protein predominantly resides on oocyte-cumulus cell borders of sheep ovarian secondary and antral follicles, displaying species-specific distribution in follicular tissues.

On the other hand, Cx43 in sheep was identified to be situated between cumulus cells and also between the oocyte and cumulus cells. Some staining was additionally observed on the oocyte side of the zona pellucida (Pant et al., 2005). In line with our results, Cx43 in most

species has been localized at the cellular borders of granulosa/cumulus cells and at the interface between the oocyte and the surrounding cumulus cells.

Consistent with earlier research, OTC has been shown to cause the under-expression of Cx43 protein in mice (Lee et al., 2008). Furthermore, a separate study in sheep highlighted a decrease in the gene expression of *Cx43* in vitrified ovarian tissue followed by *in vitro* culture, suggesting that follicular cells are more susceptible to cryoinjuries compared to oocytes (Sampaio da Silva et al., 2016). It's important to note that this specific study in sheep concentrated on secondary follicles hence a similar observation here in both antral and secondary follicles is consistent. Additionally, the slow recovery of cellular metabolism after vitrification is known to negatively influence protein translation (Choi et al., 2008; Segino et al., 2005). Moreover, *in vitro* culture, whether applied to isolated follicles or follicles within ovarian tissue, has been reported to reduce Cx43 expression (Sampaio da Silva et al., 2016). These findings suggest that vitrification and subsequent in vitro culture can impair the expression of Cx43 by slowing cellular metabolism and protein synthesis, which may compromise follicular cell communication and viability.

Consequently, both Cx37 and Cx43 mRNA expression were detected in both fresh and vitrified ovarian tissue, and no significant differences were observed between the two groups . This aligns with findings by Kristensen et al. (Kristensen et al., 2015), who reported that the mRNA expression of Cx37 and Cx43 in human ovaries remained unaffected by cryopreservation. In terms of protein expression, Cx37 showed similar levels between fresh and vitrified tissue, while Cx43 was not observed in vitrified tissue. This is consistent with previous studies that demonstrated lower Cx43 expression in cryopreserved ovarian tissues across different species, such as mice (Boland and Gosden, 1994) and felines (Luciano et al., 2009), and this lower expression has been associated with compromised follicular development. Although these results were obtained following vitrification, they are comparable to the

observations in this study as slow freezing has been shown to be more detrimental to follicles compared to vitrification.

In another study, the complementary deoxy ribonucleic acid (cDNA) array data analysis revealed abnormal gene expression in granulosa cells from antral follicles of subcutaneously transplanted cryopreserved mouse ovarian tissue (Lee et al., 2008). The most significant abnormality was found in the gene coding for gap junction proteins, particularly Cx43. Both mRNA and protein expression of Cx43 in granulosa cells were significantly lower compared to control (fresh) ovaries. Cx37, the corresponding connexin on GV oocytes, was also under expressed. Extensive apoptosis was observed in granulosa cells from the cryopreserved, transplanted ovarian tissue.

The findings suggest impaired cell-cell adhesion or interaction between cumulus/granulosa cells and oocytes in WOCP tissue, potentially explaining the poor development of oocytes from antral follicles, *in vitro* and the disconnection of cumulus cells of oocytes retrieved from WOCP tissue as observed in **Chapter 2**, despite oocytes surviving freezing and thawing.

3.5 LIMITATION AND RECOMMENDATIONS

The major limitation of this study is that the observer performing the qualitative assessment of the staining patterns and distribution within the ovarian tissue was not blinded to the treatment group. This introduced the potential for observer bias, since prior knowledge of treatment allocation may have unconsciously influenced interpretations of staining intensity, distribution, or the selection of representative images. While the observer was experienced in histological analysis, awareness of treatment assignment posed a greater methodological concern than the fact that only one observer was involved. Had blinding been implemented,

the reliance on a single trained observer would likely have been sufficient. As qualitative assessments inherently involve some subjectivity, the absence of blinding increases the risk of systematic bias, potentially skewing results and limiting the robustness of conclusions regarding treatment effectiveness. This limitation could have been reduced by having an external individual label the slides to conceal treatment status prior to analysis.

Additionally, the absence of quantitative measurements for the assessment of Cx37 and Cx43 in this study, such as western blotting for protein expression levels, enzyme-linked immunosorbent assays (ELISA) for concentration quantification, or flow cytometry to determine cellular distribution percentages, limits the ability to provide more objective and reproducible data. Quantitative methods like these offer systematic, standardized analysis, reducing variability from individual interpretation. The sole reliance on qualitative technique (i.e., subjective scoring of immunohistochemical staining) may introduce bias, potentially affecting the overall reliability and generalizability of the study findings.

Another limitation includes the inherent variability among individual sheep samples, potentially influencing Ki67 percentages due to factors like variations in tissue quality and specific characteristics of the animal subjects. The relatively small sample size of sheep specimens might constrain the generalization of the findings to the broader population. Methodologically, while Ki67 provides valuable insights into cell proliferation, it may not capture the full functional complexity of cumulus cells.

In future investigations, incorporating blinded assessment of tissue samples would substantially reduce observer bias and improve the rigor of qualitative analysis. Employing multiple independent observers and incorporating quantitative measurements would additionally strengthen the validity of the findings by providing a more objective, reproducible evaluation of Cx37 and Cx43 expression in ovarian tissue. Finally, future studies involving

larger sample sizes may provide deeper insights into the impact of cryopreservation on gap junctional proteins and cumulus cell proliferation.

3.6 CONCLUSION

In conclusion, the results suggest that both Cx37 and Cx43 exhibit consistent presence in specific locations within the ovarian tissue, but cryopreservation, particularly WOCP by slow freezing, may lead to alterations in their distribution and intensity, emphasizing the impact of cryopreservation on the gap junctional network in ovarian tissue.

CHAPTER FOUR: THE EFFECT OF WOCP ON TRANSCRIPTOME AND GLOBAL DNA METHYLATION OF THE SHEEP OVARY

4.1 INTRODUCTION

There are two inherent risks in WOCP and TP. The first one, which is the risk of malignant cell reimplantation, is only applicable in cancer patients. This is the risk that cancer cells from the original tumour could be transplanted back into the body along with the ovarian tissue (Rosendahl et al., 2013). This risk exists with both cortical strip transplantation and WOCP, but it is thought to be higher with WOCP because more tissue is being transplanted. However, to reduce the risk of malignant cell reimplantation, it is recommended to freeze an ovarian biopsy separately from the whole ovary (Eijkenboom et al., 2022). This biopsy can then be tested for cancer cells before the whole ovary is transplanted. The second risk is that the procedure is all-or-nothing which means that if anything goes wrong during the surgery or transplantation, all follicles in the ovary will be lost. This is in contrast to cortical strip transplantation, where multiple attempts can be made with the remaining frozen fragments. An adverse outcome may be cryopreservation problems and clot formation during auto-transplantation. Cryopreservation problems can occur if the tissue is not frozen properly, which can damage the follicles. Clot formation during auto-transplantation can block or reduce blood supply to the ovary, which can also cause follicular damage. Although Campbell et al. (2014) demonstrated an effective freezing procedure and anti-thrombotic strategy in sheep which resulted in 100% (14/14) restoration of ovarian function, with high rates of natural fertility (pregnancy rate: 64% (9/14); live birth rate: 29% (4/14)), histological examination 11 to 23 months later revealed a 60–70% follicle survival rate (Campbell et al., 2014).

Prior to this, other experiments faced rapid loss of follicles after transplantation. This includes the first report of live birth after transplantation of cryopreserved whole ovine ovary

in 2006 where follicle survival after 18–19 months was only 1.7% to 7.6% of that in non-transplanted control ovaries (Imhof et al., 2006). There became a need for improvements in techniques related to whole ovary cryopreservation and transplantation. In a study by Onions et al, which examined the effects of an anti-apoptotic agent called sphingosine-1-phosphate (S-1-P) on the efficiency of ovarian cryopreservation, the experiment showed that while fresh controls and freshly perfused ovarian transplants maintained vascular patency, cryopreserved transplants experienced a cessation of blood flow, resulting in blood clots in the ovarian artery and ovarian medulla. The study also found a significant loss of follicles in cryopreserved ovaries after transplantation and observed increased levels of proliferation and apoptosis in these ovaries compared to their initial state. (Onions et al., 2008). These studies indicate that further investigations can expand our understanding and knowledge surrounding follicle survival after cryopreservation could potentially lead to further advancement in treatment protocols, improving primordial/transitional follicle survival for many years.

Transcriptomic analysis is a powerful tool that can be used to study the ovary. It can be used to identify genes that are involved in different aspects of ovarian function, such as folliculogenesis, oocyte quality, ovulation, and hormone production. As the transcriptomic profile of the ovary changes in response to environmental exposures, such as pollutants and toxins leading to possible damage to the ovaries (Sharara et al., 1998; Yao et al., 2023) and to infertility, applying these techniques here after WOCP will give us some insight into those changes that may have occurred during the process of cryopreservation.

Secondly, epigenetics which was initially coined in the 1940s by Conrad Waddington (Chatterjee et al., 2017) and has now been defined as ‘‘the study of changes in gene function that are mitotically and/or meiotically heritable and that do not entail a change in DNA sequence’’ (Wu and Morris, 2001). These epigenetic mechanisms or marks include DNA methylation, histone post-translational modification and non-coding RNA (ncRNAs). DNA

methylation has been found to occur at the 5th carbon of cytosine residues mostly in CpG dinucleotides in mammals and is associated with transcriptional silencing, imprinting, X-chromosome inactivation and the silencing of repetitive and centromeric sequences (Goldberg et al., 2007). On the other hand, histone post-translational modifications alter the chromatin structure by the addition or removal of functional groups (acetyl, methyl, phosphoryl) on histone proteins, which wrap around DNA. This tends to affect DNA stability and the transcription machinery (Fan et al., 2015). Lastly, non-coding RNAs, which are transcribed from DNA but not translated into proteins, have been found to be essential for cell fate decisions (Pauli et al., 2011), controlling several levels of gene expression (Qureshi and Mehler, 2012) and have important roles in signalling networks and the epigenome (Quinn and Chang, 2016).

During oogenesis, epigenetic factors play a major role in regulating gene expression. The first phase of oogenesis (primary oocyte until it is arrested in prophase I of meiosis) is characterized by intense transcription, followed by a phase of meiotic activity and transcriptional silencing (Christou-Kent et al., 2020). During this second phase (resumption of meiosis), changes in gene expression are dependent on the translation and degradation of transcripts. This is crucial for assembling the molecular machinery required for meiotic progression, fertilisation, and embryo development (Reyes and Ross, 2016; Sendžikaitė and Kelsey, 2019). The transcripts content shows that temporal changes in gene expression are mostly regulated via epigenetic mechanisms and associated with oocyte competencies (Conti and Franciosi, 2018). Therefore, any factors that influence genome integrity and transcript synthesis/repression, stability, and association with the translation machinery can have a major impact on protein expression and crucial biological processes (Albertini and Olsen, 2013).

A few studies have been carried out to assess some epigenetic markers in oocytes following cryopreservation. Some of these studies carried out in mouse, pig and cattle oocytes

have demonstrated aberrant changes in DNA methylation (Hu et al., 2012). Vitrified mouse oocytes for instance demonstrated an abnormal pattern of the H4K12 acetylation after pronuclear formation, which in turn affects chromatin assembly and development of fertilised oocytes (Suo et al., 2010). Similarly, both slow freezing and vitrification have caused a significant reduction in global DNA methylation levels of bovine oocytes (Urrego et al., 2014).

It is important that WOCP does prolong follicle survival after transplantation, is not harmful to oocyte development, future pregnancies and does not pose concern in the health of offspring that may be obtained from the oocytes post cryopreservation. It is necessary to ensure the effect of cryopreservation conditions (e.g., type and concentration of CPA) on epigenetic status and their possible biological implications for the offspring are fully assessed to improve the safety and efficacy of cryopreservation.

4.1.2 Rationale and hypothesis

Building on the observations detailed in Chapters 2 and 3, where the cryopreservation process was associated with increased apoptosis, perturbed maturation, and a disconnection between cumulus and oocytes in antral follicles, additional molecular studies are warranted. These studies should delve into critical genes involved in oocyte and follicle development, apoptosis, cell division, spindle checkpoint regulation, imprinted genes, early indicators of follicle loss (a significant concern post-transplantation), DNA methylation, and other epigenetic-related genes. Such investigations are essential for a more comprehensive understanding of the effects of the cryopreservation technique on ovarian molecular processes.

To achieve this, transcriptomic analysis emerges as a promising and innovative approach, offering an opportunity to explore and comprehend the molecular changes occurring in sheep ovaries post-cryopreservation. In animal studies focused on oocyte vitrification, research findings have indicated that the procedure can induce alterations in global DNA

methylation (Zhao et al., 2013) and impact gene expression profiles (Anchamparuthy et al., 2010; Barberet et al., 2020; Dai et al., 2015). Consequently, it is hypothesised that the slow freezing of the whole ovary induces changes in the transcriptomic profile of ovarian tissue, potentially influencing oocyte development, especially in transitional follicle stages, as well as cell-cell communication and DNA methylation processes. This molecular insight will contribute to a more nuanced understanding of the implications of cryopreservation at the transcriptomic level.

4.1.3 Aims and objectives

The aim of this study was to investigate whether the cryopreservation of whole sheep ovaries causes transcriptional and DNA methylation changes in the tissue.

The study aimed to investigate the immediate effects of whole ovarian slow freezing on the global transcriptome dynamics on the ovary using the microarray technique and the global DNA methylation in the ovarian cortex using enzyme-linked immunoassay (ELISA).

4.2 METHODS AND MATERIALS

4.2.1 Experimental design

Sheep ovaries (n=6) from three different animals were used in this study. For each animal, one ovary was cryopreserved (n=3) following the protocol described in **Chapter 2.2.2**, while the contralateral ovary served as a fresh control (n=3). Following thawing of the cryopreserved ovaries or immediately after heparin perfusion for the fresh controls, the ovarian cortex was obtained using a skin grafting device (Rosenberg micro-dermatome; 4Med Ltd.). The dermatome was adjusted to obtain a consistent depth of 1 mm across all samples, ensuring that only the outer cortical layer of the ovary was excised. From each ovary, cortical strips measuring approximately 10–12 mm in length and 5–7 mm in width were excised, producing

fragments of ~50–80 mm² surface area and ~1 mm depth. Given that a whole sheep ovary typically measures ~20–25 mm in length and ~10–15 mm in width, the sampled fragments therefore represented only a small proportion (approximately 10–15%) of the total ovarian cortex. These fragments were used for RNA extraction (microarray; **Figure 4.1-2b**) and DNA extraction (global DNA methylation; **Figure 4.1-2a**).

A limitation of this sampling method is that the ovarian cortex is not uniform in its biological composition: follicle density and distribution, stromal composition, and vascular patterns vary across different cortical regions. By sampling only narrow strips of the outer cortex, there is a risk that the material analysed may not be fully representative of the entire ovary. Consequently, the findings reflect molecular and histological features of the sampled regions only, and caution is required in extrapolating them to the whole ovary. Although this method was selected to ensure consistent sampling depth across both groups, it nevertheless introduces variability depending on local follicle density and stromal patterning, which should be considered when interpreting the data.

.

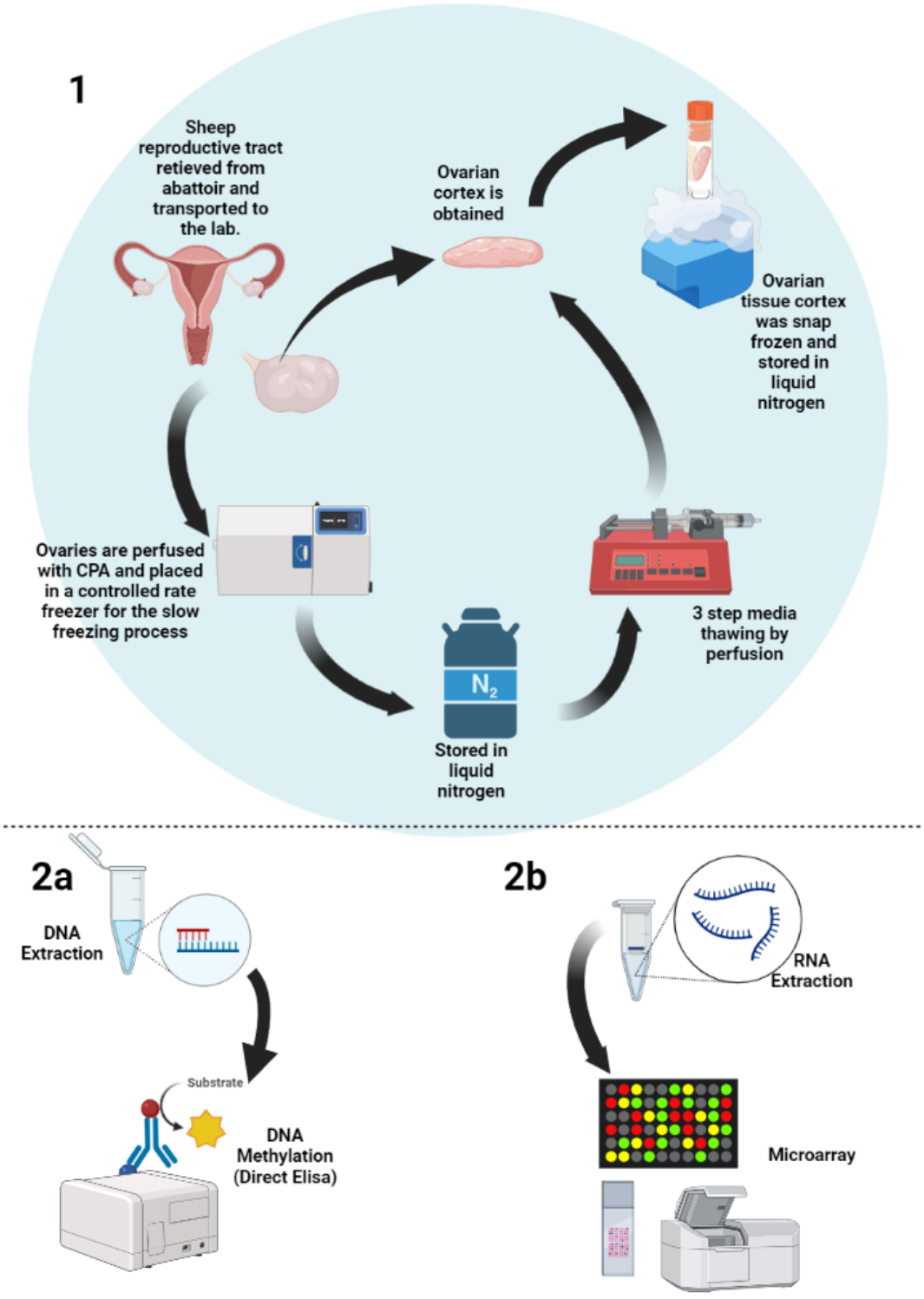

Figure 4.1 Diagram with the experimental design showing (1) cryopreservation and thawing of the ovary, (2a) DNA extraction of the ovarian cortex for global DNA methylation and (2b) RNA extraction for Microarray. Image was created using Biorender.

4.2.2 Ovarian tissue disruption and purification of total RNA

The RNA extraction was carried out using the RNeasy Mini Kit (Qiagen, USA) following manufacturer's protocol (**Figure 4.2**). Ovarian cortex stored in -80C freezer was retrieved with 30 mg of each sample weighed, disrupted in 600µl of Buffer RLT containing 1% β-mercaptoethanol (Thermo Fisher Scientific™, UK) and homogenized using the TissueLyser system (Qiagen, USA). The sample was then centrifuged ≥8000 x g and the supernatant transferred into a clean microcentrifuge tube supplied by Qiagen, USA. A volume of 70% ethanol was added to the lysate at a 1:1 ratio and mixed by pipetting. A total volume of 700µl of the ethanol-lysate mixture was then applied to the RNeasy Mini spin column and centrifuged for 15 s at ≥8000 x g. The flow-through was discarded and the column was further washed with 700µl Buffer RW1 which was subsequently followed by 500µl Buffer RPE, twice, each of which was centrifuged at for 2min at ≥8000 x g to efficiently wash away contaminants. The column was then transferred into a new 1.5 ml collection tube (Eppendorf AG, Germany) where 50µl RNase-free water was directly released onto the spin column membrane and centrifuged for 1 min at ≥8000 x g to elute the RNA.

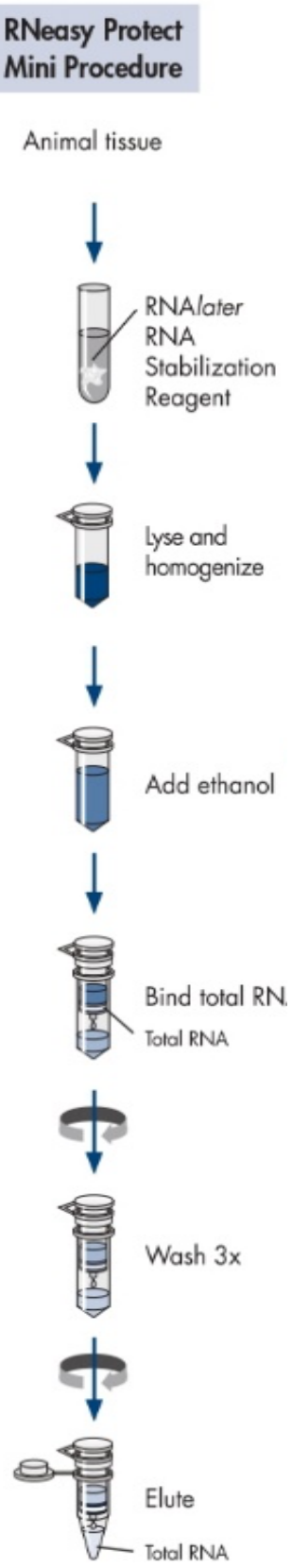

Figure 4.2 Total RNA extraction from tissue using the RNeasy Mini Kit (Qiagen, USA)

4.2.3 Microarray (Fresh & WOCP sheep ovarian tissue)

The microarray was carried out using the GeneChip™ Ovine Gene 1.0 ST Array by Thermo Fisher Scientific. Following extraction, total RNA with 260/230 > 1.5 measured with the NanoDrop™ 1000 Spectrophotometer (Thermo Fisher Scientific Inc., UK), was used in the microarray experiments which was carried out at the Nottingham Arabidopsis Stock Centre of the University of Nottingham (Dr M Castellanos Uribe; School of Biosciences, Sutton Bonington Campus, Loughborough, LE12 5RD, UK). Total RNA quality and integrity was evaluated (Agilent-2100 Bioanalyzer System) and only samples surpassing the minimal quality threshold (RIN > 8.0) were used in the subsequent microarray assessment. Complementary DNA (cDNA) was generated from 50 ng/µl of total RNA as per the GeneChip™ WT-PLUS Reagents (Thermo Fisher Scientific/Affymetrix, UK) and followed by *in vitro* transcription to produce cRNA, end-labelled and hybridised for 16 h at 45˚C to Clariom™ S Human Arrays (Thermo Fisher Scientific/Affymetrix, UK). Washing and staining steps were performed by a GeneChip Fluidics station 450 and scanning was done using ™ Scanner 3000 7G System (Thermo Fisher Scientific/Affymetrix, UK) according to manufacturer's instructions (**Figure 4.3**). Also, at the Nottingham Arabidopsis Stock Centre of the University of Nottingham, the raw CEL files were normalised using RMA background correction with quantile normalisation, log base 2 transformation by Dr M Castellanos Uribe. Differentially expressed genes were considered significant when p-value was < 0.05, FDR (false discovery rate) ≤ 0.05 with Benjamini-Hochberg correction, and fold-change of >1.0 or < -1.0.

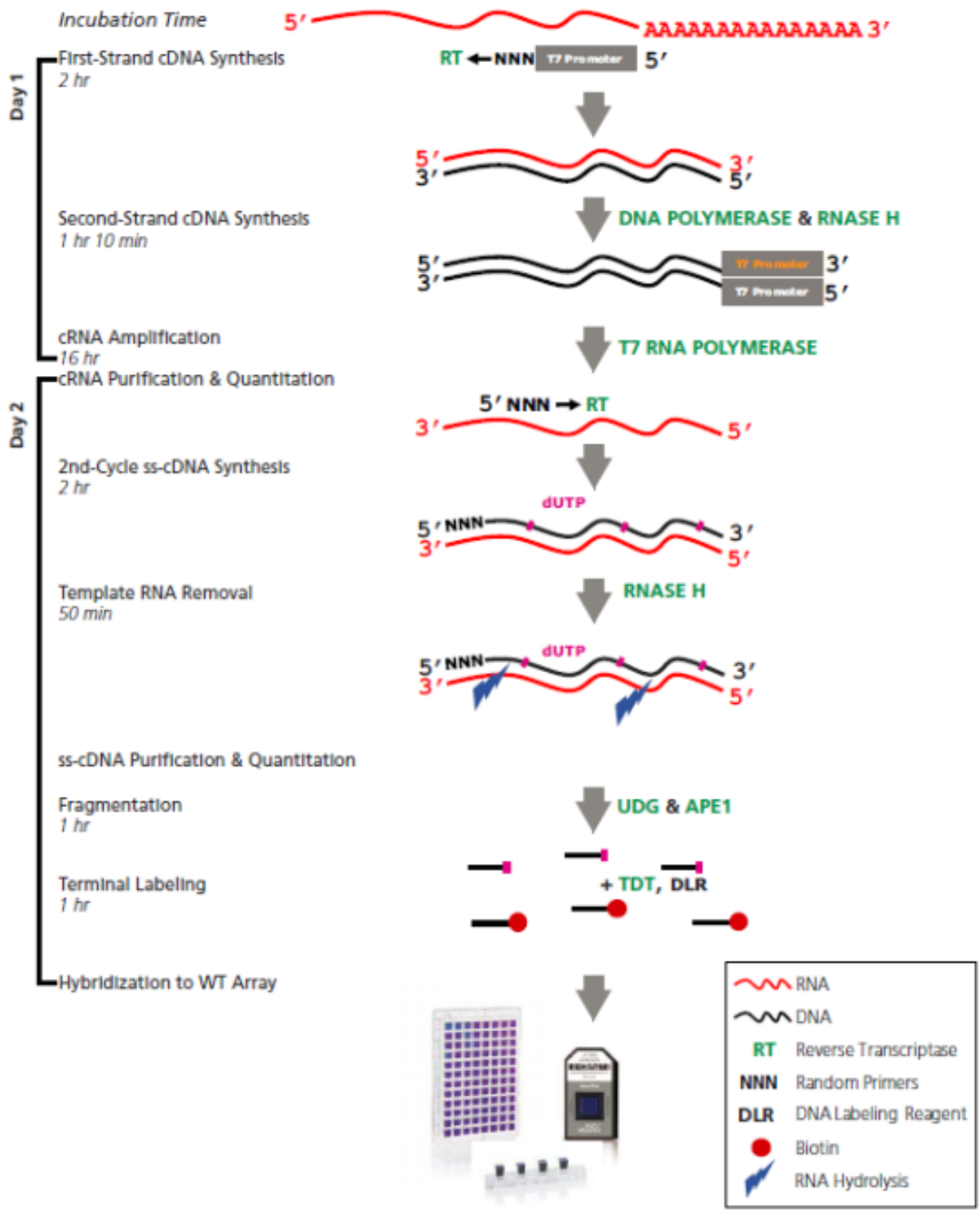

Figure 4.3 Microarray syntheses of total RNA using GeneChip™ Whole Transcript (WT) Expression Arrays by Thermo Fisher Scientific/ Affimetrix UK. The process begins with cDNA synthesis; it's amplification and purification and finally the hybridisation of the WT array.

4.2.4 Microarray confirmation using polymerase chain reaction (PCR)

For each sample that was analysed by microarray, an appropriate volume of RNA product was stored at -80˚C to be used for validation of the microarray results. cDNA templates were produced as described in **section 4.2.5.1** which was followed by relative quantification by PCR as described in **section 4.2.5.2** below. **Figure 4.4** below briefly displays the workflow of this gene expression protocol.

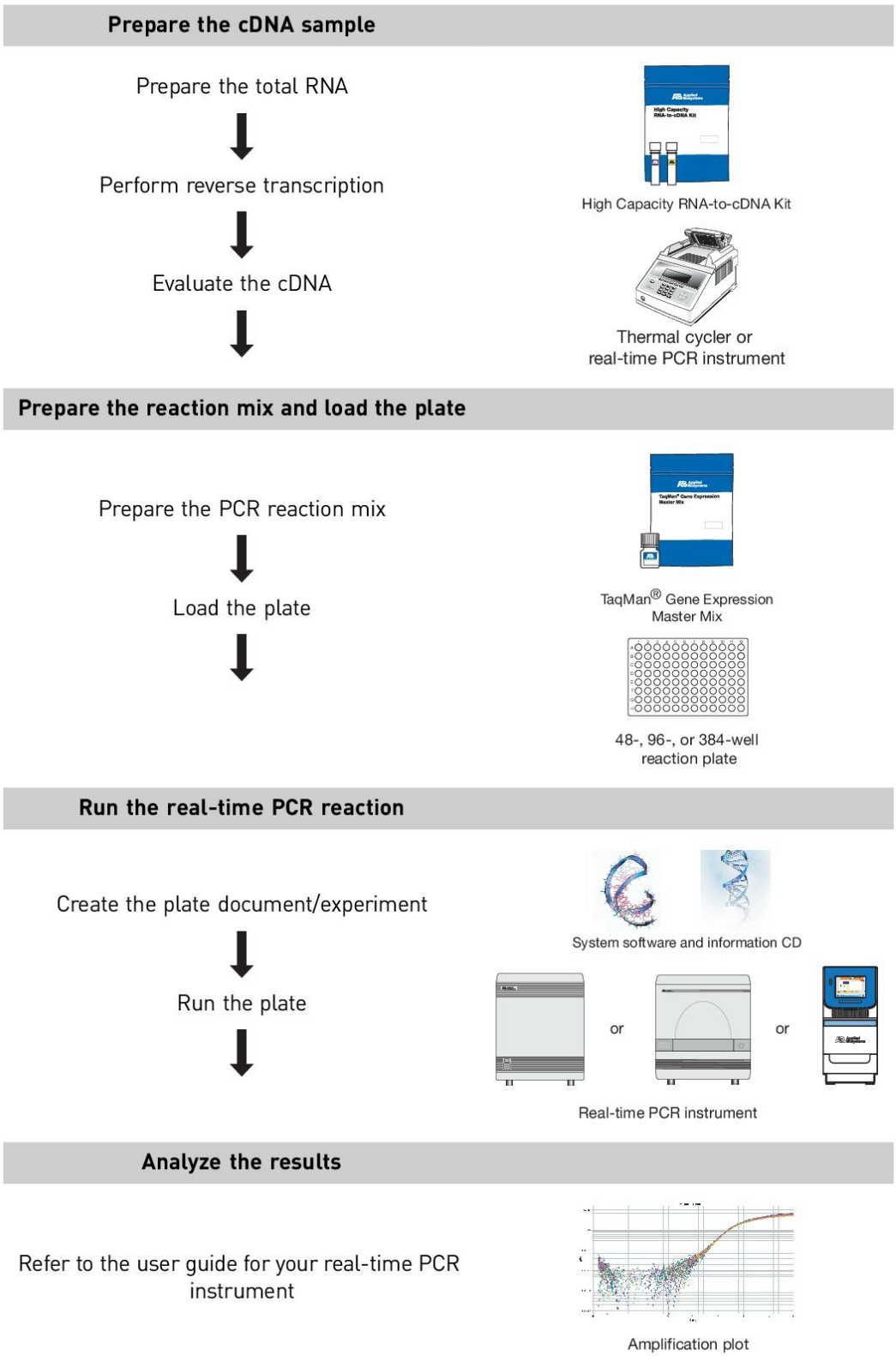

Figure 4.4 Workflow of the gene expression protocol

4.2.5.1 cDNA synthesis from Total RNA

The High-Capacity RNA-to-cDNA™ Kit from Thermo Fisher Scientific Inc., UK was used for cDNA synthesis. Following the manufacturer's protocol, the following reagents were used: 10X RT buffer, 25X dNTP mix (100 mM), 10X RT random primers, MultiScribe™ Reverse Transcriptase. The master mix was prepared by combining these reagents (**Table 4.1**). A volume of 10 µl of the master mix was added to each individual tube, followed by 10 µl of RNA sample (200ng/ µl). The reaction tubes were sealed, centrifuged, and placed on ice. The thermal cycler (7500 Fast Real-Time PCR System; Applied Biosystems, UK) was programmed to follow the conditions in **Table 4.2**.

Table 4.1 The reagents and quantities for cDNA library building from RNA

Component	Volume
10X RT Buffer	2.0 µl
25X dNTP Mix (100 mM)	0.8 µl
10X RT Random Primers	2.0 µl
MultiScribe™ Reverse Transcriptase	1.0 µl
RNase Inhibitor	1.0 µl
Nuclease-free H2O	3.2 µl
Total per reaction	**10.0 µl**

Table 4.2 The cycling conditions for cDNA library building from RNA

Settings	Step 1	Step 2	Step 3	Step 4
Temperature	25°C	37°C	85°C	4°C
Time	10 minutes	120 minutes	5 minutes	Hold

The reverse transcription reaction took approximately 2 hours to complete. Once the reaction was finished, PCR assays were performed.

4.2.5.2 Relative quantification using Polymerase Chain Reaction (PCR)

The relative quantification was performed in triplicate and reactions prepared using TaqMan™ Fast Advanced Master Mix (Thermo Fisher, UK) on a 96–well plate. Prior to real-time PCR the assays were stored frozen and protected from light. The 60X assays were then diluted to 20X working stocks with RNase-free water. The Master Mix was thawed on ice and mixed thoroughly. Samples and assay solutions were thawed on ice, vortexed and centrifuged to resuspend. PCR Reaction Mix was prepared by combining the Master Mix, assay, and nuclease-free water in the quantities presented in **Table 4.3**. The PCR reaction plate was prepared by transferring the PCR Reaction Mix to each well and adding 1 µl cDNA template or nuclease-free water for the negative control. The plate document or plate file was set up with the appropriate thermal-cycling conditions (**Table 4.4**). The PCR reaction plate was run on the 7500 Fast Real-Time PCR System (Applied Biosystems, UK). The data was analysed by viewing the amplification plots, setting the baseline and threshold values, and using the comparative Ct method.

Table 4.3 The reagents and quantities for the PCR master mix

Component	Volume per reaction	Final concentration
TaqMan™ Fast Advanced Master Mix (2X)	5.0 µl	1X
TaqMan™ Assay (20X)	0.5 µl	1X
Nuclease-free water	3.5 µl	-
Total volume of PCR Reaction Mix per reaction	**9.0 µl**	**-**

Table 4.4 The cycling conditions for PCR

Settings	Incubation	Polymerase activation	PCR (40 cycles)	
	Hold	**Hold**	**Denature**	**Anneal / extend**
Temperature	50°C	95°C	95°C	60°C
Time	2 minutes	20 seconds	3 seconds	30 seconds

4.2.5 DNA Extraction

Using the Qiagen DNeasy Blood & Tissue Kits (Qiagen, USA), total DNA from the ovarian tissue was extracted and purified according to the protocol provided. Prior to beginning the procedure, Buffer AW1 and Buffer AW2 were supplied as concentrates and each was diluted with ethanol (100%) to obtain a working solution before initial usage. The ovarian tissues were retrieved from storage in liquid nitrogen, cut and weighed into individual pieces of 25 mg while in a tray on dry ice to keep it frozen. The weighed pieces were placed in a 1.5ml centrifuge tube and further crushed into small pieces, equilibrated to room temperature (15–

25°C) and into which 180 µl Buffer ATL was added. A 20 µl volume of Proteinase K was added and mixed thoroughly by vortexing and incubated in a preheated incubator with a rocking platform at 56°C until the tissue was completely lysed, for a maximum of 3 hours. During incubation, the samples were vortexed at one-hour intervals to accelerate tissue lysis.

After lysis, the mixture was vortexed for 15 seconds and 200 µl Buffer AL was added to the sample and mixed thoroughly by vortexing. A volume of 200 µl ethanol (96–100%), was added and mixed thoroughly by vortexing, yielding a homogeneous solution.

The mixture was then transferred into the DNeasy Mini spin column placed in a 2 ml collection tube and centrifuged at ≥6000 x g (8000 rpm) for a minute. The flow-through and collection tube was discarded and the DNeasy Mini spin column was placed in a new 2 ml collection tube. A 500 µl volume of Buffer AW1 was added to the spin column and centrifuged for 1 min at ≥6000 x g (8000 rpm). This step was followed by an addition of 500 µl Buffer AW2 after discarding the flow through with the collection tube and centrifuged for 3 min at 20,000 x g (14,000 rpm) to dry the DNeasy membrane of residual ethanol. The flow-through and collection tube were discarded to complete the washing and purification of the DNA bound to the membrane of the DNeasy Mini spin column. The DNeasy mini spin column was carefully removed and placed in a clean 1.5 ml for the collection of the DNA elution. A volume of 200 µl Buffer AE was pipetted directly onto the DNeasy membrane, incubated at room temperature for 1 min, and then centrifuged for 1 min at ≥ 6000 x g (8000 rpm) to elute DNA.

The total DNA yield was determined by measuring the concentration of the eluate by absorbance at 260nm using the NanoDrop™ 1000 Spectrophotometer (Thermo Fisher Scientific Inc., UK) and values between 0.1 – 1.0 were considered accurate. The remaining isolated genomic DNA was stored at –20°C until global DNA methylation assessment.

4.2.6 Global DNA Methylation

The global DNA methylation was quantified colorimetrically using the Global DNA Methylation Assay Kit (5 Methyl Cytosine, Colorimetric, ab233486, Abcam Plc, UK). In this assay, DNA is bound to strip-wells that are specifically treated to have a high DNA affinity. The methylated fraction of DNA is detected using capture and detection antibodies and then quantified colorimetrically by reading the absorbance in a microplate spectrophotometer (**Figure 4.5**).

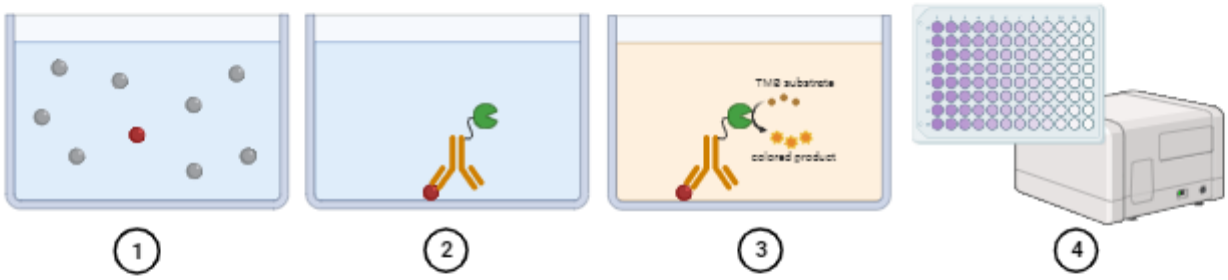

Figure 4.5 A summary of the global methylation assay process. 1) 100ng of sample DNA is added to wells, 2) detection complex solution is added, 3) colour developer solution is added, 4) absorbance at 450nm is measured with a microplate spectrophotometer. Plate is washed between each stage. Created with BioRender.com

Briefly, a fresh set of standards were prepared prior to the experiment: 1 µl of Positive Control was diluted with 9 µl of Negative Control (NC) to prepare the Diluted Positive Control, six (6) concentration points for the control were prepared by combining Positive Control (PC), Diluted Positive Control, and Negative Control according to **Table 4.5**. These volumes were sufficient for one standard curve in duplicate (12 wells total) and the Positive Control concentrations are based on per assay well, not per microliter.

Table 4.5 The quantities and volume for the preparation of the standards

Positive Control Well	Positive Control (PC) (5.0%)	Diluted Positive Control (0.5%)	Negative Control (NC)
0.1%	0.0 µl	1.0 µl	9.0 µl
0.2%	0.0 µl	1.0 µl	4.0 µl
0.5%	0.0 µl	3.0 µl	3.0 µl
1.0%	1.0 µl	0.0 µl	9.0 µl
2.0%	1.0 µl	0.0 µl	4.0 µl
5.0%	3.0 µl	0.0 µl	3.0 µl

The sample DNA was relatively pure with a 260/280 ratio of greater than 1.6. It was diluted with Nuclease-free water to 100 ng DNA per reaction. All materials and prepared reagents were equilibrated to room temperature and gently agitated prior to assay start. All standards, controls, and samples were assayed in duplicate loaded vertically instead of horizontally.

For DNA binding, 100 µl of Binding Solution and 2 µl of Negative Control were added to the negative control wells. Binding Solution (100 µl) and Positive Control (2 µl) at different concentrations (0.1%-5%) were added to the positive control wells to generate a standard curve (**Table 4.5**). For each sample well, 100 µl of Binding Solution and 100 ng of the sample DNA (2 µl) were added. The samples were loaded vertically to reduce cross variation between replicates.

The total DNA in the positive control wells was also 100 ng per well, with the different methylation percentages (0.1%, 0.2%, 0.5%, 1%, 2%, and 5%). The positive controls were assayed in parallel with the samples in the same plate. The solution was then mixed by gently

tilting the plate from side to side to ensure adequate and even coating of the bottom of the well after which the plate was sealed and incubated at 37°C for 60 minutes.

During the last 10 minutes of sample incubation, the 5-mC Detection Complex Solution was prepared. In each 1 ml of diluted 1X Wash Buffer, 1 µl of 5-mC Antibody (1000X), was added, mixed, and then 1 µl of Signal Indicator (1000X) and 0.5 µl of Enhancer Solution (1000X) were added after which the solution was mixed.

After the incubation, the Binding Solution was removed from each well and each well was washed three times with 150 µl of Wash Buffer (1X). The plate was then incubated at room temperature for 50 minutes after which 50 µl of the 5-mC Detection Complex Solution was added to each simultaneously using a multichannel pipette. The solution was removed, and wells washed five times with 150 µl of Wash Buffer (1X).

Using a multichannel pipette, 100 µl of the Developer Solution was added to each well column, simultaneously in a vertical fashion to ensure replicates developed at the same time. Colour development was monitored for up to 4 minutes, as the 5% Positive Control wells would turn deep blue in the presence of methylated DNA. The enzyme reaction was ceased immediately by adding 100 µl of Stop Solution in the same fashion as the detection complex solution. Within 2-15 minutes, the absorbance was read on a microplate reader at 450 nm.

4.2.7 Data analysis

4.2.7.1 Microarray

Partek Genomics Suite

Firstly, the Affymetrix CEL Files were imported into Partek® Genomics Suite™ 6.6 and the quality checked using RMA background correction with quantile normalisation, log base 2 transformation with adjustment for GC content. An exploratory analysis using a

principal components analysis (PCA) scatter plot was used to explore the resemblance of the samples to each other.

A 3-way analysis of variance (ANOVA) along with a volcano plot was used for identifying differentially regulated expressing larger or smaller intensity values in the data set and a list of genes was generated that are significantly different (p-value threshold of 0.05) between cryopreserved ovaries and the fresh ovaries with an absolute difference bigger than 1fold.

Gene Set Enrichment Analysis (GSEA)

The GSEA analysis of the genes that differed significantly ($p<0.05$) was carried out using WebGestalt 2019 version (Liao et al., 2019). Gene ontology (GO, Biological Process noRedundant) and pathway (KEGG) analyses were carried out using the following parameters: minimum number of genes for a category = 3, Significance level = TOP 100, Number of Permutations = 1000, Collapse Method = Mean.

4.2.7.2 Analysing Real-time PCR (RT-qPCR) results

To validate the results of the microarray analysis, an appropriate volume (minimum of 3 µl) of RNA product from each sample was stored at -80˚C. cDNA templates were created from the RNA products using the High Capacity cDNA Reverse Transcription Kit (Thermo Fisher Scientific™, UK) and PCR was carried out. The cycle threshold (Ct) values for each gene were determined and normalized with GAPDH and B2M (Thermo Fisher Scientific™, UK) housekeeping genes. The difference between the Ct values for the control and cryopreserved sample values (ΔCt) were used to compare the expression of each gene between the two groups. The difference between the ΔCt values for the microarray and PCR results values (ΔΔCt) were used to calculate the fold change in gene expression between the two groups. T-tests were used to compare the expression of each gene across the two groups. A

correlation test was used to determine the consistency between the microarray and PCR results. A p value of <0.05 was considered significant for all tests.

4.2.7.3 DNA methylation

In order to calculate the percentage of methylated DNA, a standard curve was generated using the mean absorbance/ optical density (OD) values against the positive control (PC) at each percentage point in GraphPad Prism 9. Firstly, an XY data table was created entering the optical density/absorbance (OD) values (Y) versus the positive (PC) at each percentage point (X). The sample OD (Y) values were also entered into the data set and the data set was analysed using nonlinear regression by interpolation using the hyperbola equation (X is concentration – one site specific binding) which is Y = Bmax*X/(Kd + X). The percentage of methylated DNA (5-mC) in total DNA was then calculated using the following formula:

$$5 - mC\% = \frac{Sample\ OD - Negative\ Control\ OD}{Slope\ \times S} * 100\%$$

S is the amount of input sample DNA in ng and in this case, this is 100ng.

A paired, nonparametric t test (Wilcoxon test) was then used to compare the level of 5-mC in the control group verses the WOCP group.

4.3 RESULTS

4.3.1 RNA Extraction

The concentration of RNA for each sample was >250 ng RNA/µl, and the purity (260/280) were in the acceptable range (all between 1.85 - 2.25). The RNA integrity number (RIN) score of the RNA samples were above 8. There were no visible contaminants or degradation observed. Based on these results, the RNA extraction was successful for all samples, and the RNA was of good quality, suitable for downstream application in microarray.

4.3.2 Microarray - Partek analysis

Partek analysis was done by Dr M Castellanos Uribe at the Nottingham Arabidopsis Stock Centre of the University of Nottingham. A PCA plot was generated from the ovarian cortical samples (n=3 control; and n=3 WOCP). Two clusters of data representing control (fresh) (C – blue) and WOCP (W- red) samples are observed in **Figure 4.6**. Three-dimensional concentration ellipsoids were fitted to the graph, which allowed us to visualize the homogeneity and heterogeneity of expression profiles within and between the groups. The two ellipsoids are clearly separated and spaced apart in the graph, indicating that there is a difference in the overall profile of gene expression between the two groups. The dots within each ellipsoid (samples within each group) are relatively close, which means that these samples have similar expression profiles and should therefore be included in downstream analysis.

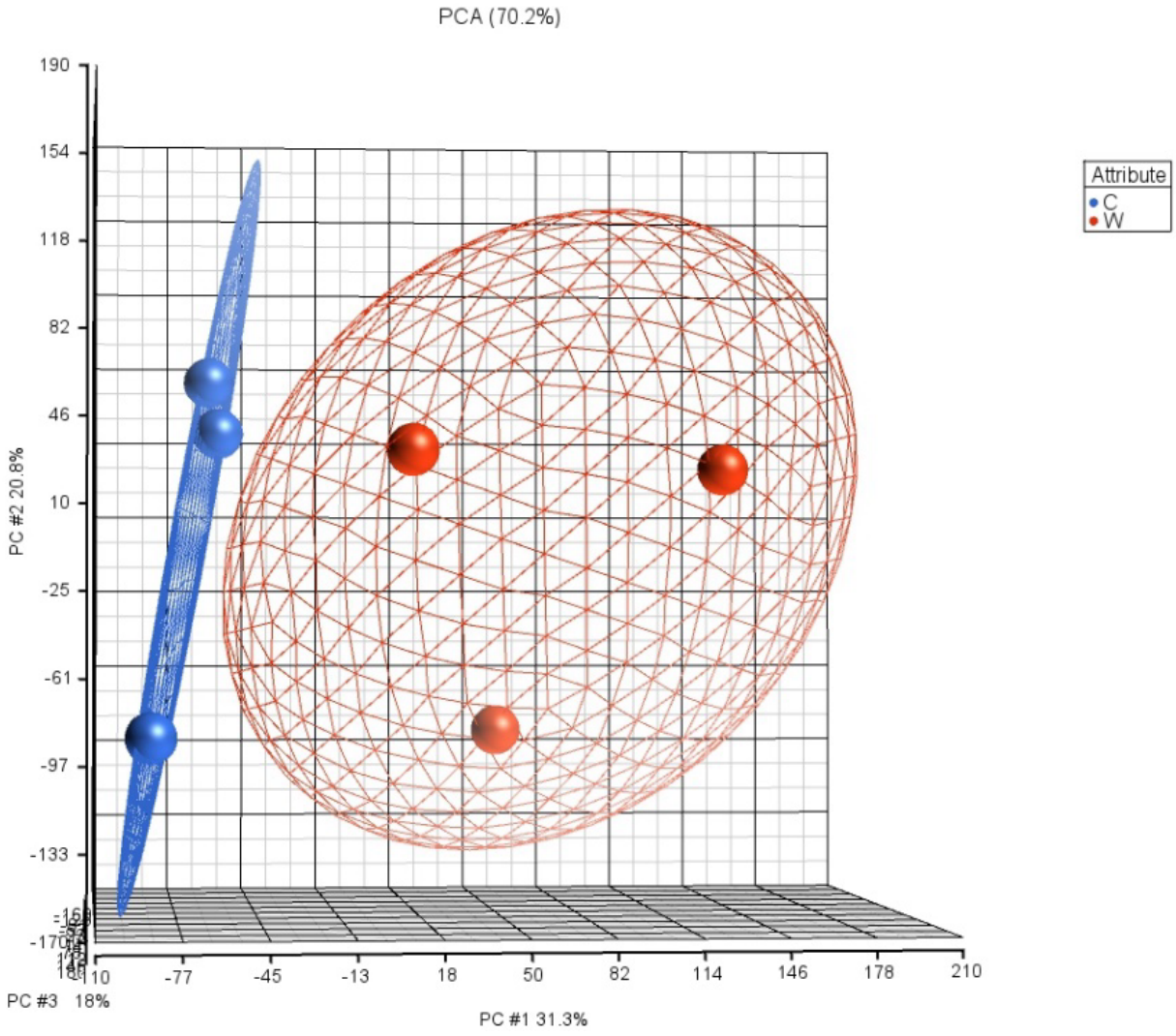

Figure 4.6 The PCA scatter plot of the gene expression data of the control group and WOCP group. Each dot represents a sample; blue coloured dot represents the control ovaries (C) and the red coloured dots represent the whole ovary cryopreserved (W) group.

Additionally, a volcano plot was generated to identify the genes which are differentially expressed between the two groups which may be statistically significant compared to the control samples (**Figure 4.7**). The x-axis shows the fold change in gene expression which is the magnitude of that change relative to the control group, and the y-axis shows the p-value which is the measure of the likelihood of the observed change in gene expression is due to chance.

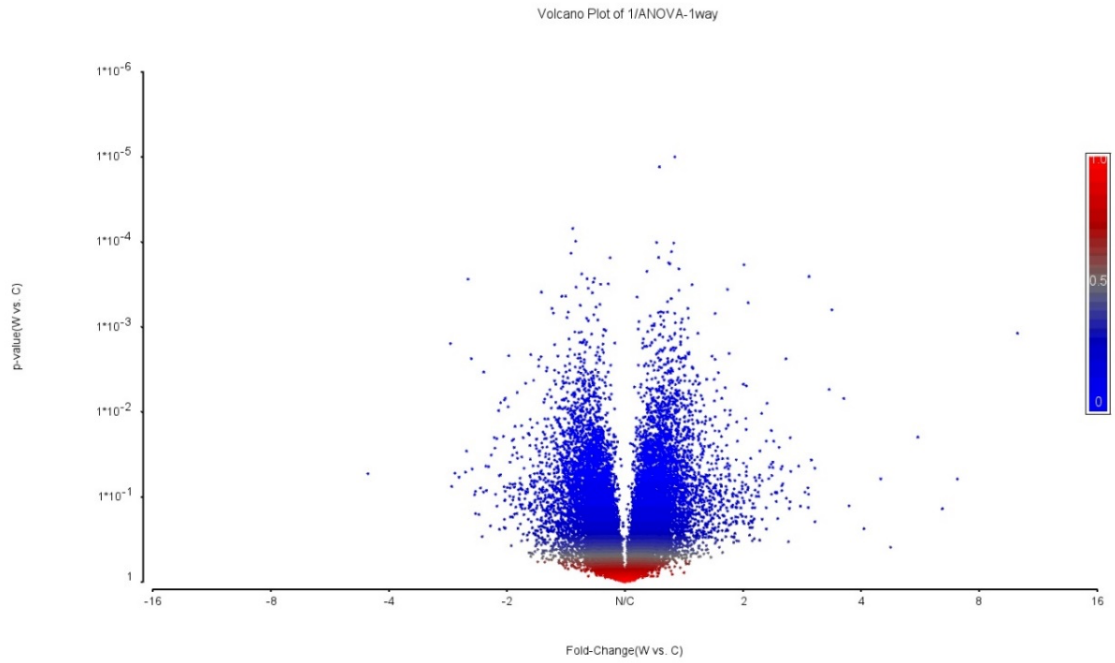

Figure 4.7 A volcano plot of 24,596 genes analysed with the microarray chip. Each dot represents one gene. The X-axis represents fold change, and the Y-axis represents the p-value calculated with 3-way ANOVA.

The initial gene list consisted of 24,596 genes, some of which were unidentified. After applying a p-value of less than 0.05 (a 5% chance that the result occurred by chance), 2,557 genes remained, of which 726 were unidentified and 1,831 were identified. When an FDR was applied, no genes remained as being statistically different. However, when an FDR was not applied, the unidentified genes were excluded and fold-change of >1.0 or < -1.0, a total of 114 genes remained as the top genes.

In other words, the initial filtering based on a p-value < 0.05 identified 2,557 genes as potentially differentially expressed at an individual gene level. However, when an FDR correction was applied to account for the multiple testing problem, no genes remained statistically significant. This indicates that the initial pool of 2,557 genes likely contained a high proportion of false positives, and the evidence for widespread differential expression was not strong enough to withstand the stringent FDR control. In contrast, when FDR correction

was not applied and unidentified genes were excluded, applying a fold-change threshold of >1.0 or < -1.0 resulted in a set of 114 genes. However, this list of 114 genes is more susceptible to containing false positives because the effects of testing thousands of genes simultaneously were not accounted for.

Given these outcomes, the decision was made to acknowledge the absence of statistically significant genes after correction for multiple testing and not to pursue FDR-adjusted results further. Instead, the uncorrected list of 114 genes, filtered by both p-value and fold-change, was explored on an exploratory, hypothesis-generating basis only, rather than being interpreted as definitive evidence of differential expression. This approach was considered the most balanced, as it maintains transparency about the limitations of the dataset while still allowing potentially interesting gene expression patterns to be highlighted for future validation using independent, quantitative techniques.

4.3.3 Gene Set Enrichment Analysis (GSEA)

Gene Ontology (GO) analysis was carried out for the 1,831 differentially expressed genes (after excluding the unidentified genes) (FDR > 0.05; p < 0.05) to classify genes based on their biological and molecular function, and their cellular location. The GO slim summaries of each categorized function are found below as analysed from WEB-based Gene Set Analysis Toolkit (WebGestalt). The following results were based on this new total of 1501 unique entrezgene IDs (numerical identifiers assigned by the National Center for Biotechnology Information (NCBI) to each gene record in their Entrez Gene database**)** which were successfully mapped.

As shown in **Figure 4.8**, the biological processes that registered the most number of genes are metabolic process (593 genes) and biological regulation (521 genes) which are genes surrounding energy production, hormone synthesis, oocyte development, transcription and

translation (**Appendix C**). Other categories affected by whole ovarian cryopreservation is cell communication with 226 genes affected in this category. Also, we see developmental process (216 genes), cell proliferation (70 genes), reproduction (46 genes) and growth (38 genes) processes that are likely linked to oogenesis, folliculogenesis and cell development.

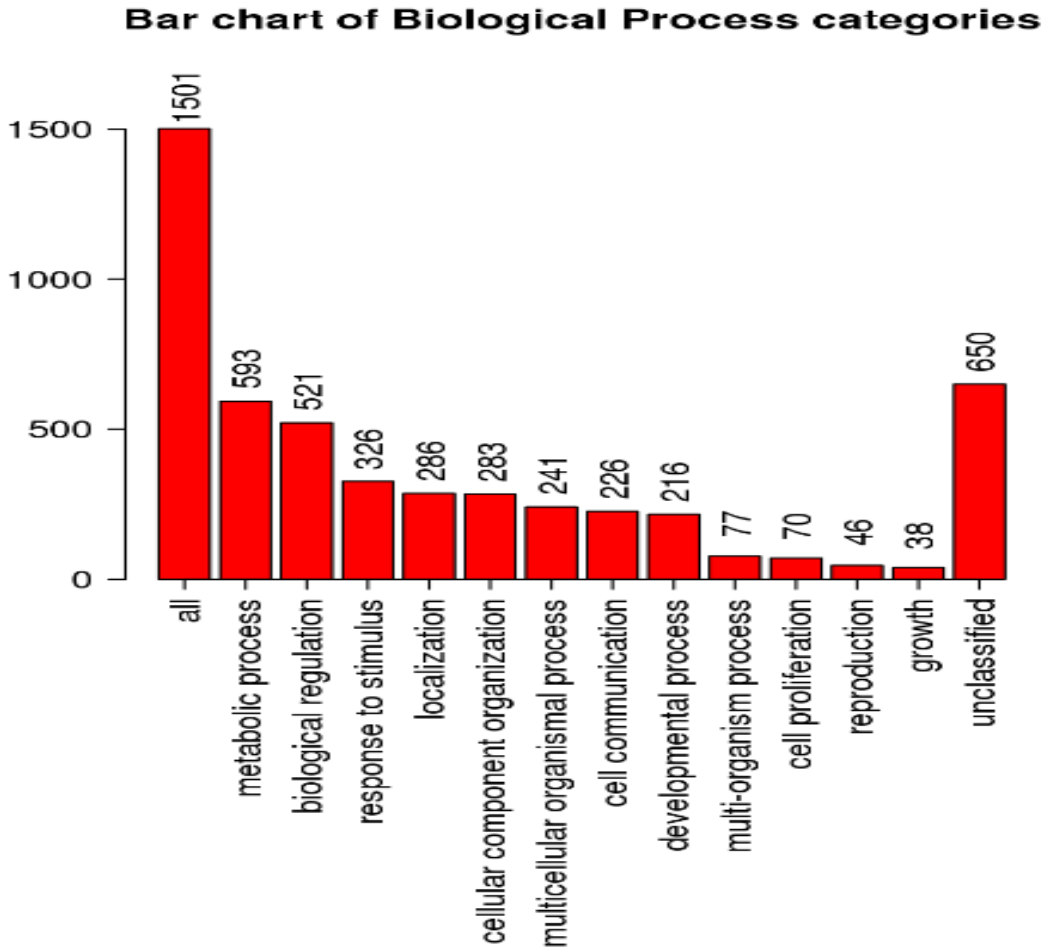

Figure 4.8 Gene ontology summary for the differentially expressed entrezgene IDs involved in biological process. The height of the bar for each chart represents the number of entrezgene IDs in each process and the exact number of entrezgene IDs involved is stated above each bar.

GSEA revealed several biological terms significantly enriched in the dataset (**Figure 4.9**). The terms exhibiting statistically significant positive Normalized Enrichment Scores

(NES) included "regulation of signalling receptor activity" and "NADH dehydrogenase complex assembly," suggesting an upregulation of genes associated with these processes. Notably, "methylation" also showed a statistically significant enrichment (FDR ≤0.05) but with a negative NES, indicating a significant downregulation of genes associated with this process. Several other biological categories displayed non-significant enrichment (FDR > 0.05), with varying positive and negative NES.

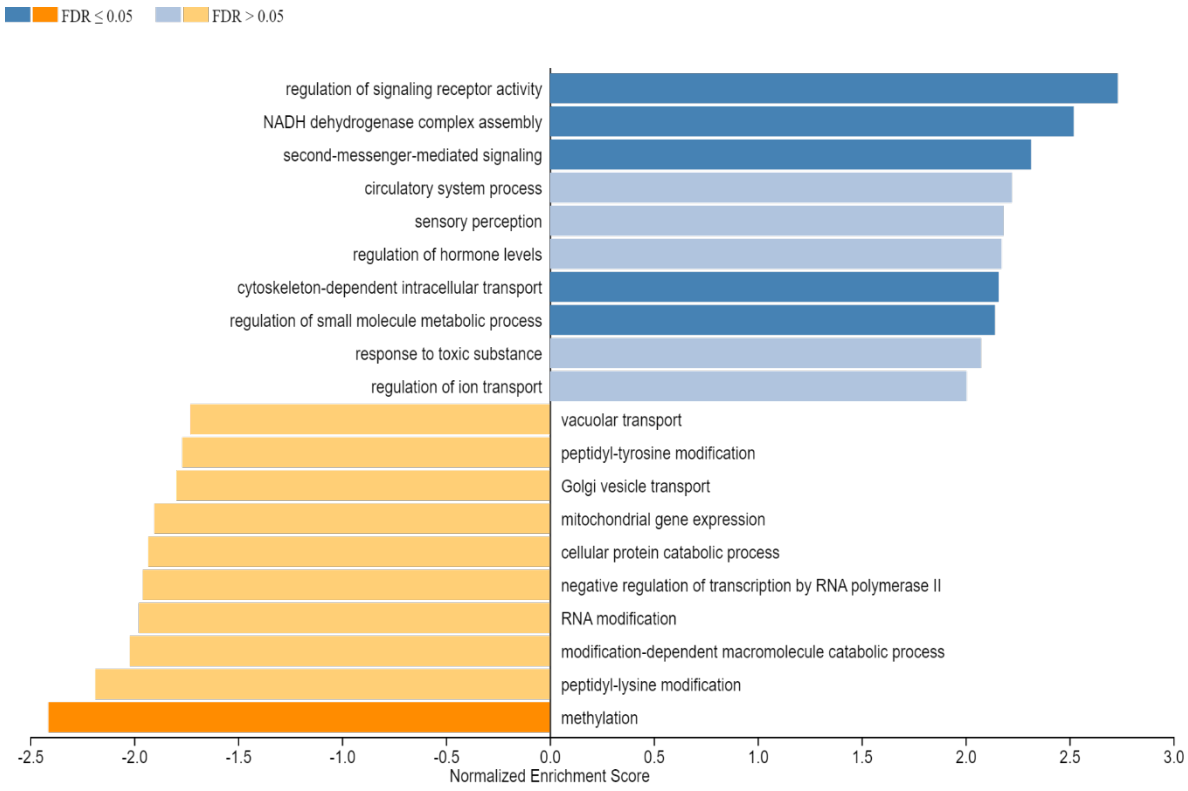

Figure 4.9 Bar chart of the GSEA. The x axis shows the normalised enrichment score given by WebGestalt. Blue bars represent biological process up regulated in the WOCP samples and yellow bars represent processes downregulated compared to the control samples. FDR was ≤0.05 for the deeper coloured categories.

Table 4.6 Genes involved in some categories of biological processes. Boldened genes are genes also found in the top genes (no FDR).

Biological regulation	Regulation of signalling receptor activity (part of signalling)	AGRP, BMP10, CCL17, CCL20, CCL22, CER1, CSF2, FGF23, GCG, GHRH, GPHA2, IL12B, IL36G, INHBE, MIA, RABEP2, RWDD1, SST, **STC2**, TNF, TRH
	Second-messenger-mediated signalling (part of signalling)	CCL20, **CMKLR1**, GHRH, GPHA2, NCALD, NOS3, PDZD3, PPP3CC, S1PR4, SRI, TNF, **TNNI3**
	Regulation of small molecule metabolic process	ANXA1, COX7A1, **FABP3**, GCG, NOS3, PDZD3, **STAR**, TNF
Cellular component organisation	NADH dehydrogenase complex assembly (part of cellular component biogenesis)	NDUFA1, NDUFA11, NDUFA13, NDUFA2, **NDUFA5**, NDUFB1, NDUFB11, NDUFB3, NDUFB6, NDUFB8, NDUFC2, NDUFS5, TAZ
Localisation	Cytoskeleton-dependent intracellular transport	AP3S1, **KIF23**, MGARP, MYO10, NDE1, TRIM46
Metabolic process	Methylation	ARID4A, ASH2L, BCDIN3D, CAMKMT, EZH1, KDM3A, **METTL16**, **METTL17**, METTL4, MTF2, NDUFAF7, NSUN4, PRMT9, RBBP5, SETD6, SETMAR, TRMT10B, TRMT11, TRMT13, VCPKMT

In the cellular component (**Figure 4.10**), the genes associated with membrane were seen to be the most affected with 394 genes differentially expressed closely followed by the genes associated with the nucleus (386 genes) and protein-containing complex (351 genes). Other cell components including cytoskeleton (85 genes), Golgi apparatus (79 genes), cell projection and ribosomes (31 genes) which are relevant to cell growth and development were also seen to express differences.

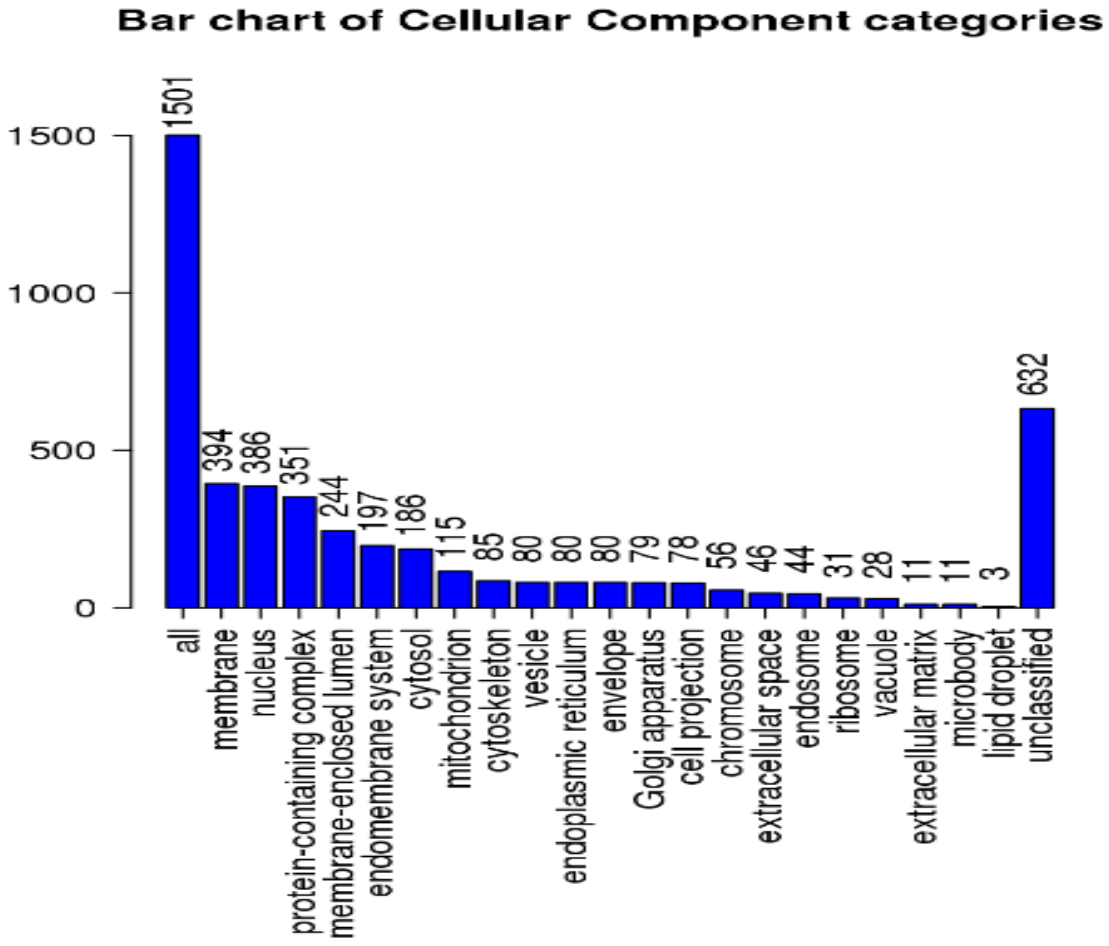

Figure 4.10 Gene ontology summary for the differentially expressed entrezgene IDs involved in cellular component. The height of the bar for each chart represents the number of entrezgene IDs in each process and the exact number of entrezgene IDs involved is stated above each bar.

GSEA revealed several biological terms significantly enriched (FDR < 0.05) in the dataset (**Figure 4.11**). The terms exhibiting statistically significant positive NES included

"respiratory chain," "mitochondrial protein complex," and "NADH dehydrogenase complex," suggesting an upregulation of genes associated with these mitochondrial processes. Conversely, several biological terms displayed statistically significant negative NES (FDR ≤ 0.05), thus “transferase complex”, "vacuole" and "Golgi apparatus part," indicating a significant downregulation of genes associated with these cellular components. Several other biological terms displayed non-significant enrichment (FDR > 0.05) with varying positive and negative NES.

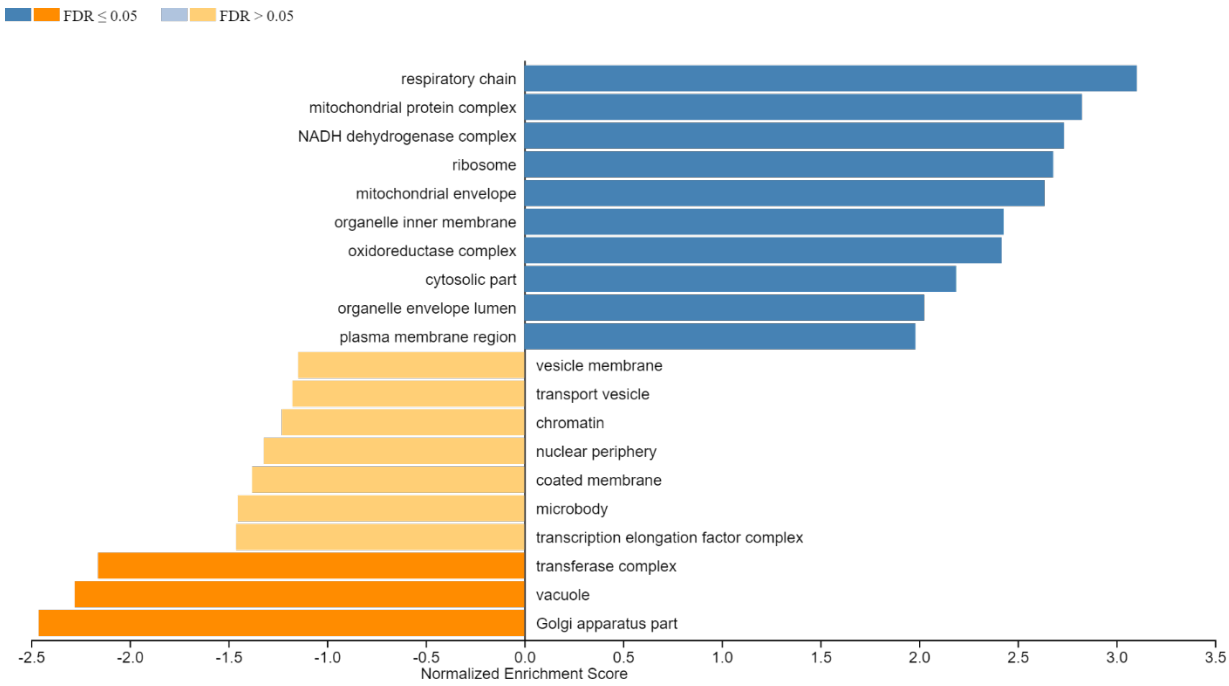

Figure 4.11 Bar chart of the GSEA. The x axis shows the normalised enrichment score given by WebGestalt. Blue bars represent cellular process up regulated in the WOCP samples and yellow bars represent processes downregulated compared to the control samples. FDR was ≤0.05 for the deeper coloured categories.

In the molecular function category (**Figure 4.12**), functions included protein binding (331 genes), nucleic acid binding (202 genes), transferase activity (132 genes), hydrolase activity (122 genes), nucleotide binding (95 genes), transporter activity (67 genes), molecular

transducer activity (41 genes), enzyme regulator activity (38 genes), and structural molecule activity (37 genes).

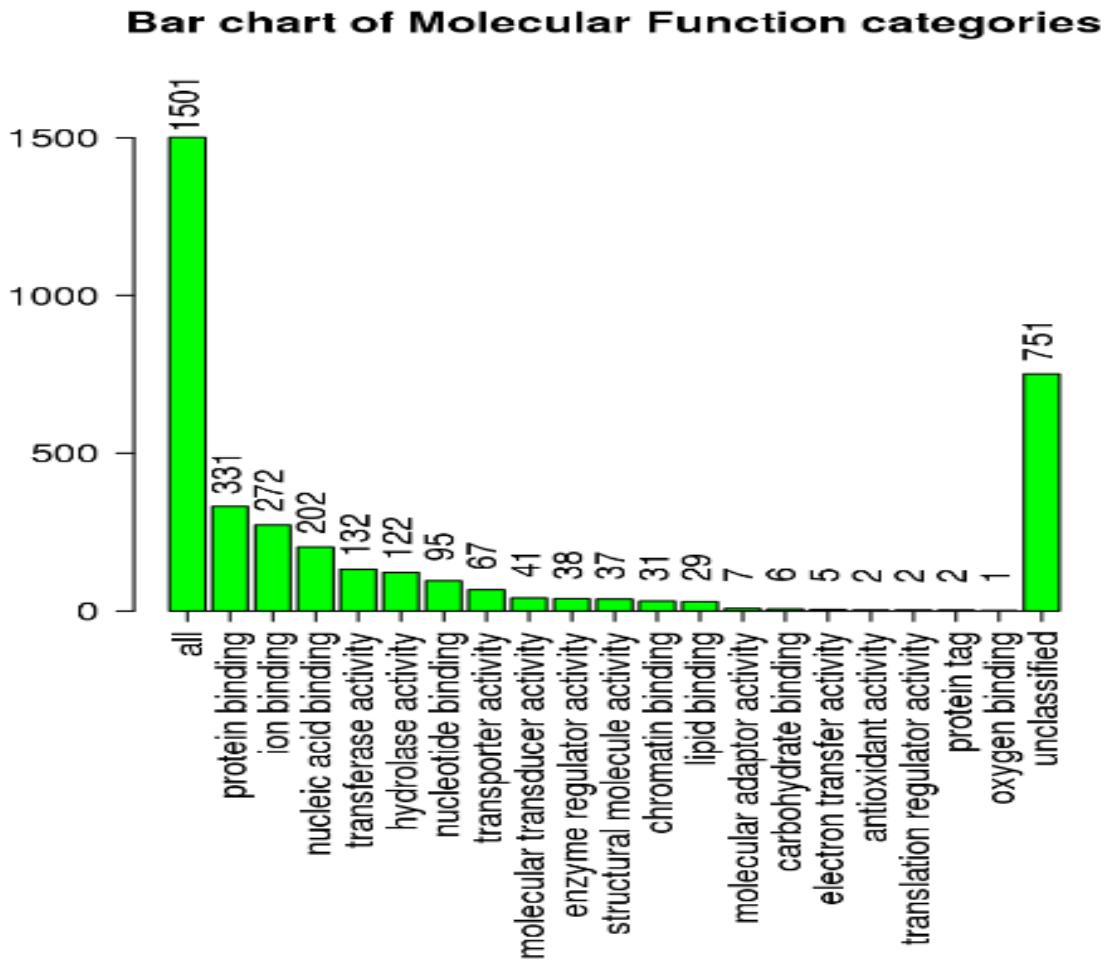

Figure 4.12 Gene ontology summary for the differentially expressed entrezgene IDs involved in molecular function. The height of the bar for each chart represents the number of entrezgene IDs in each process and the exact number of entrezgene IDs involved is stated above each bar.

GSEA results (**Figure 4.13**), highlighted key molecular functions with significantly altered gene expression. A significant upregulation (FDR $\leq$ 0.05) in genes associated with "structural molecule activity," "receptor regulator activity," "cytoskeletal protein binding," and "passive transmembrane transporter activity," as indicated by their positive NES. Conversely, there was a significant downregulation (FDR > 0.05) in genes related to "ubiquitin-like protein

transferase activity," "catalytic activity, acting on RNA," and "transferase activity, transferring one-carbon groups," as shown by their negative NES. Several other molecular function terms, including "electron transfer activity" and "regulatory region nucleic acid binding," did not reach statistical significance (FDR > 0.05).

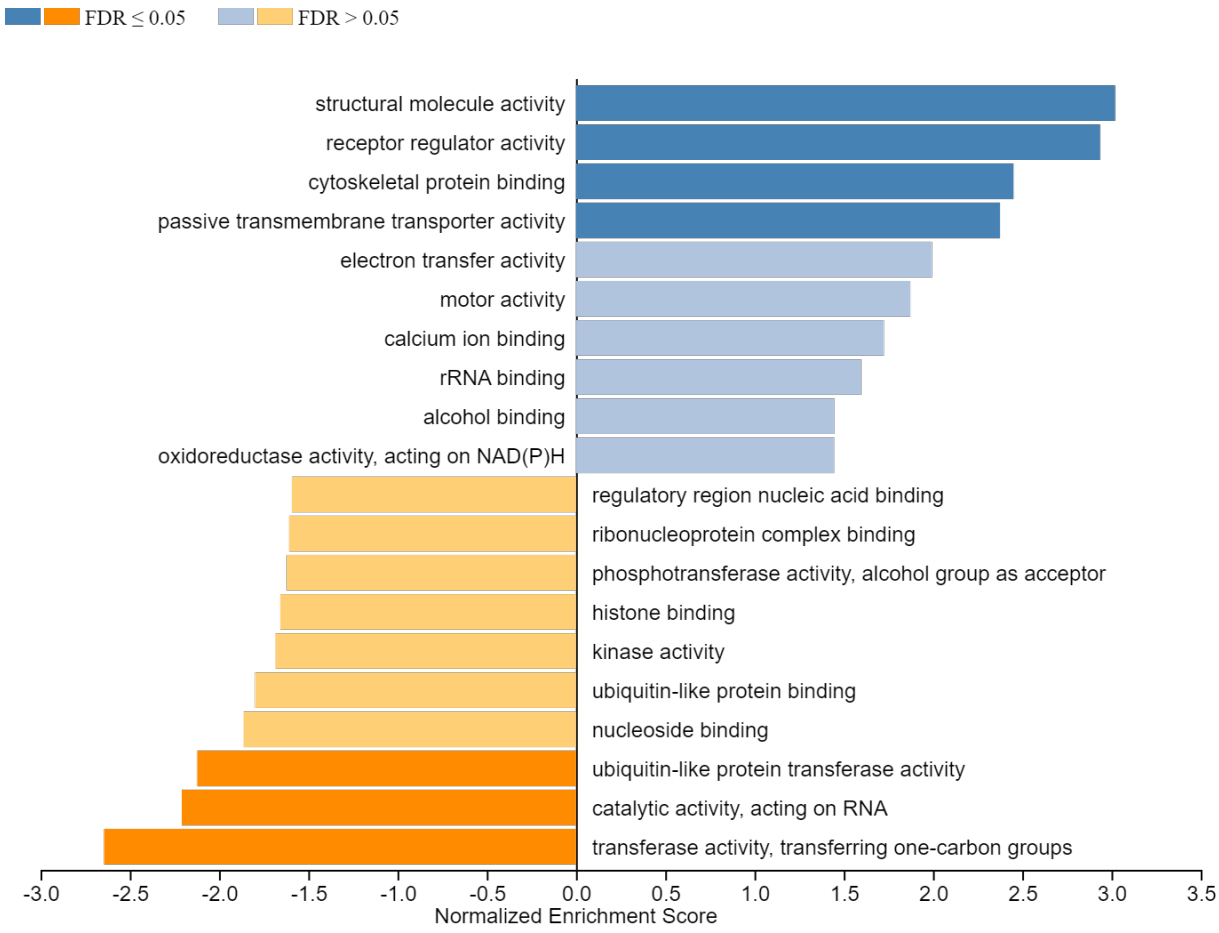

Figure 4.13 Bar chart of the GSEA. The x axis shows the normalised enrichment score given by WebGestalt. Blue bars represent molecular process up-regulated in the WOCP samples and yellow bars represent processes downregulated compared to the control samples. FDR was ≤0.05 for the deeper coloured categories.

4.3.5 Pathway analysis

4.3.5.1 KEGG Pathway

The Kyoto Encyclopaedia of Genes and Genomes (KEGG) 2019 was used as the reference database for the pathway analysis. A total of 115 pathways were identified. These

pathways include signalling pathways (cytokine-cytokine receptor interaction – 18 genes, mTOR signalling pathway – 16 genes), cellular processes (ribosome – 22 genes, lysosome – 15, autophagy – 14 genes), metabolic pathways (Huntington disease – 27 genes, thermogenesis 27 genes, Alzheimer disease - 24) hippo signalling pathway (9 genes) and FoxO signalling pathway (9 genes) (**Figure 4.14**).

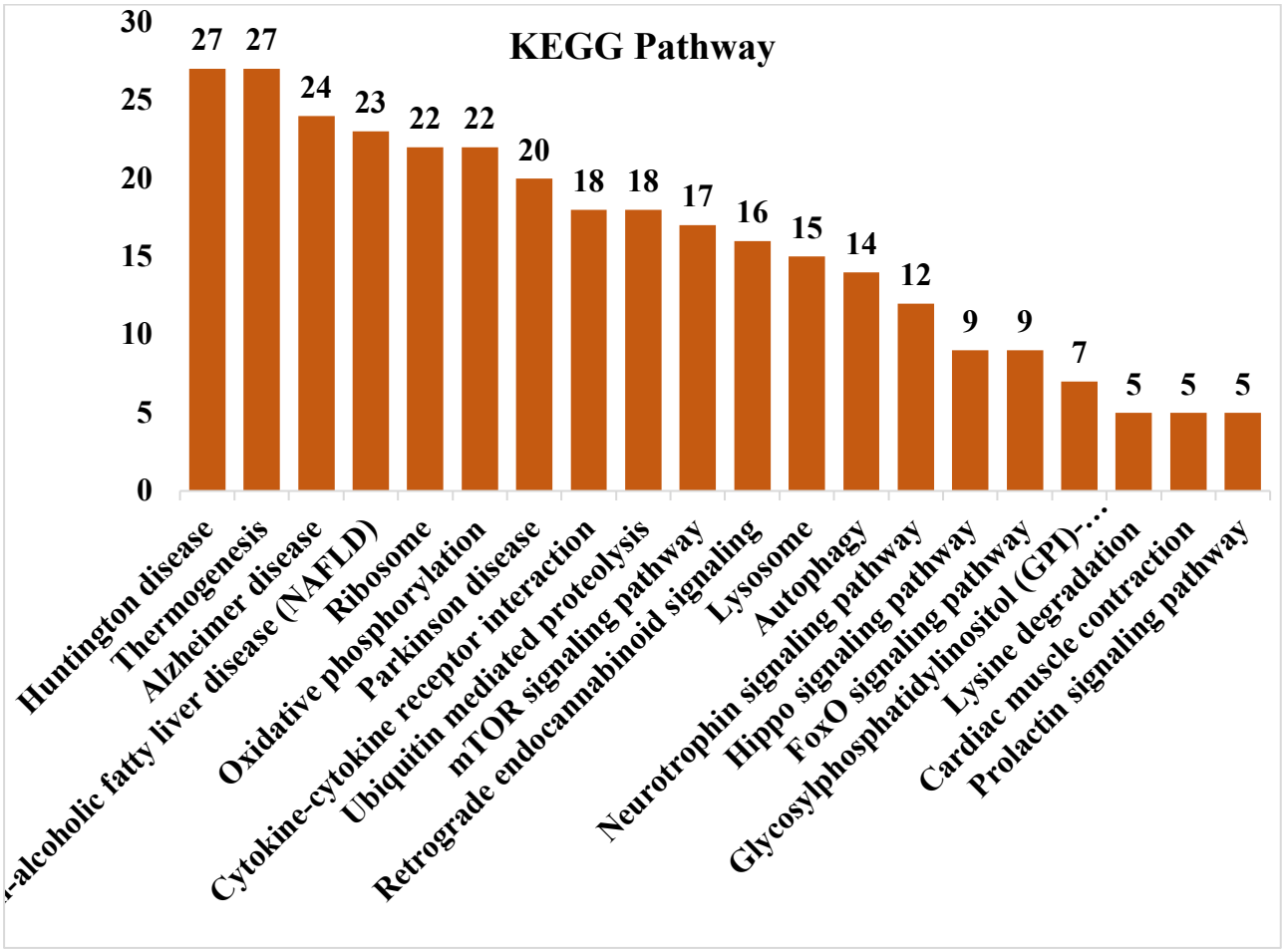

Figure 4.14 KEGG pathways associated with the differentially expressed genes in WCOP tissues as compared to control (fresh) tissue. The height of the bar represents the number of genes in each process and the exact number of genes involved is given above each bar.

Table 4.7 KEGG pathway map of the enriched genes from Figure 4.15

Human Diseases	• Neurodegenerative disease	• Huntington disease • Alzheimer disease • Parkinson disease
	• Endocrine and metabolic disease	• Non-alcoholic fatty liver disease
Organismal Systems	• Environmental adaptation	• Thermogenesis
	• Nervous system	• Retrograde endocannabinoid signalling • Neurotrophin signalling pathway
	• Circulatory system	• Cardiac muscle contraction
	• Endocrine system	• Prolactin signalling pathway
Genetic Information Processing	• Translation	• Ribosome
	• Folding, sorting and degradation	• Ubiquitin mediated proteolysis
Metabolism	• Energy metabolism	• Oxidative phosphorylation
	• Glycan biosynthesis and metabolism	• Glycosylphosphatidylinositol (GPI)-anchor biosynthesis
	• Amino acid metabolism	• Lysine degradation
Environmental Information Processing	• Signalling molecules and interaction	• Cytokine-cytokine receptor interaction
	• Signal transduction	• mTOR signalling pathway • Hippo signalling pathway • FoxO signalling pathway
Cellular Processes	• Transport and catabolism	• Lysosome • Autophagy

Among the 1501 unique entrezgene IDs, 566 IDs are annotated to the KEGG pathway category, were used for the enrichment analysis. Based on these parameters, 50 positive related categories and 50 negative related categories were identified as enriched categories, in which 40 most significant categories and representatives in the reduced sets are shown in this bar chart (**Figure 4.15**).

Analysis of gene set enrichment (**Figure 4.15**) found a significant increase (FDR ≤ 0.05) in the expression of genes belonging to pathways like "Ribosome," "Parkinson disease," "Non-alcoholic fatty liver disease (NAFLD)," and "Oxidative phosphorylation," as indicated by their positive NES. In contrast, the "Autophagy" and “Lysine degradation” pathway exhibited a significant decrease (FDR < 0.05) in gene expression, demonstrated by its negative NES. Other pathways examined, such as "Pancreatic secretion" and "Cell cycle," did not show statistically significant enrichment (FDR > 0.05).

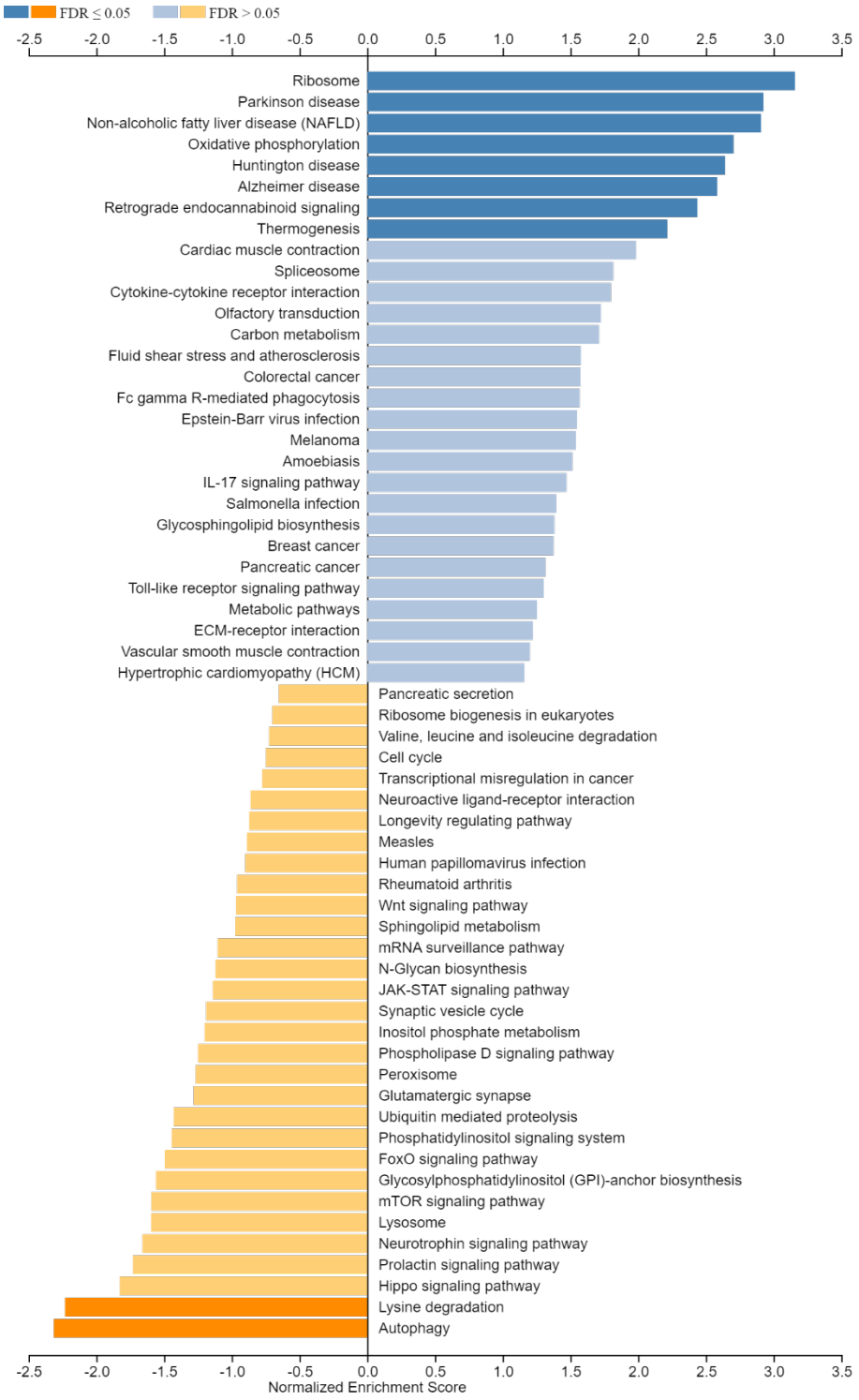

Figure 4.15 Bar chart of the GSEA. The x axis shows the normalised enrichment score given by WebGestalt. Blue bars represent KEGG pathway up regulated in the WOCP samples and yellow bars represent processes downregulated compared to the control samples. FDR was ≤0.05 for the deeper coloured categories.

4.3.6 Enriched differential genes involved in pathways with FDR ≤0.05, growth, development and apoptosis

Among the differentially expressed genes, 10 pathways had an FDR ≤ 0.05 (8 up-regulated, 2 down-regulated). The genes within these differently expressed pathways are displayed in **Table 4.8**.

Table 4.8 Differentially expressed genes involved in pathways with FDR ⩽ 0.05

Pathway	Up regulated genes	Down regulated genes
Ribosome	FAU, MRPL11, MRPL24, MRPL35, MRPL9, MRPS11, MRPS15, RPL11, RPL22L1, RPL27, RPL29, RPL37, RPL38, RPL39, RPL3L, RPL5, RPL8, RPLP0, RPLP2, RPS18, RPS24, RPS6	
Parkinson disease	COX5B, COX7A1, NDUFA1, NDUFA11, NDUFA13, NDUFA2, NDUFA4, NDUFA5, NDUFB1, NDUFB11, NDUFB3, NDUFB6, NDUFB8, NDUFC2, NDUFS5, SDHB, UBE2L3, UQCRFS1, VDAC1	
Non-alcoholic fatty liver disease (NAFLD)	BAX, COX5B, COX7A1, JUN, NDUFA1, NDUFA11, NDUFA13, NDUFA2, NDUFA4, NDUFA5, NDUFB1, NDUFB11, NDUFB3, NDUFB6, NDUFB8, NDUFC2, NDUFS5, SDHB, TNF, UQCRFS1	
Oxidative phosphorylation	ATP4A, COX5B, COX7A1, NDUFA1, NDUFA11, NDUFA13, NDUFA2, NDUFA4, NDUFA5, NDUFB1, NDUFB11, NDUFB3, NDUFB6, NDUFB8, NDUFC2,	

	NDUFS5, PPA1, SDHB, UQCRFS1	
Huntington disease	AP2S1, BAX, COX5B, COX7A1, DNAH17, NDUFA1, NDUFA11, NDUFA13, NDUFA2, NDUFA4, NDUFA5, NDUFB1, NDUFB11, NDUFB3, NDUFB6, NDUFB8, NDUFC2, NDUFS5, SDHB, UQCRFS1, VDAC1	
Alzheimer disease	COX5B, COX7A1, NDUFA1, NDUFA11, NDUFA13, NDUFA2, NDUFA4, NDUFA5, NDUFB1, NDUFB11, NDUFB3, NDUFB6, NDUFB8, NDUFC2, NDUFS5, PPP3CC, SDHB, TNF, UQCRFS1	
Retrograde endocannabinoid signalling	GABRQ, NDUFA1, NDUFA11, NDUFA13, NDUFA2, NDUFA4, NDUFA5, NDUFB1, NDUFB11, NDUFB3, NDUFB6, NDUFB8, NDUFC2, NDUFS5	
Thermogenesis	COX5B, COX7A1, GCG, NDUFA1, NDUFA11, NDUFA13, NDUFA2, NDUFA4, NDUFA5, NDUFB1, NDUFB11, NDUFB3, NDUFB6, NDUFB8, NDUFC2, NDUFS5, RPS6, SDHB, UQCRFS1	
Autophagy		ATG16L1, ATG9A, CFLAR, ERN1, LAMP2, MTMR3, MTMR4, PDPK1, PIK3C3, PIK3R1, PRKAA1, PRKACB, TRAF6, UVRAG
Lysine degradation		ALDH9A1, CAMKMT, EZH1, HYKK, SETMAR

4.3.6 Microarray confirmation using PCR

In total, 10 genes (5 upregulated and 5 downregulated) of interest were chosen for validation by RT-qPCR using the same tissue RNA as for the array analysis. These genes were selected based on their fold change values and their biological function. These genes were BMP10 (bone morphogenetic protein 10), GHRH (growth hormone releasing hormone), MRPL24 (mitochondrial ribosomal protein L24), BAX (BCL2 associated X), apoptosis, RPL22L1 (ribosomal protein L22-like) which were all upregulated, and METTL17 (methyltransferase like 17), METTL4 (methyltransferase like 4), CBX5 (chromobox 5), KAT7 lysine acetyltransferase 7, EZH1 (enhancer of zeste 1 polycomb repressive complex 2 subunit) which were all downregulated. **Table 4.9** summarizes the expression profiles and fold change values for the 10 genes as generated by microarray and the validation by PCR.

Table 4.9 The genes selected for the validation of microarray results with PCR. The interest (reason for selection), the enrichment score, nature of regulation and fold change for both microarray and PCR values.

Gene name	Function	Discovery set by microarray	Fold change by Microarray	Fold change by PCR
BMP10	Follicle growth, ovulation, inflammation	Up	1.3542	-
GHRH	Cell maturation, cAMP-mediated signalling	Up	1.35958	2.05406
MRPL24	RNA Binding	Up	1.1716	1.2375
BAX	germ cell development, intrinsic apoptotic signalling pathway in response to DNA damage	Up	1.54833	1.4834
RPL22L1	Follicle growth and development	Up	1.61499	1.4211
METTL17	Methylation, translation, mitochondrial ribosome binding, methyltransferase activity	Down	-1.63314	-1.1944
METTL4	nucleic acid binding, RNA methyltransferase activity,	Down	-1.43805	-1.6587

	regulation of mitochondrial DNA replication, regulation of mitochondrial transcription			
CBX5	chromatin binding, DNA-binding transcription factor binding, histone deacetylase binding, methylated histone binding, cellular response to DNA damage stimulus, negative regulation of transcription by RNA polymerase II	Down	-1.45012	-1.7843
KAT7	histone acetyltransferase activity, histone H3-K14 acetylation, histone H4-K12 acetylation, histone H4-K5 acetylation, histone H4-K8 acetylation, positive regulation of histone H4 acetylation	Down	-1.43424	-1.6429
EZH1	histone H3-K27, methylation	Down	-1.40632	-1.3872

4.3.9 Changes in global 5-hmC levels in response to WOCP

The examination of global 5-methylcytosine (5-mC) levels in the ovary in response to WOCP revealed a marginal increase in the 5-mC level (0.26%) in WOCP-treated tissue compared to the control tissue (0.24%). Despite data indicating a rise in global 5-hydroxymethylcytosine (5-hmC) levels due to WOCP, no statistically significant change in overall 5-mC levels was observed (**Figure 4.16**).

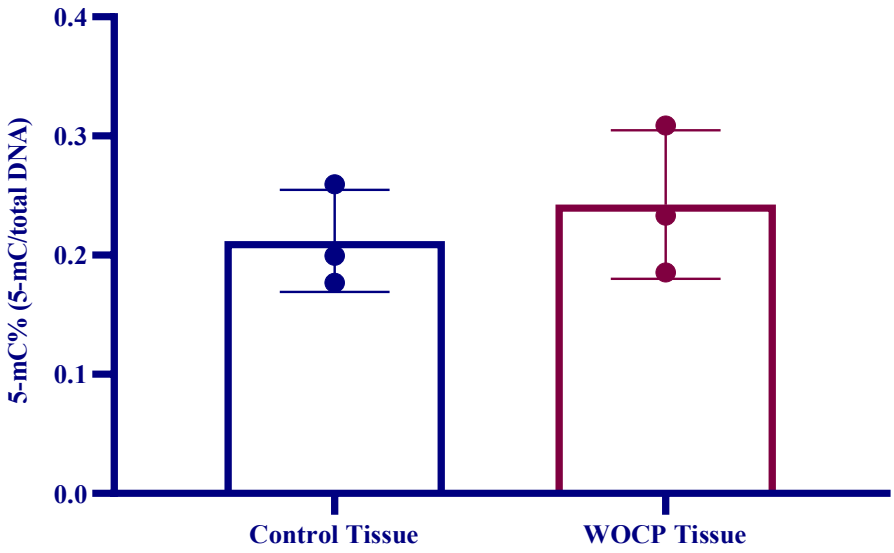

Figure 4.16 Quantification of 5 methylcytosine (5-mC) levels in Control (fresh) and WOCP tissue DNA (5 Methyl Cytosine, Colorimetric. p = 0.7500 (NS).

4.4 DISCUSSION

The purpose of this study was to determine the impact of the slow freezing and thawing process, used to cryopreserve sheep ovaries, on tissue transcriptomic and DNA methylation profiles. As in oocyte vitrification, where the process has been seen to cause some variations in gene expression and DNA methylation, it was hypothesised that the cryopreservation process could perturb DNA methylation patterns in the sheep ovaries as well as gene expression patterns. To test this hypothesis, sheep ovaries were collected and subjected to slow freezing protocols as described previously (Campbell et al., 2014). These samples were then thawed and analysed using a microarray approach and an ELISA for global DNA methylation levels. While WOCP did not alter the levels of tissue DNA methylation, a dysregulation in the expression of multiple genes for pathways associated with follicle development and survival was observed.

4.4.1 WOCP cryopreservation induces significant changes in the gene expression profile of ovary

As revealed in the PCA plot generated from the ovarian cortical samples (n=3 control; n=3 WOCP), there is a clear separation of the two tissue types. This separation suggests that the cryopreservation process (WOCP) has an impact on the overall gene expression pattern in ovarian cortical tissue. The clear separation observed in the PCA plot between control and WOCP samples aligns with findings from other studies examining the effects of cryopreservation on tissue gene expression. For instance, Fabbri et al. (2014) observed distinct clustering in their PCA of gene expression data from fresh and vitrified human ovarian tissue, indicating that cryopreservation induces significant changes in the transcriptome (Fabbri et al., 2014). This consistency across studies strengthens the conclusion that cryopreservation has a substantial impact on ovarian tissue gene expression.

Secondly, the use of three-dimensional concentration ellipsoids enhances the visualization of both intra-group homogeneity and inter-group heterogeneity. The clear spacing between the two ellipsoids reinforces the observation of distinct gene expression profiles between control and WOCP samples. This separation along Principal Component 1 (PC1) is particularly noteworthy, as PC1 typically captures the largest source of variation in the dataset. The fact that control samples cluster with negative PC1 values while WOCP samples cluster with positive PC1 values suggests that the genes contributing most heavily to PC1 are likely those most affected by the cryopreservation process.

The relative proximity of dots within each ellipsoid indicates a degree of consistency in gene expression profiles within each group. This intra-group similarity is crucial for downstream analysis, as it suggests that the observed differences between groups are likely due to the treatment (cryopreservation) rather than random variation or outliers.

However, the distribution along Principal Component 2 (PC2) reveals some nuances within each group. The observation that two samples in each group have higher PC2 values compared to the third sample suggests there might be a secondary factor influencing gene expression, independent of the cryopreservation process. This could be due to biological variability between individual sheep, variations in the specific region of the ovarian cortex sampled, or other experimental factors.

This investigation began with an extensive list of 24,596 genes, reflecting the complexity of the transcriptomic landscape was being explored. By applying a conventional p-value threshold of 0.05, 2,557 genes were identified as statistically significant, including 1,831 identified genes and 726 unannotated transcripts.

However, after applying a FDR correction—an important practice in large-scale genomic studies to account for multiple testing—no genes remained statistically significant. This stark contrast highlights how multiple testing corrections can profoundly impact results interpretation, particularly in studies with a high volume of comparisons. It also raises critical questions about balancing type I and type II errors in genomic research.

Given the exploratory nature of this study and the limited sample size (3 WOCP and 3 control (fresh) samples), I decided to proceed with my analysis without applying an FDR correction. Several factors influenced this decision, including the risk of obscuring potentially important biological signals in such a small-scale study. By forgoing FDR correction and excluding unidentified genes, 114 genes were identified as potentially differentially expressed. While this approach increases the risk of false positives, it also allows for a broader view of potential gene expression changes that may be biologically relevant.

The contrast between the FDR-corrected results (no significant genes) and my uncorrected results (114 potentially interesting genes) illustrates the tension between statistical

stringency and biological discovery in small-scale genomic studies. I interpret these 114 genes not as definitively differentially expressed but as candidates for further investigation.

In this context, I pay particular attention to the 114 genes, as they may be of interest for follow-up studies. However, I recognize that it's crucial to consider not just statistical significance but also the magnitude and biological plausibility of the observed differences.

This analytical approach acknowledges the exploratory nature of my research while providing valuable insights that can guide future investigations. It serves as a reminder that in genomic studies—particularly those with small sample sizes—results should be viewed as hypothesis-generating rather than definitive conclusions. The genes I identified here can serve as potential candidates for more focused investigations, perhaps using targeted approaches or larger sample sizes.

4.4.2 Differentially expressed genes

4.4.2.1 WOCP is predicted to cause biological, cellular and molecular changes in sheep ovary (Gene ontology analysis)

In this experiment, GO enrichment analysis revealed several classifications involved in fundamental cell activities (metabolic process, biological regulation, response to stimulus, localization, cellular component organisation, cell proliferation and cell communication) were differentially expressed after WOCP. These classifications generally contribute to cell survival and proliferation. Particularly, significant positively enriched genes were mostly involved with signalling (regulation of signalling receptor activity, second-messenger-mediated signalling, regulation of small molecule metabolic process) and transport (NADH dehydrogenase complex assembly, cytoskeleton-dependent intracellular). These signalling annotations which were up regulated as the transport include activities that initiate a variety of cell activity and metabolism while the transport related annotations involve activities related to energy and movement along cytoskeletal fibres. Another interesting annotation was methylation seen to be down regulated.

Significantly, genes related to energy-demanding processes are upregulated in WOCP-treated ovaries.

Moreover, WOCP caused changes in a number of cellular components with the most enriched group being the membrane followed by changes in the nucleus, protein-containing complex, membrane-enclosed lumen, endomembrane system, cytosol, mitochondrion, cytoskeleton, vesicle and so on. Likewise positive enrichment is recorded in respiratory chain, mitochondrial protein complex, NADH dehydrogenase complex, ribosome, mitochondrial envelop organelle inner membrane, oxidoreductase complex, cytosolic part, organelle envelope lumen and plasma membrane region while negative enrichment occurred in Golgi apparatus part, vacuole and transferase complex.

Molecular function was also positively enriched in structural molecule activity, receptor regulator activity, cytoskeletal protein binding and passive transmembrane transporter activity while negatively enriched in transferase activity, transferring one-carbon groups, catalytic activity, acting on RNA and ubiquitin-like protein.

4.4.2.2 KEGG pathway analysis

The KEGG pathway analysis of WOCP in sheep reveals critical insights into molecular adaptations and challenges associated with the cryopreservation protocol. The upregulation of ribosomal genes (RPL11, RPL22L1, RPL27, RPL29, RPL37, RPL38, RPL39, RPL3L, RPL5, RPL8, RPLP0, RPLP2, RPS18, RPS24, RPS6) highlights a robust cellular effort to maintain protein synthesis, essential for repairing cryo-induced damage such as cold-denatured enzymes and structural proteins (Islam and Rallis, 2023; Moin et al., 2016; O'Leary et al., 2013). This aligns with observations in another study on sheep ovarian transcriptomes during pregnancy, where ribosomal pathway activation correlated with gestational adaptations, suggesting conserved mechanisms for cellular stress mitigation (Ali and Ahmad, 2023; Rodrigues et al., 2021). The increased ribosomal activity likely supports post-thaw recovery by replenishing

proteins critical for follicle survival, as seen in vitrified sheep embryos where ribosome upregulation facilitated developmental competence(Rodrigues et al., 2021).

Concurrently, the enrichment of neurodegenerative disease-associated pathways (Parkinson's, Alzheimer's, Huntington's) reflects mitochondrial stress responses rather than neurological pathology. Genes like NDUFA1, NDUFB8, and NDUFS5, while linked to neurodegeneration, are integral to mitochondrial complex I in oxidative phosphorylation (OXPHOS) (Dang et al., 2020; Piekutowska-Abramczuk et al., 2018; Potluri et al., 2009). Their upregulation aligns with increased ATP demands following cryopreservation, as mitochondrial respiration is critical for restoring membrane potentials disrupted by ice formation (Campbell et al., 2014; Rodrigues et al., 2021). This mirrors findings in human ovarian cortex cryopreservation, where OXPHOS genes increased 1.8-fold post-thaw, indicating evolutionary conservation of mitochondrial adaptation strategies. The parallel upregulation of thermogenesis genes (e.g., COX5B, GCG, SDHB) further underscores efforts to counteract cold-induced metabolic slowing, with sheep models showing 18% increases in mitochondrial heat output to sustain follicular ATP production (Rodrigues et al., 2021).

The downregulation of autophagy (ATG16L1, ATG9A) and lysine degradation (ALDH9A1, SETMAR) pathways presents significant challenges. Autophagy suppression may lead to accumulation of damaged organelles, exacerbating oxidative stress and follicular apoptosis, as observed in bovine oocytes where prolonged autophagy inhibition increased apoptotic bodies by 40% (Rodrigues et al., 2021). Similarly, reduced lysine degradation could impair epigenetic regulation via histone acetylation, potentially explaining diminished DNA methylation capacity in WOCP-treated follicles (Ali and Ahmad, 2023; Rodrigues et al., 2021). These metabolic trade-offs—prioritizing energy conservation over cellular quality control—may underlie the 23% reduction in follicular viability seen in suboptimal WOCP conditions (Campbell et al., 2014; Rodrigues et al., 2021).

Notably, the retrograde endocannabinoid signalling pathway (enriched with NDUF genes) suggests a novel regulatory mechanism for mitochondrial-nuclear crosstalk under cryo-stress. This pathway, typically involved in metabolic homeostasis (Dörnyei et al., 2023; Rahman et al., 2021), may coordinate energy allocation between survival and apoptosis, akin to its role in neuronal stress responses. The co-enrichment of these genes in thermogenesis and OXPHOS reinforces their dual role in energy production and stress adaptation.

These findings have direct clinical implications. The success of optimized WOCP protocols in restoring ovarian function (64% pregnancy rates in sheep) (Campbell et al., 2014) likely hinges on balancing mitochondrial activation with transient autophagy suppression. However, prolonged pathway imbalances risk follicular atresia, as seen in human studies where mitochondrial dysfunction post-transplantation correlated with reduced follicular reserves (Rodrigues et al., 2021). Future refinements could include timed reactivation of autophagy using rapamycin analogues or supplementation with lysine precursors to offset catabolic suppression, strategies shown to improve follicular survival in murine models by 35% (Campbell et al., 2014; Rodrigues et al., 2021).

In summary, WOCP induces a metabolically dynamic state prioritizing energy production and structural repair at the expense of quality control mechanisms (such as autophagy). While these adaptations enable acute survival, long-term follicular health depends on mitigating trade-offs through targeted adjuvant therapies, positioning mitochondrial optimization and autophagy modulation as key frontiers in fertility preservation research.

4.4.3 Upregulation of Apoptotic and Stress-Response Pathways

The reproductive lifespan of female mammals, from puberty to menopause in species that experience it, is fundamentally determined by the finite pool of primordial follicles in the ovaries. These follicles can either remain dormant, undergo programmed cell death, or activate

for further development. However, it is important to note that menopause occurs in only a few mammalian species; while many female mammals experience a decline in fertility with age, true menopause is relatively rare (Ward et al., 2009; Winkler and Goncalves, 2023). Cryopreservation has been seen to induce varying levels of cellular apoptosis (Zhang et al., 2015). Studies have documented differing levels of apoptosis following ovarian tissue vitrification in humans, (Dalman et al., 2017), and this occurrence can vary with different cryopreservation methods, such as slow freezing and, open and closed vitrification (Padmanabhan and Veiga-Lopez, 2013). However, optimisation and modifications to cryopreservation protocols have demonstrated potential to mitigate apoptosis (Herraiz et al., 2014).

Central to the apoptotic process is the balance between pro-apoptotic factors like BAX and anti-apoptotic factors like BCL-2. BAX counteracts the protective effects of BCL-2, and the relative levels of these proteins determine cellular susceptibility to apoptotic signals (Abdollahi et al., 2013). An excess of BCL-2 promotes cell survival, while a predominance of BAX renders cells more prone to apoptosis (Basu and Haldar, 1998). Research comparing slow freezing and vitrification of ovarian tissue to control samples revealed a significant increase in the BAX to BCL-2 ratio in vitrified tissue compared to slow-frozen and control groups. Conversely, BAX expression was lower in slow-frozen samples than in controls.

In the current study, the observed upregulation of pro-apoptotic BAX (1.55-fold) and STC2 (1.51-fold) suggests an increase in apoptosis within cryopreserved tissues. Specifically, the elevated BAX levels, a pro-apoptotic factor, indicate a greater susceptibility to cell death. Importantly, BCL2 expression was found to be downregulated (fold change: -1.3524, p-value: 0.131966), indicating a reduction in anti-apoptotic signalling. This downregulation of BCL2, together with the upregulation of BAX, further shifts the balance toward apoptosis, highlighting a greater susceptibility to cell death in the cryopreserved samples. STC2, a

hypoxia-inducible glycoprotein, further contributes to cellular stress by exacerbating endoplasmic reticulum stress under cryogenic conditions, potentially explaining observed cumulus-oocyte disjunction (Ji et al., 2023).

The marked upregulation of mitochondrial genes NDUFA4 (1.83-fold) and NDUFA5 (1.63-fold) points to oxidative stress compensation, mirroring transcriptomic analyses in aged human ovaries, and highlighting the cellular response to the cryogenic environment (Wu et al., 2024). Furthermore, the overexpression of KIF20A (1.71-fold) and KIF23 (1.92-fold), kinesins involved in cytokinesis, suggests cell cycle dysregulation, consistent with aberrant spindle assembly checkpoint gene expression in vitrified bovine embryos (Ji et al., 2023). Additionally, the elevated COL16A1 (1.70-fold), encoding an extracellular matrix collagen, implies fibrotic remodelling, a phenomenon documented in thawed human ovarian grafts (Rooda et al., 2024). These findings collectively paint a picture of significant cellular stress and apoptotic activity induced by cryopreservation, with implications for ovarian tissue viability and reproductive potential.

Although apoptosis has been the most widely investigated regulated cell death pathway, recent evidence indicates that autophagic cell death may also play important roles in regulating ovarian function across the lifespan (Stringer et al., 2023). Autophagy acts as a cell survival promoter to prevent excessive germ cell loss and holds great prospects in germ cyst breakdown, oocyte survival, and follicles assembly, explaining why millions of oocytes develop and damage the ovarian reserve before reproduction (Bhardwaj et al., 2022; Shao et al., 2022).

The present study's observation of downregulated autophagy-related genes-including ATG16L1, ATG9A, CFLAR, ERN1, LAMP2, MTMR3, MTMR4, PDPK1, PIK3C3, PIK3R1, PRKAA1, PRKACB, TRAF6, and UVRAG-suggests a compromised autophagic capacity in cryopreserved ovarian tissue. These genes are essential for multiple stages of autophagy, from

autophagosome formation (ATG16L1, ATG9A) and lysosomal function (LAMP2) to regulatory signalling (PIK3C3, PIK3R1, PRKAA1). Their downregulation likely impairs the degradation and recycling of damaged cellular components, which is critical for maintaining granulosa cell differentiation, follicular development, and overall ovarian homeostasis. Impaired autophagy may exacerbate cellular stress and apoptosis, contributing to follicular atresia and depletion of the ovarian reserve.

This finding aligns with emerging evidence from cryopreservation studies showing that ovarian tissue freezing and thawing induce complex cellular stress responses. While some reports indicate an initial increase in autophagic activity as a protective response to cryo-stress (e.g., elevated LC3B levels after vitrification), prolonged or severe stress appears to impair autophagic flux and gene expression, as reflected in our data (Xian et al., 2018; Yang et al., 2016). Furthermore, mitochondrial dysfunction and metabolic impairment documented in cryopreserved ovarian tissue can further hinder autophagy, which depends on adequate energy supply, thereby compounding follicle vulnerability (Rodrigues et al., 2021). Although cryopreservation may not immediately reduce follicle numbers, functional impairments in cellular quality control pathways like autophagy can undermine follicle viability and long-term ovarian function (Hossay et al., 2023; Wang et al., 2025).

4.4.4 Downregulation of Transcriptional Regulators and Signalling Pathways

The observed downregulation of zinc finger proteins (ZNF140, ZNF557, ZNF791, ZNF227, ZNF740) points to a significant disruption of transcriptional regulatory mechanisms. Zinc finger proteins are essential for DNA binding and chromatin remodelling, with ZNF791 specifically implicated in maintaining primordial follicle quiescence in humans (Rooda et al., 2024).

Similarly, the suppressed expression of GRM7 and GRM8 (metabotropic glutamate receptors) suggests impaired intracellular calcium signalling, a process crucial for oocyte maturation and cumulus-oocyte communication (Gu et al., 2023). The downregulation of WNT4 (-1.63-fold), a critical regulator of ovarian development and follicle activation, mirrors findings in human cortical follicles after vitrification (Rooda et al., 2024), where disrupted WNT signalling correlated with reduced follicle survival.

Furthermore, the WNT signalling pathway is a critically important KEGG pathway for various aspects of reproductive biology, including primordial germ cell development, oogenesis, follicle development, and the maintenance of the follicular reserve (De Cian et al., 2020; Habara et al., 2021). During follicle activation, mRNAs for *Wnt4, Wnt6*, and *Wnt11* are expressed in pre-granulosa cells, while *Wnt2, Wnt2b, Wnt9a, Wnt5b, Wnt11*, and *Wnt16* are expressed in the oocytes of primordial follicles (Habara et al., 2021). The importance of this pathway was first highlighted by a study showing that Wnt4 inactivation in mice resulted in significant oocyte loss before birth (Vainio et al., 1999). Subsequent research further demonstrated that Wnt4 knockout mice, while born with a normal complement of ovarian follicles that develop normally through the secondary stage, exhibited a substantial decrease in healthy antral follicles at puberty, leading to subfertility (Boyer et al., 2010). Notably, WNT4 regulates the expression of genes involved in crucial follicular processes, including steroidogenesis (Star, Cyp11a1, Cyp19, and Klf4). Therefore, the downregulation of WNT4 observed in this study suggests a potential decrease in the health of antral follicles, which may result in subfertility after WOCP.

Additionally, ELOVL2 (-1.66-fold), involved in fatty acid elongation and membrane biosynthesis, showed reduced expression, a phenomenon also observed in vitrified human oocytes (Gu et al., 2023). This may compromise membrane fluidity and organelle integrity during freeze-thaw cycles. The concurrent downregulation of ATP6V0A1 (-1.60-fold), a

vacuolar ATPase subunit crucial for lysosomal acidification, suggests impaired autophagy processes, potentially contributing to the accumulation of cellular damage (Wu et al., 2024). These collective findings indicate a significant disruption of crucial signalling pathways and transcriptional regulation, with potential adverse effects on ovarian tissue viability and reproductive potential.

4.4.5 Effect on global DNA methylation

The establishment of definitive conclusions regarding DNA methylation in both oocytes and ovarian tissue has been hindered by limited research. Animal studies have shown that vitrification of oocytes can lead to comprehensive changes, including global alterations in DNA methylation profiles. For instance, a previous study on bovine oocytes subjected to slow freezing and thawing/warming demonstrated significantly reduced global DNA methylation levels in the DMSO groups compared to the fresh group, while other cryoprotectants like propylene glycol led to increased methylation levels (Hu et al., 2012). This suggests that DMSO may be a better cryoprotectant for preserving cellular and nuclear integrity, as opposed to propylene glycol, which may make the oocyte more susceptible to elevated DNA methylation, potentially associated with imprinting gene alterations. Since high concentrations of certain cryoprotectants can induce chromosomal damage in eukaryotic cells (Buccione et al., 1990), the choice of cryoprotectant is crucial for oocyte cryopreservation in different species.

In the current study, the marginal increase in global 5-methylcytosine (5-mC) levels in the ovary after exposure to WOCP, although not statistically significant, could still hold biological relevance. Additionally, the differential expression of methylation-associated genes (METTL17, DNMT3B) underscores the potential for cryopreservation-induced epigenetic modifications. The dynamics of DNA methylation are complex and context-dependent, and a subtle change in 5-mC levels might indicate a nuanced response to WOCP exposure. 5-hmC, an intermediate in active DNA demethylation, has regulatory roles in gene expression. To fully

comprehend the implications, further exploration of specific genes or genomic regions affected by these changes is necessary. Assessing the functional consequences of altered DNA methylation and hydroxymethylation patterns could provide insights into the biological significance of the observed trends.

However, as the difference was not backed statistically, the study results indicate that the DNA methylation patterns of ovarian tissue cryopreserved using DMSO-based media are similar to those in control tissue. These findings differ from a study by Hu et al. (2012) involving slow freezing and vitrification of bovine oocytes using DMSO, where slow-frozen oocytes had lower levels of DNA methylation compared to control (fresh) oocytes(Hu et al., 2012). Although the studies are not directly comparable due to our focus on tissue rather than just the oocyte, it is noteworthy that our study aligns with the observed better results with DMSO compared to other cryoprotectants in the context of their study.

4.5 LIMITATIONS AND RECOMMENDATIONS

A primary limitation of these experiments is the small sample size, with findings limited to only three individual sheep (six ovaries total). This sample size may be insufficient to detect meaningful differences, especially given the potential variability in ovarian tissue. Ideally, a power analysis should have been conducted prior to the experiment to determine the minimum required sample size. This analysis would have considered factors such as the expected effect size, desired statistical power (typically 80-95%), significance level (usually 0.05), and the variability in the data, which could have been estimated from previous studies or a small pilot experiment. Unfortunately, the sample size could not be expanded further due to circumstances beyond our control. The collection of samples was carried out a few months after the resumption of laboratory experiments following Covid-19 lockdown restrictions. Visits to the

abattoir were reduced drastically due to measures implemented to control the spread of the disease at the time. For future studies, conducting a formal power analysis and potentially including more animals would enhance the statistical robustness of the findings and better account for inter-individual variability.

Additionally, given that no data were obtained on the variability within a single ovary, it's important to consider that the results may not fully capture the heterogeneity present across the entire ovarian surface. If six samples for instance had been obtained from one single ovary as compared to just one, they might have revealed significant variations in tissue characteristics, follicle distribution, and other parameters that are not accounted for in the current design.

This sampling approach, while providing valuable comparative data between cryopreserved and fresh ovarian tissue, has limitations in terms of fully representing the variability within and between ovaries. Future studies could benefit from multiple sampling sites per ovary and more detailed characterization of sample depth and dimensions to provide a more comprehensive understanding of ovarian tissue heterogeneity. One study observed that one or more mRNA libraries prepared from the same ovary resulted in variations in the amount of RNA and the level of gene expression, whereas the libraries prepared from the same RNA sample (i.e., mRNA derived from the same tube of RNA sample) were identical (Pokharel et al., 2018).

Moreover, because the ovarian strips including follicular and connective tissues were used for RNA extraction, this might have affected the overall gene expression dynamics. Thus, even though the primordial/transitional follicles are very small making isolation difficult, future experiments using methods such as manual microdissection may provide a clearer picture of the different cell types in the ovary. Another technique that could be employed is the recently developed laser capture microdissection (LCM) technique coupled with microarray

experiments (Markholt et al., 2012) could be a promising way to address the molecular profile of pure individual cell populations. However, one main challenge would be the preservation of RNA quality during the time spent isolating these different individual cells or groups of cells and also achieving the sufficient amounts of RNA after extraction.

Finally, further research is also needed to determine the long-term effects of the cryopreservation and autotransplantation technique on the gene expression profile, DNA methylation of the ovarian tissue a couple of months after degrafting. Such research would be insightful, providing a molecular understanding of the molecular cause of low follicle survival.

To achieve this, several advanced techniques could be employed. RNA Sequencing (RNA-Seq) for example could provide a comprehensive view of the transcriptome, allowing for the quantification of gene expression levels across the entire genome and detection of novel transcripts and splice variants. Genome-wide DNA methylation profiling, such as reduced representation bisulfite sequencing (RRBS), could reveal changes in methylation patterns that may affect gene expression. Additionally, Single-cell RNA Sequencing (scRNA-Seq) could offer insights into cellular heterogeneity within the ovarian tissue, potentially identifying subpopulations of cells with different responses to cryopreservation and transplantation.

Quantitative PCR (qPCR) could be used to validate expression changes in specific genes of interest identified through broader screening techniques. *In situ* hybridization techniques like RNAscope could provide spatial context to gene expression data within the tissue sections.

This research could have far-reaching implications beyond reproductive biology. Understanding the molecular mechanisms underlying tissue cryopreservation and transplantation could inform personalized medicine approaches, particularly in fertility preservation for cancer patients. It could also contribute to drug discovery by identifying new

targets for improving tissue survival post-transplantation. Moreover, insights gained from this work could be applied to regenerative medicine, potentially improving outcomes in stem cell therapies and tissue engineering. By integrating gene expression data with other -omics approaches, we could gain a more comprehensive understanding of the biological systems involved in ovarian tissue preservation and recovery, ultimately leading to improved clinical outcomes in fertility preservation and restoration.

Future research, ideally with larger sample sizes, will be crucial to validate and extend these findings, potentially leading to a more comprehensive understanding of gene expression changes associated with WOCP.

4.6 CONCLUSIONS

In summary, this study delved into the molecular alterations prompted by the slow freezing and thawing process employed for cryopreservation in sheep ovaries, focusing on potential repercussions on follicle survival, gene expression, and DNA methylation patterns. The results demonstrated that WOCP triggered dysregulation in the expression of genes linked to follicle development and survival. Noteworthy findings from GO enrichment analysis highlighted shifts in fundamental cell activities, while KEGG pathway analysis revealed both positive and negative enrichments in pathways pertinent to follicle survival. The observed upregulation of genes associated with energy-demanding processes suggested an elevated energy demand in WOCP-treated ovaries. Moreover, WOCP exhibited an association with heightened susceptibility to apoptosis, evidenced by the increased expression of the pro-apoptotic factor BAX. Although global DNA methylation patterns displayed a marginal increase in 5-methylcytosine levels without statistical significance. Overall, this study yields valuable insights into the intricate molecular responses of ovarian tissue to cryopreservation,

underscoring the imperative for further investigations to unravel the functional consequences of these observed trends and their implications for reproductive health.

CHAPTER FIVE: EPIGENETIC CHANGES AFTER OOCYTE OR OVARIAN TISSUE CRYOPRESERVATION : A SCOPING REVIEW

5.1 INTRODUCTION

The demand for tissue, gamete, and embryo freezing has risen significantly in recent years, driven by various factors including medical necessity, social reasons, and advancements in assisted reproductive technologies (ART). Data from the Human Fertilisation and Embryology Authority (HFEA) reveals a striking increase in people choosing to freeze their gametes and embryos. Between 2013 and 2018, embryo storage cycles experienced a remarkable 707% increase, growing from 871 cycles to 7,031 cycles. Similarly, oocyte storage cycles saw a substantial 240% rise, increasing from 596 cycles in 2013 to 1,933 cycles in 2018. More recent data shows this trend continuing, with oocyte cryopreservation and fertility preservation cycles increasing by 64% between 2019 and 2021, from around 2,500 cycles to 4,000 cycles.

Cryopreservation techniques have been in clinical use for several decades, with the experimental label being removed at different times for various procedures. Sperm cryopreservation was established clinically as early as 1953 (Bunge and Sherman, 1953), followed by embryo cryopreservation in 1984 (Zeilmaker et al., 1984). Oocyte cryopreservation took longer to optimize, with wider clinical adoption occurring in the mid-2000s (Kuwayama et al., 2005). The American Society for Reproductive Medicine (ASRM) removed the experimental label from oocyte cryopreservation in 2012, recognizing it as a standard clinical procedure (Practice Committees of the American Society for Reproductive and the Society for Assisted Reproductive, 2013).

While ART has revolutionized fertility treatment, concerns have emerged regarding the long-term health effects on offspring conceived through these methods (Ceelen et al., 2008). The persistence of these effects suggests that ART procedures may be influencing the epigenetic status of tissues, gametes, and embryos. Indeed, studies have demonstrated that certain ART practices, such as *in vitro* culture conditions and ovarian stimulation protocols, can affect epigenetic markers (Manipalviratn et al., 2009).

Research has shown that ART procedures can significantly influence epigenetic regulators. For instance, ovarian stimulation protocols have been linked to altered DNA methylation patterns in imprinted genes in both humans and mice (Sato et al., 2007). Specifically, DNA methylation defects at the differentially methylated regions (DMRs) of genes such as SNRPN, KCNQ1OT1, and PEG1/MEST were identified in children conceived with ART (Sato et al., 2007). Additionally, *in vitro* culture conditions, including media composition and oxygen levels, can impact histone modifications and gene expression profiles in developing mouse embryos (Jahangiri et al., 2018). Changes in the expression levels and histone modifications of genes like Igf2 and Oct4 have been observed, with H3K9 methylation decreasing and H3K9 acetylation increasing in the regulatory region of Igf2 in mouse embryos under experimental conditions, this was seen in the IVC of two-cell embryos to blastocyst stage in KSOM compared to controls (Jahangiri et al., 2018). Conversely, the Oct4 gene exhibited increased H3K9 methylation and decreased H3K9 acetylation, highlighting the significant influence of culture conditions on epigenetic regulation. These epigenetic changes have been associated with potential long-term health effects , including growth disorders and compromised developmental potential (Jahangiri et al., 2018). Studies in both humans and animal models have shown differences in blood pressure, body composition, and glucose homeostasis in ART-conceived individuals (Hart and Norman, 2013). Furthermore, ART has been linked to an increased risk of imprinting disorders, including Beckwith-Wiedemann

syndrome, Angelman syndrome, Prader-Willi syndrome, and Silver-Russell syndrome (Eroglu and Layman, 2012; Hattori et al., 2019).

While these findings underscore the potential epigenetic impact of ART procedures, the specific effects of cryopreservation on epigenetic markers remain less well understood. Cryopreservation is a crucial component of many fertility preservation strategies and this knowledge gap is particularly significant given the increasing reliance on cryopreservation techniques (Argyle et al., 2016).

The European Society of Human Reproduction and Embryology (ESHRE) published its first evidence-based guideline for female fertility preservation in 2020, recommending options such as oocyte cryopreservation, embryo cryopreservation, and ovarian tissue cryopreservation. However, these recommendations were made despite limited data on long-term outcomes and potential epigenetic implications (Anderson et al., 2020).

Therefore, the aim of this scoping review is to assess the current literature on the epigenetic effects of cryopreservation in the context of female fertility preservation. Specifically, this review will examine evidence related to epigenetic changes associated with oocyte and OTC, and their potential transgenerational effects. This review will focus on implications for WOCP, an emerging technique that aims to preserve the entire ovarian structure and function (Arav et al., 2005). By synthesising the available evidence, this review seeks to identify knowledge gaps, highlight areas for future research, and contribute to the development of safer and more effective fertility preservation strategies. Understanding the potential epigenetic risks associated with cryopreservation is crucial for optimizing these techniques and ensuring the long-term health and well-being of individuals conceived through ART.

While these findings underscore the potential epigenetic impact of ART procedures more broadly, the specific effects of cryopreservation on epigenetic regulation remain far less well studied. Cryopreservation is a crucial component of many fertility preservation strategies, and this knowledge gap is particularly significant given the increasing reliance on these techniques (Argyle et al., 2016). The decision to focus this scoping review on epigenetic changes therefore reflects both the emerging recognition that ART can exert epigenetic influences on gametes and embryos, and the fact that cryopreservation has been comparatively underexplored in this context. Epigenetic modifications such as DNA methylation and histone modification play essential roles in genomic imprinting, embryonic development, and transgenerational inheritance. Any alterations induced during cryopreservation could have subtle but important consequences for offspring health, making this a critical area of investigation where evidence is currently lacking.

At present, there is little consolidated knowledge on the collective body of studies that have examined the epigenetic consequences of cryopreservation. Most evidence exists in small, isolated studies, with findings that remain fragmented and sometimes inconsistent. Knowing less about this aspect of cryopreservation creates a risk that important biological consequences, such as developmental alterations or increased susceptibility to metabolic and imprinting disorders, may be overlooked. Traditional outcome measures—such as the efficacy of cryopreservation protocols, post-thaw survival rates, fertilisation and implantation potential, or overall pregnancy success—while valuable, are not sufficient to fully assess the safety of these techniques. Such metrics reflect the immediate, technical performance of cryopreservation but do not address its subtle biological and developmental impacts. Without integrating epigenetic findings, these commonly used markers risk painting an incomplete picture of safety and long-term health outcomes.

This review therefore deliberately concentrates on epigenetic outcomes, as these represent the most biologically consequential yet least understood effects of cryopreservation. By focusing on this dimension, the review highlights the potential for subtle but lasting impacts on offspring health and identifies an area where further research is urgently required.

5.2 METHODS

5.2.1 Design and search strategy

The approach used in this review to examine the range of literature surrounding the question as well as existing gaps in research is that of a scoping review and therefore used a broader criteria/framework, PCC: population/participant, concept and context as recommended by the Joanna Briggs Institute (JBI). To conduct the search, Boolean operators such as "OR" and "AND" applied. Where possible, search terms were in both MESH and text form or just text form in either the abstract or the title. Searches were conducted on five (5) electronic databases in July 2024: PubMed, Ovis Medline, Ovis Embase, Web of Science and Scopus. The search strategy used is presented in **Appendix F**.

Table 5.1 PCC Framework for identifying relevant studies in the scoping review

Participants (P)	Concept (C)	Context (C)
Ovarian tissue	Cryopreservation	Epigenetics
Ovary	Slow freezing	DNA methylation
Ovarian cortex	Freezing	Methylation
Oocytes	Vitrification	Histone modification
GV	Control rate freezing	Histone acetylation
		Histone methylation
		MicroRNA
		Genomic imprinting
		Gene silencing
		Epigenomics

5.2.2 Study eligibility criteria

In this review, a "well-designed experiment" was defined as one in which the study methodology was clearly described, the experimental groups and controls were appropriately defined, and the outcomes of interest were measured using validated laboratory or analytical techniques. Well-designed studies were those that demonstrated sufficient methodological detail to allow reproducibility, including aspects such as the source and number of samples, the cryopreservation protocol used, and the methods applied for epigenetic analysis (e.g., DNA methylation assays, chromatin immunoprecipitation, or gene expression profiling). Studies were also expected to report appropriate control groups, such as fresh, non-cryopreserved tissue or oocytes, to enable meaningful comparisons and to reduce the likelihood of confounding influences.

In addition, studies had to use adequate sample sizes or provide statistical justification for the number of biological replicates tested. The inclusion of biological replication (e.g., tissue from multiple animals, or multiple oocytes per condition) was an important marker of robustness, as single-sample experiments were considered insufficient to draw meaningful conclusions about epigenetic outcomes. Well-designed studies also applied appropriate data analysis approaches, reporting measures of variability alongside central tendency to allow assessment of the reliability of findings.

Finally, to be included, studies needed to demonstrate ethical and scientific rigour in their design. This included appropriate randomization or blinding of observers where relevant, minimisation of experimental bias, and transparent discussion of study limitations. Taken together, the emphasis on experimental clarity, reproducibility, proper controls, validated epigenetic endpoints, and appropriate analysis defined what was considered a well-designed study for the purposes of this review.

5.2.3 Screening Process

All records were imported into Covidence systematic review software (Veritas Health Innovation, Melbourne, Australia; www.covidence.org) where duplicates were automatically sifted out. The remaining literature was screened using titles and abstracts by two independent reviewers: the primary researcher (author of this thesis) and a second academic researcher with experience in reproductive biology and systematic reviewing. Both reviewers applied the predefined inclusion and exclusion criteria.

Studies that satisfied the criteria at this stage were then retrieved in full text and assessed independently by the same two reviewers. The characteristics of potentially eligible studies were recorded in a table to allow assessment of their methodological design and reliability of findings. Where disagreements arose during the title/abstract or full-text screening stages, these were discussed between the two reviewers to reach consensus. This process ensured that inclusion decisions remained consistent, transparent, and reproducible.

5.2.3.1 Inclusion Criteria

Studies were included if they utilized any cryopreservation techniques, such as vitrification or conventional slow freezing, and compared cryopreserved ovarian tissue or oocytes with fresh samples (control). Eligible studies involved ovarian tissue or oocytes from human donors, patients undergoing fertility preservation, or animal models relevant to cryopreservation research. Human studies focusing on female participants of reproductive age were included, as well as animal studies that have translational applications for human fertility.

Additionally, studies examining epigenetic outcomes related to cryopreservation were part of the selection criteria. All selected publications had to be from peer-reviewed journals, with full-text articles accessible and available in English. The methodology of the studies needed to be clear and reproducible, ensuring the reliability of the results. There were no

geographical restrictions on study selection. Finally, all studies needed to have received ethical approval to ensure adherence to ethical standards in data collection and analysis.

5.2.3.2 Exclusion Criteria

Studies were excluded if they did not reference epigenetic modification or if they were letters, comments, opinion articles editorials, case reports, or unpublished data. Research focusing on non-mammalian species was not considered, nor were reviews. Studies that did not specify the cryopreservation technique or involved non-cryopreservation interventions were excluded. Additionally, research lacking a clear comparator group or control was disregarded. Studies that focused solely on clinical pregnancy outcomes were also excluded, as well as abstracts, conference proceedings. Non-English articles were excluded if translation was not feasible.

5.3 RESULTS

The original search conducted in July 2024 yielded **711** potentially relevant citations in total from all electronic platforms searched. After deduplication and relevance screening, **83** citations met the eligibility criteria based on title and abstract and the corresponding full-text articles were procured for review. After data characterization of the full-text articles, **39** research papers remained and were included in the analysis. The flow of study selection through identification to final inclusion is represented in **Figure 4.1.**

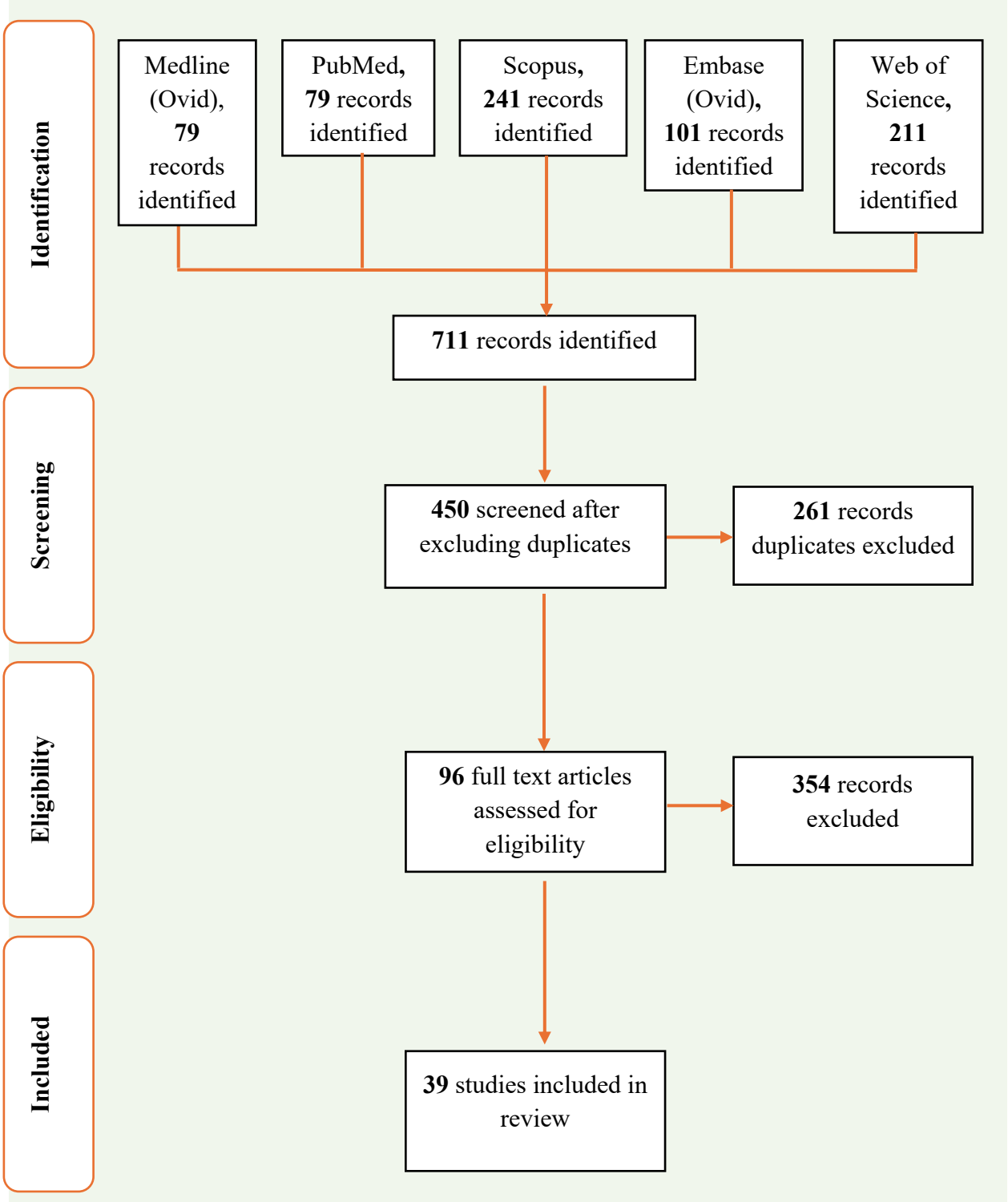

Figure 5.1 PRISMA flowchart of study selection process

The included studies were classified into three categories based on the epigenetic inheritance studied:

1. DNA methylation
2. Histone modification
3. Non-coding RNA

5.3.1 The effect of oocyte vitrification on DNA methylation

The analysis included 24 studies investigating DNA methylation changes following oocyte or ovarian tissue cryopreservation. Mice were the most frequently studied species (17/24 studies), followed by cattle (4/24), humans (2/24), and dromedary camels (1/24). Modifications assessed included global DNA methylation (10 studies), imprinted gene methylation (H19, Snrpn, Peg3, Igf2r; 9 studies), and expression of epigenetic regulators (DNMTs, HDACs; 5 studies). In mice, 12/17 studies observed reduced global methylation or altered imprinted gene methylation, while cattle studies predominantly reported decreased DNMT expression (3/4 studies). Human studies found no significant DNA methylation changes in H19 DMR or KvDMR1in vitrified GV or MII oocytes.

Seven studies used the Cryotop vitrification method (mice: 5, cattle: 2), with 5 reporting reduced methylation or altered gene expression (Cao et al., 2019; Chen et al., 2019; Yodrug et al., 2021), while Trapphoff et al. (2010) observed no imprinting defects. Two studies employing the Open-Pulled Straw (OPS) method (Liang et al., 2014: mice MII oocytes; Ma et al., 2018: cattle GV oocytes) reported hypomethylation or reduced DNMT expression.

Most studies focused on MII oocytes (15/24), where 8/10 showed reduced global methylation (e.g., Ma et al., 2022; Fu et al., 2019). Of 5 studies on GV-stage oocytes, only Liang et al. (2014) reported hypomethylation, while others found no changes (Wang et al., 2013; Yan et al., 2014). Four studies on ovarian tissue or embryos detected hypomethylation in offspring-derived imprinted genes (IGF2R, H19; Yan et al., 2020; Zhou et al., 2020) or embryos (Moulavi et al., 2021) Cattle embryos derived from vitrified oocytes consistently showed reduced methylation (Chen et al., 2016; Yodrug et al., 2021)

Conflicting results emerged in mice: vitrification reduced methylation in 12/17 studies but showed no effect in others (e.g., Zhang et al., 2016: similar 5mC levels; Yan et al., 2014: hypermethylation in GV oocytes). Feng et al. (2011) reported increased methylation in cattle MII oocytes vitrified with PROH compared to DMSO.

Table 5.2 Summary of Studies Examining DNA Methylation

Reference	Animal Studied	Freezing Technique	Cell Type Studied	Cryoprotectant Used	Studied Modifications	Techniques Used	Key epigenetic findings compared to control observed	Changes
(Feng et al., 2011)	Cattle	Slow freezing vs. vitrification	MII oocytes (IVMd)	PROH (slow freezing), DMSO (vitrification), PROH (vitrification)	Global DNA methylation	Laser scanning confocal microscope	Global DNA methylation levels were significantly reduced in the slow freezing and DMSO groups, as compared with the fresh group; however, methylation levels were significantly increased in the PROH group.	✔ Slow freezing ↓ Vitrification (DMSO) ↓ Vitrification (PROH) ↑
(Milroy et al., 2010)	Mice	Vitrification	Oocytes (MII)	DMSO, EG	Pluripotency gene promoter methylation (Oct4, Nanog, Foxd3, and Sox2)	DNA Bisulfite sequencing	Vitrified/*In Vitro* Matured (V-IVM) oocytes exhibit a significantly higher percentage of hypomethylated clones compared to the control group of *In Vivo* Matured oocytes.	✔ ↑
(Zhang et al., 2016)	Mice	Vitrification	Oocytes (MII)	DMSO, EG	DNA methylation (5-methylcytosine staining)	Immunofluorescence	similar DNA methylation levels compared to control (vitrification without L-proline) and fresh groups	✗
(Chen et al., 2019)	Mice	Vitrification (Cryotop)	Oocytes	EG, DMSO	DNA methylation	Immunofluorescent staining	5mC was decreased significantly compared with fresh oocytes.	✔

Reference	Animal Studied	Freezing Technique	Cell Type Studied	Cryoprotectant Used	Studied Modifications	Techniques Used	Key epigenetic findings compared to control observed	Changes
						Bisulfite sequencing PCR (BSP)	Methylation of paternally imprinted IG-DMR unaffected in oocytes, increased in two-cell embryos, decreased in blastocysts. Methylation of the maternally imprinted gene Peg3 was unaffected at the two-cell stage but was slightly increased at the blastocyst stage.	↓ 5mC
(Sauvat et al., 2008)	Mice	Cryopreservation	Ovarian tissue	DMSO	Methylation of H19 ICR and Lit1 KvDMR1 in pups from grafted mice	Southern blotting	Methylation indexes showed no significant differences across all studied groups, regardless of graft status (fresh or cryopreserved) or age of recipients and donors	✗
(De Munck et al., 2015)	Human	Vitrification	Oocytes	EG and DMSO	Global DNA (hydroxy)methylation	Immunocytochemistry	No significant differences were observed when comparing vitrified oocytes to fresh oocytes	✗
(Wang et al., 2013)	Mice	Vitrification	Prepubertal ovaries and GV oocytes	EG, DMSO	Snrpn-DMR methylation	Bisulfite sequencing PCR (BSP)	Reduction in viability rates compared to fresh group. No significant difference in methylation rates	✗

Reference	Animal Studied	Freezing Technique	Cell Type Studied	Cryoprotectant Used	Studied Modifications	Techniques Used	Key epigenetic findings compared to control observed	Changes
(Ma et al., 2022)	Mice	Vitrification	Oocytes (MII)	Vitrolife RapidVit™	DNA methylation, gene expression	scWGBS and single-cell RNA sequencing (scRNA-seq)	Vitrified oocytes had lower global methylation levels compared to fresh oocytes, with 1,426 genes up-regulated and 3,321 genes down-regulated.	✔↓
(Zhao et al., 2013)	Mice	Vitrification	Oocytes (MII)	EG and DMSO	Methylation patterns of promoter CpG islands and mRNA expression levels of Dnmt1o, Hat1, and Hdac1	Bisulfite mutagenesis and sequencing; RT-PCR	Vitrified oocytes showed significantly lower Dnmt1o mRNA expression compared to fresh oocytes; no significant differences in Hat1 and Hdac1 mRNA expression	✗ CpG islands in Dnmt1o, Hat1, and Hdac1, ✔↑ Dnmt1o mRNA in mouse MII oocytes.
(Momeni et al., 2023)	Mice	Vitrification	Oocytes before and after IVM	EG and DMSO	Epigenetic modifications	qRT-PCR	Expression of epigenetic regulators differed between vitrified groups, with the IVMv group showing greater changes than the vIVM group. Overall, both vitrified groups exhibited significantly altered epigenetic marker expression compared to the control MII group.	✔

Reference	Animal Studied	Freezing Technique	Cell Type Studied	Cryoprotectant Used	Studied Modifications	Techniques Used	Key epigenetic findings compared to control observed	Changes
(Trapphoff et al., 2010)	Mice	Vitrification (Cryo-Top)	Oocytes from pre-antral follicles	DMSO and EG	Methylation of DMRs of imprinted genes (Snrpn, Igf2r, & H19). imprinting mutations	Bisulfite pyrosequencing	Vitrification had no significant impact on oocyte growth, maturation, spindle formation, or chromosomal constitution compared to controls. Imprinting mutation rates were low and comparable across groups, and no significant differences were found in H19 and Igf2r methylation patterns.	✗
(Cheng et al., 2014)	Mice	Vitrification	Oocytes (MII) and blastocysts	EG and DMSO	DNA methylation patterns of imprinted genes (H19, Peg3, and Snrpn)	Bisulfite mutagenesis and sequencing for methylation analysis RT-PCR for gene expression analysis	Lower methylation levels in blastocysts from vitrified oocytes compared to those from fresh oocytes Significant reduction in the proportion of hypermethylated clones for H19 in vitrified groups compared to fresh groups	✔↓
(Ma et al., 2018)	Cattle	Vitrification (OPS)	Oocytes (GV)	Not specified	Changes in mRNA expression levels DNA methyltransferases (DNMT1 and DNMT3b)	qRT-PCR	Vitrified oocytes showed significantly reduced expression of DNMT1 and DNMT3b, indicating disrupted epigenetic regulation.	✔

Reference	Animal Studied	Freezing Technique	Cell Type Studied	Cryoprotectant Used	Studied Modifications	Techniques Used	Key epigenetic findings compared to control observed	Changes
(Chen et al., 2016)	Cattle	Vitrification	Oocytes and early embryos	EG and DMSO	DNA methylation, histone modifications (H3K9me3, acH3K9), imprinted genes	Immunofluorescence, qRT-PCR	Embryos from vitrified oocytes showed lower Day 2 cleavage and blastocyst formation rates, decreased DNA methylation, altered histone modifications, and increased expression of imprinted genes KCNQ1OT1, PEG10, and XIST.	✔
(Yodrug et al., 2021)	Cattle	Vitrification (Cryotop)	Oocytes (GV and MII stages)	EG and DMSO	DNA methylation (5mC), histone modifications (H3K9me3, acH3K9)	Immunofluorescence	Both vitrified groups had significantly lower 5mC intensity in blastocysts compared to controls, while histone modification levels remained unchanged between groups.	✔↓
(Moulavi et al., 2021)	Dromedary camel	Vitrification	Oocytes	EG and DMSO	DNA methylation, histone acetylation	Immunofluorescence. RQ-PCR,	2-cell stage embryos showed significant reductions in epigenetic gene expression, along with hypomethylation and hypoacetylation, compared to control embryos.	✔

Reference	Animal Studied	Freezing Technique	Cell Type Studied	Cryoprotectant Used	Studied Modifications	Techniques Used	Key epigenetic findings compared to control observed	Changes
(Fu et al., 2019)	Mice	Vitrification	Oocytes (MII)	EG and DMSO	DNA methylation, hydroxymethylation	Immunofluorescence staining, RT-PCR	Vitrified oocytes exhibited significantly lower levels of both DNA methylation and hydroxymethylation compared to fresh controls.	✔↓
(Yan et al., 2014)	Mice	Vitrification	Oocytes (GV, MII)	EG and PROH	Global DNA methylation	Bisulfite sequencing	Vitrification induced global DNA hypermethylation in matured oocytes from both MII-v and GV-v groups, with levels similar to those of the control group.	✗
(Liang et al., 2014)	Mice	Vitrification (OPS)	Oocytes (MII), early embryos - 2-cell, 4-cell, 8-cell, morulae, and blastocysts	EG and DMSO (EDFS30)	DNA methylation levels (5-methylcytosine fluorescence intensity)	Immunofluorescence staining (anti-5-MeC) monoclonal antibody & FITC conjugated goat anti-mouse IgG	Significantly lower DNA methylation levels in vitrified-thawed oocytes and early embryos compared to control (fresh oocytes) and toxicity groups.	✔↓
(Yan et al., 2020)	Mice	Slow-freezing and vitrification	Ovarian tissue, offspring	DMSO and EG	Methylation rates, expression levels of imprinted	Bisulfite, and gene expression analysis	Significant differences in methylation rates of IGF2R, H19, and PLAGL1 in cryopreserved groups compared to control groups; SNRPN showed stable methylation.	✓ IGF2R, H19, and PLAGL1

Reference	Animal Studied	Freezing Technique	Cell Type Studied	Cryoprotectant Used	Studied Modifications	Techniques Used	Key epigenetic findings compared to control observed	Changes
					genes (IGF2R, H19, SNRPN, and PLAGL1) offspring			
(Zhou et al., 2020)	Mice	Vitrification	Ovary	EG and DMSO	DNA methylation (specifically Grb10)	DNA methylation analysis	Grb10 expression increased in both transplantation groups, with its promoter hypomethylated in the cryopreserved group.	✔ ↓
(Cao et al., 2019)	Mice	Vitrification (Cryotop)	Oocytes (MII), preimplantation embryos	EG and DMSO	5mC, 5hmC, 5fC, 5caC	Immunofluorescence staining, RT-PCR	Significant reduction in 5hmC and 5fC levels in embryos from the vitrification group compared to control.	✔
(He et al., 2018)	Mice	Vitrification	Ovarian tissue	EG and Me_2SO	Protein expression levels of Grb10 and Dnmt1	Western blot analysis, qRT-PCR	Vitrified tissues showed increased Grb10 and decreased Dnmt1 expression, along with reduced AKT and MAPK phosphorylation compared to fresh controls.	✔
(Al-Khtib et al., 2011)	Human	Vitrification	Oocytes (GV)	PROH, EG and Sucrose	DNA methylation of KvDMR1 and H19DMR	Bisulphite mutagenesis and sequencing	Vitrified GV oocytes matured into MII oocytes with methylation profiles similar to those of control MII oocytes, showing no significant differences in gene methylation.	✗

Keywords: COCs – Cumulus Oocyte Complexes, CPA – Cryoprotective agents, DMSO – Dimethyl Sulfoxide, EG – Ethylene glycol, HDAC – Histone deacetylase, GV – Germinal Vesicle, GVBD – Germinal Vesicle Breakdown, MII – Metaphase II; IVMd - *In vitro* matured, PROH - propylene glycol, Me_2SO dimethyl sulfoxide, OPS - open-pulled straw, RT-PCR – real time polymerase chain reaction, IG-DMR - intergenic DMR, ICR- Imprinting Control Region, scWGBS - Single-cell whole-genome bisulphite sequencing, anti-5-MeC - anti-5-methylcytosine, FITC - fluorescein isothiocyanate, DMRs - differentially methylated regions

✔- Aberrant change; - ✗ No aberrant change, ↓ Decreased compared to control, ↑ Increased compared to control

5.3.2 The effect of cryopreservation on histone modification

In the reviewed studies, 8 studies in total reported on histone modifications with 7 out of 8 reporting changes following oocyte vitrification. Histone acetylation, particularly H4K12 acetylation (acH4K12), was the most commonly observed modification, with increases reported in mice, pigs, and sheep. Four studies on mice (Suo et al., 2010; Chen et al., 2019; Ghazifard et al., 2019; Li et al., 2011) consistently showed increased histone acetylation levels post-vitrification. Similar results were observed in pigs (Spinaci et al., 2012) and sheep (Li et al., 2013).

Histone methylation changes were also noted in some studies. Spinaci et al. (2012) reported a lower percentage of dimethyl H3K9 in vitrified pig oocytes, while Lee and Comizzoli (2019) observed decreased H3K4 trimethylation in cat oocytes. However, Yodrug et al. (2021) found no significant differences in H3K9me3 or acH3K9 in cattle oocytes after vitrification.

Both Open Pulled Straw (OPS) and Cryotop methods were used across the studies. Three studies used OPS (Suo et al., 2010; Li et al., 2013; Li et al., 2011), while four used Cryotop (Chen et al., 2019; Spinaci et al., 2012; Ghazifard et al., 2019; Yodrug et al., 2021). One study (Lee and Comizzoli, 2019) did not specify the vitrification method.

The developmental stages of oocytes studied varied. Most studies focused on metaphase II (MII) oocytes, but some included other stages. Li et al. (2013) examined oocytes at GV, GVBD, MI, and MII stages, while Lee and Comizzoli (2019) studied GV-stage oocytes. Yodrug et al. (2021) included both GV and MII stages in their study.

Table 5.3 Summary of Studies Examining Histone Modification

Reference	Animal Studied	Freezing Technique	Cell Type Studied	Cryoprotectant Used	Studied Modifications	Techniques Used	Changes compared to control observed	Change
(Suo et al., 2010)	Mice	Vitrification (OPS)	Oocytes (and resp. zygotes)	EG, DMSO, Ficoll-70, Sucrose	Histone acetylation (acH4K12)	Immunofluorescence	AcH4K12 levels significantly higher in vitrified oocytes compared to fresh controls	✓
(Chen et al., 2019)	Mice	Vitrification (Cyrotop)	Oocytes	EG, DMSO, Ficoll-70, Sucrose	Histone acetylation	Immunofluorescence	H3K9ac levels were abnormally increased by oocyte vitrification	✓ ↑ H3K9ac
(Spinaci et al., 2012)	Pig	Vitrification (Cyrotop)	Oocytes (MII)	EG, DMSO, sucrose	Histone acetylation (H4), methylation (H3K9)	Immunofluorescence	Control oocytes showed a lower percentage of hyperacetylated H4 and a higher percentage of positive dimethyl H3K9 compared to vitrified oocytes.	✓
(Li et al., 2013)	Sheep	Vitrification (OPS)	Oocytes	EG, DMSO, Ficoll, Sucrose	Histone acetylation (acH4K12, acH4K16)	Immunofluorescence	Significant increases in acH4K12 and acH4K16 levels in vitrified oocytes compared to fresh controls at GV, MI, and MII stages; no significant difference at GVBD stage	✓ ↑
(Ghazifard et al., 2019)	Mice	Vitrification (Cyrotop)	Oocytes (MII)	EG, DMSO, sucrose	Histone acetylation (acH4K12)	Immunofluorescence	AcH4K12 modification significantly increased in oocytes that were vitrified, compared to the fresh oocytes.	✓ ↑

Reference	Animal Studied	Freezing Technique	Cell Type Studied	Cryoprotectant Used	Studied Modifications	Techniques Used	Changes compared to control observed	Change
(Li et al., 2011)	Mice	Vitrification (OPS)	Oocytes, *in vitro*-fertilized embryos	EG, DMSO, Ficoll, Sucrose	HDAC1 expression	Immunofluorescence	HDAC1 expression in the vitrified group was significantly lower ($P<0.05$) than that in the control and toxicity groups at all developmental stages except for the blastocyst.	✓↓
(Yodrug et al., 2021)	Cattle	Vitrification (Cyrotop)	Oocytes (GV and MII stages)	EG, DMSO, and sucrose	histone modifications (H3K9me3, acH3K9)	Immunofluorescence	no significant differences in histone modifications between vitrified and control groups.	✗
(Lee and Comizzoli, 2019)	Cat	Vitrification	Oocytes (GV)	EG, DMSO, and sucrose	H3K4me3, H3K9me3	Immunofluorescence	H3K4me3 intensity was lowered after vitrification while H3K9me3 levels was maintained	✓ ↓ H3K4me3 ✗H3K9me3

Keywords: CPA – Cryoprotective agents, DMSO – Dimethyl Sulfoxide, EG – Ethylene glycol, HDAC – Histone deacetylase, GV – Germinal Vesicle, MII – Metaphase II; IVMd - *In vitro* matured, PROH - propylene glycol, OPS - open pulled straws, miR - microRNA, RT-qPCR - Reverse Transcription Quantitative Polymerase Chain Reaction, GO - Gene Ontology, KEGG - Kyoto Encyclopedia of Genes and Genomes, acH4K12 - histone H4 at lysine K12, H3K9ac - histone H3 lysine 9 acetylation, HDAC - histone deacetyltransferases, H3K4me3 - histone H3 trimethylation at lysine 4, H3K9me3 - - histone H3 trimethylation at lysine 9

✓- Aberrant change; -✗No aberrant change, ↓ Decreased compared to control, ↑ Increased compared to control

5.3.3 The effect of cryopreservation on non-coding RNA

Three studies examined the effects of cryopreservation on miRNA expression in mammalian oocytes and ovarian tissue. Wang et al. (2018) found that overexpression of HDAC6 or depletion of miR-762 improved survival and developmental potential of vitrified mouse oocytes. Li et al. (2019) observed significant changes in miRNA expression in vitrified mouse oocytes, with 22 differentially expressed miRNAs, including upregulation of miR-21-3p and downregulation of miR-465c-5p1. Islam et al. (2019) reported downregulation of miRNA-193b and miRNA-320A, and upregulation of miRNA-24 in cryopreserved-cultured sheep ovarian cortical tissue.

Table 5.4 Summary of Studies Examining MicroRNA Expression

Reference	Animal Studied	Freezing Technique	Cell Type Studied	CPA Used	Studied Modifications	Techniques Used	Changes compared to control observed	Change
(Wang et al., 2018)	Mice	Vitrification	Oocytes	EG and DMSO	Overexpression of HDAC6 and depletion of miR-762	Western blot, RT-qPCR, luciferase-reporter activity assay, transfection experiments	Oocytes with low HDAC6 levels had significantly lower survival rates (93.5 vs 99.1%), cleavage rates (54.0 vs 73.6%), and blastocyst rates (39.7 vs 69.6%) compared to those with high HDAC6 levels. Overexpression of HDAC6 or depletion of miR-762 improves the survival, cleavage, and blastocyst development of cryopreserved oocytes after recovery, indicating that HDAC6 plays a critical role in oocyte survival and developmental potential during cryopreservation.	✔↑
(Li et al., 2019)	Mice	Vitrification	Oocytes	DMSO and EG	MicroRNA expression	Small RNA sequencing RT-qPCR GO and KEGG Western blot Luciferase activity assay	Significant changes in miR expression levels in vitrified oocytes compared to fresh oocytes ($P < 0.05$) Differential expression of 22 miRs in vitrified oocytes compared to fresh oocytes Upregulation of miR-21-3p and downregulation of miR-465c-5p	✔ ↑ miR-21-3p ↓ miR-465c-5p

Reference	Animal Studied	Freezing Technique	Cell Type Studied	CPA Used	Studied Modifications	Techniques Used	Changes compared to control observed	Change
(Islam et al., 2019)	Sheep	Slow freezing	Ovarian cortical tissue	DMSO	interplay between ovarian steroid production and miRNA expression	Rt PCR for miRNA expression analysis	The expression of miRNA-193b was downregulated in cryopreserved-cultured tissues, while miRNA-24 was upregulated.	✓ ↓ of miRNA-193b and miRNA-320A ↑ miRNA-24

Keywords: CPA – Cryoprotective agents, DMSO – Dimethyl Sulfoxide, EG – Ethylene glycol, HDAC – Histone deacetylase, GV – Germinal Vesicle, MII – Metaphase II; IVMd - *In vitro* matured, PROH - propylene glycol, miR - microRNA, RT-qPCR - Reverse Transcription Quantitative Polymerase Chain Reaction, GO - Gene Ontology, KEGG - Kyoto Encyclopedia of Genes and Genomes

✔- Aberrant change; - ✗ No aberrant change, ↓ Decreased compared to control, ↑ Increased compared to control

5.4 DISCUSSION

This scoping review provides an extensive summary of current knowledge regarding the epigenetic impacts of cryopreservation on female fertility, with a focus on oocyte and ovarian tissue vitrification. The review underscores the intricate nature of epigenetic modifications and their potential effects on reproductive outcomes and long-term health. Research consistently indicates that cryopreservation—particularly vitrification—can induce notable epigenetic changes in oocytes and ovarian tissues. These changes, which encompass alterations in DNA methylation, histone modifications, and microRNA expression, can modify chromatin structure and gene accessibility, thereby affecting gene expression. Moreover, the persistence of these modifications from fertilisation through early embryonic development raises significant concerns about possible transgenerational consequences. Although most investigations have centred on isolated oocytes or fragmented ovarian tissue, these findings carry considerable implications for WOCP. In such cases, preserving the entire ovarian structure introduces further complexities related to tissue architecture and cellular interactions that may impact epigenetic outcomes. Ultimately, achieving a balance between effective structural preservation and the maintenance of epigenetic integrity remains a critical challenge for optimizing fertility preservation strategies and safeguarding the long-term health of future offspring.

5.4.1 DNA Methylation Alterations

The findings from the 24 studies examining DNA methylation changes after oocyte and ovarian tissue cryopreservation show insights into the epigenetic consequences of fertility preservation techniques. Overall, two-thirds of the studies (16/24) reported aberrant changes in DNA methylation patterns following cryopreservation, predominantly manifesting as reduced global methylation or altered imprinted gene methylation. This suggests that cryopreservation

protocols, while preserving cell viability, may introduce subtle yet potentially consequential epigenetic modifications that could impact developmental competence.

The differential responses observed across species highlight important biological variations in oocyte resilience to cryopreservation-induced stress. Mouse models, representing the majority of studies (17/24), demonstrated the highest susceptibility to methylation alterations, with 12/17 studies reporting hypomethylation or imprinting aberrations. This sensitivity in mice may reflect their evolutionary adaptation to rapid reproduction rather than long-term gamete preservation as in cryopreservation (Santos and Dean, 2004). Cattle studies consistently showed reduced DNMT expression or global hypomethylation following vitrification, suggesting disrupted methylation maintenance. Most notably, human oocytes appeared more resilient, with both studies finding no significant methylation differences at H19DMR or KvDMR1 after vitrification (Al-Khtib et al., 2011; De Munck et al., 2015). This apparent resilience in human oocytes warrants further investigation, as it may reflect either genuine epigenetic stability or limitations in detection methods used which was narrow focusing on these specific imprinting regions. The overall epigenetic landscape of human oocytes remains underexplored and compared to the animal models, especially mice, human oocytes have not been studied as intensively on a genome-wide level, signalling a critical gap in our understanding and raising concern as the other studies have indicated a potential for hypomethylation effects which could have implications for the imprinting processes in human oocytes. The single dromedary camel study (Moulavi et al., 2021) showing hypomethylation in 2-cell embryos post-fertilization provides a valuable comparison point for non-model organisms, though its relevance to oocyte-specific epigenetic states is limited due to active post-fertilisation reprogramming involving protamine-to-histone exchange and TET3-mediated oxidation of 5-methylcytosine (Cheng et al., 2019; Gou et al., 2020; Zhang et al., 2020).

Another variable worth looking at is the cryopreservation method and cryoprotectant composition employed in these studies as they are critical determinants of epigenetic outcomes. The widely used Cryotop vitrification method, while efficient for oocyte survival, was associated with reduced methylation in 5/7 studies, suggesting optimisation for viability may not necessarily preserve epigenetic integrity. Similarly, all three studies employing the Open-Pulled Straw (OPS) method reported hypomethylation, indicating that rapid cooling techniques may induce common epigenetic perturbations regardless of species. The contrasting effects of different cryoprotectants are particularly evident in the Feng et al. (2011) study, where PROH increased methylation while DMSO decreased it in cattle oocytes. This chemical-specific effect suggests that cryoprotectants interact differentially with cellular epigenetic machinery, possibly through direct effects on DNA methyltransferase activity or indirectly via osmotic and oxidative stress pathways as well as their permeability (El Kamouh et al., 2023; Kopeika et al., 2014; Ma et al., 2022). For instance, DMSO's methyl groups may facilitate DNA methylation via reactive oxygen species (ROS)-driven mechanisms, while PROH's lower permeability could limit such interactions. These findings underscore the need for cryopreservation protocols that consider epigenetic preservation alongside cell viability.

The developmental stage of oocytes during cryopreservation appears to significantly influence epigenetic vulnerability. MII oocytes showed the most consistent methylation changes (8/10 studies reporting hypomethylation), potentially due to their unique chromatin configuration with condensed chromosomes and spindle structures that may be particularly susceptible to cryoinjury (Iussig et al., 2019). In contrast, GV oocytes demonstrated epigenetic resilience, with only 1/3 studies reporting methylation changes. This stage-specific vulnerability aligns with current understanding of dynamic epigenetic reprogramming during oocyte maturation, where the transition from GV to MII involves extensive chromatin remodelling and refinement of methylation patterns (Katz-Jaffe et al., 2009).

MII oocytes with condensed chromatin are more susceptible to cryoinjury due to their structural and functional characteristics. The condensed chromatin and meiotic spindle in MII oocytes are highly sensitive to temperature fluctuations and osmotic stress during cryopreservation, leading to microtubule depolymerization and chromosomal misalignment. Additionally, the large size and high water content of MII oocytes increase vulnerability to intracellular ice formation and osmotic shock during cooling (Ledwaba et al., 2025). The transcriptionally silent state of MII oocytes limits their ability to repair cryodamage, as they rely on pre-existing maternal mRNAs and proteins until embryonic genome activation (Eroglu et al., 2020). Furthermore, cryoprotectant exposure can induce parthenogenetic activation or cytoskeletal disruption, exacerbating chromosomal abnormalities and developmental incompetence (Szurek and Eroglu, 2011). The combination of these factors-structural fragility, limited repair capacity, and cryoprotectant toxicity-renders MII oocytes particularly prone to cryoinjury compared to GV oocytes, which retain a more flexible chromatin structure and active transcriptional machinery for stress response (Brambillasca et al., 2013; Eroglu et al., 2020).

The consistent hypomethylation observed in embryos derived from cryopreserved oocytes (4/4 studies) suggests that initial epigenetic alterations may persist through early development, potentially affecting imprinted gene expression and developmental trajectory. These stage-specific vulnerabilities provide insight into the molecular mechanisms underlying cryopreservation induced epigenetic changes, likely involving disruption of DNA methyltransferase activity (Sendžikaitė and Kelsey, 2019), altered chromatin structure and accessibility (Falk et al., 2018; Reyes Palomares and Rodriguez-Wallberg, 2022), or impaired methyl donor metabolism (Ishii et al., 2014).

The results have significant implications for assisted reproductive technologies and fertility preservation practices. The species-specific responses suggest caution in extrapolating

findings from animal models to human clinical applications. The absence of methylation changes reported in human oocyte studies (Al-Khtib et al., 2011; De Munck et al., 2015) does not conclusively demonstrate resilience, as these findings are limited to specific imprinted regions (H19DMR and KvDMR1) and small sample sizes. Genome-wide analyses and larger-scale studies are needed to assess the broader epigenetic impact of cryopreservation on human oocytes. The observation that different cryoprotectants induce distinct methylation changes suggests opportunities for protocol optimization focused specifically on epigenetic preservation. Particularly concerning is the persistence of methylation changes in embryos derived from cryopreserved material, as seen in studies by Yan et al. (2020) and Zhou et al. (2020), raises concerns about potential developmental impacts, though these do not yet meet transgenerational criteria. These findings highlight the need for comprehensive epigenetic assessment in addition to traditional measures of cryopreservation success (survival, fertilization, and cleavage rates) when evaluating preservation protocols for clinical use.

The inconsistencies observed across some studies reflect methodological differences in both cryopreservation techniques and epigenetic analysis methods. Studies employing high-resolution techniques like bisulfite sequencing (Chen et al., 2019; Cheng et al., 2014; Milroy et al., 2010; Yan et al., 2020) detected subtle changes that may be missed by immunofluorescence approaches, suggesting some negative findings might reflect methodological limitations rather than true epigenetic stability. Future research should employ standardized protocols and combine genome-wide methylation profiling, transcriptomics, and long-term developmental monitoring to comprehensively evaluate the impact of cryopreservation (El Kamouh et al., 2023; Kopeika et al., 2014). Additionally, the focus on imprinted genes in many studies reflects their known susceptibility to environmental perturbations, but genome-wide approaches as in Ma et al., 2022 suggest broader epigenetic impacts that warrant further investigation. Long-term follow-up studies examining

development beyond the blastocyst stage would provide valuable insights into the developmental consequences of these epigenetic alterations. Ultimately, these findings collectively emphasize the need to incorporate epigenetic considerations into the development and optimization of cryopreservation protocols for reproductive medicine and fertility preservation.

5.4.2 Histone Modifications

Analysis of vitrified oocytes across multiple studies revealed a consistent pattern of histone modification disturbances that may significantly impact oocyte developmental competence. The predominant finding of increased histone acetylation, particularly H4K12 acetylation, across mice (Ghazifard et al., 2019; Suo et al., 2010), sheep (Li et al., 2013), and pigs (Spinaci et al., 2012) suggests a conserved stress response to vitrification. These acetylation changes are critically important because they can directly influence chromatin structure and accessibility, potentially leading to aberrant gene expression during critical developmental windows (Bannister and Kouzarides, 2011). For instance, the hyperacetylation of H4K12 observed by Suo et al. (2010) in mouse oocytes correlated with abnormal acetylation patterns in resulting zygotes, indicating that these epigenetic disruptions can persist beyond fertilization.

The observed changes in histone methylation patterns further complicate the epigenetic landscape of vitrified oocytes. Lee and Comizzoli (2019) reported decreased H3K4me3 (a mark associated with active transcription) in cat oocytes, while Spinaci et al. (2012) observed reduced H3K9 dimethylation in pig oocytes. These methylation changes could significantly alter gene expression regulation and chromatin compaction necessary for proper oocyte function. Interestingly, Yodrug et al. (2021) found no significant changes of H3K9me3 and acH3K9 in cattle oocytes, suggesting possible species-specific resilience to vitrification-

induced epigenetic alterations, or that different histone marks may be affected in different species.

The decreased HDAC1 expression reported by Li et al. (2011) in mouse oocytes provides a potential mechanism for the observed hyperacetylation. HDAC1 is a key enzyme responsible for removing acetyl groups from histones (Haberland et al., 2009), and its downregulation would naturally lead to increased histone acetylation (de Ruijter et al., 2003). This finding creates a direct link between enzyme activity changes and the altered epigenetic landscape following vitrification. The study's observation that HDAC1 suppression persisted from oocytes through early embryo development but normalized by the blastocyst stage suggests a potential for epigenetic recovery during later developmental stages (Li et al., 2011).

The comparison between OPS and Cryotop vitrification methods reveals that epigenetic disruptions occur regardless of the specific technique employed. Both methods led to increased histone acetylation in mouse oocytes (Suo et al., 2010; Chen et al., 2019; Ghazifard et al., 2019), suggesting that the fundamental process of vitrification, rather than specific methodological differences, may be responsible for these epigenetic alterations. This has important implications for clinical practice, as it suggests that modifying vitrification protocols alone may not be sufficient to prevent epigenetic disruptions.

The stage-specific responses observed by Li et al. (2013), where significant increases in acH4K12 and acH4K16 occurred in GV, MI, and MII stages but not at GVBD in sheep oocytes, highlight the dynamic nature of chromatin during oocyte maturation and its varying susceptibility to cryopreservation-induced alterations. This temporal sensitivity could provide valuable insights for optimizing the timing of vitrification procedures to minimize epigenetic disruptions based on oocyte developmental stage.

5.4.3 MicroRNA Expression

The studies reviewed offer compelling evidence that cryopreservation induces significant alterations in microRNA (miRNA) expression patterns in oocytes and ovarian tissue with potential implications for epigenetic inheritance and the efficacy of fertility preservation techniques.

Wang et al. (2018) demonstrated that the regulation of histone deacetylase 6 (HDAC6) expression, controlled in part by miR-762, plays a crucial role in oocyte viability after vitrification. Their research revealed that mouse oocytes with lower HDAC6 levels exhibited significantly reduced survival rates (93.5% vs 99.1%), cleavage rates (54.0% vs 73.6%), and blastocyst rates (39.7% vs 69.6%) compared to those with higher HDAC6 levels. Importantly, they discovered that the manipulation of this epigenetic pathway through HDAC6 overexpression or miR-762 suppression could enhance post-thaw oocyte survival and developmental potential. This finding suggests that specific miRNAs can serve as potential targets for improving cryopreservation outcomes.

Li et al. (2019) expanded our understanding of cryopreservation-induced miRNA changes by employing next-generation sequencing to comprehensively profile miRNA expression in vitrified mouse oocytes. Their study identified 22 differentially expressed miRNAs following vitrification, with notable upregulation of miR-21-3p and downregulation of miR-465c-5p. The authors observed that PTEN, a potential target of miR-21-3p, showed reduced expression at both transcriptional and post-transcriptional levels in vitrified oocytes. This alteration could have significant implications for cellular pathways involved in oocyte maturation and early embryonic development, as PTEN is known to regulate cell growth, survival, and metabolism (Endicott and and Miller, 2024).

Islam et al. (2019) provided valuable insights into the effects of cryopreservation on ovarian tissue, reporting that slow freezing of sheep ovarian cortical tissue led to downregulation of miRNA-193b and miRNA-320A, along with upregulation of miRNA-24. This study is particularly relevant to whole ovary cryopreservation as it examines miRNA changes in a complex tissue rather than isolated oocytes. The authors also investigated the relationship between these miRNA alterations and steroid production, suggesting that cryopreservation-induced epigenetic changes may affect the endocrine function of preserved ovarian tissue.

These three studies share several important similarities. First, they all demonstrate that cryopreservation, regardless of the specific technique employed or tissue type, induces measurable changes in miRNA expression patterns. Second, they suggest that these alterations may have functional consequences for cellular processes critical to reproductive success, including oocyte survival, maturation, and developmental potential. Third, they highlight the potential for targeted interventions to mitigate the adverse effects of cryopreservation on reproductive tissues.

However, notable differences exist among these studies. Wang et al. (2018) focused specifically on the HDAC6-miR-762 regulatory axis in oocytes, whereas Li et al. (2019) took a broader approach, examining global miRNA expression changes. Islam et al. (2019) extended the investigation to ovarian tissue, introducing the additional complexity of tissue-specific responses and the interplay between different cell types. Furthermore, the studies employed different cryopreservation methods (vitrification versus slow freezing) and examined different species (mice versus sheep), which may account for some variations in their findings.

The findings from these studies can help explain one another in several ways. For instance, the specific regulatory relationship between miR-762 and HDAC6 identified by

Wang et al. (2018) provides a mechanistic explanation for how miRNA alterations might affect oocyte viability after cryopreservation. They found that among several HDAC6-targeting miRNAs expressed in mouse oocytes, only miR-762 significantly inhibits HDAC6 protein translation by binding specifically to the 3′-UTR of HDAC6 mRNA. This interaction does not affect HDAC6 mRNA levels but reduces HDAC6 protein expression. Functionally, suppressing miR-762 or overexpressing HDAC6 in oocytes improved survival, cleavage, and blastocyst formation rates after vitrification, indicating that miR-762 negatively regulates HDAC6 and that modulating this axis can enhance oocyte viability post-cryopreservation. Thus, miR-762 acts as a post-transcriptional regulator of HDAC6, providing a mechanistic explanation for how miRNA alterations influence oocyte survival and developmental competence after freezing (Wang et al., 2018). This mechanism could potentially apply to some of the differentially expressed miRNAs identified in Li et al.'s (2019) broader profiling study. Similarly, the tissue-level changes observed by Islam et al. (2019) may reflect the cumulative effects of cellular-level alterations similar to those described in the oocyte studies.

These results align with and extend previous findings in the literature. Zhao et al. (2011) previously reported that vitrification can alter gene expression patterns in mouse oocytes, while Monzo et al. (2012) observed changes in mRNA expression in human oocytes following cryopreservation. The specific miRNA changes identified in these three studies provide a potential mechanism for these gene expression alterations, as miRNAs are known to regulate mRNA stability and translation. Furthermore, the findings are consistent with broader research on stress-induced epigenetic changes (primarily to the epigenetic modifications triggered by cellular stress during the freezing and thawing process), such as those reported by Salas-Huetos et al. (2014) in the context of sperm cryopreservation.

5.4.4 Implications for Whole Ovary Cryopreservation (WOCP)

The epigenetic alterations observed in isolated oocytes and tissue fragments have significant implications for WOCP. As an emerging technique aiming to preserve the entire ovarian structure and function (Arav et al., 2005), WOCP introduces additional complexity in terms of tissue architecture and cellular heterogeneity. The varied epigenetic responses observed across different cell types suggest that the diverse cellular composition of the intact ovary may result in differential epigenetic vulnerabilities during cryopreservation.

The tissue-level miRNA changes observed by Islam et al. (2019) in ovarian cortical tissue provide the most direct evidence of epigenetic alterations relevant to WOCP. The finding that these changes affected steroid production highlights how epigenetic disruptions could impact not only reproductive but also endocrine functions of preserved ovarian tissue. This is particularly relevant for whole ovary cryopreservation, where maintaining both reproductive and hormonal functions is essential.

The observed differential effects of cryoprotectants on DNA methylation patterns suggest that optimising cryoprotectant composition for whole ovary protocols requires consideration of epigenetic preservation alongside structural protection. The vascular architecture of the whole ovary presents additional challenges, as uniform cryoprotectant perfusion becomes more complex, potentially resulting in regional variations in epigenetic alterations dependent on exposure to cryoprotectants and cooling/warming rates.

5.5 CONCLUSION

This comprehensive scoping review provides substantial evidence that cryopreservation techniques employed for female fertility preservation induce significant epigenetic alterations that may persist through early embryonic development and potentially

impact offspring health. The evidence spanning DNA methylation patterns, histone modifications, and microRNA expression profiles collectively suggests that while cryopreservation successfully preserves structural and functional aspects of female reproductive tissues, it may compromise epigenetic integrity with potential long-term consequences.

For WOCP, these findings have particularly significant implications. The complex cellular composition and architecture of the intact ovary present unique challenges for preserving epigenetic integrity. The observed tissue-specific responses to cryopreservation, particularly those noted in ovarian cortical tissue studies, suggest that different cell types within the ovary may exhibit varying epigenetic vulnerabilities. Furthermore, the interactions between different ovarian compartments during the freezing and thawing processes may introduce additional epigenetic perturbations not observed in isolated oocyte or tissue fragment studies.

Significant knowledge gaps remain in our understanding of epigenetic inheritance following female fertility preservation. First, the apparent resilience of human oocytes to cryopreservation-induced epigenetic alterations observed in limited studies requires further investigation with larger sample sizes and more comprehensive epigenetic profiling. Second, long-term follow-up studies examining development beyond the blastocyst stage and into adulthood are critically needed to assess the full impact of these epigenetic alterations on offspring health and development. Third, the mechanisms underlying cryopreservation-induced epigenetic changes, particularly the molecular pathways linking cryoinjury to specific epigenetic perturbations, remain poorly understood.

Future research should prioritize several key areas: (1) comprehensive epigenome-wide studies using high-resolution techniques to capture subtle epigenetic alterations in human reproductive tissues; (2) longitudinal studies tracking epigenetic changes from cryopreserved

tissue through fertilization, embryonic development, and into offspring; (3) comparative studies between different cryopreservation protocols specifically optimized for epigenetic preservation; and (4) development of targeted interventions to mitigate cryopreservation-induced epigenetic disruptions, such as the HDAC6 overexpression or miR-762 suppression strategies demonstrated to enhance post-thaw oocyte outcomes.

For clinical practice, these findings emphasize the need to incorporate epigenetic assessments alongside traditional measures of cryopreservation success when evaluating preservation protocols. The species-specific responses observed caution against direct extrapolation from animal models to human applications. Additionally, the differential effects of cryoprotectants and developmental stage-specific vulnerabilities suggest opportunities for protocol optimization focused specifically on epigenetic preservation. For WOCP, careful epigenetic evaluation should be integrated from the earliest stages of protocol development to ensure not only structural and functional preservation but also epigenetic integrity of this complex reproductive tissue.

In conclusion, while fertility preservation through cryopreservation offers invaluable opportunities for maintaining reproductive potential, the epigenetic consequences of these techniques warrant careful consideration. Continued research and protocol refinement are essential to minimize epigenetic disruptions and ensure the long-term health and well-being of individuals conceived through assisted reproductive technologies utilizing cryopreserved material.

CHAPTER SIX: GENERAL DISCUSSION AND CONCLUSIONS

6.1 GENERAL DISCUSSION

Despite significant progress and documented live births in animal models such as sheep, there remain unresolved questions regarding the efficacy of WOCP and thawing protocols, necessitating further investigations before their potential application in animal production, conservation, or clinical contexts. Traditionally, the success of cryopreservation has been assessed through post-thaw cell survival rates. However, emerging evidence suggests deviations from oocyte physiology during cryopreservation, impacting elements like zona hardening, meiotic spindle, DNA fragmentation, and epigenetic marks. This prompted the initiation of the present study. Initially, a literature review was undertaken to define the specific objectives of the thesis and establish the technical approach for subsequent studies. A series of experiments followed, each designed based on the insights gained from the preceding one, aiming to provide a comprehensive analysis of the subject. Sheep were chosen as the experimental model due to several physiological similarities with humans, previous successful experiments with the species and the availability of biological material from nearby abattoirs. The study's specific aims were elaborated upon in individual experimental chapters.

The study commenced with a focus on the oocytes within the antral follicle, identified as particularly susceptible to the cryopreservation process due to their elevated water content compared to various other follicle types in the ovary. Considering the prolonged duration observed in prior studies for experimental subjects to recover ovarian function, it became apparent that live birth did not originate from antral follicles. Initially, the investigation targeted the maturation potential of antral follicle oocytes. However, upon oocyte aspiration, a disconnection with cumulus cells was noted, hindering the ability of oocytes to attain nuclear

maturation. Using PI, a biological stain, the cell membrane integrity was evaluated, revealing no significant differences. Subsequent exploration focused on DNA fragmentation by apoptosis using TUNEL, uncovering notable distinctions. The chromatin configuration of the oocytes was then examined to establish any correlation with the experimental groups. This inquiry was succeeded by an immunohistochemistry histology test aimed at identifying intercellular communication proteins connexin 37 and 43 within the ovarian tissue. Finally, the transcriptomic profile and DNA methylation of the ovarian cortex were scrutinised to identify potential changes in genes vital to follicle survival, oocyte development, cell-cell communication, spindle cytoskeleton, and checkpoint processes.

The findings reported in this thesis are novel and form a strong basis for further and advanced research into the whole ovarian cryopreservation technique for fertility preservation. The main results and conclusions are;

1. Morphological grading of oocytes retrieved from sheep antral follicles of WOCP are comparable to the control, however, the structure of the COC was damaged as the oocytes were completely striped of their cumulus cells.
2. Following IVM, antral follicle oocytes subjected to WOCP exhibited a significant reduction in nuclear maturation rates compared to the control group.
3. While WOCP demonstrated a higher percentage of cell membrane disruption assessed through PI staining compared to the control group, the difference did not reach statistical significance, suggesting potential resilience of oocyte viability post-WOCP.
4. Oocytes cryopreserved *in situ* within an antral follicle during whole ovarian cryopreservation exhibited an elevated apoptosis index, as revealed by the TUNEL assay, compared to the control group. This higher apoptotic index suggests increased DNA fragmentation in the oocytes, implying potential effects on oocyte integrity following cryopreservation.

5. Chromatin configuration classifications revealed variations in both control and WOCP groups, with a significant increase in decondensed chromatin fibres in WOCP oocytes compared to the control, indicating alterations in chromatin structure following cryopreservation.
6. WOCP and subsequent warming, has an impact on the expression patterns of connexins, particularly Cx37 and Cx43, in the ovarian tissue.
7. WOCP significantly alters the gene expression profile of sheep ovarian tissue. PCA analysis clearly showed distinct gene expression patterns between control and cryopreserved samples.
8. WOCP induces a complex cellular stress response aimed at survival, but potentially at the cost of long-term ovarian health. The study observed upregulation of genes related to protein synthesis (ribosomal genes) and mitochondrial stress (neurodegenerative disease-associated pathways like OXPHOS and thermogenesis), indicating efforts to repair damage and generate energy. However, it also noted the downregulation of crucial cellular quality control pathways like autophagy and lysine degradation, which could lead to accumulated damage and compromise follicular viability over time.
9. WOCP activates pro-apoptotic pathways and disrupts key regulatory signalling, potentially impacting ovarian function and fertility. Upregulation of pro-apoptotic genes (like BAX and STC2) and downregulation of anti-apoptotic genes (like BCL2) indicate increased cellular susceptibility to death. Additionally, the suppression of important transcriptional regulators (zinc finger proteins) and signalling pathways (GRM7, GRM8, WNT4) suggests a broad disruption of processes vital for follicle development, oocyte maturation, and overall ovarian homeostasis.
10. Global DNA methylation patterns in the ovary following exposure to WOCP showed a marginal increase in 5-methylcytosine (5-mC) levels, which was not statistically significant.

11. Cryopreservation, particularly vitrification, induces significant epigenetic changes in oocytes and ovarian tissues. These alterations include changes in DNA methylation (often hypomethylation), histone modifications (e.g., increased acetylation), and microRNA expression, which can affect gene expression and potentially have transgenerational consequences.
12. Oocyte developmental stage and cryopreservation methods influence epigenetic outcomes. MII oocytes appear more vulnerable to cryoinjury and methylation changes than GV oocytes. Additionally, different cryoprotectants and techniques (like Cryotop and OPS vitrification) can lead to distinct epigenetic perturbations, highlighting the need for optimization beyond just cell viability.
13. Epigenetic alterations persist into early embryonic development, raising concerns about long-term offspring health, and warrant further investigation.

The in-depth exploration into the repercussions of WOCP on antral follicle oocytes, as elucidated in this study, unravels a complex interplay of molecular and cellular responses that significantly shape their growth, maturation, and developmental competence. Employing a multifaceted approach that encompasses assessments of DNA fragmentation, morphological alterations, cumulus cell interactions, gene expression, and chromatin configuration provides a nuanced and comprehensive understanding of the intricate consequences of cryopreservation on ovarian tissue.

Consistently, the results highlight the inhibitory impact of WOCP, through the slow freezing method as described by Campbel et al (2014), on the developmental potential of antral follicle oocytes. The observed decline in maturation rates, coupled with an increase in apoptosis and morphological abnormalities, underscores the detrimental effects incurred during the cryopreservation process. These findings align with existing literature emphasizing the

challenges associated with preserving the integrity of delicate structures within ovarian tissue, ultimately leading to compromised oocyte quality and competence (Li et al., 2008; Macaulay et al., 2016; Rana et al., 2013).

The crucial role of cryoprotective agents (CPAs) and the cryopreservation method itself in influencing oocyte viability and functionality is highlighted in the study. It stresses the importance of meticulous optimization in cryopreservation protocols to alleviate the observed adverse effects. The link between the slow freezing process and increased susceptibility to apoptosis, evidenced by TUNNEL in antral follicle oocytes and heightened expression of pro-apoptotic factors like BAX in ovarian tissue, emphasizes the continuous necessity for refining cryopreservation techniques. This revelation sheds light on the impact of WOCP on cell death processes. The elevated expression of the pro-apoptotic factor BAX indicates a heightened susceptibility to apoptosis, potentially impacting the quantity of primordial follicles and, consequently, the reproductive lifespan of female mammals. Furthermore, the recognition of the potential involvement of autophagic cell death in regulating ovarian function underscores the intricate nature of cellular responses to cryopreservation, emphasizing the imperative need for further exploration in this context.

A pivotal aspect of the study is the investigation into the chromatin configuration of WOCP oocytes, revealing significant alterations. The observed increase in condensed patterns (SNE) and decondensed patterns (NSN) raises intriguing questions about potential adaptive responses or defensive mechanisms deployed by oocytes during cryopreservation. The early condensation observed may serve as a protective strategy, compactly packaging chromatin fibres to shield against cryodamage, presenting an interesting avenue for future research into the adaptive responses of oocytes to cryopreservation stress.

The study delves into the critical role of cumulus cells in oocyte maturation and competence, emphasizing the importance of maintaining their integrity during cryopreservation. Disruptions in the granulosa-oocyte interface, reflected in changes in connexin proteins Cx37 and Cx43, are implicated in the observed deficiencies in oocyte development from antral follicles post WOCP. The nuanced impact of cryopreservation parameters, including the type of cryoprotectant, temperature modifications, and the method employed, underscores the complexity of preserving the delicate balance of cellular and molecular interactions within the whole ovarian tissue.

The observed dysregulation in gene expression, particularly those associated with fundamental cellular activities such as metabolic processes, cell communication, and energy-demanding pathways, raises concerns about the overall health and functionality of the cryopreserved ovaries. Notably, the upregulation of genes related to signalling, transport, and energy-demanding processes, as well as the positive enrichment in respiratory chain-related pathways, indicates an increased energy demand in WOCP ovaries.

6.2 LIMITATIONS OF SHEEP MODELS

There are a few limitations of using sheep as a model for WOCP that may hinder the direct applicability of findings to human fertility preservation. One such limitation is the difference in actual ovarian size and tissue architecture. While sheep ovaries are similar in structure, they are still smaller than human ovaries, which affects the diffusion of cryoprotectants and the uniformity of cooling during the freezing process. This discrepancy means that protocols optimised in sheep may not work effectively in human ovaries, where the risk of incomplete cryoprotectant penetration and uneven cooling increases the likelihood of tissue damage, particularly in the medulla and vascular structures (Wallin et al., 2009).

Another limitation is the survival rate of primordial follicles after cryopreservation and transplantation. In sheep, studies have shown that the majority of primordial follicles do not survive, primarily due to ischemic injury before revascularization rather than direct cryodamage (Anderson et al., 2017; Hongyan et al., 2021). This challenge is also present in human tissue, but the extent of ischemic loss and the mechanisms involved may differ due to species-specific vascular and metabolic factors. As a result, the follicular survival and subsequent fertility outcomes observed in sheep may not accurately predict those in humans.

Additionally, sheep are seasonal breeders with reproductive cycles that differ from those of humans, who are non-seasonal and have a more continuous pattern of follicular recruitment. This difference can influence the interpretation of functional recovery and fertility restoration after transplantation, potentially limiting the relevance of sheep data for human clinical scenarios (Campbell et al., 2014).

6.3 GENERAL CONCLUSIONS

In conclusion, this comprehensive study delved into the intricate molecular alterations induced by the slow freezing and thawing process employed for cryopreservation in sheep ovaries. The investigation focused on potential repercussions on various aspects such as follicle survival, gene expression, DNA methylation patterns, and the maturation potential of oocytes.

The outcomes regarding DNA fragmentation, morphological assessment, and cumulus cell loss unequivocally pointed towards the challenges antral follicle oocytes from WOCP tissue face in attaining maturation to the MII stage of meiosis. Despite uncertainties surrounding cytoplasmic maturation, the sustained cytoplasmic activity, as indicated by colourless oocytes after 24 hours of maturation, suggests ongoing energy utilisation and G6PDH activity. The application of BCB staining provided valuable insights into post-WOCP

and IVM oocyte cytoplasmic activity, reinforcing the predictive value of the BCB test for oocyte quality and developmental competence. The prolonged colourless state and swift dye loss in BCB-positive oocytes indicated ongoing energy utilisation and G6PDH activity.

The study also highlighted notable influences of WOCP on the chromatin configuration of antral follicle oocytes, potentially impacting gene expression, transcriptional activity, and meiotic competence. The increased prevalence of decondensed chromatin in WOCP oocytes hinted at a more transcriptionally active state, potentially favourable for progressing through meiosis. However, further studies are warranted to directly assess meiotic progression and embryonic development to fully understand the reproductive implications of WOCP exposure.

Moreover, the investigation into the expression of gap junction proteins Cx37 and Cx43 within ovarian tissue indicated consistent presence in specific locations, but cryopreservation, particularly WOCP by slow freezing, appeared to lead to alterations in their distribution and intensity. This emphasises the impact of cryopreservation on the gap junctional network in ovarian tissue.

Finally, the study on gene expression and DNA methylation patterns following cryopreservation demonstrated dysregulation in genes linked to follicle development and survival. Noteworthy findings from GO enrichment and KEGG pathway analyses highlighted shifts in fundamental cell activities and pathways relevant to follicle survival. The observed upregulation of genes associated with energy-demanding processes and heightened susceptibility to apoptosis in WOCP-treated ovaries underscores the complex molecular responses to cryopreservation.

In summary, this research provides valuable insights into the intricate molecular responses of ovarian tissue to cryopreservation, emphasizing the need for further investigations to unravel the functional consequences of these observed trends and their implications for

reproductive health. The findings contribute to the growing body of knowledge in reproductive biology and cryobiology, guiding future research aimed at refining cryopreservation techniques and ensuring their safety and efficacy in preserving fertility.

REFERENCES

AbdelHafez, F.F., Desai, N., Abou-Setta, A.M., Falcone, T., Goldfarb, J., 2010. Slow freezing, vitrification and ultra-rapid freezing of human embryos: a systematic review and meta-analysis. Reproductive biomedicine online 20, 209-222.

Abdollahi, M., Salehnia, M., Salehpour, S., Ghorbanmehr, N., 2013. Human ovarian tissue vitrification/warming has minor effect on the expression of apoptosis-related genes. Iranian Biomedical Journal 17, 179-186.

Abedelahi, A., Rezaei-Tavirani, M., Mohammadnejad, D., 2013. Fertility preservation among the cancer patients by ovarian tissue cryopreservation, transplantation, and follicular development. Iranian Journal of Cancer Prevention 6, 123.

Ackert, C.L., Gittens, J.E., O'Brien, M.J., Eppig, J.J., Kidder, G.M., 2001. Intercellular communication via connexin43 gap junctions is required for ovarian folliculogenesis in the mouse. Dev Biol 233, 258-270.

Aflatoonian, N., Pourmasumi, S., Aflatoonian, A., Eftekhar, M., 2013. Duration of storage does not influence pregnancy outcome in cryopreserved human embryos. Iranian journal of reproductive medicine 11, 843-846.

Ajayi, A.F., Akhigbe, R.E., 2020. Staging of the estrous cycle and induction of estrus in experimental rodents: an update. Fertility research and practice 6, 5.

Al-aghbari, A.M., Menino, A.R., 2002. Survival of oocytes recovered from vitrified sheep ovarian tissues. Animal reproduction science 71, 101-110.

Al-Khtib, M., Perret, A., Khoueiry, R., Ibala-Romdhane, S., Blachère, T., Greze, C., Lornage, J., Lefèvre, A., 2011. Vitrification at the germinal vesicle stage does not affect the methylation profile of H19 and KCNQ1OT1 imprinting centers in human oocytes subsequently matured in vitro. Fertility and sterility 95, 1955-1960.

Albertini, D.F., Combelles, C., Benecchi, E., Carabatsos, M.J., 2001. Cellular basis for paracrine regulation of ovarian follicle development. Reproduction 121, 647-653.

Albertini, D.F., Olsen, R., 2013. Effects of fertility preservation on oocyte genomic integrity. Advances in experimental medicine and biology 761, 19-27.

Albertini, D.F., Sanfins, A., Combelles, C.M., 2003. Origins and manifestations of oocyte maturation competencies. Reproductive biomedicine online 6, 410-415.

Albright, F., Smith, P.H., Fraser, R., 1942. A syndrome characterized by primary ovarian insufficiency and decreased stature: report of 11 cases with a digression on hormonal control of axillary and pubic hair. Am J Med Sci 204, 625-648.

Ali, H., Ahmad, S., 2023. “Comparative Analysis of Ovarian Transcriptome Changes Across Gestational Stages in Kari Sheep”. bioRxiv, 2023.2011.2020.567795.

Ali, J., Shelton, J.N., 1993. Design of vitrification solutions for the cryopreservation of embryos. Journal of reproduction and fertility 99, 471-477.

Alm, H., Torner, H., Löhrke, B., Viergutz, T., Ghoneim, I., Kanitz, W., 2005. Bovine blastocyst development rate in vitro is influenced by selection of oocytes by brillant cresyl blue staining before IVM as indicator for glucose-6-phosphate dehydrogenase activity. Theriogenology 63, 2194-2205.

Almodin, C.G., Minguetti-Camara, V.C., Paixao, C.L., Pereira, P.C., 2010. Embryo development and gestation using fresh and vitrified oocytes. Human reproduction 25, 1192-1198.

Amorim, C.A., Curaba, M., Van Langendonckt, A., Dolmans, M.M., Donnez, J., 2011. Vitrification as an alternative means of cryopreserving ovarian tissue. Reproductive biomedicine online 23, 160-186.

Anchamparuthy, V.M., Pearson, R.E., Gwazdauskas, F.C., 2010. Expression pattern of apoptotic genes in vitrified-thawed bovine oocytes. Reproduction in domestic animals = Zuchthygiene 45, e83-90.

Andersen, C.Y., Silber, S.J., Bergholdt, S.H., Jorgensen, J.S., Ernst, E., 2012. Long-term duration of function of ovarian tissue transplants: case reports. Reproductive biomedicine online 25, 128-132.

Anderson, E.L., Baltus, A.E., Roepers-Gajadien, H.L., Hassold, T.J., de Rooij, D.G., van Pelt, A.M., Page, D.C., 2008. Stra8 and its inducer, retinoic acid, regulate meiotic initiation in both spermatogenesis and oogenesis in mice. Proceedings of the National Academy of Sciences of the United States of America 105, 14976-14980.

Anderson, R.A., Amant, F., Braat, D., D'Angelo, A., Chuva de Sousa Lopes, S.M., Demeestere, I., Dwek, S., Frith, L., Lambertini, M., Maslin, C., Moura-Ramos, M., Nogueira, D., Rodriguez-Wallberg, K., Vermeulen, N., 2020. ESHRE guideline: female fertility preservation. Hum Reprod Open 2020, hoaa052.

Anderson, R.A., Wallace, W.H.B., Telfer, E.E., 2017. Ovarian tissue cryopreservation for fertility preservation: clinical and research perspectives. Human Reproduction Open 2017.

Antinori, M., Licata, E., Dani, G., Cerusico, F., Versaci, C., Antinori, S., 2007. Cryotop vitrification of human oocytes results in high survival rate and healthy deliveries. Reproductive biomedicine online 14, 72-79.

Arav, A., Natan, Y., 2009. Directional freezing: a solution to the methodological challenges to preserve large organs. Seminars in reproductive medicine 27, 438-442.

Arav, A., Revel, A., Nathan, Y., Bor, A., Gacitua, H., Yavin, S., Gavish, Z., Uri, M., Elami, A., 2005. Oocyte recovery, embryo development and ovarian function after cryopreservation and transplantation of whole sheep ovary. Human reproduction 20, 3554-3559.

Argyle, C.E., Harper, J.C., Davies, M.C., 2016. Oocyte cryopreservation: where are we now? Human reproduction update 22, 440-449.

Baerwald, A.R., Adams, G.P., Pierson, R.A., 2011. Ovarian antral folliculogenesis during the human menstrual cycle: a review. Human reproduction update 18, 73-91.

Bahrami, Z., Hatamian, N., Talkhabi, M., Zand, E., Mottershead, D.G., Fathi, R., 2022. Granulosa Cell Conditioned Medium Enhances The Rate of Mouse Oocyte In Vitro Maturation and Embryo Formation. Cell Journal (Yakhteh) 24, 620.

Bahroudi, Z., Zarnaghi, M.R., Izadpanah, M., Abedelahi, A., Niknafs, B., Nasrabadi, H.T., Seghinsara, A.M., 2022. Review of ovarian tissue cryopreservation techniques for fertility preservation. Journal of Gynecology Obstetrics and Human Reproduction 51, 102290.

Bannister, A.J., Kouzarides, T., 2011. Regulation of chromatin by histone modifications. Cell research 21, 381-395.

Barberet, J., Barry, F., Choux, C., Guilleman, M., Karoui, S., Simonot, R., Bruno, C., Fauque, P., 2020. What impact does oocyte vitrification have on epigenetics and gene expression? Clinical epigenetics 12, 121.

Barnes, F.L., Kausche, A., Tiglias, J., Wood, C., Wilton, L., Trounson, A., 1996. Production of embryos from in vitro-matured primary human oocytes. Fertility and sterility 65, 1151-1156.

Basu, A., Haldar, S., 1998. The relationship between Bcl2, Bax and p53: Consequences for cell cycle progression and cell death. Molecular human reproduction 4, 1099-1109.

Bhardwaj, J.K., Paliwal, A., Saraf, P., Sachdeva, S.N., 2022. Role of autophagy in follicular development and maintenance of primordial follicular pool in the ovary. Journal of cellular physiology 237, 1157-1170.

Bianchi, V., Macchiarelli, G., Borini, A., Lappi, M., Cecconi, S., Miglietta, S., Familiari, G., Nottola, S.A., 2014. Fine morphological assessment of quality of human mature oocytes after slow freezing or vitrification with a closed device: a comparative analysis. Reproductive biology and endocrinology : RB&E 12, 110.

Bojic, S., Murray, A., Bentley, B.L., Spindler, R., Pawlik, P., Cordeiro, J.L., Bauer, R., de Magalhães, J.P., 2021. Winter is coming: the future of cryopreservation. BMC biology 19, 56.

Boland, N., Gosden, R., 1994. Effects of epidermal growth factor on the growth and differentiation of cultured mouse ovarian follicles. Reproduction 101, 369-374.

Borowczyk, E., Johnson, M.L., Bilski, J.J., Borowicz, P., Redmer, D.A., Reynolds, L.P., Grazul-Bilska, A.T., 2006a. Gap junctional connexin 37 is expressed in sheep ovaries. Endocrine 30, 223-230.

Borowczyk, E., Johnson, M.L., Bilski, J.J., Borowicz, P.P., Redmer, D.A., Reynolds, L.P., Grazul-Bilska, A.T., 2006b. Expression of gap junctional connexins 26, 32, and 43 mRNA in ovarian preovulatory follicles and corpora lutea in sheep. Canadian Journal of Physiology and Pharmacology 84, 1011-1020.

Bouniol-Baly, C., Hamraoui, L., Guibert, J., Beaujean, N., Szöllösi, M.S., Debey, P., 1999. Differential transcriptional activity associated with chromatin configuration in fully grown mouse germinal vesicle oocytes. Biology of reproduction 60, 580-587.

Bowles, J., Knight, D., Smith, C., Wilhelm, D., Richman, J., Mamiya, S., Yashiro, K., Chawengsaksophak, K., Wilson, M.J., Rossant, J., Hamada, H., Koopman, P., 2006. Retinoid signaling determines germ cell fate in mice. Science 312, 596-600.

Bowles, J., Koopman, P., 2007. Retinoic acid, meiosis and germ cell fate in mammals. Development (Cambridge, England) 134, 3401-3411.

Boyer, A., Lapointe, É., Zheng, X., Cowan, R.G., Li, H., Quirk, S.M., Demayo, F.J., Richards, J.S., Boerboom, D., 2010. WNT4 is required for normal ovarian follicle development and female fertility. The FASEB Journal 24, 3010-3025.

Brambillasca, F., Guglielmo, M.C., Coticchio, G., Mignini Renzini, M., Dal Canto, M., Fadini, R., 2013. The current challenges to efficient immature oocyte cryopreservation. Journal of assisted reproduction and genetics 30, 1531-1539.

Bray, F., Ferlay, J., Soerjomataram, I., Siegel, R.L., Torre, L.A., Jemal, A., 2018. Global cancer statistics 2018: GLOBOCAN estimates of incidence and mortality worldwide for 36 cancers in 185 countries. CA: a cancer journal for clinicians 68, 394-424.

Brezina, P.R., Zhao, Y., 2012. The ethical, legal, and social issues impacted by modern assisted reproductive technologies. Obstetrics and gynecology international 2012, 686253.

Brison, D., Cutting, R., Clarke, H., Wood, M., 2012. ACE consensus meeting report: oocyte and embryo cryopreservation Sheffield 17.05. 11. Human Fertility 15, 69-74.

Broer, S.L., Broekmans, F.J., Laven, J.S., Fauser, B.C., 2014. Anti-Müllerian hormone: ovarian reserve testing and its potential clinical implications. Human reproduction update 20, 688-701.

Buccione, R., Schroeder, A.C., Eppig, J.J., 1990. Interactions between somatic cells and germ cells throughout mammalian oogenesis. Biology of reproduction 43, 543-547.

Bunge, R.G., Sherman, J.K., 1953. Fertilizing capacity of frozen human spermatozoa. Nature 172, 767-768.

Cahill, D.J., Wardle, P.G., Harlow, C.R., Hull, M.G., 1998. Onset of the preovulatory luteinizing hormone surge: diurnal timing and critical follicular prerequisites. Fertility and sterility 70, 56-59.

Cakmak, H., Rosen, M.P., 2013. Ovarian stimulation in cancer patients. Fertility and sterility 99, 1476-1484.

Campbell, B.K., Hernandez-Medrano, J., Onions, V., Pincott-Allen, C., Aljaser, F., Fisher, J., McNeilly, A.S., Webb, R., Picton, H.M., 2014. Restoration of ovarian function and natural fertility following the cryopreservation and autotransplantation of whole adult sheep ovaries. Human reproduction 29, 1749-1763.

Candelaria, J.I., Rabaglino, M.B., Denicol, A.C., 2020. Ovarian preantral follicles are responsive to FSH as early as the primary stage of development. The Journal of endocrinology 247, 153-168.

Cao, Y.X., Xing, Q., Li, L., Cong, L., Zhang, Z.G., Wei, Z.L., Zhou, P., 2009. Comparison of survival and embryonic development in human oocytes cryopreserved by slow-freezing and vitrification. Fertility and sterility 92, 1306-1311.

Cao, Z., Zhang, M., Xu, T., Chen, Z., Tong, X., Zhang, D., Wang, Y., Zhang, L., Gao, D., Luo, L., Khan, I.M., Zhang, Y., 2019. Vitrification of murine mature metaphase II oocytes perturbs DNA methylation reprogramming during preimplantation embryo development. Cryobiology 87, 91-98.

Carabatsos, M.J., Sellitto, C., Goodenough, D.A., Albertini, D.F., 2000. Oocyte-granulosa cell heterologous gap junctions are required for the coordination of nuclear and cytoplasmic meiotic competence. Dev Biol 226, 167-179.

Carroll, J., Marangos, P., 2013. The DNA damage response in mammalian oocytes. Frontiers in Genetics 4.

Catala, M.G., Izquierdo, D., Uzbekova, S., Morato, R., Roura, M., Romaguera, R., Papillier, P., Paramio, M.T., 2011. Brilliant Cresyl Blue stain selects largest oocytes with highest mitochondrial activity, maturation-promoting factor activity and embryo developmental competence in prepubertal sheep. Reproduction 142, 517-527.

Catalini, L., Fedder, J., 2020. Characteristics of the endometrium in menstruating species: lessons learned from the animal kingdom†. Biology of reproduction 102, 1160-1169.

Ceelen, M., van Weissenbruch, M.M., Vermeiden, J.P., van Leeuwen, F.E., Delemarre-van de Waal, H.A., 2008. Growth and development of children born after in vitro fertilization. Fertility and sterility 90, 1662-1673.

Cha, K.-Y., Chian, R.-C., 1998. Maturation in vitro of immature human oocytes for clinical use. Human reproduction update 4, 103-120.

Chatterjee, A., Saha, D., Niemann, H., Gryshkov, O., Glasmacher, B., Hofmann, N., 2017. Effects of cryopreservation on the epigenetic profile of cells. Cryobiology 74, 1-7.

Chen, C., 1986. Pregnancy after human oocyte cryopreservation. Lancet 1, 884-886.

Chen, H., Zhang, L., Deng, T., Zou, P., Wang, Y., Quan, F., Zhang, Y., 2016. Effects of oocyte vitrification on epigenetic status in early bovine embryos. Theriogenology 86, 868-878.

Chen, H., Zhang, L., Wang, Z., Chang, H., Xie, X., Fu, L., Zhang, Y., Quan, F., 2019. Resveratrol improved the developmental potential of oocytes after vitrification by modifying the epigenetics. Molecular reproduction and development 86, 862-870.

Cheng, H., Zhang, J., Zhang, S., Zhai, Y., Jiang, Y., An, X., Ma, X., Zhang, X., Li, Z., Tang, B., 2019. Tet3 is required for normal in vitro fertilization preimplantation embryos development of bovine. Molecular reproduction and development 86, 298-307.

Cheng, K.-R., Fu, X.-W., Zhang, R.-N., Jia, G.-X., Hou, Y.-P., Zhu, S.-E., 2014. Effect of oocyte vitrification on deoxyribonucleic acid methylation of H19, Peg3, and Snrpn differentially methylated regions in mouse blastocysts. Fertility and sterility 102, 1183-1190.e1183.

Chian, R.C., Tan, S.L., 2002. Maturational and developmental competence of cumulus-free immature human oocytes derived from stimulated and intracytoplasmic sperm injection cycles. Reproductive biomedicine online 5, 125-132.

Childs, A.J., Cowan, G., Kinnell, H.L., Anderson, R.A., Saunders, P.T.K., 2011. Retinoic Acid Signalling and the Control of Meiotic Entry in the Human Fetal Gonad. PloS one 6, e20249.

Cho, E., Kim, Y.Y., Noh, K., Ku, S.-Y., 2019. A new possibility in fertility preservation: The artificial ovary. Journal of Tissue Engineering and Regenerative Medicine 13, 1294-1315.

Choi, J., Lee, B., Lee, E., Yoon, B.-K., Bae, D., Choi, D., 2008. Cryopreservation of ovarian tissues temporarily suppresses the proliferation of granulosa cells in mouse preantral follicles. Cryobiology 56, 36-42.

Christou-Kent, M., Dhellemmes, M., Lambert, E., Ray, P.F., Arnoult, C., 2020. Diversity of RNA-Binding Proteins Modulating Post-Transcriptional Regulation of Protein Expression in the Maturing Mammalian Oocyte. Cells 9.

Clowse, M.E., Behera, M.A., Anders, C.K., Copland, S., Coffman, C.J., Leppert, P.C., Bastian, L.A., 2009. Ovarian preservation by GnRH agonists during chemotherapy: a meta-analysis. Journal of women's health (2002) 18, 311-319.

Cobo, A., Diaz, C., 2011. Clinical application of oocyte vitrification: a systematic review and meta-analysis of randomized controlled trials. Fertility and sterility 96, 277-285.

Cobo, A., García-Velasco, J.A., Coello, A., Domingo, J., Pellicer, A., Remohí, J., 2016. Oocyte vitrification as an efficient option for elective fertility preservation. Fertility and sterility 105, 755-764. e758.

Cobo, A., Garrido, N., Pellicer, A., Remohí, J., 2015. Six years' experience in ovum donation using vitrified oocytes: report of cumulative outcomes, impact of storage time, and development of a predictive model for oocyte survival rate. Fertility and sterility 104, 1426-1434. e1428.

Cobo, A., Kuwayama, M., Perez, S., Ruiz, A., Pellicer, A., Remohi, J., 2008. Comparison of concomitant outcome achieved with fresh and cryopreserved donor oocytes vitrified by the Cryotop method. Fertility and sterility 89, 1657-1664.

Cobo, A., Remohi, J., Chang, C.C., Nagy, Z.P., 2011. Oocyte cryopreservation for donor egg banking. Reproductive biomedicine online 23, 341-346.

Conti, M., Chang, R.J., 2016. Chapter 125 - Folliculogenesis, Ovulation, and Luteogenesis, in: Jameson, J.L., De Groot, L.J., de Kretser, D.M., Giudice, L.C., Grossman, A.B., Melmed, S., Potts, J.T., Weir, G.C. (Eds.), Endocrinology: Adult and Pediatric (Seventh Edition). W.B. Saunders, Philadelphia, pp. 2179-2191.e2173.

Conti, M., Franciosi, F., 2018. Acquisition of oocyte competence to develop as an embryo: integrated nuclear and cytoplasmic events. Human reproduction update 24, 245-266.

Coticchio, G., Dal Canto, M., Mignini Renzini, M., Guglielmo, M.C., Brambillasca, F., Turchi, D., Novara, P.V., Fadini, R., 2015. Oocyte maturation: gamete-somatic cells interactions,

meiotic resumption, cytoskeletal dynamics and cytoplasmic reorganization. Human reproduction update 21, 427-454.

Coulam, C.B., Adamson, S.C., Annegers, J.F., 1986. Incidence of premature ovarian failure. Obstetrics and gynecology 67, 604-606.

Craig, J., Orisaka, M., Wang, H., Orisaka, S., Thompson, W., Zhu, C., Kotsuji, F., Tsang, B.K., 2007. Gonadotropin and intra-ovarian signals regulating follicle development and atresia: the delicate balance between life and death. Frontiers in bioscience : a journal and virtual library 12, 3628-3639.

Da Silva-Buttkus, P., Jayasooriya, G., Mora, J., Mobberley, M., Ryder, T., Baithun, M., Stark, J., Franks, S., Hardy, K., 2008. Effect of cell shape and packing density on granulosa cell proliferation and formation of multiple layers during early follicle development in the ovary. Journal of Cell Science 121, 3890-3900.

Dai, J., Wu, C., Muneri, C.W., Niu, Y., Zhang, S., Rui, R., Zhang, D., 2015. Changes in mitochondrial function in porcine vitrified MII-stage oocytes and their impacts on apoptosis and developmental ability. Cryobiology 71, 291-298.

Dalman, A., Deheshkar Gooneh Farahani, N.S., Totonchi, M., Pirjani, R., Ebrahimi, B., Rezazadeh Valojerdi, M., 2017. Slow freezing versus vitrification technique for human ovarian tissue cryopreservation: An evaluation of histological changes, WNT signaling pathway and apoptotic genes expression. Cryobiology 79, 29-36.

Dang, Q.L., Phan, D.H., Johnson, A.N., Pasapuleti, M., Alkhaldi, H.A., Zhang, F., Vik, S.B., 2020. Analysis of Human Mutations in the Supernumerary Subunits of Complex I. Life (Basel, Switzerland) 10.

De Cian, M.C., Gregoire, E.P., Le Rolle, M., Lachambre, S., Mondin, M., Bell, S., Guigon, C.J., Chassot, A.A., Chaboissier, M.C., 2020. R-spondin2 signaling is required for oocyte-driven intercellular communication and follicular growth. Cell death and differentiation 27, 2856-2871.

De La Fuente, R., Eppig, J.J., 2001. Transcriptional activity of the mouse oocyte genome: companion granulosa cells modulate transcription and chromatin remodeling. Dev Biol 229, 224-236.

De La Fuente, R., Viveiros, M.M., Burns, K.H., Adashi, E.Y., Matzuk, M.M., Eppig, J.J., 2004. Major chromatin remodeling in the germinal vesicle (GV) of mammalian oocytes is dispensable for global transcriptional silencing but required for centromeric heterochromatin function. Developmental Biology 275, 447-458.

De Munck, N., Petrussa, L., Verheyen, G., Staessen, C., Vandeskelde, Y., Sterckx, J., Bocken, G., Jacobs, K., Stoop, D., De Rycke, M., Van de Velde, H., 2015. Chromosomal meiotic segregation, embryonic developmental kinetics and DNA (hydroxy)methylation analysis consolidate the safety of human oocyte vitrification. Molecular human reproduction 21, 535-544.

de Ruijter, A.J., van Gennip, A.H., Caron, H.N., Kemp, S., van Kuilenburg, A.B., 2003. Histone deacetylases (HDACs): characterization of the classical HDAC family. The Biochemical journal 370, 737-749.

Deanesly, R., 1954. Immature rat ovaries grafted after freezing and thawing. Journal of Endocrinology 11, 197-NP.

Debey, P., Szöllösi, M.S., Szöllösi, D., Vautier, D., Girousse, A., Besombes, D., 1993. Competent mouse oocytes isolated from antral follicles exhibit different chromatin organization and follow different maturation dynamics. Molecular reproduction and development 36, 59-74.

Demond, H., Khan, S., Castillo-Fernandez, J., Hanna, C.W., Kelsey, G., 2025. Transcriptome and DNA methylation profiling during the NSN to SN transition in mouse oocytes. BMC Molecular and Cell Biology 26, 2.

Dhali, A., Javvaji, P.K., Kolte, A.P., Francis, J.R., Roy, S.C., Sejian, V., 2017. Temporal expression of cumulus cell marker genes during in vitro maturation and oocyte developmental competence. Journal of assisted reproduction and genetics 34, 1493-1500.

Dinh, T., Son, W.Y., Demirtas, E., Dahan, M.H., 2022. How long can oocytes be frozen with vitrification and still produce competent embryos? A series of six cases. Obstetrics & gynecology science.

Dolmans, M.M., Falcone, T., Patrizio, P., 2020. Importance of patient selection to analyze in vitro fertilization outcome with transplanted cryopreserved ovarian tissue. Fertility and sterility 114, 279-280.

Dong, J., Albertini, D.F., Nishimori, K., Kumar, T.R., Lu, N., Matzuk, M.M., 1996. Growth differentiation factor-9 is required during early ovarian folliculogenesis. Nature 383, 531-535.

Donnez, J., Dolmans, M.-M., 2017. Fertility preservation in women. New England Journal of Medicine 377, 1657-1665.

Donnez, J., Dolmans, M.M., 2015a. Ovarian cortex transplantation: 60 reported live births brings the success and worldwide expansion of the technique towards routine clinical practice. Journal of assisted reproduction and genetics 32, 1167-1170.

Donnez, J., Dolmans, M.M., 2015b. Ovarian tissue freezing: current status. Current opinion in obstetrics & gynecology 27, 222-230.

Donnez, J., Dolmans, M.M., Demylle, D., Jadoul, P., Pirard, C., Squifflet, J., Martinez-Madrid, B., van Langendonckt, A., 2004. Livebirth after orthotopic transplantation of cryopreserved ovarian tissue. Lancet 364, 1405-1410.

Donnez, J., Dolmans, M.M., Pellicer, A., Diaz-Garcia, C., Sanchez Serrano, M., Schmidt, K.T., Ernst, E., Luyckx, V., Andersen, C.Y., 2013. Restoration of ovarian activity and pregnancy after transplantation of cryopreserved ovarian tissue: a review of 60 cases of reimplantation. Fertility and sterility 99, 1503-1513.

Donnez, J., Jadoul, P., Squifflet, J., Van Langendonckt, A., Donnez, O., Van Eyck, A.-S., Marinescu, C., Dolmans, M.-M., 2010. Ovarian tissue cryopreservation and transplantation in cancer patients. Best practice & research Clinical obstetrics & gynaecology 24, 87-100.

Dörnyei, G., Vass, Z., Juhász, C.B., Nádasy, G.L., Hunyady, L., Szekeres, M., 2023. Role of the Endocannabinoid System in Metabolic Control Processes and in the Pathogenesis of Metabolic Syndrome: An Update. Biomedicines 11.

Downs, S.M., Humpherson, P.G., Leese, H.J., 1998. Meiotic induction in cumulus cell-enclosed mouse oocytes: involvement of the pentose phosphate pathway. Biology of reproduction 58, 1084-1094.

Dumesic, D.A., Meldrum, D.R., Katz-Jaffe, M.G., Krisher, R.L., Schoolcraft, W.B., 2015. Oocyte environment: follicular fluid and cumulus cells are critical for oocyte health. Fertility and sterility 103, 303-316.

Dunlop, C.E., Anderson, R.A., 2014. The regulation and assessment of follicular growth. Scandinavian Journal of Clinical and Laboratory Investigation 74, 13-17.

Durli, I., Paz, A.H.R., Terraciano, P.B., Passos, E.P., Cirne-Lima, E.O., 2014. Comparative analysis of two cryopreservation systems of ovarian tissues in female Wistar rats. JBRA assisted reproduction 18, 7-11.

Eijkenboom, L., Saedt, E., Zietse, C., Braat, D., Beerendonk, C., Peek, R., 2022. Strategies to safely use cryopreserved ovarian tissue to restore fertility after cancer: a systematic review. Reproductive biomedicine online 45, 763-778.

Einenkel, R., Schallmoser, A., Sänger, N., 2022. Metabolic and secretory recovery of slow frozen-thawed human ovarian tissue in vitro. Molecular human reproduction 28.

El Cury-Silva, T., Nunes, M.E.G., Casalechi, M., Comim, F.V., Rodrigues, J.K., Reis, F.M., 2021. Cryoprotectant agents for ovarian tissue vitrification: Systematic review. Cryobiology 103, 7-14.

El Kamouh, M., Brionne, A., Sayyari, A., Laurent, A., Labbé, C., 2023. Cryopreservation effect on DNA methylation profile in rainbow trout spermatozoa. Scientific reports 13, 19029.

Endicott, S.J., and Miller, R.A., 2024. PTEN activates chaperone-mediated autophagy to regulate metabolism. Autophagy 20, 216-217.

Eroglu, A., Layman, L.C., 2012. Role of ART in imprinting disorders. Seminars in reproductive medicine 30, 92-104.

Eroglu, B., Szurek, E.A., Schall, P., Latham, K.E., Eroglu, A., 2020. Probing lasting cryoinjuries to oocyte-embryo transcriptome. PloS one 15, e0231108.

Esencan, E., Simsek, B., Seli, E., 2021. Analysis of female demographics in the United States: life expectancy, education, employment, family building decisions, and fertility service utilization. Current Opinion in Obstetrics and Gynecology 33, 170-177.

Estudillo, E., Jiménez, A., Bustamante-Nieves, P.E., Palacios-Reyes, C., Velasco, I., López-Ornelas, A., 2021. Cryopreservation of Gametes and Embryos and Their Molecular Changes. International journal of molecular sciences 22.

Fabbri, R., Porcu, E., Marsella, T., Rocchetta, G., Venturoli, S., Flamigni, C., 2001. Human oocyte cryopreservation: new perspectives regarding oocyte survival. Human reproduction 16, 411-416.

Fabbri, R., Vicenti, R., Macciocca, M., Pasquinelli, G., Paradisi, R., Battaglia, C., Martino, N.A., Venturoli, S., 2014. Good preservation of stromal cells and no apoptosis in human ovarian tissue after vitrification. BioMed research international 2014, 673537.

Fadini, R., Brambillasca, F., Renzini, M.M., Merola, M., Comi, R., De Ponti, E., Dal Canto, M.B., 2009. Human oocyte cryopreservation: comparison between slow and ultrarapid methods. Reproductive biomedicine online 19, 171-180.

Fahy, G.M., Wowk, B., Wu, J., 2006. Cryopreservation of complex systems: the missing link in the regenerative medicine supply chain. Rejuvenation research 9, 279-291.

Fair, T., Hulshof, S., Hyttel, P., Greve, T., Boland, M., 1997. Nucleus ultrastructure and transcriptional activity of bovine oocytes in preantral and antral follicles. Molecular reproduction and development 46, 208-215.

Falk, M., Falková, I., Kopečná, O., Bačíková, A., Pagáčová, E., Šimek, D., Golan, M., Kozubek, S., Pekarová, M., Follett, S.E., Klejdus, B., Elliott, K.W., Varga, K., Teplá, O., Kratochvílová, I., 2018. Chromatin architecture changes and DNA replication fork collapse are critical features in cryopreserved cells that are differentially controlled by cryoprotectants. Scientific reports 8, 14694.

Fan, J., Krautkramer, K.A., Feldman, J.L., Denu, J.M., 2015. Metabolic regulation of histone post-translational modifications. ACS Chem Biol 10, 95-108.

Feng, H.L., Hu, W., Marchesi, D., Qiao, J., Hershlag, A., 2011. The effect of slow-freeze versus vitrification on the oocyte: an animal model. Fertility and sterility 96, S77.

Fenton, A.J., 2015. Premature ovarian insufficiency: Pathogenesis and management. Journal of mid-life health 6, 147-153.

Ferrer-Roda, M., Izquierdo, D., Gil, A., Oliveira, M.E.F., Paramio, M.T., 2024. Oocyte Competence of Prepubertal Sheep and Goat Oocytes: An Assessment of Large-Scale Chromatin Configuration and Epidermal Growth Factor Receptor Expression in Oocytes and Cumulus Cells. International journal of molecular sciences 25.

Findlay, J., Hutt, K., Hickey, M., Anderson, R., 2015. How is the number of primordial follicles in the ovarian reserve established? Biology of reproduction, 111.

Ford, E.A., Beckett, E.L., Roman, S.D., McLaughlin, E.A., Sutherland, J.M., 2020. Advances in human primordial follicle activation and premature ovarian insufficiency. Reproduction 159, R15-R29.

Fortune, J.E., 1994. Ovarian follicular growth and development in mammals. Biology of reproduction 50, 225-232.

Fu, L., Chang, H., Wang, Z., Xie, X., chen, H., lei, Z., Zhang, Y., Quan, F., 2019. The effects of TETs on DNA methylation and hydroxymethylation of mouse oocytes after vitrification and warming. Cryobiology 90, 41-46.

Gao, H.H., Li, Z.P., Wang, H.P., Zhang, L.F., Zhang, J.M., 2016. Cryopreservation of whole bovine ovaries: comparisons of different thawing protocols. European journal of obstetrics, gynecology, and reproductive biology 204, 104-107.

Ge, L., Sui, H.-S., Lan, G.-C., Liu, N., Wang, J.-Z., Tan, J.-H., 2008. Coculture with cumulus cells improves maturation of mouse oocytes denuded of the cumulus oophorus: observations of nuclear and cytoplasmic events. Fertility and sterility 90, 2376-2388.

Gellert, S.E., Pors, S.E., Kristensen, S.G., Bay-Bjørn, A.M., Ernst, E., Yding Andersen, C., 2018. Transplantation of frozen-thawed ovarian tissue: an update on worldwide activity published in peer-reviewed papers and on the Danish cohort. Journal of assisted reproduction and genetics 35, 561-570.

Ghazifard, A., Salehi, M., Ghaffari Novin, M., Bandehpour, M., Keshavarzi, S., Fallah Omrani, V., Dehghani-Mohammadabadi, M., Masteri Farahani, R., Hosseini, A., 2019. Anacardic Acid Reduces Acetylation of H4K12 in Mouse Oocytes during Vitrification. Cell journal 20, 552-558.

Gilbert, S.F., 2000. Developmental Biology, 6th edition.

Gilchrist, R.B., Ritter, L.J., Armstrong, D.T., 2004. Oocyte-somatic cell interactions during follicle development in mammals. Animal reproduction science 82-83, 431-446.

Goldberg, A.D., Allis, C.D., Bernstein, E., 2007. Epigenetics: a landscape takes shape. Cell 128, 635-638.

Goldberg, G.S., Valiunas, V., Brink, P.R., 2004. Selective permeability of gap junction channels. Biochimica et Biophysica Acta - Biomembranes 1662, 96-101.

Golezar, S., Ramezani Tehrani, F., Khazaei, S., Ebadi, A., Keshavarz, Z., 2019. The global prevalence of primary ovarian insufficiency and early menopause: a meta-analysis. Climacteric 22, 403-411.

Gook, D.A., Edgar, D.H., 2007. Human oocyte cryopreservation. Human reproduction update 13, 591-605.

Gook, D.A., Osborn, S.M., Johnston, W.I., 1993. Cryopreservation of mouse and human oocytes using 1,2-propanediol and the configuration of the meiotic spindle. Human reproduction 8, 1101-1109.

Gook, D.A., Osborn, S.M., Johnston, W.I., 1995. Parthenogenetic activation of human oocytes following cryopreservation using 1,2-propanediol. Human reproduction 10, 654-658.

Gosden, R.G., Baird, D.T., Wade, J.C., Webb, R., 1994. Restoration of fertility to oophorectomized sheep by ovarian autografts stored at -196 degrees C. Human reproduction 9, 597-603.

Gou, L.T., Lim, D.H., Ma, W., Aubol, B.E., Hao, Y., Wang, X., Zhao, J., Liang, Z., Shao, C., Zhang, X., Meng, F., Li, H., Zhang, X., Xu, R., Li, D., Rosenfeld, M.G., Mellon, P.L., Adams, J.A., Liu, M.F., Fu, X.D., 2020. Initiation of Parental Genome Reprogramming in Fertilized Oocyte by Splicing Kinase SRPK1-Catalyzed Protamine Phosphorylation. Cell 180, 1212-1227.e1214.

Granot, I., Bechor, E., Barash, A., Dekel, N., 2002. Connexin43 in rat oocytes: developmental modulation of its phosphorylation. Biology of reproduction 66, 568-573.

Grazul-Bilska, A.T., Redmer, D.A., Bilski, J.J., Jablonka-Shariff, A., Doraiswamy, V., Reynolds, L.P., 1998. Gap junctional proteins, connexin 26, 32, and 43 in sheep ovaries throughout the estrous cycle. Endocrine 8, 269-279.

Grazul-Bilska, A.T., Reynolds, L.P., Redmer, D.A., 1997. Gap Junctions in the Ovaries1. Biology of reproduction 57, 947-957.

Griesinger, G., Schultz, L., Bauer, T., Broessner, A., Frambach, T., Kissler, S., 2011. Ovarian hyperstimulation syndrome prevention by gonadotropin-releasing hormone agonist triggering of final oocyte maturation in a gonadotropin-releasing hormone antagonist protocol in combination with a "freeze-all" strategy: a prospective multicentric study. Fertility and sterility 95, 2029-2033, 2033.e2021.

Griffin, J., Emery, B.R., Huang, I., Peterson, C.M., Carrell, D.T., 2006. Comparative analysis of follicle morphology and oocyte diameter in four mammalian species (mouse, hamster, pig, and human). Journal of experimental & clinical assisted reproduction 3, 2.

Groome, N.P., Illingworth, P.J., O'Brien, M., Pai, R., Rodger, F.E., Mather, J.P., McNeilly, A.S., 1996. Measurement of dimeric inhibin B throughout the human menstrual cycle. The Journal of clinical endocrinology and metabolism 81, 1401-1405.

Gu, R., Ge, N., Huang, B., Fu, J., Zhang, Y., Wang, N., Xu, Y., Li, L., Peng, X., Zou, Y., Sun, Y., Sun, X., 2023. Impacts of vitrification on the transcriptome of human ovarian tissue in patients with gynecological cancer. Front Genet 14, 1114650.

Gualtieri, R., Kalthur, G., Barbato, V., Di Nardo, M., Adiga, S.K., Talevi, R., 2021. Mitochondrial Dysfunction and Oxidative Stress Caused by Cryopreservation in Reproductive Cells. Antioxidants (Basel, Switzerland) 10.

Gupta, S.K., Chakravarty, S., Suraj, K., Bansal, P., Ganguly, A., Jain, M.K., Bhandari, B., 2007. Structural and functional attributes of zona pellucida glycoproteins. Society of Reproduction and Fertility supplement 63, 203-216.

Gutnisky, C., Dalvit, G.C., Thompson, J.G., Cetica, P.D., 2014. Pentose phosphate pathway activity: effect on in vitro maturation and oxidative status of bovine oocytes. Reproduction, Fertility and Development 26, 931-942.

Guzel, Y., Oktem, O., 2017. Understanding follicle growth in vitro: Are we getting closer to obtaining mature oocytes from in vitro-grown follicles in human? Molecular reproduction and development 84, 544-559.

Habara, O., Logan, C.Y., Kanai-Azuma, M., Nusse, R., Takase, H.M., 2021. WNT signaling in pre-granulosa cells is required for ovarian folliculogenesis and female fertility. Development (Cambridge, England) 148.

Haberland, M., Montgomery, R.L., Olson, E.N., 2009. The many roles of histone deacetylases in development and physiology: implications for disease and therapy. Nature reviews. Genetics 10, 32-42.

Hansen, K., Knowlton, N., Thyer, A., Charleston, J., Soules, M., Klein, N., 2008. A new model of reproductive aging: the decline in ovarian non-growing follicle number from birth to menopause. Human reproduction, 699-708.

Hardy, K., Wright, C.S., Franks, S., Winston, R.M.L., 2000. In Vitro maturation of oocytes. British Medical Bulletin 56, 588-602.

Hart, R., Norman, R.J., 2013. The longer-term health outcomes for children born as a result of IVF treatment: Part I--General health outcomes. Human reproduction update 19, 232-243.

Hattori, H., Hiura, H., Kitamura, A., Miyauchi, N., Kobayashi, N., Takahashi, S., Okae, H., Kyono, K., Kagami, M., Ogata, T., Arima, T., 2019. Association of four imprinting disorders and ART. Clinical epigenetics 11, 21.

He, Y., Su, Y., Zeng, J., Chong, W., Hu, X., Zhang, Y., Peng, X., 2022. Cancer-specific survival after diagnosis in men versus women: A pan-cancer analysis. MedComm 3, e145.

He, Z.-y., Wang, H.-Y., Zhou, X., Liang, X.-y., Yan, B., Wang, R., Ma, L.-h., Wang, Y.-l., 2018. Evaluation of vitrification protocol of mouse ovarian tissue by effect of DNA methyltransferase-1 and paternal imprinted growth factor receptor-binding protein 10 on signaling pathways. Cryobiology 80, 89-95.

Health, O., 2006. In vitro fertilization and multiple pregnancies: an evidence-based analysis. Ontario Health Technol Assess Ser 6, 1-63.

Heape, W., 1900. Memoirs: The" Sexual Season" of Mammals and the Relation of the" Pro-œstrum" to Menstruation. Journal of Cell Science 2, 1-70.

Henzl, M.R., Smith, R.E., Boost, G., Tyler, E.T., 1972. Lysosomal concept of menstrual bleeding in humans. The Journal of clinical endocrinology and metabolism 34, 860-875.

Herraiz, S., Novella-Maestre, E., Rodríguez, B., Díaz, C., Sánchez-Serrano, M., Mirabet, V., Pellicer, A., 2014. Improving ovarian tissue cryopreservation for oncologic patients: slow freezing versus vitrification, effect of different procedures and devices. Fertility and sterility 101, 775-784.

Hirshfield, A.N., 1991. Development of follicles in the mammalian ovary. Int Rev Cytol 124, 43-101.

Hongyan, C., Xue, Y., Honglan, Z., Yi, L., Xudong, l., Xiaohong, C., Heng, C., 2021. An experimental study on autologous transplantation of fresh ovarian tissue in sheep. Gynecology and Obstetrics Clinical Medicine 1, null.

Hoshino, Y., 2018. Updating the markers for oocyte quality evaluation: intracellular temperature as a new index. Reproductive medicine and biology 17, 434-441.

Hossay, C., Donnez, J., Dolmans, M.M., 2020. Whole Ovary Cryopreservation and Transplantation: A Systematic Review of Challenges and Research Developments in Animal Experiments and Humans. Journal of clinical medicine 9.

Hossay, C., Tramacere, F., Cacciottola, L., Camboni, A., Squifflet, J.L., Donnez, J., Dolmans, M.M., 2023. Follicle outcomes in human ovarian tissue: effect of freezing, culture, and grafting. Fertility and sterility 119, 135-145.

Hu, W., Marchesi, D., Qiao, J., Feng, H.L., 2012. Effect of slow freeze versus vitrification on the oocyte: an animal model. Fertility and sterility 98, 752-760 e753.

Huang, F.J., Chang, S.Y., Tsai, M.Y., Lin, Y.C., Kung, F.T., Wu, J.F., Lu, Y.J., 1999. Relationship of the human cumulus-free oocyte maturational profile with in vitro outcome parameters after intracytoplasmic sperm injection. Journal of assisted reproduction and genetics 16, 483-487.

Hunt, C.J., 2011. Cryopreservation of Human Stem Cells for Clinical Application: A Review. Transfusion medicine and hemotherapy : offizielles Organ der Deutschen Gesellschaft fur Transfusionsmedizin und Immunhamatologie 38, 107-123.

Imhof, M., Bergmeister, H., Lipovac, M., Rudas, M., Hofstetter, G., Huber, J., 2006. Orthotopic microvascular reanastomosis of whole cryopreserved ovine ovaries resulting in pregnancy and live birth. Fertility and sterility 85 Suppl 1, 1208-1215.

Imhof, M., Hofstetter, G., Bergmeister, H., Rudas, M., Kain, R., Lipovac, M., Huber, J., 2004. Cryopreservation of a Whole Ovary As a Strategy for Restoring Ovarian Function. Journal of assisted reproduction and genetics 21, 459-465.

Isachenko, V., Rahimi, G., Dattena, M., Mallmann, P., Baikoshkarova, S., Kellerwessel, E., Otarbaev, M., Shalakhmetova, T., Isachenko, E., 2014. Whole ovine ovaries as a model for human: perfusion with cryoprotectants in vivo and in vitro. BioMed research international 2014, 409019.

Ishii, D., Matsuzawa, D., Matsuda, S., Tomizawa, H., Sutoh, C., Shimizu, E., 2014. Methyl donor-deficient diet during development can affect fear and anxiety in adulthood in C57BL/6J mice. PloS one 9, e105750.

Islam, N., Sunday Paul, U., Alhamdan, R., Hernandez-Medrano, J., Campbell, B.K., Marsters, P., Maalouf, W.E., 2019. Steroids and miRNAs in assessment of ovarian tissue damage following cryopreservation. Journal of Molecular Endocrinology 62, 207-216.

Islam, R.A., Rallis, C., 2023. Ribosomal Biogenesis and Heterogeneity in Development, Disease, and Aging. Epigenomes 7.

Iussig, B., Maggiulli, R., Fabozzi, G., Bertelle, S., Vaiarelli, A., Cimadomo, D., Ubaldi, F.M., Rienzi, L., 2019. A brief history of oocyte cryopreservation: Arguments and facts. Acta obstetricia et gynecologica Scandinavica 98, 550-558.

Jaffe, L.A., Egbert, J.R., 2017. Regulation of Mammalian Oocyte Meiosis by Intercellular Communication Within the Ovarian Follicle. Annual review of physiology 79, 237-260.

Jahangiri, M., Shahhoseini, M., Movaghar, B., 2018. The Effect of Vitrification on Expression and Histone Marks of Igf2 and Oct4 in Blastocysts Cultured from Two-Cell Mouse Embryos. Cell journal 19, 607-613.

Jang, T.H., Park, S.C., Yang, J.H., Kim, J.Y., Seok, J.H., Park, U.S., Choi, C.W., Lee, S.R., Han, J., 2017. Cryopreservation and its clinical applications. Integrative medicine research 6, 12-18.

Jensen, A.K., Kristensen, S.G., Macklon, K.T., Jeppesen, J.V., Fedder, J., Ernst, E., Andersen, C.Y., 2015. Outcomes of transplantations of cryopreserved ovarian tissue to 41 women in Denmark. Human reproduction 30, 2838-2845.

Ji, P., Liu, Y., Yan, L., Jia, Y., Zhao, M., Lv, D., Yao, Y., Ma, W., Yin, D., Liu, F., Gao, S., Wusiman, A., Yang, K., Zhang, L., Liu, G., 2023. Melatonin improves the vitrification of sheep morulae by modulating transcriptome. Frontiers in Veterinary Science 10.

Johnson, M.L., Redmer, D.A., Reynolds, L.P., Bilski, J.J., Grazul-Bilska, A.T., 2002. Gap junctional intercellular communication of bovine granulosa and thecal cells from antral follicles: Effects of luteinizing hormone and follicle-stimulating hormone. Endocrine 18, 261-270.

Kageyama, S., Liu, H., Kaneko, N., Ooga, M., Nagata, M., Aoki, F., 2007. Alterations in epigenetic modifications during oocyte growth in mice. Reproduction 133, 85-94.

Karlsson, J.O.M., 2002. Cryopreservation: Freezing and vitrification [3]. Science 296, 655-656.

Kasapoğlu, I., Seli, E., 2020. Mitochondrial dysfunction and ovarian aging. Endocrinology 161.

Katz-Jaffe, M.G., McReynolds, S., Gardner, D.K., Schoolcraft, W.B., 2009. The role of proteomics in defining the human embryonic secretome. Molecular human reproduction 15, 271-277.

Kawamura, K., Cheng, Y., Suzuki, N., Deguchi, M., Sato, Y., Takae, S., Ho, C.H., Kawamura, N., Tamura, M., Hashimoto, S., Sugishita, Y., Morimoto, Y., Hosoi, Y., Yoshioka, N., Ishizuka, B., Hsueh, A.J., 2013. Hippo signaling disruption and Akt stimulation of ovarian follicles for infertility treatment. Proceedings of the National Academy of Sciences of the United States of America 110, 17474-17479.

Kelsey, T.W., Dodwell, S.K., Wilkinson, A.G., Greve, T., Andersen, C.Y., Anderson, R.A., Wallace, W.H., 2013. Ovarian volume throughout life: a validated normative model. PloS one 8, e71465.

Khattak, H., Malhas, R., Craciunas, L., Afifi, Y., Amorim, C.A., Fishel, S., Silber, S., Gook, D., Demeestere, I., Bystrova, O., Lisyanskaya, A., Manikhas, G., Lotz, L., Dittrich, R., Colmorn, L.B., Macklon, K.T., Hjorth, I.M.D., Kristensen, S.G., Gallos, I., Coomarasamy, A., 2022. Fresh and cryopreserved ovarian tissue transplantation for preserving reproductive and endocrine function: a systematic review and individual patient data meta-analysis. Human reproduction update 28, 400-416.

Kidder, G.M., Mhawi, A.A., 2002. Gap junctions and ovarian folliculogenesis. Reproduction 123, 613-620.

Kim, B., Ryu, K.J., Lee, S., Kim, T., 2021. Changes in telomere length and senescence markers during human ovarian tissue cryopreservation. Scientific reports 11, 2238.

Kolibianaki, E., Goulis, D., Kolibianakis, E., 2020. Ovarian tissue cryopreservation and transplantation to delay menopause: Facts and fiction. Maturitas 142, 64-67.

Komorowska, B., 2016. Autoimmune premature ovarian failure. Menopause Review/Przegląd Menopauzalny 15, 210-214.

Kopeika, J., Thornhill, A., Khalaf, Y., 2014. The effect of cryopreservation on the genome of gametes and embryos: principles of cryobiology and critical appraisal of the evidence. Human reproduction update 21, 209-227.

Korkidakis, A., Au, J., Albert, A., Havelock, J., 2021. Higher blastocyst implantation in frozen versus fresh embryo transfers in good prognosis patients. Minerva obstetrics and gynecology 73, 776-781.

Koubova, J., Menke, D.B., Zhou, Q., Capel, B., Griswold, M.D., Page, D.C., 2006. Retinoic acid regulates sex-specific timing of meiotic initiation in mice. Proceedings of the National Academy of Sciences of the United States of America 103, 2474-2479.

Kratochvílová, I., Kopečná, O., Bačíková, A., Pagáčová, E., Falková, I., Follett, S.E., Elliott, K.W., Varga, K., Golan, M., Falk, M., 2019. Changes in Cryopreserved Cell Nuclei Serve as Indicators of Processes during Freezing and Thawing. Langmuir : the ACS journal of surfaces and colloids 35, 7496-7508.

Kristensen, S.G., Andersen, C.Y., 2018. Cryopreservation of Ovarian Tissue: Opportunities Beyond Fertility Preservation and a Positive View Into the Future. Frontiers in endocrinology 9, 347.

Kristensen, S.G., Ebbesen, P., Andersen, C.Y., 2015. Transcriptional profiling of five isolated size-matched stages of human preantral follicles. Molecular and cellular endocrinology 401, 189-201.

Kuleshova, L., Gianaroli, L., Magli, C., Ferraretti, A., Trounson, A., 1999. Birth following vitrification of a small number of human oocytes: case report. Human reproduction 14, 3077-3079.

Kuwayama, M., 2007. Highly efficient vitrification for cryopreservation of human oocytes and embryos: the Cryotop method. Theriogenology 67, 73-80.

Kuwayama, M., Vajta, G., Kato, O., Leibo, S.P., 2005. Highly efficient vitrification method for cryopreservation of human oocytes. Reproductive biomedicine online 11, 300-308.

Labrune, E., Jaeger, P., Santamaria, C., Fournier, C., Benchaib, M., Rabilloud, M., Salle, B., Lornage, J., 2020. Cellular and Molecular Impact of Vitrification Versus Slow Freezing on Ovarian Tissue. Tissue engineering. Part C, Methods 26, 276-285.

Lainas, T.G., Sfontouris, I.A., Zorzovilis, I.Z., Petsas, G.K., Lainas, G.T., Iliadis, G.S., Kolibianakis, E.M., 2009. Management of severe OHSS using GnRH antagonist and blastocyst cryopreservation in PCOS patients treated with long protocol. Reproductive biomedicine online 18, 15-20.

Lamas-Toranzo, I., Pericuesta, E., Bermejo-Álvarez, P., 2018. Mitochondrial and metabolic adjustments during the final phase of follicular development prior to IVM of bovine oocytes. Theriogenology 119, 156-162.

Lambertini, M., Horicks, F., Del Mastro, L., Partridge, A.H., Demeestere, I., 2019a. Ovarian protection with gonadotropin-releasing hormone agonists during chemotherapy in cancer patients: From biological evidence to clinical application. Cancer treatment reviews 72, 65-77.

Lambertini, M., Richard, F., Nguyen, B., Viglietti, G., Villarreal-Garza, C., 2019b. Ovarian Function and Fertility Preservation in Breast Cancer: Should Gonadotropin-Releasing Hormone Agonist be administered to All Premenopausal Patients Receiving Chemotherapy? Clinical medicine insights. Reproductive health 13, 1179558119828393.

Larman, M.G., Katz-Jaffe, M.G., Sheehan, C.B., Gardner, D.K., 2007. 1,2-propanediol and the type of cryopreservation procedure adversely affect mouse oocyte physiology. Human reproduction 22, 250-259.

Ledwaba, M.R., O'Neill, H.A., Thema, M.A., Maqhashu, A., Mphaphathi, M.L., 2025. Techniques for In Vitro Fertilisation of Vitrified Cattle Oocytes: Challenges and New Developments. Agriculture 15, 363.

Lee, P.C., Comizzoli, P., 2019. Desiccation and supra-zero temperature storage of cat germinal vesicles lead to less structural damage and similar epigenetic alterations compared to cryopreservation. Molecular reproduction and development 86, 1822-1831.

Lee, R.K., Li, S.H., Lu, C.H., Ho, H.Y., Chen, Y.J., Yeh, H.I., 2008. Abnormally low expression of connexin 37 and connexin 43 in subcutaneously transplanted cryopreserved mouse ovarian tissue. Journal of assisted reproduction and genetics 25, 489-497.

Levi Setti, P.E., Smeraldi, A., Menduni, F., Parini, V., Levi, S., Desgrò, M., 2013. Comparison of fresh and warmed transfer of blastocysts developed day 5 or day 6. Fertility and sterility 100, S505.

Li, G.P., Bunch, T.D., White, K.L., Rickords, L., Liu, Y., Sessions, B.R., 2006. Denuding and centrifugation of maturing bovine oocytes alters oocyte spindle integrity and the ability of cytoplasm to support parthenogenetic and nuclear transfer embryo development. Molecular reproduction and development 73, 446-451.

Li, J., Yang, X., Liu, F., Song, Y., Liu, Y., 2019. Evaluation of differentially expressed microRNAs in vitrified oocytes by next generation sequencing. The International Journal of Biochemistry & Cell Biology 112, 134-140.

Li, J.J., Fu, X.W., Mo, X.H., Yue, M.X., Jia, B.Y., Zhu, S.E., 2013. Vitrification alters acH4K12 and acH4K16 levels in sheep oocytes at various developmental stages. Small Ruminant Research 112, 108-113.

Li, J.J., Pei, Y., Zhou, G.B., Suo, L., Wang, Y.P., Wu, G.Q., Fu, X.W., Hou, Y.P., Zhu, S.E., 2011. Histone deacetyltransferase1 expression in mouse oocyte and their in vitro-fertilized embryo: effect of oocyte vitrification. Cryo letters 32, 13-20.

Li, M., Zhu, Y., Wei, J., Chen, L., Chen, S., Lai, D., 2023. The global prevalence of premature ovarian insufficiency: a systematic review and meta-analysis. Climacteric 26, 95-102.

Li, Q., McKenzie, L.J., Matzuk, M.M., 2008. Revisiting oocyte-somatic cell interactions: in search of novel intrafollicular predictors and regulators of oocyte developmental competence. Molecular human reproduction 14, 673-678.

Li, Z., Wang, Y.A., Ledger, W., Edgar, D.H., Sullivan, E.A., 2014. Clinical outcomes following cryopreservation of blastocysts by vitrification or slow freezing: a population-based cohort study. Human reproduction 29, 2794-2801.

Liang, Y., Fu, X.-W., Li, J.-J., Yuan, D.-S., Zhu, S.-E., 2014. DNA methylation pattern in mouse oocytes and their in vitro fertilized early embryos: effect of oocyte vitrification. Zygote 22, 138-145.

Lin, Y., Gill, M.E., Koubova, J., Page, D.C., 2008. Germ Cell-Intrinsic and -Extrinsic Factors Govern Meiotic Initiation in Mouse Embryos. Science 322, 1685-1687.

Liu, Y., Sui, H.S., Wang, H.L., Yuan, J.H., Luo, M.J., Xia, P., Tan, J.H., 2006. Germinal vesicle chromatin configurations of bovine oocytes. Microscopy research and technique 69, 799-807.

Locatelli, Y., Calais, L., Duffard, N., Lardic, L., Monniaux, D., Piver, P., Mermillod, P., Bertoldo, M.J., 2019. In vitro survival of follicles in prepubertal ewe ovarian cortex cryopreserved by slow freezing or non-equilibrium vitrification. Journal of assisted reproduction and genetics 36, 1823-1835.

Luciano, A.M., Chigioni, S., Lodde, V., Franciosi, F., Luvoni, G.C., Modina, S.C., 2009. Effect of different cryopreservation protocols on cytoskeleton and gap junction mediated communication integrity in feline germinal vesicle stage oocytes. Cryobiology 59, 90-95.

Luciano, A.M., Modina, S., Vassena, R., Milanesi, E., Lauria, A., Gandolfi, F., 2004. Role of Intracellular Cyclic Adenosine 3′,5′-Monophosphate Concentration and Oocyte-Cumulus Cells Communications on the Acquisition of the Developmental Competence during In Vitro Maturation of Bovine Oocyte. Biology of reproduction 70, 465-472.

Ma, J.Y., Li, M., Luo, Y.B., Song, S., Tian, D., Yang, J., Zhang, B., Hou, Y., Schatten, H., Liu, Z., Sun, Q.Y., 2013. Maternal factors required for oocyte developmental competence in mice: transcriptome analysis of non-surrounded nucleolus (NSN) and surrounded nucleolus (SN) oocytes. Cell Cycle 12, 1928-1938.

Ma, Y., Long, C., Liu, G., Bai, H., Ma, L., Bai, T., Zuo, Y., Li, S., 2022. WGBS combined with RNA-seq analysis revealed that Dnmt1 affects the methylation modification and gene expression changes during mouse oocyte vitrification. Theriogenology 177, 11-21.

Ma, Y., Pan, B., Yang, H., Qazi, I.H., Wu, Z., Zeng, C., Zhang, M., Meng, Q., Zhou, G., 2018. Expression of CD9 and CD81 in bovine germinal vesicle oocytes after vitrification followed by in vitro maturation. Cryobiology 81, 206-209.

Macaulay, A.D., Gilbert, I., Scantland, S., Fournier, E., Ashkar, F., Bastien, A., Saadi, H.A.S., Gagné, D., Sirard, M.-A., Khandjian, É.W., 2016. Cumulus cell transcripts transit to the bovine oocyte in preparation for maturation. Biology of reproduction 94, 16, 11-11.

Maclaran, K., Horner, E., Panay, N., 2010. Premature ovarian failure: long-term sequelae. Menopause international 16, 38-41.

Magnusson, V., Feitosa, W.B., Goissis, M.D., Yamada, C., Tavares, L.M., D'Avila Assumpcao, M.E., Visintin, J.A., 2008. Bovine oocyte vitrification: effect of ethylene glycol concentrations and meiotic stages. Animal reproduction science 106, 265-273.

Maltaris, T., Beckmann, M.W., Mueller, A., Hoffmann, I., Kohl, J., Dittrich, R., 2007. Significant loss of primordial follicles after prolonged gonadotropin stimulation in xenografts of cryopreserved human ovarian tissue in severe combined immunodeficient mice. Fertility and sterility 87, 195-197.

Mandawala, A.A., Harvey, S.C., Roy, T.K., Fowler, K.E., 2016. Cryopreservation of animal oocytes and embryos: Current progress and future prospects. Theriogenology 86, 1637-1644.

Manipalviratn, S., DeCherney, A., Segars, J., 2009. Imprinting disorders and assisted reproductive technology. Fertility and sterility 91, 305-315.

Manjunatha, B., Gupta, P., Devaraj, M., Ravindra, J., Nandi, S., 2007. Selection of developmentally competent buffalo oocytes by brilliant cresyl blue staining before IVM. Theriogenology 68, 1299-1304.

Markholt, S., Grøndahl, M.L., Ernst, E.H., Andersen, C.Y., Ernst, E., Lykke-Hartmann, K., 2012. Global gene analysis of oocytes from early stages in human folliculogenesis shows high expression of novel genes in reproduction. Molecular human reproduction 18, 96-110.

Martinez-Burgos, M., Herrero, L., Megias, D., Salvanes, R., Montoya, M.C., Cobo, A.C., Garcia-Velasco, J.A., 2011. Vitrification versus slow freezing of oocytes: effects on morphologic appearance, meiotic spindle configuration, and DNA damage. Fertility and sterility 95, 374-377.

Martinez-Madrid, B., Camboni, A., Dolmans, M.M., Nottola, S., Van Langendonckt, A., Donnez, J., 2007. Apoptosis and ultrastructural assessment after cryopreservation of whole human ovaries with their vascular pedicle. Fertility and sterility 87, 1153-1165.

Martinez, C.A., Rizos, D., Rodriguez-Martinez, H., Funahashi, H., 2023. Oocyte-cumulus cells crosstalk: New comparative insights. Theriogenology 205, 87-93.

Mathias, F.J., D'Souza, F., Uppangala, S., Salian, S.R., Kalthur, G., Adiga, S.K., 2014. Ovarian tissue vitrification is more efficient than slow freezing in protecting oocyte and granulosa cell DNA integrity. Systems Biology in Reproductive Medicine 60, 317-322.

Matsunaga, R., Funahashi, H., 2017. Supplementation with cumulus cell masses improves the in vitro meiotic competence of porcine cumulus–oocytes complexes derived from small follicles. Reproduction in Domestic Animals 52, 672-679.

Matzuk, M.M., Burns, K.H., Viveiros, M.M., Eppig, J.J., 2002. Intercellular communication in the mammalian ovary: oocytes carry the conversation. Science 296, 2178-2180.

McLaughlin, M., Patrizio, P., Kayisli, U., Luk, J., Thomson, T.C., Anderson, R.A., Telfer, E.E., Johnson, J., 2011. mTOR kinase inhibition results in oocyte loss characterized by empty follicles in human ovarian cortical strips cultured in vitro. Fertility and sterility 96, 1154-1159. e1151.

Meirow, D., Nugent, D., 2001. The effects of radiotherapy and chemotherapy on female reproduction. Human reproduction update 7, 535-543.

Melton, C.M., Zaunbrecher, G.M., Yoshizaki, G., Patio, R., Whisnant, S., Rendon, A., Lee, V.H., 2001. Expression of connexin 43 mRNA and protein in developing follicles of prepubertal porcine ovaries. Comparative Biochemistry and Physiology - B Biochemistry and Molecular Biology 130, 43-55.

Men, H., Monson, R.L., Parrish, J.J., Rutledge, J.J., 2003. Detection of DNA damage in bovine metaphase II oocytes resulting from cryopreservation. Molecular reproduction and development 64, 245-250.

Mhatre, P., Mhatre, J., Magotra, R., 2005. Ovarian transplant: a new frontier. Transplantation proceedings 37, 1396-1398.

Mihm, M., Evans, A., 2008. Mechanisms for Dominant Follicle Selection in Monovulatory Species: A Comparison of Morphological, Endocrine and Intraovarian Events in Cows, Mares and Women. Reproduction in Domestic Animals 43, 48-56.

Miki, H., Ogonuki, N., Inoue, K., Baba, T., Ogura, A., 2006. Improvement of Cumulus-free Oocyte Maturation In Vitro and Its Application to Microinsemination with Primary Spermatocytes in Mice. Journal of Reproduction and Development 52, 239-248.

Milenkovic, M., Diaz-Garcia, C., Wallin, A., Brannstrom, M., 2012. Viability and function of the cryopreserved whole rat ovary: comparison between slow-freezing and vitrification. Fertility and sterility 97, 1176-1182.

Milenkovic, M., Gharemani, M., Bergh, A., Wallin, A., Mölne, J., Fazlagic, E., Eliassen, E., Kahn, J., Brännström, M., 2011. The human postmenopausal ovary as a tool for evaluation of cryopreservation protocols towards whole ovary cryopreservation. Journal of assisted reproduction and genetics 28, 453-460.

Milroy, C., Liu, L., Hammoud, S., Hammoud, A., Carrell, D.T., 2010. Differential methylation of pluripotentcy factors in in-vitro matured and vitrified in-vitro matured mouse oocytes. Fertility and sterility 94, S137.

Mira, A., 1998. Why is Meiosis Arrested? Journal of Theoretical Biology 194, 275-287.

Miyara, F., Migne, C., Dumont-Hassan, M., Le Meur, A., Cohen-Bacrie, P., Aubriot, F.X., Glissant, A., Nathan, C., Douard, S., Stanovici, A., Debey, P., 2003. Chromatin configuration and transcriptional control in human and mouse oocytes. Molecular reproduction and development 64, 458-470.

Moin, M., Bakshi, A., Saha, A., Dutta, M., Madhav, S.M., Kirti, P.B., 2016. Rice Ribosomal Protein Large Subunit Genes and Their Spatio-temporal and Stress Regulation. Frontiers in Plant Science 7.

Momeni, A., Haghpanah, T., Nematollahi-Mahani, S.N., Ashourzadeh, S., Eftekhar-Vaghefi, S.H., 2023. Comparing the effects of vitrification, before and after mouse oocyte in vitro maturation on developmental competence, changes in epigenetic regulators and stress oxidative response. Biochemical and Biophysical Research Communications 679, 179-190.

Momenimovahed, Z., Taheri, S., Tiznobaik, A., Salehiniya, H., 2019. Do the Fertility Drugs Increase the Risk of Cancer? A Review Study. Frontiers in endocrinology 10, 313.

Motta, P., Makabe, S., Notttola, S., 1997. The ultrastructure of human reproduction. 1. The natural history of the female germ cell: origin, migration and differentiation inside the developing ovary. Human reproduction update 3, 281-297.

Moulavi, F., Saadeldin, I.M., Swelum, A.A., Tasdighi, F., Hosseini-Fahraji, H., Hosseini, S.M., 2021. Oocyte vitrification induces loss of DNA methylation and histone acetylation in the resulting embryos derived using ICSI in dromedary camel. Zygote 29, 383-392.

Moussa, M., Shu, J., Zhang, X., Zeng, F., 2014. Cryopreservation of mammalian oocytes and embryos: current problems and future perspectives. Science China. Life sciences 57, 903-914.

Nagy, Z.P., Chang, C.C., Shapiro, D.B., Bernal, D.P., Elsner, C.W., Mitchell-Leef, D., Toledo, A.A., Kort, H.I., 2009. Clinical evaluation of the efficiency of an oocyte donation program using egg cryo-banking. Fertility and sterility 92, 520-526.

Nakamura, Y., Obata, R., Okuyama, N., Aono, N., Hashimoto, T., Kyono, K., 2017. Residual ethylene glycol and dimethyl sulphoxide concentration in human ovarian tissue during warming/thawing steps following cryopreservation. Reproductive biomedicine online 35, 311-313.

Newton, H., Aubard, Y., Rutherford, A., Sharma, V., Gosden, R., 1996. Low temperature storage and grafting of human ovarian tissue. Human reproduction 11, 1487-1491.

Nisolle, M., Casanas-Roux, F., Qu, J., Motta, P., Donnez, J., 2000. Histologic and ultrastructural evaluation of fresh and frozen-thawed human ovarian xenografts in nude mice. Fertility and sterility 74, 122-129.

Norris, R.P., Freudzon, M., Mehlmann, L.M., Cowan, A.E., Simon, A.M., Paul, D.L., Lampe, P.D., Jaffe, L.A., 2008. Luteinizing hormone causes MAP kinase-dependent phosphorylation and closure of connexin 43 gap junctions in mouse ovarian follicles: one of two paths to meiotic resumption. Development (Cambridge, England) 135, 3229-3238.

Nottola, S.A., Albani, E., Coticchio, G., Palmerini, M.G., Lorenzo, C., Scaravelli, G., Borini, A., Levi-Setti, P.E., Macchiarelli, G., 2016. Freeze/thaw stress induces organelle remodeling and membrane recycling in cryopreserved human mature oocytes. Journal of assisted reproduction and genetics 33, 1559-1570.

Nuttinck, F., Peynot, N., Humblot, P., Massip, A., Dessy, F., Fléchon, J.E., 2000. Comparative immunohistochemical distribution of Connexin 37 and Connexin 43 throughout folliculogenesis in the bovine ovary. Molecular reproduction and development 57, 60-66.

O'Leary, M.N., Schreiber, K.H., Zhang, Y., Duc, A.C., Rao, S., Hale, J.S., Academia, E.C., Shah, S.R., Morton, J.F., Holstein, C.A., Martin, D.B., Kaeberlein, M., Ladiges, W.C., Fink, P.J., Mackay, V.L., Wiest, D.L., Kennedy, B.K., 2013. The ribosomal protein Rpl22 controls ribosome composition by directly repressing expression of its own paralog, Rpl22l1. PLoS genetics 9, e1003708.

Obata, R., Nakumura, Y., Okuyama, N., Sasaki, C., Ogura, Y., Aono, N., Hamano, S., Hashimoto, T., Kyono, K., 2018. Comparison of Residual Dimethyl Sulfoxide (DMSO) and

Ethylene Glycol (EG) Concentration in Bovine Ovarian Tissue During Warming Steps Between Slow Freezing and Vitrification. Cryo letters 39, 251-254.

Oktay, K., Briggs, D., Gosden, R.G., 1997. Ontogeny of follicle-stimulating hormone receptor gene expression in isolated human ovarian follicles. The Journal of clinical endocrinology and metabolism 82, 3748-3751.

Oktay, K., Cil, A.P., Bang, H., 2006. Efficiency of oocyte cryopreservation: a meta-analysis. Fertility and sterility 86, 70-80.

Oktay, K., Harvey, B.E., Partridge, A.H., Quinn, G.P., Reinecke, J., Taylor, H.S., Wallace, W.H., Wang, E.T., Loren, A.W., 2018. Fertility Preservation in Patients With Cancer: ASCO Clinical Practice Guideline Update. Journal of clinical oncology : official journal of the American Society of Clinical Oncology 36, 1994-2001.

Oktay, K., Karlikaya, G., 2000. Ovarian function after transplantation of frozen, banked autologous ovarian tissue. The New England journal of medicine 342, 1919.

Oktem, O., Oktay, K., 2008. The ovary: anatomy and function throughout human life. Annals of the New York Academy of Sciences 1127, 1-9.

Oktem, O., Urman, B., 2010. Understanding follicle growth in vivo. Human reproduction 25, 2944-2954.

Onions, V.J., Mitchell, M.R., Campbell, B.K., Webb, R., 2008. Ovarian tissue viability following whole ovine ovary cryopreservation: assessing the effects of sphingosine-1-phosphate inclusion. Human reproduction 23, 606-618.

Onions, V.J., Webb, R., Pincott-Allen, C., Picton, H.M., Campbell, B.K., 2013. The effects of whole ovarian perfusion and cryopreservation on endothelial cell-related gene expression in the ovarian medulla and pedicle. Molecular human reproduction 19, 205-215.

Onofre, J., Baert, Y., Faes, K., Goossens, E., 2016. Cryopreservation of testicular tissue or testicular cell suspensions: a pivotal step in fertility preservation. Human reproduction update 22, 744-761.

Padmanabhan, V., Veiga-Lopez, A., 2013. Sheep models of polycystic ovary syndrome phenotype. Molecular and cellular endocrinology 373, 8-20.

Palmerini, M.G., Antinori, M., Maione, M., Cerusico, F., Versaci, C., Nottola, S.A., Macchiarelli, G., Khalili, M.A., Antinori, S., 2014. Ultrastructure of immature and mature human oocytes after cryotop vitrification. The Journal of reproduction and development 60, 411-420.

Pant, D., Reynolds, L.P., Luther, J.S., Borowicz, P.P., Stenbak, T.M., Bilski, J.J., Weigl, R.M., Lopes, F., Petry, K., Johnson, M.L., Redmer, D.A., Grazul-Bilska, A.T., 2005. Expression of connexin 43 and gap junctional intercellular communication in the cumulus-oocyte complex in sheep. Reproduction 129, 191-200.

Parmegiani, L., Accorsi, A., Cognigni, G.E., Bernardi, S., Troilo, E., Filicori, M., 2010. Sterilization of liquid nitrogen with ultraviolet irradiation for safe vitrification of human oocytes or embryos. Fertility and sterility 94, 1525-1528.

Parmegiani, L., Cognigni, G., Bernardi, S., Cuomo, S., Ciampaglia, W., Infante, F., De Fatis, C.T., Arnone, A., Maccarini, A., Filicori, M., 2011. Efficiency of aseptic open vitrification and hermetical cryostorage of human oocytes. Reproductive biomedicine online 23, 505-512.

Patrizio, P., Bromer, J., Johnson, J., Martel, M., Silber, S., Arav, A., 2008. Cryopreservation of eleven whole human ovaries: histology, immunohistochemistry and technical details. Fertility and sterility 90, S38.

Pauli, A., Rinn, J.L., Schier, A.F., 2011. Non-coding RNAs as regulators of embryogenesis. Nature Reviews Genetics 12, 136.

Pavone, M.E., Innes, J., Hirshfeld-Cytron, J., Kazer, R., Zhang, J., 2011. Comparing thaw survival, implantation and live birth rates from cryopreserved zygotes, embryos and blastocysts. Journal of human reproductive sciences 4, 23-28.

Pegg, D., 1987. Mechanisms of freezing damage, Symposia of the Society for Experimental Biology, pp. 363-378.

Pegg, D.E., 2002. The History and Principles of Cryopreservation. Seminars in reproductive medicine 20, 005-014.

Pegg, D.E., 2007. Principles of cryopreservation. Methods in molecular biology 368, 39-57.

Pereira, R.M., Marques, C.C., 2008. Animal oocyte and embryo cryopreservation. Cell and Tissue Banking 9, 267-277.

Pfeifer, S., Butts, S., Dumesic, D., Fossum, G., Gracia, C., La Barbera, A., Mersereau, J., Odem, R., Paulson, R., Penzias, A., Pisarska, M., Rebar, R., Reindollar, R., Rosen, M., Sandlow, J., Vernon, M., Widra, E., 2016. Fertility drugs and cancer: a guideline. Fertility and sterility 106, 1617-1626.

Piekutowska-Abramczuk, D., Assouline, Z., Mataković, L., Feichtinger, R.G., Koňařiková, E., Jurkiewicz, E., Stawiński, P., Gusic, M., Koller, A., Pollak, A., Gasperowicz, P., Trubicka, J., Ciara, E., Iwanicka-Pronicka, K., Rokicki, D., Hanein, S., Wortmann, S.B., Sperl, W., Rötig, A., Prokisch, H., Pronicka, E., Płoski, R., Barcia, G., Mayr, J.A., 2018. NDUFB8 Mutations Cause Mitochondrial Complex I Deficiency in Individuals with Leigh-like Encephalomyopathy. American journal of human genetics 102, 460-467.

Pinkerton, J.H., Mc, K.D., Adams, E.C., Hertig, A.T., 1961. Development of the human ovary--a study using histochemical technics. Obstetrics and gynecology 18, 152-181.

Pokharel, K., Peippo, J., Honkatukia, M., Seppälä, A., Rautiainen, J., Ghanem, N., Hamama, T.M., Crowe, M.A., Andersson, M., Li, M.H., Kantanen, J., 2018. Integrated ovarian mRNA and miRNA transcriptome profiling characterizes the genetic basis of prolificacy traits in sheep (Ovis aries). BMC genomics 19, 104.

Polge, C., Smith, A.U., Parkes, A.S., 1949. Revival of spermatozoa after vitrification and dehydration at low temperatures. Nature 164, 666.

Porcu, E., 1999. Cycles of human oocyte cryopreservation and intracytoplasmic sperm injection: results of 112 cycles. Fertility and sterility 72, S2.

Porcu, E., Fabbri, R., Seracchioli, R., Ciotti, P.M., Magrini, O., Flamigni, C., 1997. Birth of a healthy female after intracytoplasmic sperm injection of cryopreserved human oocytes. Fertility and sterility 68, 724-726.

Potluri, P., Davila, A., Ruiz-Pesini, E., Mishmar, D., O'Hearn, S., Hancock, S., Simon, M., Scheffler, I.E., Wallace, D.C., Procaccio, V., 2009. A novel NDUFA1 mutation leads to a progressive mitochondrial complex I-specific neurodegenerative disease. Molecular genetics and metabolism 96, 189-195.

Practice Committee of American Society for Reproductive, M., 2019. Fertility preservation in patients undergoing gonadotoxic therapy or gonadectomy: a committee opinion. Fertility and sterility 112, 1022-1033.

Practice Committee of the American Society for Reproductive Medicine. Electronic address, a.a.o., 2021. Evidence-based outcomes after oocyte cryopreservation for donor oocyte in vitro fertilization and planned oocyte cryopreservation: a guideline. Fertility and sterility 116, 36-47.

Practice Committees of the American Society for Reproductive, M., the Society for Assisted Reproductive, T., 2013. Mature oocyte cryopreservation: a guideline. Fertility and sterility 99, 37-43.

Qiao, J., Wang, Z.-B., Feng, H.-L., Miao, Y.-L., Wang, Q., Yu, Y., Wei, Y.-C., Yan, J., Wang, W.-H., Shen, W., 2014. The root of reduced fertility in aged women and possible therapentic options: current status and future perspects. Molecular aspects of medicine 38, 54-85.

Quaresma, M., Coleman, M.P., Rachet, B., 2015. 40-year trends in an index of survival for all cancers combined and survival adjusted for age and sex for each cancer in England and Wales, 1971-2011: a population-based study. Lancet 385, 1206-1218.

Quinn, J.J., Chang, H.Y., 2016. Unique features of long non-coding RNA biogenesis and function. Nature reviews. Genetics 17, 47-62.

Qureshi, I.A., Mehler, M.F., 2012. Emerging roles of non-coding RNAs in brain evolution, development, plasticity and disease. Nature reviews. Neuroscience 13, 528-541.

Rahman, S.M.K., Uyama, T., Hussain, Z., Ueda, N., 2021. Roles of Endocannabinoids and Endocannabinoid-Like Molecules in Energy Homeostasis and Metabolic Regulation: A Nutritional Perspective. Annual review of nutrition 41, 177-202.

Rana, S., Gautam, S., Gahlawat, S., 2013. Cryobiological effects of cryoprotectants on morphology of cumulus oocyte complexes (COCs) of sheep using vitrification. 2277-4122.

Reddy, P., Liu, L., Adhikari, D., Jagarlamudi, K., Rajareddy, S., Shen, Y., Du, C., Tang, W., Hämäläinen, T., Peng, S.L., Lan, Z.J., Cooney, A.J., Huhtaniemi, I., Liu, K., 2008. Oocyte-specific deletion of Pten causes premature activation of the primordial follicle pool. Science 319, 611-613.

Renata Gaya Avelar, S., Ramos Moura, R., de Sousa, F., Pereira, A., Castro Almeida, K., Henrique Sousa Melo, C., Carlos Teles Filho, A., Gérard, B., Magalhães Melo, L., Teixeira, D., Freitas, V., 2012. Oocyte production and in vitro maturation in Canindé goats following hormonal ovarian stimulation. Animal reproduction 9, 2012.

Reyes, J.M., Ross, P.J., 2016. Cytoplasmic polyadenylation in mammalian oocyte maturation. Wiley interdisciplinary reviews. RNA 7, 71-89.

Reyes Palomares, A., Rodriguez-Wallberg, K.A., 2022. Update on the Epigenomic Implication of Embryo Cryopreservation Methods Applied in Assisted Reproductive Technologies With Potential Long-Term Health Effects. Frontiers in Cell and Developmental Biology Volume 10 - 2022.

Rienzi, L., Cobo, A., Paffoni, A., Scarduelli, C., Capalbo, A., Vajta, G., Remohí, J., Ragni, G., Ubaldi, F.M., 2012. Consistent and predictable delivery rates after oocyte vitrification: an observational longitudinal cohort multicentric study. Human reproduction 27, 1606-1612.

Rienzi, L., Gracia, C., Maggiulli, R., LaBarbera, A.R., Kaser, D.J., Ubaldi, F.M., Vanderpoel, S., Racowsky, C., 2016. Oocyte, embryo and blastocyst cryopreservation in ART: systematic review and meta-analysis comparing slow-freezing versus vitrification to produce evidence for the development of global guidance. Human reproduction update 23, 139-155.

Rienzi, L., Romano, S., Albricci, L., Maggiulli, R., Capalbo, A., Baroni, E., Colamaria, S., Sapienza, F., Ubaldi, F., 2010. Embryo development of fresh 'versus' vitrified metaphase II oocytes after ICSI: a prospective randomized sibling-oocyte study. Human reproduction 25, 66-73.

Rodgers, R.J., Irving-Rodgers, H.F., 2010. Formation of the ovarian follicular antrum and follicular fluid. Biology of reproduction 82, 1021-1029.

Rodrigues, A.Q., Picolo, V.L., Goulart, J.T., Silva, I.M.G., Ribeiro, R.B., Aguiar, B.A., Ferreira, Y.B., Oliveira, D.M., Lucci, C.M., de Bem, A.F., Paulini, F., 2021. Metabolic activity in cryopreserved and grafted ovarian tissue using high-resolution respirometry. Scientific reports 11, 21517.

Rodrıguez-González, E., Lopez-Bejar, M., Velilla, E., Paramio, M., 2002. Selection of prepubertal goat oocytes using the brilliant cresyl blue test. Theriogenology 57, 1397-1409.

Rooda, I., Hassan, J., Hao, J., Wagner, M., Moussaud-Lamodière, E., Jääger, K., Otala, M., Knuus, K., Lindskog, C., Papaikonomou, K., Gidlöf, S., Langenskiöld, C., Vogt, H., Frisk, P., Malmros, J., Tuuri, T., Salumets, A., Jahnukainen, K., Velthut-Meikas, A., Damdimopoulou, P., 2024. In-depth analysis of transcriptomes in ovarian cortical follicles from children and adults reveals interfollicular heterogeneity. Nature Communications 15, 6989.

Rosendahl, M., Greve, T., Andersen, C.Y., 2013. The safety of transplanting cryopreserved ovarian tissue in cancer patients: a review of the literature. Journal of assisted reproduction and genetics 30, 11-24.

Rudnicka, E., Kruszewska, J., Klicka, K., Kowalczyk, J., Grymowicz, M., Skórska, J., Pięta, W., Smolarczyk, R., 2018. Premature ovarian insufficiency - aetiopathology, epidemiology, and diagnostic evaluation. Przeglad menopauzalny = Menopause review 17, 105-108.

Russell, D.L., Gilchrist, R.B., Brown, H.M., Thompson, J.G., 2016. Bidirectional communication between cumulus cells and the oocyte: old hands and new players? Theriogenology 86, 62-68.

Russo, V., Martelli, A., Berardinelli, P., Di Giacinto, O., Bernabo, N., Fantasia, D., Mattioli, M., Barboni, B., 2007. Modifications in chromatin morphology and organization during sheep oogenesis. Microscopy research and technique 70, 733-744.

Sampaio da Silva, A.M., Bruno, J.B., de Lima, L.F., Ribeiro de Sá, N.A., Lunardi, F.O., Ferreira, A.C., Vieira Correia, H.H., de Aguiar, F.L., Araújo, V.R., Lobo, C.H., de Alencar Araripe Moura, A., Campello, C.C., Smitz, J., de Figueiredo, J.R., Ribeiro Rodrigues, A.P., 2016. Connexin 37 and 43 gene and protein expression and developmental competence of isolated ovine secondary follicles cultured in vitro after vitrification of ovarian tissue. Theriogenology 85, 1457-1467.

Santos, F., Dean, W., 2004. Epigenetic reprogramming during early development in mammals. Reproduction 127, 643-651.

Sathananthan, A.H., Trounson, A., Freeman, L., 1987. Morphology and fertilizability of frozen human oocytes. Gamete research 16, 343-354.

Sato, A., Otsu, E., Negishi, H., Utsunomiya, T., Arima, T., 2007. Aberrant DNA methylation of imprinted loci in superovulated oocytes. Human reproduction 22, 26-35.

Sauvat, F., Capito, C., Sarnacki, S., Poirot, C., Bachelot, A., Meduri, G., Dandolo, L., Binart, N., 2008. Immature cryopreserved ovary restores puberty and fertility in mice without alteration of epigenetic marks. PloS one 3, e1972.

Schuster, T.G., Keller, L.M., Dunn, R.L., Ohl, D.A., Smith, G.D., 2003. Ultra-rapid freezing of very low numbers of sperm using cryoloops. Human reproduction 18, 788-795.

Segino, M., Ikeda, M., Hirahara, F., Sato, K., 2005. In vitro follicular development of cryopreserved mouse ovarian tissue. Reproduction 130, 187-192.

Sendžikaitė, G., Kelsey, G., 2019. The role and mechanisms of DNA methylation in the oocyte. Essays in biochemistry 63, 691-705.

Senturk, E., Manfredi, J.J., 2013. p53 and cell cycle effects after DNA damage. Methods in molecular biology 962, 49-61.

Shao, T., Ke, H., Liu, R., Xu, L., Han, S., Zhang, X., Dang, Y., Jiao, X., Li, W., Chen, Z.J., Qin, Y., Zhao, S., 2022. Autophagy regulates differentiation of ovarian granulosa cells through degradation of WT1. Autophagy 18, 1864-1878.

Shapira, M., Dolmans, M.-M., Silber, S., Meirow, D., 2020. Evaluation of ovarian tissue transplantation: results from three clinical centers. Fertility and sterility 114, 388-397.

Sharara, F.I., Seifer, D.B., Flaws, J.A., 1998. Environmental toxicants and female reproduction 44Additional references are available from the authors. Fertility and sterility 70, 613-622.

Shen, H.P., Ding, C.M., Chi, Z.Y., Kang, Z.Z., Tan, W.S., 2003. [Effects of different cooling rates on cryopreservation of hematopoietic stem cells from cord blood]. Sheng Wu Gong Cheng Xue Bao 19, 489-492.

Siegel, R., Naishadham, D., Jemal, A., 2012. Cancer statistics, 2012. CA: a cancer journal for clinicians 62, 10-29.

Silber, S.J., Grudzinskas, G., Gosden, R.G., 2008. Successful pregnancy after microsurgical transplantation of an intact ovary. New England Journal of Medicine 359, 2617-2618.

Simon, A.M., Chen, H., Jackson, C.L., 2006. Cx37 and Cx43 localize to zona pellucida in mouse ovarian follicles. Cell communication & adhesion 13, 61-77.

Simon, L.E., Kumar, T.R., Duncan, F.E., 2020. In vitro ovarian follicle growth: a comprehensive analysis of key protocol variables†. Biology of reproduction 103, 455-470.

Skinner, M.K., 2005. Regulation of primordial follicle assembly and development. Human reproduction update 11, 461-471.

Smith, G.D., Serafini, P.C., Fioravanti, J., Yadid, I., Coslovsky, M., Hassun, P., Alegretti, J.R., Motta, E.L., 2010. Prospective randomized comparison of human oocyte cryopreservation with slow-rate freezing or vitrification. Fertility and sterility 94, 2088-2095.

Söhl, G., Willecke, K., 2004. Gap junctions and the connexin protein family. Cardiovascular research 62, 228-232.

Spinaci, M., Vallorani, C., Bucci, D., Tamanini, C., Porcu, E., Galeati, G., 2012. Vitrification of pig oocytes induces changes in histone H4 acetylation and histone H3 lysine 9 methylation (H3K9). Veterinary research communications 36, 165-171.

Stachecki, J.J., Cohen, J., 2004. An overview of oocyte cryopreservation. Reproductive biomedicine online 9, 152-163.

Stachecki, J.J., Munné, S., Cohen, J., 2004. Spindle organization after cryopreservation of mouse, human, and bovine oocytes. Reproductive biomedicine online 8, 664-672.

Stachowiak, E.M., Papis, K., Kruszewski, M., Iwanenko, T., Bartlomiejczyk, T., Modlinski, J.A., 2009. Comparison of the level(s) of DNA damage using Comet assay in bovine oocytes subjected to selected vitrification methods. Reproduction in domestic animals = Zuchthygiene 44, 653-658.

Stoop, D., Cobo, A., Silber, S., 2014. Fertility preservation for age-related fertility decline. Lancet 384, 1311-1319.

Stoop, D., De Munck, N., Jansen, E., Platteau, P., Van den Abbeel, E., Verheyen, G., Devroey, P., 2012. Clinical validation of a closed vitrification system in an oocyte-donation programme. Reproductive biomedicine online 24, 180-185.

Strączyńska, P., Papis, K., Morawiec, E., Czerwiński, M., Gajewski, Z., Olejek, A., Bednarska-Czerwińska, A., 2022. Signaling mechanisms and their regulation during in vivo or in vitro maturation of mammalian oocytes. Reproductive biology and endocrinology : RB&E 20, 37.

Stringer, J.M., Alesi, L.R., Winship, A.L., Hutt, K.J., 2023. Beyond apoptosis: evidence of other regulated cell death pathways in the ovary throughout development and life. Human reproduction update 29, 434-456.

Sun, Y., Sun, X., Dyce, P., Shen, W., Chen, H., 2017. The role of germ cell loss during primordial follicle assembly: a review of current advances. International Journal of Biological Sciences, 449-457.

Sung, H., Ferlay, J., Siegel, R.L., Laversanne, M., Soerjomataram, I., Jemal, A., Bray, F., 2021. Global Cancer Statistics 2020: GLOBOCAN Estimates of Incidence and Mortality Worldwide for 36 Cancers in 185 Countries. CA: a cancer journal for clinicians 71, 209-249.

Sunkara, S.K., Siozos, A., Bolton, V.N., Khalaf, Y., Braude, P.R., El-Toukhy, T., 2010. The influence of delayed blastocyst formation on the outcome of frozen-thawed blastocyst transfer: a systematic review and meta-analysis. Human reproduction 25, 1906-1915.

Suo, L., Meng, Q., Pei, Y., Fu, X., Wang, Y., Bunch, T.D., Zhu, S., 2010. Effect of cryopreservation on acetylation patterns of lysine 12 of histone H4 (acH4K12) in mouse oocytes and zygotes. Journal of assisted reproduction and genetics 27, 735-741.

Szell, A.Z., Bierbaum, R.C., Hazelrigg, W.B., Chetkowski, R.J., 2013. Live births from frozen human semen stored for 40 years. Journal of assisted reproduction and genetics 30, 743-744.

Szurek, E.A., Eroglu, A., 2011. Comparison and avoidance of toxicity of penetrating cryoprotectants. PloS one 6, e27604.

Talukder, M., Iqbal, A., Khandoker, M.A.M., Zahangir Alam, M., 2011. Collection grading and evaluation of cumulus-oocyte-complexes for in vitro maturation in sheep. Bangladesh Veterinarian 28.

Tanpradit, N., Comizzoli, P., Srisuwatanasagul, S., Chatdarong, K., 2015. Positive impact of sucrose supplementation during slow freezing of cat ovarian tissues on cellular viability, follicle morphology, and DNA integrity. Theriogenology 83, 1553-1561.

Teilmann, S.C., 2005. Differential expression and localisation of connexin-37 and connexin-43 in follicles of different stages in the 4-week-old mouse ovary, Molecular and cellular endocrinology, 1-2 ed, pp. 27-35.

Terren, C., Fransolet, M., Ancion, M., Nisolle, M., Munaut, C., 2019. Slow freezing versus vitrification of mouse ovaries: from ex vivo analyses to successful pregnancies after auto-transplantation. Scientific reports 9, 19668.

Torre, A., Vertu-Ciolino, D., Mazoyer, C., Selva, J., Lornage, J., Salle, B., 2016a. Safeguarding Fertility With Whole Ovary Cryopreservation and Microvascular Transplantation: Higher Follicular Survival With Vitrification Than With Slow Freezing in a Ewe Model. Transplantation 100, 1889-1897.

Torre, L.A., Siegel, R.L., Ward, E.M., Jemal, A., 2016b. Global Cancer Incidence and Mortality Rates and Trends--An Update. Cancer epidemiology, biomarkers & prevention : a publication of the American Association for Cancer Research, cosponsored by the American Society of Preventive Oncology 25, 16-27.

Trapphoff, T., El Hajj, N., Zechner, U., Haaf, T., Eichenlaub-Ritter, U., 2010. DNA integrity, growth pattern, spindle formation, chromosomal constitution and imprinting patterns of mouse oocytes from vitrified pre-antral follicles. Human reproduction 25, 3025-3042.

Ubaldi, F., Anniballo, R., Romano, S., Baroni, E., Albricci, L., Colamaria, S., Capalbo, A., Sapienza, F., Vajta, G., Rienzi, L., 2010. Cumulative ongoing pregnancy rate achieved with oocyte vitrification and cleavage stage transfer without embryo selection in a standard infertility program. Human reproduction 25, 1199-1205.

Urrego, R., Rodriguez-Osorio, N., Niemann, H., 2014. Epigenetic disorders and altered gene expression after use of Assisted Reproductive Technologies in domestic cattle. Epigenetics 9, 803-815.

Vainio, S., Heikkilä, M., Kispert, A., Chin, N., McMahon, A.P., 1999. Female development in mammals is regulated by Wnt-4 signalling. Nature 397, 405-409.

Vajta, G., Rienzi, L., Ubaldi, F.M., 2015. Open versus closed systems for vitrification of human oocytes and embryos. Reproductive biomedicine online 30, 325-333.

Van der Ven, H., Liebenthron, J., Beckmann, M., Toth, B., Korell, M., Krüssel, J., Frambach, T., Kupka, M., Hohl, M.K., Winkler-Crepaz, K., Seitz, S., Dogan, A., Griesinger, G., Häberlin, F., Henes, M., Schwab, R., Sütterlin, M., von Wolff, M., Dittrich, R., 2016a. Ninety-five orthotopic transplantations in 74 women of ovarian tissue after cytotoxic treatment in a fertility preservation network: tissue activity, pregnancy and delivery rates. Human reproduction 31, 2031-2041.

Van der Ven, H., Liebenthron, J., Beckmann, M., Toth, B., Korell, M., Krussel, J., Frambach, T., Kupka, M., Hohl, M.K., Winkler-Crepaz, K., Seitz, S., Dogan, A., Griesinger, G., Haberlin, F., Henes, M., Schwab, R., Sutterlin, M., von Wolff, M., Dittrich, R., Ferti, P.n., 2016b. Ninety-five orthotopic transplantations in 74 women of ovarian tissue after cytotoxic treatment in a fertility preservation network: tissue activity, pregnancy and delivery rates. Human reproduction 31, 2031-2041.

Veitch, G.I., Gittens, J.E., Shao, Q., Laird, D.W., Kidder, G.M., 2004. Selective assembly of connexin37 into heterocellular gap junctions at the oocyte/granulosa cell interface. J Cell Sci 117, 2699-2707.

Vermeulen, M., Giudice, M.G., Del Vento, F., Wyns, C., 2019. Role of stem cells in fertility preservation: current insights. Stem cells and cloning : advances and applications 12, 27-48.

Vincent, C., Johnson, M.H., 1992. Cooling, cryoprotectants, and the cytoskeleton of the mammalian oocyte. Oxford reviews of reproductive biology 14, 73-100.

Vitale, F., Dolmans, M.-M., 2024. Comprehensive Review of In Vitro Human Follicle Development for Fertility Restoration: Recent Achievements, Current Challenges, and Future Optimization Strategies. Journal of clinical medicine 13, 1791.

Vozzi, C., Formenton, A., Chanson, A., Senn, A., Sahli, R., Shaw, P., Nicod, P., Germond, M., Haefliger, J.A., 2001. Involvement of connexin 43 in meiotic maturation of bovine oocytes. Reproduction 122, 619-628.

Walker, Z., Lanes, A., Ginsburg, E., 2022. Oocyte cryopreservation review: outcomes of medical oocyte cryopreservation and planned oocyte cryopreservation. Reproductive Biology and Endocrinology 20, 10.

Wallace, W.H., Kelsey, T.W., 2010. Human ovarian reserve from conception to the menopause. PloS one 5, e8772.

Wallin, A., Ghahremani, M., Dahm-Kähler, P., Brännström, M., 2009. Viability and function of the cryopreserved whole ovary: in vitro studies in the sheep. Human reproduction 24, 1684-1694.

Wang, H.-Y., Li, Y.-H., Sun, L., Gao, X., You, L., Wang, Y., Ma, J.-L., Chen, Z.-J., 2013. Allotransplantation of cryopreserved prepubertal mouse ovaries restored puberty and fertility without affecting methylation profile of Snrpn-DMR. Fertility and sterility 99, 241-247.e244.

Wang, X., Pepling, M.E., 2021. Regulation of Meiotic Prophase One in Mammalian Oocytes. Frontiers in Cell and Developmental Biology 9.

Wang, Y., Yang, R., Zhang, B., Zhang, Y., Zhao, Y., Jiang, D., Mao, Y., Tang, B., Zhang, X., 2025. Advances in mammalian ovarian tissue cryopreservation. Animals and Zoonoses.

Wang, Y., Zhang, M.-l., Zhao, L.-w., Kuang, Y.-p., Xue, S.-g., 2018. Enhancement of the efficiency of oocyte vitrification through regulation of histone deacetylase 6 expression. Journal of assisted reproduction and genetics 35, 1179-1185.

Ward, E.J., Parsons, K., Holmes, E.E., Balcomb, K.C., 3rd, Ford, J.K., 2009. The role of menopause and reproductive senescence in a long-lived social mammal. Frontiers in zoology 6, 4.

Wear, H.M., McPike, M.J., Watanabe, K.H., 2016. From primordial germ cells to primordial follicles: a review and visual representation of early ovarian development in mice. Journal of ovarian research 9, 36.

Webber, L., Davies, M., Anderson, R., Bartlett, J., Braat, D., Cartwright, B., Cifkova, R., de Muinck Keizer-Schrama, S., Hogervorst, E., Janse, F., 2016. European Society for Human Reproduction and Embryology (ESHRE) Guideline Group on POI. ESHRE Guideline: management of women with premature ovarian insufficiency. Human reproduction 31, 926-937.

Westphal, J.R., Gerritse, R., Braat, D.D.M., Beerendonk, C.C.M., Peek, R., 2017. Complete protection against cryodamage of cryopreserved whole bovine and human ovaries using DMSO as a cryoprotectant. Journal of assisted reproduction and genetics 34, 1217-1229.

Whaley, D., Damyar, K., Witek, R.P., Mendoza, A., Alexander, M., Lakey, J.R., 2021. Cryopreservation: An Overview of Principles and Cell-Specific Considerations. Cell transplantation 30, 963689721999617.

Wigglesworth, K., Lee, K.B., O'Brien, M.J., Peng, J., Matzuk, M.M., Eppig, J.J., 2013. Bidirectional communication between oocytes and ovarian follicular somatic cells is required for meiotic arrest of mammalian oocytes. Proceedings of the National Academy of Sciences of the United States of America 110, E3723-E3729.

Winkler, I., Goncalves, A., 2023. Do mammals have menopause? Cell 186, 4729-4733.

Wongsrikeao, P., Otoi, T., Yamasaki, H., Agung, B., Taniguchi, M., Naoi, H., Shimizu, R., Nagai, T., 2006. Effects of single and double exposure to brilliant cresyl blue on the selection of porcine oocytes for in vitro production of embryos. Theriogenology 66, 366-372.

Wood, T.C., Wildt, D.E., 1997. Effect of the quality of the cumulus-oocyte complex in the domestic cat on the ability of oocytes to mature, fertilize and develop into blastocysts in vitro. Journal of reproduction and fertility 110, 355-360.

Woods, E.J., Benson, J.D., Agca, Y., Critser, J.K., 2004. Fundamental cryobiology of reproductive cells and tissues. Cryobiology 48, 146-156.

Wu, C., Morris, J.R., 2001. Genes, genetics, and epigenetics: a correspondence. Science 293, 1103-1105.

Wu, M., Tang, W., Chen, Y., Xue, L., Dai, J., Li, Y., Zhu, X., Wu, C., Xiong, J., Zhang, J., Wu, T., Zhou, S., Chen, D., Sun, C., Yu, J., Li, H., Guo, Y., Huang, Y., Zhu, Q., Wei, S., Zhou, Z., Wu, M., Li, Y., Xiang, T., Qiao, H., Wang, S., 2024. Spatiotemporal transcriptomic changes of human ovarian aging and the regulatory role of FOXP1. Nature Aging 4, 527-545.

Xian, Y., Li, B., Pan, P., Wang, Y., Pei, X., Yang, Y., 2018. Role of Autophagy in Ovarian Cryopreservation by Vitrification. Cryo letters 39, 201-210.

Xiao, Z., Wang, Y., Li, L.L., Li, S.W., 2013. In vitro culture thawed human ovarian tissue: NIV versus slow freezing method. Cryo letters 34, 520-526.

Yan, J., Zhang, L., Wang, T., Li, R., Liu, P., Yan, L., Qiao, J., 2014. Effect of vitrification at the germinal vesicle stage on the global methylation status in mouse oocytes subsequently matured in vitro. Chinese medical journal 127, 4019-4024.

Yan, Z., Li, Q., Zhang, L., Kang, B., Fan, W., Deng, T., Zhu, J., Wang, Y., 2020. The growth and development conditions in mouse offspring derived from ovarian tissue cryopreservation and orthotopic transplantation. Journal of assisted reproduction and genetics 37, 923-932.

Yang, Y., Cheung, H.H., Law, W.N., Zhang, C., Chan, W.Y., Pei, X., Wang, Y., 2016. New Insights into the Role of Autophagy in Ovarian Cryopreservation by Vitrification. Biology of reproduction 94, 137.

Yao, X., Liu, W., Xie, Y., Xi, M., Xiao, L., 2023. Fertility loss: negative effects of environmental toxicants on oogenesis. Frontiers in Physiology 14.

Yodrug, T., Parnpai, R., Hirao, Y., Somfai, T., 2021. Effect of vitrification at different meiotic stages on epigenetic characteristics of bovine oocytes and subsequently developing embryos. Animal Science Journal 92, e13596.

Yong, K.W., Laouar, L., Elliott, J.A.W., Jomha, N.M., 2020. Review of non-permeating cryoprotectants as supplements for vitrification of mammalian tissues. Cryobiology 96, 1-11.

Younis, A.I., Toner, M., Albertini, D.F., Biggers, J.D., 1996. Cryobiology of non-human primate oocytes. Human reproduction 11, 156-165.

Zeilmaker, G.H., Alberda, A.T., van Gent, I., Rijkmans, C.M.P.M., Drogendijk, A.C., 1984. Two pregnancies following transfer of intact frozen-thawed embryos. Fertility and sterility 42, 293-296.

Zenzes, M.T., Bielecki, R., Casper, R.F., Leibo, S.P., 2001. Effects of chilling to 0 degrees C on the morphology of meiotic spindles in human metaphase II oocytes. Fertility and sterility 75, 769-777.

Zhang, D., Ren, L., Chen, G.Q., Zhang, J., Reed, B.M., Shen, X.H., 2015. ROS-induced oxidative stress and apoptosis-like event directly affect the cell viability of cryopreserved embryogenic callus in Agapanthus praecox. Plant cell reports 34, 1499-1513.

Zhang, J., Hao, L., Wei, Q., Zhang, S., Cheng, H., Zhai, Y., Jiang, Y., An, X., Li, Z., Zhang, X., Tang, B., 2020. TET3 overexpression facilitates DNA reprogramming and early development of bovine SCNT embryos. Reproduction 160, 379-391.

Zhang, J., Liu, J., Xu, K., Liu, B., DiMattina, M., 1995. Extracorporeal development and ultrarapid freezing of human fetal ova. Journal of assisted reproduction and genetics 12, 361-368.

Zhang, L., Xue, X., Yan, J., Yan, L.Y., Jin, X.H., Zhu, X.H., He, Z.Z., Liu, J., Li, R., Qiao, J., 2016. Cryobiological Characteristics of L-proline in Mammalian Oocyte Cryopreservation. Chinese medical journal 129, 1963-1968.

Zhang, T., He, M., Zhang, J., Tong, Y., Chen, T., Wang, C., Pan, W., Xiao, Z., 2023. Mechanisms of primordial follicle activation and new pregnancy opportunity for premature ovarian failure patients. Frontiers in Physiology 14.

Zhao, X.M., Ren, J.J., Du, W.H., Hao, H.S., Wang, D., Qin, T., Liu, Y., Zhu, H.B., 2013. Effect of vitrification on promoter CpG island methylation patterns and expression levels of DNA methyltransferase 1o, histone acetyltransferase 1, and deacetylase 1 in metaphase II mouse oocytes. Fertility and sterility 100, 256-261.

Zhou, X., Yan, B., Xu, X., Yu, X.-L., Fu, X.-F., Cai, Y.-F., Xu, Y.-Y., Tang, Y.-G., Zhang, X.-Z., Wang, H.-Y., 2020. Risk and mechanism of glucose metabolism disorder in the offspring conceived by female fertility maintenance technology. Cryobiology 96, 68-75.

Zhou, X.H., Zhang, D., Shi, J., Wu, Y.J., 2016. Comparison of vitrification and conventional slow freezing for cryopreservation of ovarian tissue with respect to the number of intact primordial follicles: A meta-analysis. Medicine 95, e4095.

Zhu, J., Moawad, A.R., Wang, C.Y., Li, H.F., Ren, J.Y., Dai, Y.F., 2018. Advances in in vitro production of sheep embryos. International journal of veterinary science and medicine 6, S15-S26.

Zuccotti, M., Piccinelli, A., Giorgi Rossi, P., Garagna, S., Redi, C.A., 1995. Chromatin organization during mouse oocyte growth. Molecular reproduction and development 41, 479-485.

Zuccotti, M., Ponce, R.H., Boiani, M., Guizzardi, S., Govoni, P., Scandroglio, R., Garagna, S., Redi, C.A., 2002. The analysis of chromatin organisation allows selection of mouse antral oocytes competent for development to blastocyst. Zygote 10, 73-78.

Online sources

UniProt Available at: www.uniprot.org

Webgestalt Available at: www. https://www.webgestalt.org

APPENDICES

A. Studies of transplantation of cryopreserved whole ovaries in animal models

Species	Freezing Technique	Follow - up	Outcome
R*at*	Slow freezing	≥60 days	• 4/7 (57%) resumed estrous cycles after 12 - 2.5 days • 1/7 (14.3%) conceived, but no live birth • Follicle counts (baseline vs. postgrafting): ($p < 0.01$)
Rabbit	Slow freezing	6 months	• 10/12 (83.3%) resumed ovarian function after 1 week • No IVF attempts • Follicle counts (baseline vs. postgrafting): &(18.68 _ 3.86 vs. 13.99 _ 3.21; $p < 0.0001$)
R*at*	Slow freezing	≥42 days	• 8/10 (80%) resumed estrous cycles after 14 _ 3 days • 2/10 (20%) conceived • Follicle counts: not mentioned
R*at*	Slow freezing	8 months	• 5/25 (20%) died from early postoperative complications (infection/anastomotic thrombosis) 14/20 (80%) resumed estrous cycles after 14 _ 3 days • 4/20 (20%) conceived, yielding healthy offspring + second and third generations of rats from the initial offspring • Follicle counts: ($p < 0.05$)
Sheep	Slow freezing	8–10 days	• 11/11 (100%) immediate vascular patency • 3/11 (27%) maintained vascular patency after 8–10 days • Follicle counts (patent vs. non-patent): (3.67 _ 2.08 vs. 0.250 _ 0.463; $p = 0.001$)

Directional freezing	6 years	• 5/8 (62.5%) immediate vascular patency!3/8 failure due to venous thrombosis (n = 1), torn artery (n = 1) and unknown reason (n = 1) • 3/8 (37.5%) resumed P cyclicity 34 to 69 weeks after transplantation; 2/8 (25%): oocyte aspiration + embryo development up to the 8-cell stage • 2/8 (25%) maintained ovarian function for up to 3 years and 1/8 (12.5%) for up to 6 years
Slow freezing	18–19 months	• 6/8 (75%) long-term vascular patency • 4/8 (50%) resumed ovarian function 6 months after transplantation and P cyclicity resumed 12–14 months postgrafting • 1/8 (12.5%) spontaneous pregnancy yielding healthy offspring • Follicle survival rate: 1.7–7.6%
Slow freezing	8–10 days	• Successful vascular patency after 8–10 days: • 5/8 with end-to-end anastomosis (WOCT = 3/6; fresh = 2/2) 2/6 with end-to-side anastomosis (WOCT = 1/4; fresh = 1/2) • 0/7 with fish-mouth anastomosis (WOCT = 0/5; fresh = 0/2)
Slow freezing	5 months	• 2/8 (25%) resumed ovarian function • No information on maintained vascular patency 3 COCs obtained after FSH stimulation; 2 developed to metaphase II after in vitro maturation, but no fertilization
Vitrification	12 months	• 1/5 (20%) long-term vascular patency!4/5 failure due to lumbo-ovarian pedicle thrombosis (n = 2), arterial thrombosis (n = 1) and pneumopathy (n = 1) (pedicle non-analyzable) • 1/5 (20%) resumed ovarian function 6 months after transplantation • Follicle counts: total follicle loss
Slow freezing	7 months	• 7/8 (87.5%) immediate and long-term vascular patency (In 1 case = freezing device malfunction excluded from further analysis) • 3/7 (42.9%) resumed ovarian cyclicity • Follicles (pregrafting vs. postgrafting): (36.7 _ 5.7 vs. 2.3 _ 1.0; $p < 0.05$)

Slow freezing	7 days	• 4/4 (100%) immediate vascular patency • 1/4 (25%) vascular patency at degrafting. 3/4 (75%): arterial thrombosis + FMS extravasation in the medulla • Follicle density (pregrafting vs. postgrafting): (0.42 vs. 0.02; $p < 0.001$)
Slow freezing	3 months	• 15/15 (100%) immediate vascular patency • 4/15 (27%) restored ovarian function within 7 weeks of transplantation • Follicle density within the functioning ovary (pregrafting vs. postgrafting): (2.48 _ 0.98 vs. 1.43 _ 0.10)
Slow freezing	11–23 months	• 14/14 (100%) immediate and long-term vascular patency • 14/14 (100%) restored ovarian function within 3 weeks of transplantation • 9/14 (64%) pregnancies + 4/14 (29%) and healthy live births. One offspring gave birth to second-generation lambs • Follicle survival rate: 60–70%
Slow freezing vs Vitrification	3 years	• 6/6 (100%) immediate vascular patency with slow freezing vs. 67% (4/6) with vitrification (1 death occurred in both groups) • 5/5 slow freezing + 6/6 vitrification (100%): restored hormone production • 1/5 (20%) pregnancy and live birth of healthy offspring in the slow-frozen group. No pregnancy in the vitrified group • Follicle survival rates (slow freezing vs. vitrification): 0.017% 0.019% vs.0.3% 0.5% ($p = 0.047$)

B. Top genes generated by Partek (p<0.05)

Gene Symbol	p-value(W vs. C)	Fold-Change(W vs. C)
LOC101106730	0.0207254	-2.12201
LOC105602036	0.0148673	-1.90741
LOC101105010	0.0340058	-1.83304
LOC101105099	0.0199883	-1.81844
GUCY2C	0.0459845	-1.80881
LOC105605488	0.00459671	-1.79213
TMEM107	0.0178447	-1.76399
MAP10	0.00212783	-1.73789
SPAG16	0.0152463	-1.72632
C8orf4	0.0430532	-1.71664
ZNF140	0.0248459	-1.68775
ZNF557	0.0268985	-1.68082
GRM8	0.0209547	-1.67841
ELOVL2	0.0433671	-1.66313
ZNF791	0.00290661	-1.66033
GRM7	0.00241864	-1.65675
PPP2R2B	0.0296415	-1.65561
GRM8	0.0325696	-1.65218
MORN4	0.0287718	-1.6476
ZNF227	0.00223579	-1.63644
METTL17	0.000390658	-1.63314
WNT4	0.049045	-1.63232
TARSL2	0.0232422	-1.63077
LOC101120540	0.0394126	-1.62553
LOC101104852	0.026088	-1.62261
LOC105615374	0.0173605	-1.61568
PPP1R36	0.0207185	-1.60504
ATP6V0A1	0.00707077	-1.60236
TCTA	0.0120723	-1.60122
ABO	0.00329133	-1.58553
LOC101109476	0.0258664	-1.58199
ENO2	0.00300704	-1.57937
HSD17B7	0.0054651	-1.55428
BBS10	0.0439486	-1.55338
ZNF740	0.00664773	-1.54231
ZSCAN12	0.0196612	-1.54152
GRID1	0.0226529	-1.53921
RAB30	0.000604548	-1.53645
BCDIN3D	0.0155026	-1.53022
SVIP	0.0191091	-1.52634
PEX11B	0.000685382	-1.52206
CXXC4	0.0271192	-1.51998

LOC101116975	0.0220453	-1.51834
LOC101113086	0.0475331	-1.51464
ATP6V1G2	0.0329886	-1.5145
PLAGL2	0.00323498	-1.5122
IVD	0.00428835	-1.51178
METTL16	0.00161142	-1.51165
TMEM194A	0.0367988	-1.51114
THNSL1	0.0116055	-1.51049
TMEM116	0.0267399	-1.50406
ATP2B1	0.0233162	-1.50245
ZNF420	0.00768098	-1.50116
TXNL4B	0.00473575	-1.50107
STC2	0.0367711	1.50638
A4GALT	0.00971803	1.5136
LOC101102980	0.00367322	1.5279
PLSCR5	0.0412175	1.52954
SPEF1	0.00380952	1.53133
ARPC3	0.0134874	1.53351
SH3BGRL2	0.00119156	1.5337
LOC105611350	0.0192854	1.53562
PPP1R14B	0.0214687	1.53862
VDAC1	0.0203801	1.5435
LOC105603084	0.0185936	1.54704
UQCRFS1	0.00457315	1.54807
BAX	0.0180401	1.54833
KIAA1683	0.0368823	1.55782
MRPL40	0.00976081	1.55998
SSR4	0.0316592	1.56154
LOC101111518	0.0250951	1.56446
E2F3	0.0169301	1.57073
LAMTOR2	0.0131443	1.57423
IRX3	0.00706677	1.57573
LOC101118794	0.029485	1.57767
RCN1	0.0316488	1.57975
FABP3	0.00834416	1.59061
DUSP15	0.0138141	1.59845
RPL22L1	0.00412841	1.61499
NDUFA5	0.0395569	1.62502
NDUFB1	0.0249988	1.63446
DBI	0.012028	1.64853
LOC101102454	0.0406744	1.66067
SPAG7	0.0236884	1.6813
HSPB3	0.0166714	1.69597
COL16A1	0.000694092	1.69646
LOC101112402	0.0285667	1.70379
KIF20A	0.0405405	1.70834
SNRPG	0.00567543	1.71313
BMP1	0.0332014	1.72333

TNNI2	0.00694552	1.76544
HECW2	0.0287626	1.76573
TNNI3	0.00519885	1.80219
ABRACL	0.04358	1.81969
NDUFA4	0.000360271	1.82542
LOC101101998	0.0404999	1.82601
CMKLR1	0.00204717	1.84235
KIF23	0.0365799	1.92131
LOC101117112	0.0400169	2.00621
SERTM1	0.000185426	2.01032
LOC101113893	0.0119239	2.03347
LGALS1	0.0160801	2.03666
MYL6	0.00490551	2.03784
SELP	0.0353127	2.09221
ARHGAP11A	0.0287132	2.20971
DIAPH3	0.00794464	2.30179
SLC16A7	0.0445335	2.33454
LOC101118739	0.0409766	2.3631
COL1A1	0.0261244	2.47186
ANLN	0.020005	2.63938
MSMB	0.0459136	3.0461
STAR	0.0069552	3.61612
ANGPTL5	0.0198456	5.58034

C. Ancestor Chart

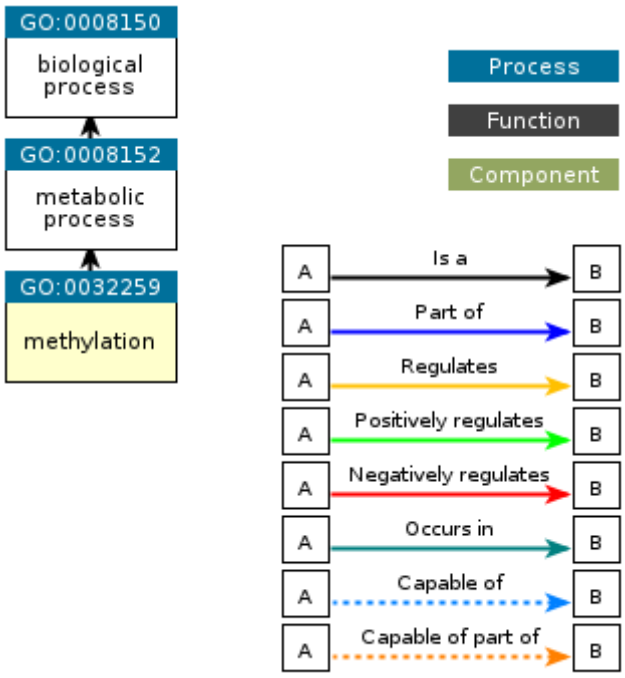

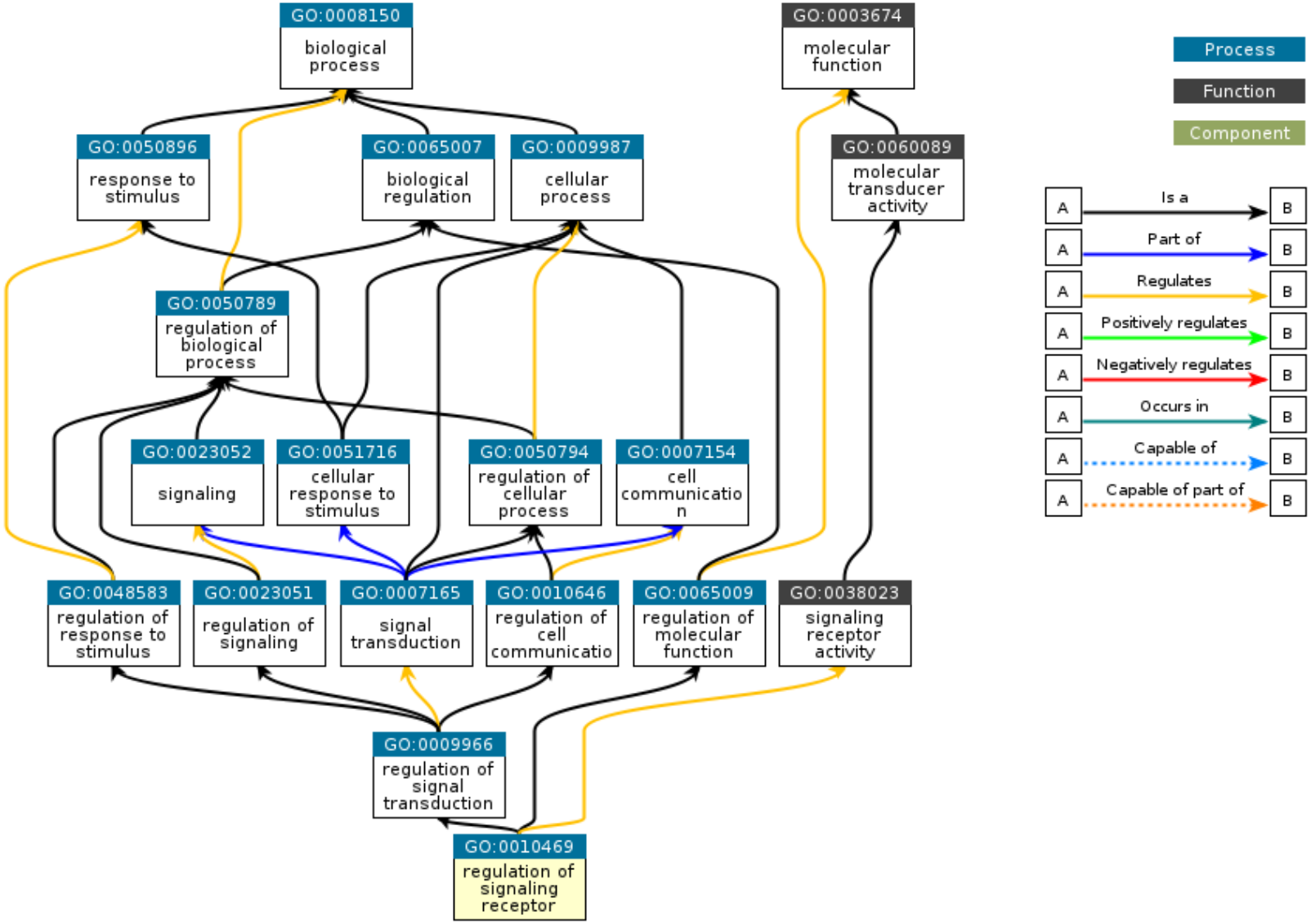
GO:0008150
biological process
GO:0003674
molecular function
Process
Function
Component
GO:0050896
response to stimulus
GO:0065007
biological regulation
GO:0009987
cellular process
GO:0060089
molecular transducer activity
A
Is a
B
A
Part of
B
A
Regulates
B
A
Positively regulates
B
A
Negatively regulates
B
A
Occurs in
B
A
Capable of
B
A
Capable of part of
B
GO:0050789
regulation of biological process
GO:0023052
signaling
GO:0051716
cellular response to stimulus
GO:0050794
regulation of cellular process
GO:0007154
cell communicatio n
GO:0048583
regulation of response to stimulus
GO:0023051
regulation of signaling
GO:0007165
signal transduction
GO:0010646
regulation of cell communicatio
GO:0065009
regulation of molecular function
GO:0038023
signaling receptor activity
GO:0009966
regulation of signal transduction
GO:0010469
regulation of signaling receptor

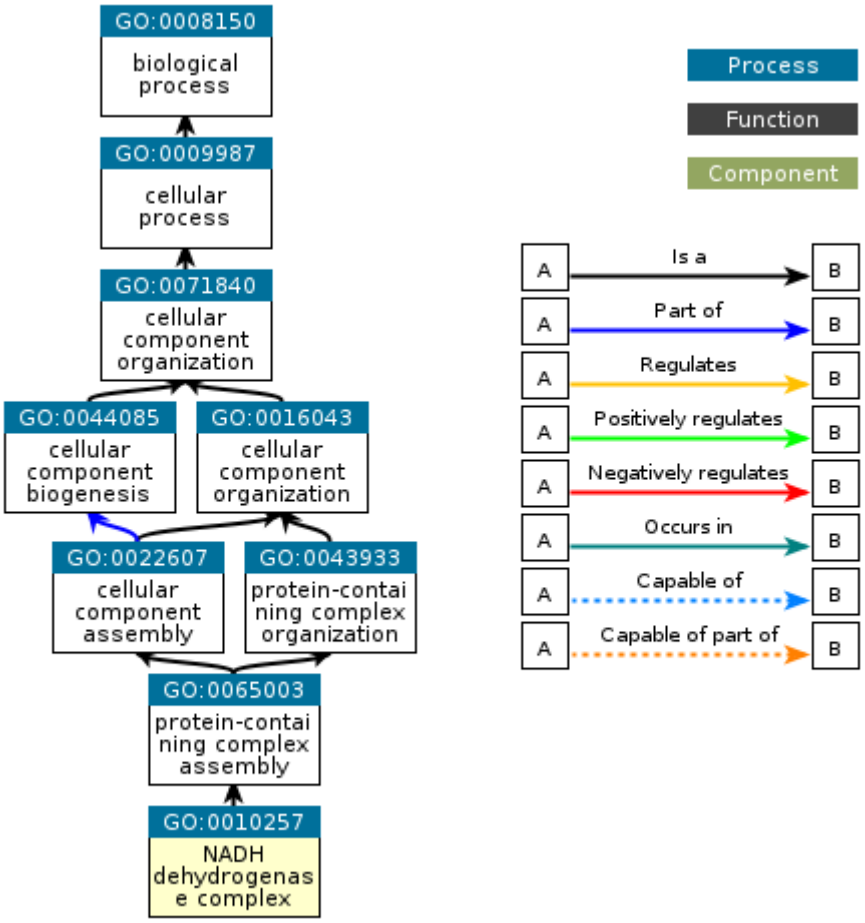
GO:0008150
biological process
GO:0009987
cellular process
GO:0071840
cellular component organization
GO:0044085
cellular component biogenesis
GO:0016043
cellular component organization
GO:0022607
cellular component assembly
GO:0043933
protein-containing complex organization
GO:0065003
protein-containing complex assembly
GO:0010257
NADH dehydrogenase complex
Process
Function
Component
A
Is a
B
A
Part of
B
A
Regulates
B
A
Positively regulates
B
A
Negatively regulates
B
A
Occurs in
B
A
Capable of
B
A
Capable of part of
B

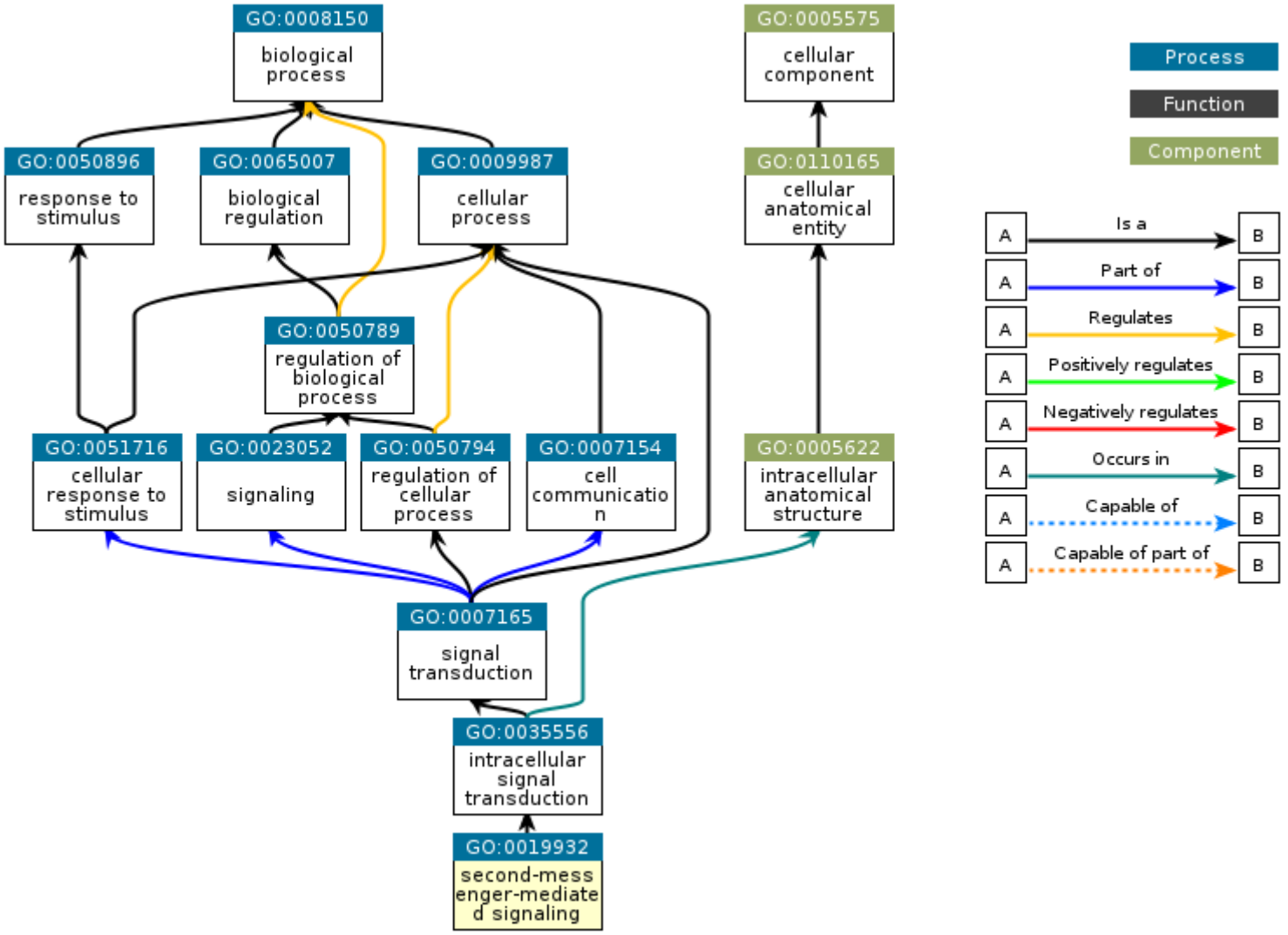
GO:0008150
biological process
GO:0005575
cellular component
Process
Function
Component
GO:0050896
response to stimulus
GO:0065007
biological regulation
GO:0009987
cellular process
GO:0110165
cellular anatomical entity
A
Is a
B
A
Part of
B
A
Regulates
B
A
Positively regulates
B
A
Negatively regulates
B
A
Occurs in
B
A
Capable of
B
A
Capable of part of
B
GO:0050789
regulation of biological process
GO:0051716
cellular response to stimulus
GO:0023052
signaling
GO:0050794
regulation of cellular process
GO:0007154
cell communicatio n
GO:0005622
intracellular anatomical structure
GO:0007165
signal transduction
GO:0035556
intracellular signal transduction
GO:0019932
second-mess enger-mediate d signaling

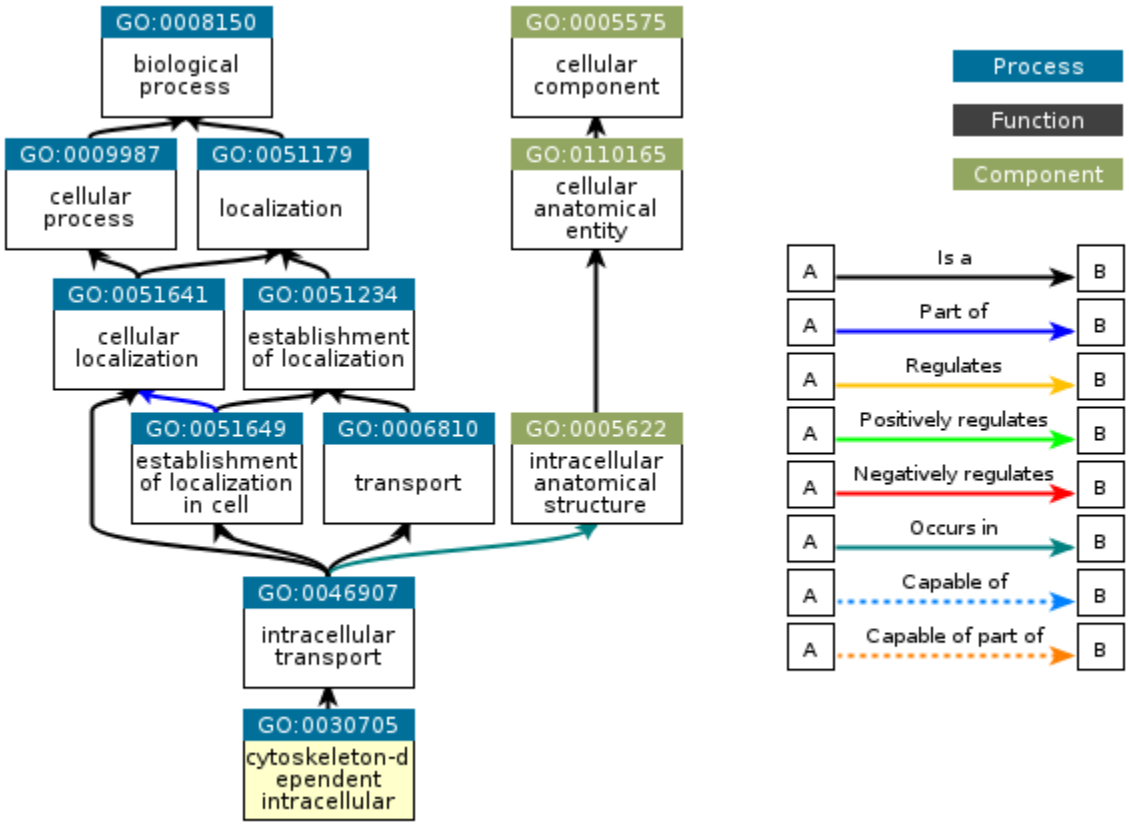
GO:0008150
biological process
GO:0005575
cellular component
Process
Function
Component
GO:0009987
cellular process
GO:0051179
localization
GO:0110165
cellular anatomical entity
A
Is a
B
GO:0051641
cellular localization
GO:0051234
establishment of localization
A
Part of
B
A
Regulates
B
GO:0051649
establishment of localization in cell
GO:0006810
transport
GO:0005622
intracellular anatomical structure
A
Positively regulates
B
A
Negatively regulates
B
A
Occurs in
B
GO:0046907
intracellular transport
A
Capable of
B
A
Capable of part of
B
GO:0030705
cytoskeleton-dependent intracellular

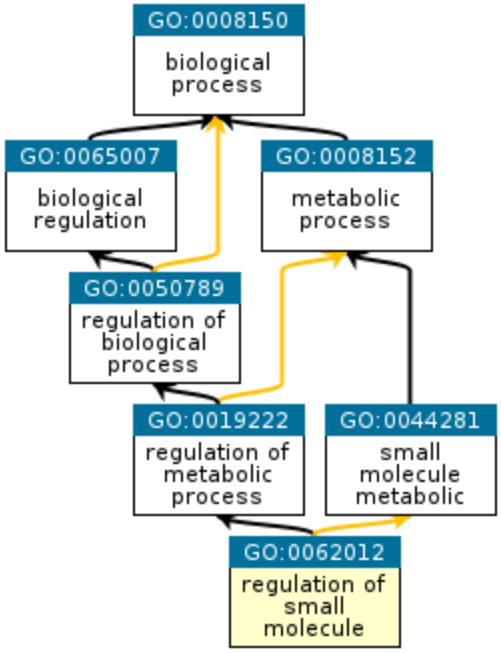
GO:0008150
biological process
GO:0065007
biological regulation
GO:0008152
metabolic process
GO:0050789
regulation of biological process
GO:0019222
regulation of metabolic process
GO:0044281
small molecule metabolic
GO:0062012
regulation of small molecule

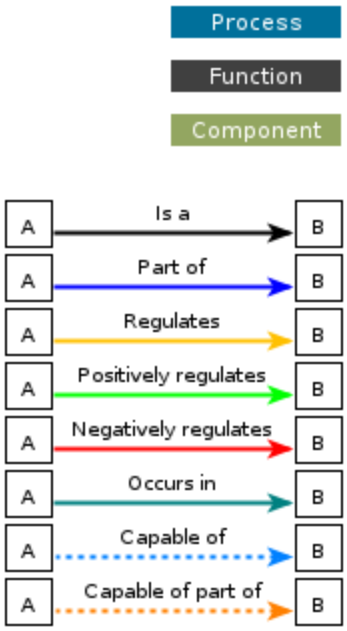
Process
Function
Component
A
Is a
B
A
Part of
B
A
Regulates
B
A
Positively regulates
B
A
Negatively regulates
B
A
Occurs in
B
A
Capable of
B
A
Capable of part of
B

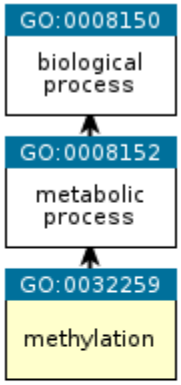
GO:0008150
biological process
GO:0008152
metabolic process
GO:0032259
methylation

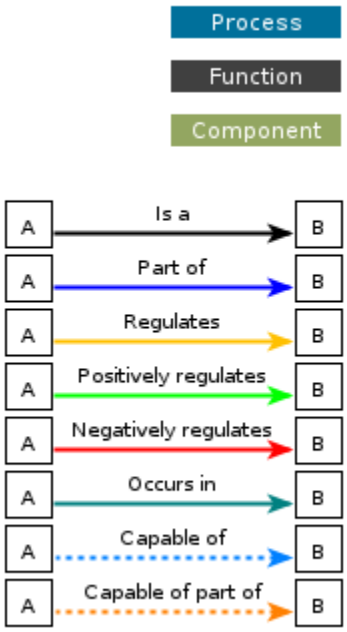
Process
Function
Component
A
Is a
B
A
Part of
B
A
Regulates
B
A
Positively regulates
B
A
Negatively regulates
B
A
Occurs in
B
A
Capable of
B
A
Capable of part of
B

D. Changes in global 5-hmC levels in response to WOCP

The PC mean OD values were seen to be in progressing percentage as expected therefore confirming the dilutions were done appropriately. The equation for the slope which went through 6 data points was Y=2.309X/ (0.4509+X) with R^2=0.9832.

The negative control, positive control at each percentage point and their corresponding mean absorbance at 450nm (OD)

5-mC concentration (%)	Mean OD (Absorbance at 450nm)
0	0
0.1	0.249
0.2	0.665
0.5	1.234
1	1.753
2	1.9025
5	2.017

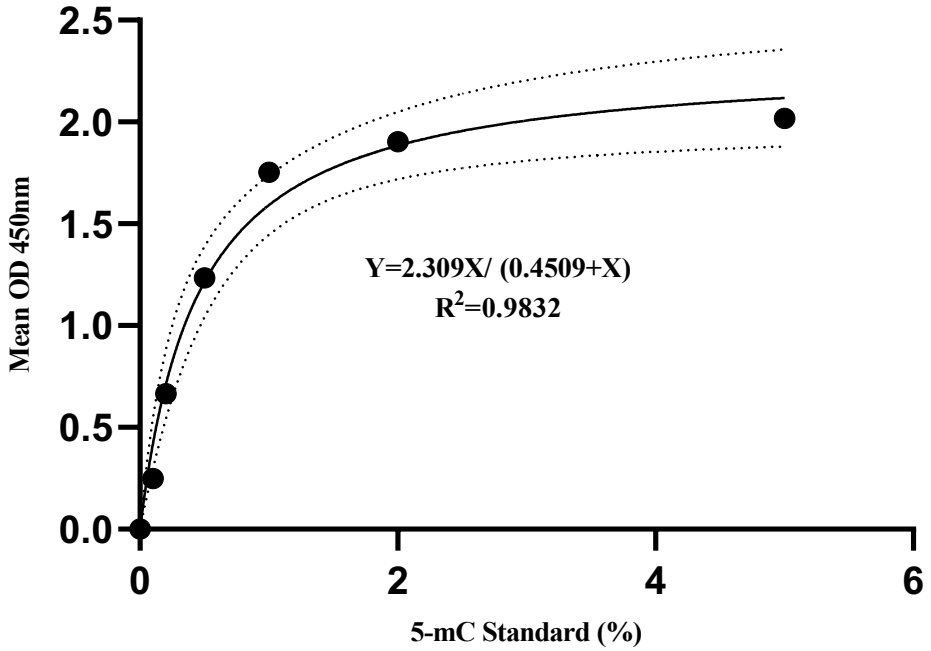

The optimal standard curve generated using the percentage 5-mC of positive controls.

E. Faculty PG Training courses

COURSE	DATES	STATUS	TRAINING POINTS
Understanding your research degree (standalone online learning course)	01/10/2018	Attended	2
Researcher Information Skills for Medicine & Health Sciences	21/11/2018	Attended	1
Introduction to Endnote for Researchers	07/12/2018	Attended	1
Structuring Your Thesis	22/02/2019	Attended	1
Project managing your research (moderated online learning course)	25/02/2019	Pending	2
Exploring Ethics in Research	12/03/2019	Attended	1
Presentation skills for researchers (all disciplines)	21/03/2019	Attended	2
Good Laboratory Practice : Fundamentals	01/03/2019	Attended	1
Good Laboratory Practice : Techniques	08/03/2019	Attended	1
Preparing for your confirmation review	29/04/2019	Attended	0
Post-genomics and bioinformatics	07/05/2019	Attended	6
Faculty postgraduate Research Forum (Medicine and Health Sciences Faculty)	25/06/2019	Attended	4

F. Search details entered

Medline (Ovid) & Embase (Ovid)

1 Ovarian tissue/

2 Ovary/

3 Ovarian cortex/

4 Oocytes/

5 Germinal Vesicle/

6 ovarian tissue*.ti,ab.

7 ovary*.ti,ab.

8 ovarian cortex.ti,ab.

9 oocytes.ti,ab.

10 GV.ti,ab.

11 1 or 2 or 3 or 4 or 5 or 6 or 7 or 8 or 9 or 10

12 Cryopreservation/

13 Slow freezing/

14 Vitrification/

15 Controlled rate freezing/

16 Freezing/

17 cryopreservation.ti,ab.

18 slow freezing.ti,ab.

19 vitrification.ti,ab.

20 controlled rate freezing.ti,ab.

21 freezing.ti,ab.

22 12 or 13 or 14 or 15 or 16 or 17 or 18 or 19 or 20 or 21

23 Epigenetics/

24 DNA methylation/

25 Methylation/

26 Histone modification/

27 Histone acetylation/

28 Histone methylation/

29 MicroRNA/

30 Genomic imprinting/

31 Gene silencing/

32 Epigenomics/

33 epigenetics.ti,ab.

34 DNA methylation.ti,ab.

35 methylation.ti,ab.

36 histone modification.ti,ab.

37 histone acetylation.ti,ab.

38 histone methylation.ti,ab.

39 microRNA.ti,ab.

40 genomic imprinting.ti,ab.

41 gene silencing.ti,ab.

42 epigenomics.ti,ab.

43 23 or 24 or 25 or 26 or 27 or 28 or 29 or 30 or 31 or 32 or 33 or 34 or 35 or 36 or 37 or 38 or 39 or 40 or 41 or 42

44 11 and 22 and 43

Pubmed

((((("Ovarian tissue"[MeSH Terms] OR "Ovarian tissue"[Title/Abstract]) OR ("Ovary"[MeSH Terms] OR "Ovary"[Title/Abstract]) OR ("Ovarian cortex"[MeSH Terms] OR "Ovarian cortex"[Title/Abstract]) OR ("Oocytes"[MeSH Terms] OR "Oocytes"[Title/Abstract]) OR ("Germinal Vesicle"[MeSH Terms] OR "Germinal Vesicle"[Title/Abstract])) AND (("Cryopreservation"[MeSH Terms] OR "Cryopreservation"[Title/Abstract]) OR ("Slow freezing"[Title/Abstract]) OR ("Vitrification"[Title/Abstract]) OR ("Controlled rate freezing"[Title/Abstract]) OR ("Freezing"[Title/Abstract])) AND (("Epigenetics"[MeSH Terms] OR "Epigenetics"[Title/Abstract]) OR ("DNA Methylation"[MeSH Terms] OR "DNA Methylation"[Title/Abstract]) OR ("Methylation"[Title/Abstract]) OR ("Histone Modification"[Title/Abstract]) OR ("Histone Acetylation"[Title/Abstract]) OR ("Histone Methylation"[Title/Abstract]) OR ("MicroRNA"[Title/Abstract]) OR ("Genomic Imprinting"[Title/Abstract]) OR ("Gene Silencing"[Title/Abstract]) OR ("Epigenomics"[Title/Abstract])))) AND ((((("Ovarian tissue"[MeSH Terms] OR "Ovarian tissue"[Title/Abstract]) OR ("Ovary"[MeSH Terms] OR "Ovary"[Title/Abstract]) OR ("Ovarian

cortex"[MeSH Terms] OR "Ovarian cortex"[Title/Abstract]) OR ("Oocytes"[MeSH Terms] OR "Oocytes"[Title/Abstract]) OR ("Germinal Vesicle"[MeSH Terms] OR "Germinal Vesicle"[Title/Abstract])) AND (("Cryopreservation"[MeSH Terms] OR "Cryopreservation"[Title/Abstract]) OR ("Slow freezing"[Title/Abstract]) OR ("Vitrification"[Title/Abstract]) OR ("Controlled rate freezing"[Title/Abstract]) OR ("Freezing"[Title/Abstract])) AND (("Epigenetics"[MeSH Terms] OR "Epigenetics"[Title/Abstract]) OR ("DNA Methylation"[MeSH Terms] OR "DNA Methylation"[Title/Abstract]) OR ("Methylation"[Title/Abstract]) OR ("Histone Modification"[Title/Abstract]) OR ("Histone Acetylation"[Title/Abstract]) OR ("Histone Methylation"[Title/Abstract]) OR ("MicroRNA"[Title/Abstract]) OR ("Genomic Imprinting"[Title/Abstract]) OR ("Gene Silencing"[Title/Abstract]) OR ("Epigenomics"[Title/Abstract])))

Scopus

((TITLE-ABS-KEY ("ovarian tissue")) OR (TITLE-ABS-KEY ("ovarian cortex")) OR (TITLE-ABS-KEY ("ovary")) OR (TITLE-ABS-KEY ("ovaries")) OR (TITLE-ABS-KEY ("embryo")) OR (TITLE-ABS-KEY ("blastocyst")) OR (TITLE-ABS-KEY ("Cleavage Stage")) OR (TITLE-ABS-KEY ("2 cell")) OR (TITLE-ABS-KEY ("4 cell")) OR (TITLE-ABS-KEY ("8 cell"))) AND ((TITLE-ABS-KEY ("cryopreservation")) OR (TITLE-ABS-KEY ("slow freezing")) OR (TITLE-ABS-KEY ("vitrification")) OR (TITLE-ABS-KEY ("control rate freezing"))) AND ((TITLE-ABS-KEY ("Epigenetic")) OR (TITLE-ABS-KEY ("DNA methylation")) OR (TITLE-ABS-KEY ("Histone modification")) OR (TITLE-ABS-KEY ("MicroRNA")) OR (TITLE-ABS-KEY ("Genomic imprint")) OR

(TITLE-ABS-KEY ("Gene silencing")) OR (TITLE-ABS-KEY ("Epigenomic")) OR (TITLE-ABS-KEY ("gene expression")) OR (TITLE-ABS-KEY ("Epigenesis")))

Web of Science

(((TS=(ovarian tissue OR ovary OR ovarian cortex OR oocytes OR germinal vesicle)) AND (TS=(cryopreservation OR slow freezing OR vitrification OR controlled rate freezing OR freezing)) AND (TS=(epigenetics OR DNA methylation OR methylation OR histone modification OR histone acetylation OR histone methylation OR microRNA OR genomic imprinting OR gene silencing OR epigenomics))))